Changes in Mitochondrial Dynamics and iNOS in the Dorsal Vagal Complex of the Brain affects Insulin Sensing, Feeding Behaviours and Body Weight Gain in Rats

Bianca Bhavani Patel

Submitted in accordance with the requirements for the degree of Doctor of Philosophy

University of Leeds

School of Biomedical Sciences

May 2020

The candidate confirms that the work submitted is her own and the appropriate credit has been given where reference has been made to the work of others.

Acknowledgements

First and foremost, I must thank my primary supervisor Beatrice Maria Filippi, you have given me invaluable guidance and encouragement throughout my PhD. You have taught me an endless list of skills both in the lab and outside of the lab, and have supported me through the tears and stress, and for that I am eternally grateful. I would also like to thank my secondary supervisor Jim Deuchars, thank you for testing me and asking me questions which I would have never thought of even if it did scare the living daylights out of me at first. You have given me the confidence to establish myself as a scientist and to think of things outside the ordinary.

I would also like to thank all the people in the Filippi lab, you have all aided me in helping complete this PhD with your baked goods, smiles in the morning and an ear to listen to me moan. In particular, Lauryn, thank you for helping me with immunohistochemistry and feeding studies. Without you by my side for the best part of my PhD, I would have undoubtedly lost my mind, thanks for sending me back to reality, motivating me and listen to my whines on a daily basis. I hope your eardrums return to normal after this. Additionally, I would like to thank the team down at CBS; Mel, Andy, David and Scott, who also put a smile on my face during a long day at my second home.

Thanks to all my friends and family who have given me the support and endless number of drinks to get me through. A special shout-out to my Ashvin Kaka, Greg, Amy and Sophie who always pretended to be interested in my data, you always made me feel special. Kish, you have given me very few words of wisdom, but you have been a decent distraction and a great encouragement for me to take holidays, and for that, I thank you.

My last thanks go to my mum, dad and sisters, without the love and backing of you guys this journey would have been twice as hard. Thank you to my two sisters, Heleyna and Sana, for always being on the other end of the phone for a useless chat. Thank you, Mum, for always sending me back up with brain food. Thank you, Dad, for always giving me the ‘motivational’ speech during my hypochondriac moments. I hope I have made you all proud.

Abstract

Worldwide obesity has nearly tripled since 1975, with over 650 million cases in 2016. Obesity can lead to many adverse metabolic effects in the cardiovascular, brain and endocrine systems. It has been previously shown, the dorsal vagal complex (DVC) of the brain regulates glucose homeostasis and controls food intake through insulin signalling in rats. In these rats, a 3-day high fat diet (HFD) has been shown to induce insulin resistance and diminishes the DVC's ability to regulate glucose metabolism and food intake, though exact mechanistic effects of this are still unknown. HFD-feeding is associated with an increase in mitochondrial fission in the DVC. Mitochondrial fission is regulated by dynamin related protein 1 (Drp1), and an increase in Drp1 activity in the DVC modulates the insulin signalling pathway. Activation of Drp1 has been correlated with increased levels of inducible nitric oxide synthase (iNOS), increased endoplasmic reticulum (ER) stress and insulin resistance in the DVC. This study has shown that activation of Drp1 in the DVC leads to an increase in body weight gain, cumulative food intake and adipose tissue, these rats are also insulin resistant compared to regular chow (RC)- fed littermates and displayed higher levels of iNOS in the DVC. Conversely inhibiting Drp1, or knocking down iNOS, in the DVC in HFD-fed rats decreased body weight gain, cumulative food intake and adipose tissue, and prevented the development of insulin resistance. In addition to this, selective inhibition of Drp1 in astrocytes of the DVC in HFD-fed rats resulted in a decrease in food intake and body weight and prevented HFD-induced insulin resistance. Finally, in diet-induced obese, insulin resistant rats, inhibition of mitochondrial fission or knocking down iNOS in the DVC restored insulin sensitivity and decreased fat deposition. This study has determined the integral role Drp1 and iNOS in the DVC and the effect this has on feeding behaviours and body weight gain, in particular I demonstrated that it is sufficient to target astrocytes in the DVC to affect insulin sensing, feeding behaviours and fat deposition.

Table of Contents

List of Figures

List of Tables

Abbreviations

α-MSH	α-melanocyte-stimulating hormone
DAPI	4',6-diamidino-2-phenylindole
MAPK	Activating mitogen activated protein kinases
ATF6	Activating transcription factor 6
ACBP	Acyl-CoA-binding protein-derived
ADP	Adenosine diphosphate
ATP	Adenosine triphosphate
AgRP	Agouti-related peptide
AD	Alzheimer's disease
APS	Ammonium persulphate
AMPK	Adenosine monophosphate activated protein kinase
AIF	Apoptosis inducing factor
ARC	Arcuate nucleus
AP	Area postrema
K_{ATP}	ATP-sensitive potassium channel
BCA	Bicinchoninic acid assay
BiP	Binding immunoglobulin protein
BBB	Blood-brain barrier
BSA	Bovine serum albumin
BAT	Brown adipose tissue
JNK	c-Jun N-terminal kinases
CO_2	Carbon dioxide
CL	Cardiolipin
CC	Central canal
CNS	Central nervous system
Cyt c	Cytochrome c

DREADD	Designer receptor exclusively activated by designer drugs
DMSO	Dimethyl sulfoxide
DTT	Dithiothreitol
DMX	Dorsal motor nucleus of the vagus
DVC	Dorsal vagal complex
ddH_2O	Double distilled water
PERK	Double stranded RNA-activated protein kinase-like ER kinase
DMEM	Dulbecco's modified eagle medium
Drp1	Dynamin-related protein 1
EGTA	Egtazic acid
ER	Endoplasmic reticulum
eNOS	Endothelial NOS
ECL	Enhanced chemiluminescence
EDTA	Ethylenediaminetetraacetic acid
eIF2α	Eukaryotic initiating factor 2 alpha
ERK	Extracellular signal-regulated kinase
Fis1	Fission 1
FOXO	Forkhead box class O
FFA	Free fatty acids
FSC	Frozen Section Compound
GFAP	Glial fibrillary acidic protein
GSK3β	Glucose synthase kinase 3 beta
GLUT4	Glucose transporter type 4
G6PASE	Glucose-6-phophatase
GSH	Glutathione
GFP	Green fluorescent protein
G-domain	GTPase domain

GED	GTPase effector domain
GDP	Guanosine diphosphate
GTP	Guanosine triphosphate
HGP	Hepatic glucose production
HFD	High fat diet
HRP	Horseradish Peroxidase
HCl	Hydrochloric acid
IHC	Immunohistochemistry
iNOS	Inducible nitric oxide synthase
PINK1	Inductive putative kinase
IMM	Inner mitochondrial membrane
Pi	Inorganic phosphate
IRE-1	Inositol-requiring enzyme 1
IRS	Insulin receptor substrate
IL	Interleukin
ICV	Intracerebroventricular
IP	Intraperitoneal
JAK	Janus-activated kinases
LH	Lateral hypothalamus
LPS	Lipopolysaccharide
LIRKO	Liver-specific insulin receptor knockout
LIRFKO	Liver-specific insulin receptor and FOXO1 knockout
MBH	Mediobasal hypothalamus
MCR	Melanocortin receptor
mRNA	Messenger ribonucleic acid
MMTS	Methyl methane thiosulfate
MDIVI-1	Mitochondrial division inhibitor 1

mtDNA	Mitochondrial DNA
MiD	Mitochondrial dynamic proteins
Mff	Mitochondrial fission factor
MFN	Mitofusin
MAP	Mitogen activated protein
MOI	Multiplicity of infection
NMDA	N-methyl-D-aspartate
nNOS	Neuronal NOS
NeuN	Neuronal nuclei
NIRKO	Neurone-specific knockdown of the insulin receptor
NPY	Neuropeptide Y
NADH	Nicotinamide adenine dinucleotide hydrogen
NAD(P)H	Nicotinamide adenine dinucleotide phosphate
NO	Nitric oxide
NOS	Nitric oxide synthase
NF-κB	Nuclear factor kappa-light-chain enhancer of activated B cells
NTS	Nucleus tractus solitarri
Ob/ob	Leptin knockout
ODN	Octadecaneuropeptide
NP-40	Octyl phenoxypolethoxylethanol 40
OPA1	Optic atrophy 1
OCT	Optimal cutting temperature medium
OMM	Outer mitochondrial membrane
PVN	Paraventricular nucleus
$OONO^{\cdot}$	Peroxynitrite
PBS	Phosphate-buffered saline
PBST	Phosphate-buffered saline triton

PEPCK	Phosphoenolpyruvate carboxykinase
PI3K	Phosphoinositide 3 kinase
PIP	Phosphatidylinositol 4,5-biphosophate
PTB	Phosphortyrosine-binding
PH	Pleckstrin homology
PPAR-γ	Proliferator-activated receptor gamma
POMC	Proopiomelanocortin
PDI	Protein disulphide isomerase
PKA	Protein kinase A
AKT	Protein kinase B
PKC	Protein kinase C
RNS	Reactive nitrogen species
ROS	Reactive oxygen species
RC	Regular Chow
RT	Room Temperature
RPM	Rotation per minute
GSNO	S-nitroglutathione
GSNOR	S-nitroglutathione reductase
ShRNA	Short hairpin RNA
SDS	Sodium dodecyl sulphate
SD	Sprague Dawley
SOCS	Suppressor of cytokine signalling
SYN	Synapsin I promotor
TMT	Tandem Mass Tag
TEMED	Tetramethylethylenediamine
TLR	Toll-like receptors
TBST	Tris-buffered saline tween 20

TBS	Tris buffered solution
TNF	Tumour necrosis factor
T2DM	Type II diabetes mellitus
UCP2	Uncoupling protein 2
UPR	Unfolded protein response
VMH	Ventromedial nucleus
WAT	White adipose tissue
XBP1	X-box binding protein 1

1 General Introduction

1.1 Insulin

1.1.1 History and Discovery

Insulin is a hormone which is released by the β-cells in the islet of Langerhans located in the pancreas (Lee and Pilch, 1994). The importance of the pancreas in the regulation of carbohydrate metabolism was first seen in 1890 (Mering and Minkowski, 1890), where removing the pancreas in a dog resulted in hyperglycaemia which subsequently led to diabetes and ketosis, ultimately resulting in death (Rosenfeld, 2002). In 1921, Fredrick Banting and Charles Best extracted a serum from a calf's pancreas which effectively lowered blood glucose in diabetic dogs. They presented their findings to Macleod, a physiologist, who recruited the biochemist J.B. Collip, to analyse this extract. With this success, Banting, Best, Collip and Macleod were awarded the Nobel Prize for the discovery of this extract, named insulin (Rosenfeld, 2002). This was a medical breakthrough for the treatment of diabetes (Quianzon and Cheikh, 2012).

1.1.2 Structure and Function

Proinsulin is synthesised from pre-proinsulin mRNA and this is the precursor of insulin which is produced in β-cells of the pancreas (Wilcox, 2005). In 1964, Dorothy Hodgkin won a Nobel Prize for using x-ray crystallography to determine protein structures, five years later, Hodgkin and colleagues successfully determined the three dimensional structure of insulin (Adams et al., 1969). Insulin is a dimer of an A-chain and a B-chain with a combined molecular mass of 5808 Da (Figure 1.1A) (Adams et al., 1969; Ward and Lawrence, 2011). Insulin binds to the α-subunit of the insulin receptor, initiating a cascade of downstream signalling.

The insulin receptor is a tetrameric protein comprised of two extracellular cysteine rich α-subunits and two tyrosine rich β-subunits, which are linked by disulphide bonds (Lee and Pilch, 1994; Saltiel and Kahn, 2001). The β-subunit is formed of three regions, the extracellular, transmembrane and cytosolic regions. The cytosolic tyrosine domain has an adenosine triphosphate (ATP) binding consensus sequence and three clusters of tyrosine which are phosphorylated in response to insulin (Lee and Pilch, 1994). Insulin binds to the α-subunit, initiating a string of events, firstly insulin binding increases the kinase activity of the β-subunits, resulting in phosphorylation of the β-subunits leading to a conformational change of the receptor, which in turn increases the tyrosine kinase activity allowing recruitment of receptor substrates (Figure 1.1B) (Saltiel and Kahn, 2001).

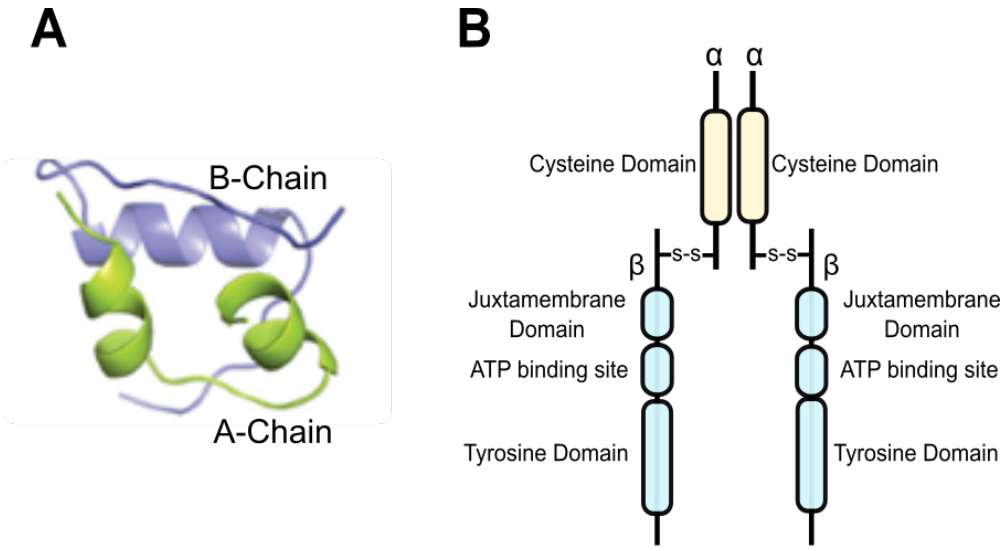

Figure 1.1 Structure of insulin and insulin receptor

A: Monomer of insulin (green represents A chain, purple represents B chain)

B: Structure of the insulin receptor

Insulin receptor substrate (IRS) proteins are a family of highly homogenous, cytoplasmic adaptor proteins that regulate signalling with insulin binding. IRS-1 and -2 are ubiquitously expressed and are mediators of insulin-dependent

mitogenesis and glucose metabolism in cells (Boucher et al., 2014; Mardilovich et al., 2009; Saltiel and Kahn, 2001; Shaw, 2011). These substrates are extremely important in development, mice with an IRS-1 knockout were born around 70% smaller than wild type mice, and remained smaller throughout their lives. In addition, these mice were insulin resistant and had impaired glucose tolerance in peripheral tissues (Araki et al., 1994; Kadowaki et al., 1996; Kido et al., 2000; Shaw, 2011). In contrast, IRS-2 knockout mice were the same size as wild type mice, however they had many tissue-specific defects (Kido et al., 2000; Saltiel and Kahn, 2001; Withers et al., 1998). IRS-2 knockout mice had smaller brains due to a decrease in neuronal proliferation, they also had a reduction in number β-cells in the pancreas as well as insulin resistance in peripheral tissues (Kido et al., 2000; Saltiel and Kahn, 2001; Withers et al., 1998). These studies therefore illustrate the importance of IRS proteins in normal protein development and function.

IRS proteins have a N-terminal pleckstrin homology (PH) domain adjacent to a phosphortyrosine-binding (PTB) domain. The PH domain directs IRS to the juxtamembrane domain on the insulin receptor where it binds and sequentially regulates tyrosine phosphorylation resulting in downstream effects (Boucher et al., 2014; Okada et al., 1994; Shaw, 2011). One of these downstream effectors is the p85 regulatory subunit of the phosphoinositide 3 kinase (PI3K) which is highly important in the activation of the serine threonine kinase, protein kinase B (AKT), which aids the metabolic regulation of insulin's actions. The PI3K catalytic subunit, p110, phosphorylates phosphatidylinositol 4,5-phosphate (PIP_2) leading to the activation of PIP_3, activating AKT (Okada et al., 1994; Shaw, 2011; Sun et al., 1993). Activation of AKT leads to downstream signalling of key substrates in

response to insulin, including inhibiting Forkhead box class O (FOXO) transcription factors (Boucher et al., 2014; Shaw, 2011). FOXO transcription factors, integrate signals from stress and nutrient deprivation to increase gluconeogenesis and glycolysis (Figure 1.2) (Shaw, 2011; Webb and Brunet, 2014). Another essential branch of the insulin signalling pathway is the mitogen activated protein kinases (MAPK) / extracellular signal-related kinases (ERK) pathway, this pathway is activated independently of the PI3K/AKT pathway

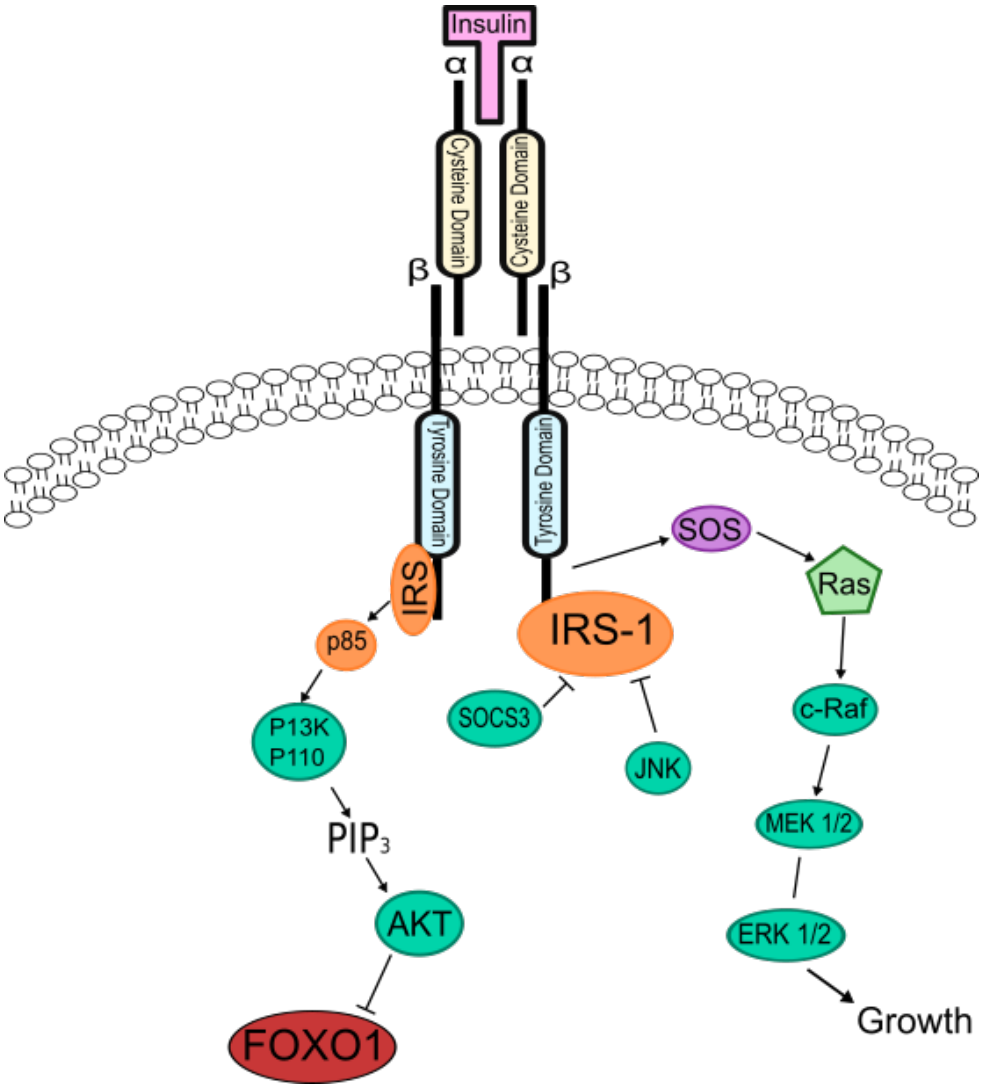

Figure 1.2 Insulin signalling pathway

Schematic representation of the insulin signalling pathways, insulin binds to the α subunits on its receptor to initiate a cascade of downstream effects. Insulin activates either the PI3K/AKT pathway or the MAPK/ERK1/2 pathway

(Boucher et al., 2014). Activated IRS proteins initiate a signalling cascade which results in serine threonine kinase Raf activation, that targets MAPK1 and -2, phosphorylating and activating MAP kinases, ERK1 and -2. ERK1 and -2 play important roles in cell proliferation and differentiation by regulating gene expression (Figure 1.2) (Boucher et al., 2014).

Insulin is secreted in response to circulating glucose levels, regulating blood glucose levels and maintaining energy homeostasis (Schwartz, 2005; Wilcox, 2005). Insulin allows uptake of glucose, free fatty acids (FFA) and amino acids, in the liver, adipose tissue and muscle which are stored as glycogen, lipids and proteins, respectively (Figure 1.3). Insulin can rapidly supress hepatic glucose production (HGP) through direct action on the liver and indirectly via adipose tissue, muscle cells and α-cells of the pancreas (Girard, 2006; Schwartz, 2005; Wilcox, 2005). Insulin's actions in the brain were first discovered nearly a century ago, since then there has been extensive research to understand its actions (Claude, 1855). Insulin in brain can initiate signalling cascades to decrease HGP through neuronal input to the liver, as well as decrease lipolysis and glucagon production (Filippi et al., 2012a; Schwartz, 2005).

In addition to controlling glucose production, insulin has a critical role in the regulation of feeding; insulin is a satiety hormone which can signal to the brain to inhibit food intake and in turn affect body weight (Figure 1.3) (Woods et al., 2006). The 'adiposity negative feedback' model was created on the premise that circulating peripheral signals inform the brain of alterations in body fat to which it responds with adaptive adjustments to stabilise fat stores. Insulin receptors are heavily concentrated in the brain, when body fat mass increases, insulin signals to the brain to inhibit food intake, suggesting insulin is a key 'ancestral negative

feedback regulator' of energy homeostasis (Clegg et al., 2003; Schwartz, 2005; Smeets et al., 2012).

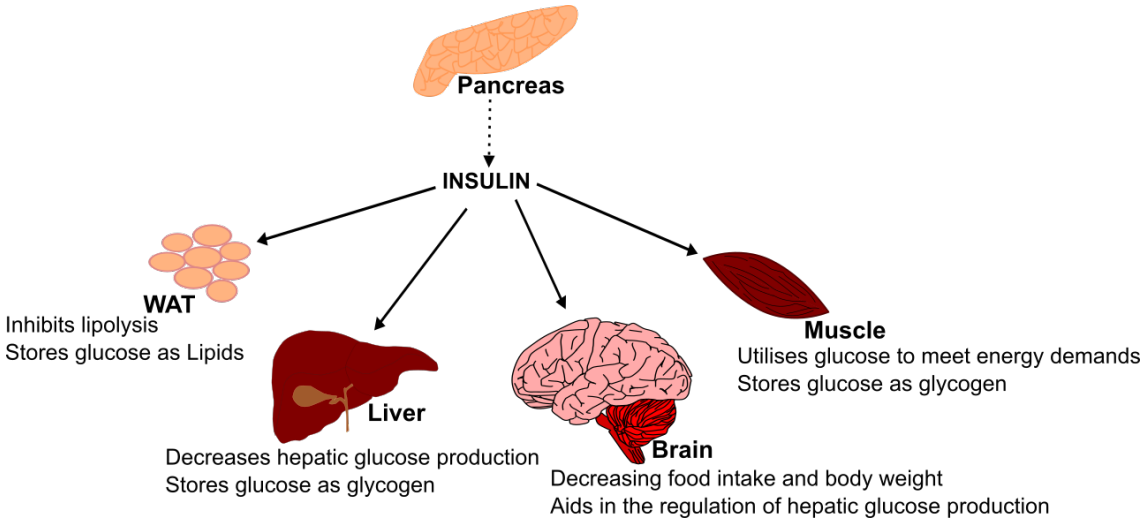

Figure 1.3 Summary of the action of insulin in the body

Insulin is released by the pancreas in response to an increase in circulating glucose, which then acts on the white adipose tissue (WAT), liver, brain and muscle to maintain euglycemia

Insulin signalling is tightly regulated, however disruption in its signalling pathway can cause insulin resistance. Insulin resistance can be defined as defects in the insulin signalling pathway, and clinically refers to impaired sensitivity to insulin required for glucose disposal. Insulin resistance results in increased levels of plasma insulin (hyperinsulinemia) required to enable glucose uptake in different areas of the body, such as the liver, muscle and fat (Wilcox, 2005). Chronic hyperinsulinemia can lead to diabetes, as the pancreas can no longer meet the demands to reached euglycemia. Studies have shown that in both human and mice, disruption of insulin signalling components results in insulin resistance and hyperglycaemia (Czech, 2017).

1.2 Insulin's mechanisms of actions in the body

1.2.1 Liver

The liver accounts for around 30% of insulin-mediated glucose disposal, HGP accounts for the majority of glucose production (Cherrington et al., 2007; Edgerton et al., 2006; Moore et al., 2012). Insulin is released constantly at a steady state to enable insulin-dependent glucose entry into the liver cells, preventing hydrolysis of triglycerides and limiting gluconeogenesis to maintain normal blood glucose levels (Cherrington, 1999; Cherrington et al., 2007; Wilcox, 2005). In a post-prandial state, insulin concentrations are increased in the blood. Insulin binds directly to hepatic insulin receptors activating insulin signalling, allowing glucose uptake, facilitating glycogen storage and decreasing HGP via inhibition of gluconeogenesis and glycolysis (Biddinger et al., 2008; Cherrington, 1999; Edgerton et al., 2006; Moore et al., 2012). The glucose transporters (GLUTs) are an important family which help facilitate glucose uptake into the liver to control blood glucose levels (Chadt and Al-Hasani, 2020). In particular, the GLUT1, -2, -5 and -8 are extremely important in glucose sensing and HGP (Chadt and Al-Hasani, 2020).

The liver is a highly important organ in glucose regulation, mice with a liver-specific insulin receptor knockout (LIRKO), were severely insulin resistant and were dramatically glucose intolerant (Biddinger et al., 2008). Insulin can control the synthesis and storage of lipids in the liver by increasing de novo lipogenesis which in turn supresses fatty acid oxidation. LIRKO mice were protected from fatty liver disease and lipid abnormalities seen in high fat diet (HFD) fed rats, despite being insulin resistant, highlighting the crucial role of insulin in stimulating

de novo lipogenesis in the liver (Biddinger et al., 2008; Cherrington et al., 2007; Titchenell et al., 2017). FOXO, is a transcription factor that is regulated by insulin and promotes many genes involved in gluconeogenesis. In a liver-specific, insulin receptor and FOXO1 knockout (LIRFKO) obese model, these mice had with improved glucose tolerance (O-Sullivan et al., 2015).

In an insulin resistant state, insulin fails to stimulate glucose uptake and suppress HGP in both pre- and post-prandial states, resulting in higher circulating blood glucose levels (Brown and Goldstein, 2008; Ferris and Kahn, 2016; Titchenell et al., 2017). In the pathophysiology of obesity and type II diabetes mellitus (T2DM), a key contributing factor is an increase in triglyceride synthesis due to increased nutrient availability (Biddinger et al., 2008; Brown and Goldstein, 2008; Ferris and Kahn, 2016; Vatner et al., 2015). Insulin has an essential role in regulating glucose homeostasis in the liver and therefore in the development of T2DM.

1.2.2 Skeletal Muscle

Skeletal muscle consumes energy in the form of glucose; insulin signals to the muscle to promote glucose uptake and net glycogen synthesis, a process controlled by GLUT4 translocation (Dimitriadis et al., 2011; Petersen and Shulman, 2018). Glucose transport is important in cell metabolism as it controls the rate of glucose utilisation. Insulin activates enzymes hexokinase and 6-phosphofructokinase in muscle leads to an increased rate of glycolysis in muscle (Dimitriadis et al., 2011; Petersen and Shulman, 2018).

Insulin resistance in skeletal muscle is characterised by excess β-oxidation, a catabolic process were fatty acids are broken down to acetyl Co-A which can be used in the electron transport chain to produce energy (Bartlett and Eaton, 2004).

Muscle-specific models of insulin resistance demonstrated a 50% decrease in glycogen synthesis in muscle, ultimately leading to T2DM (Perseghin et al., 1996; Petersen and Shulman, 2018). In addition, studies have previously shown that a blockade of hexokinase activity decreases glycogen production and glucose transport due to decreased GLUT4 translocation, resulting in insulin resistance in humans (Dohm et al., 1988). Insulin resistance in muscle has been seen in obese mice, this was due to a decrease in tyrosine kinase activity in the insulin receptor impairing intracellular signalling of insulin (Garvey et al., 1998; Petersen and Shulman, 2018). It is evident that insulin acting on the muscle is extremely important in the maintenance and functionality of skeletal muscle.

1.2.3 White adipose tissue (WAT)

Insulin facilitates glucose and FFA uptake in WAT, which in turn inhibits lipolysis and stimulates *de novo* fatty acid synthesis via activation of the GLUT4 transporter (Kusminski and Scherer, 2012; Wilcox, 2005). Insulin can enhance the expression of WAT transcription factors, such as peroxisome proliferator-activated receptor gamma (PPAR-γ) (Boden, 2009; Cignarelli et al., 2019; Scherer et al., 2011). WAT produces a variety of adipokines, including leptin and adiponectin which regulate fat cell differentiation and systemic energy balance. Adipocytes break down triglycerides to release non-esterified fatty acids into the circulation when in fasted or in high energy consuming states (Boden, 2006; Scherer et al., 2011).

WAT dysfunction can lead to uncontrolled lipolysis leading to an increase in FFA release and insulin resistance (Tokarz et al., 2018). In addition, WAT dysfunction increases the production of cytokines inducing insulin resistance by inhibiting insulin signalling cascades (Scherer et al., 2011; Wilcox, 2005). Adipocytes taken

from diabetic mice had reduced levels of GLUT4 translocation and decreased IRS-1 expression (Wilcox, 2005). Adipocytes in HFD-fed rats displayed low levels of ATP, increased lipid storage and reduced mitochondrial biogenesis leading to lipid accumulation and high levels of reactive oxygen species (ROS) as well as insulin resistance (Brand, 2010; Kusminski and Scherer, 2012).

1.2.4 Brain

In 1854, Claude Bernard, a French physiologist demonstrated the role of the brain in glucose homeostasis by puncturing the floor of the fourth ventricle which resulted in glycosuria in a rabbit (Claude, 1855). Since then, there has been extensive research into insulin's actions in the brain (Brüning, 2000; Kleinridders et al., 2014). There are many different satiety-related hormones which have been identified to have an effect in the brain, some of these include, insulin, leptin and ghrelin, to exert their actions these hormones must pass the blood brain barrier (BBB) (Banks, 2008). The BBB is a highly regulated interface between the periphery and the CNS, it maintains homeostasis in the brain (Morris et al., 2018a). The BBB regulates the movement of molecules by way of a partially permeable membrane, which protects the CNS from foreign bodies such as viruses and bacteria, while also allowing certain proteins and hormones to pass through the CNS (Banks, 2008).

The discovery that insulin could cross the BBB was made by Margolis and Altszuler, who showed that that intravenous injection of insulin peripherally caused an increase in insulin levels in the cerebrospinal fluid (Margolis and Altszuler, 1967). In 1997, Banks and colleagues demonstrated using an radioimmunoassay that insulin could pass though the BBB via a saturable transport system. The insulin receptor is highly expressed throughout the brain,

from the olfactory bulb to the brainstem (Brüning, 2000; Kleinridders et al., 2014). Insulin has many functions in the brain from regulating protein synthesis and autophagy, events which occur intracellularly that are important in aiding synaptic plasticity. In addition to this, insulin in the brain is extremely important in the regulation of food intake, energy expenditure and glucose metabolism (Kleinridders et al., 2014; Schwartz, 2005). Mice with a deletion of the insulin receptor in the brain (NIR knockout mice) presented with increased body fat and insulin resistance (Brüning, 2000), illustrating the role insulin plays in the regulation of energy balance.

Insulin can also signal indirectly to the CNS, the brain receives signals from the gastrointestinal tract and adipose tissue via neuronal and hormonal signals (Smeets et al., 2012). This information is transmitted through the afferent branch of the vagus nerve to the brainstem where the nucleus tractus solitarii (NTS) regulates autonomic functions and homeostasis (Browning and Travagli, 2011; Travagli et al., 2006). Vagal afferent neurones express the insulin receptors directly reaching multiple areas of the brain including the hypothalamus to help regulate both food intake and body weight (Schwartz, 2006; Smeets et al., 2012).

The hypothalamus is one of the most important and studied areas of the brain involved in the control of feeding and glucose homeostasis (Brüning, 2000; Obici et al., 2002a; Pocai et al., 2005; Timper and Brüning, 2017). Many studies have shown that food intake leads to activation of anorexigenic neuropeptide producing proopiomelanocortin (POMC) neurones which leads to a counterregulatory downstream effect of decreased food intake and increased energy expenditure. On the contrary, a fasted state induces the activation of orexigenic, neuropeptide-Y (NPY) and agouti-related peptide (AgRP) neurones,

which act to stimulate food intake. In addition to regulating food intake, these neurones also express the receptor for insulin (Stanley and Leibowitz, 1984; Timper and Brüning, 2017). Targeted deletion of the both the insulin and leptin receptor in POMC neurones caused a loss of central glucose regulation, determining that the direct action of insulin or leptin are essential in the maintaining glucose homeostasis (Hill et al., 2010). Mice with an insulin receptor knockout in AgRP neurones, failed to decrease HGP, determined by levels of decreased levels of interleukin-6, which has shown to suppress gluconeogenesis and an increase in levels of glucose-6-phophatase (G6PASE), an enzyme which produces glucose (Könner et al., 2007). Concluding that insulin binds to its receptor on AgRP-expressing neurones, decreasing firing and resulting in decreased HGP (Könner et al., 2007). Such findings illustrate the crucial role of hypothalamic insulin signalling on feeding behaviours and glucose homeostasis.

In addition to regulating feeding, hypothalamic insulin is also important for sympathetic nervous outflow to the brown adipose tissue (BAT), a main function of which is to regulate body temperature (Bamshad et al., 1999; Kleinridders et al., 2014). Many hypothalamic nuclei have been shown to control BAT thermogenesis, such as the arcuate nucleus (ARC), dorsal medial hypothalamus, the paraventricular hypothalamus (PVN) and the lateral hypothalamus (LH) (Labbé et al., 2015). Injection of insulin into the hypothalamus activates BAT and induces hyperthermia, an effect which was lost in mice who had a neurone-specific knockdown of the insulin receptor (NIRKO) (Labbé et al., 2015; Plum, 2006). NPY in the ARC of the hypothalamus has been shown to be critical in the function of BAT, NPY signalling leads to a decrease in tyrosine hydroxylase, the rate-limiting enzyme in synthesising catecholamines, in the PVN, locus coeruleus

and the brainstem which in turn decreases BAT thermogenesis. HFD-fed mice with a knockdown of NPY had increase mRNA of tyrosine hydroxylase and improved BAT function compared to HFD-fed controls (Shi et al., 2013).

There is growing evidence that insulin is important in memory, cognition and behaviour (Lee et al., 2016). Insulin resistance in the brain induces dopaminergic dysfunction leading to anxiety and behavioural disorders (Kleinridders et al., 2015). Activation of neurones in hippocampal slices with insulin, increased neurotransmitter release from presynaptic terminals and promoted synaptic plasticity by modulating long term potentiation and long-term depression (Van Der Heide et al., 2005; Lee et al., 2011). Post-synaptically in the hippocampus, activation of the PI3K pathway is essential for translocation of the glutamate receptor to the plasma membrane during synaptic plasticity (Lee et al., 2011; Schmitz et al., 2018). Hippocampal slices of mice lacking IRS-2 had a decrease in N-methyl-D-aspartate (NMDA) receptor synaptic plasticity and PI3K downstream targets, which could underlie cognitive defects linked to insulin signalling (Costello et al., 2012). Illustrating the of importance insulin signalling in synaptic plasticity and cognition.

Insulin resistance leading to T2DM has been linked to the development of Alzheimer's disease (AD) (Boyt et al., 1999; Ferreira et al., 2018; Perry et al., 2010). Insulin resistance can influence amyloid-β plaque deposition, which impairs synaptic plasticity and memory formation; many studies have shown that insulin signalling is impaired in the brain of AD patients (Boyt et al., 1999; Hiltunen et al., 2012). HFD-fed mice overexpressing amyloid precursor protein and presenilin, a protein important in amyloid-β plaque formation, presented with hyperglycaemia, poor spatial learning and increased amyloid-β plaques,

illustrating regulatory mechanisms which link T2DM and AD (Hiltunen et al., 2012). However, the underlying mechanisms of this and the role of insulin in the development of AD are still unknown (Boyt et al., 1999; Ferreira et al., 2018).

1.2.4.1 Mediobasal hypothalamus

The mediobasal hypothalamus (MBH) is situated adjacent to the third ventricle of the brain and is a region that responds to insulin to modulate food intake and glucose metabolism. The MBH is comprised of the ARC, PVN, VMH and LH, together they regulate glucose homeostasis (Roh et al., 2016). Hormones and nutrients in the systemic circulation and cerebrospinal fluid can easily access the hypothalamic ARC as it is in close contact with the median eminence, this region is rich in fenestrated capillaries close to the BBB (Rodríguez et al., 2010; Roh et al., 2016). As mentioned previously, the ARC has two distinct neuronal populations involved in satiety: the orexigenic NPY and AgRP neurones, and the anorexigenic POMC and cocaine- and amphetamine-regulated transcript neuropeptides producing neurones (Roh et al., 2016; Schwartz, 2005).

The neuropeptide α-melanocyte-stimulating hormone (α-MSH), is produced by the post-transcriptional processing of POMC, once released it binds to melanocortin 3 and 4-receptor (MC3R and MC4R, respectively), and initiates catabolic pathways resulting in a decrease in food intake and increase in energy expenditure (Figure 1.4) (Cowley et al., 2001; Raffan et al., 2016; Roh et al., 2016; Schwartz, 2005). POMC neurones are stimulated by insulin and leptin and function to inhibit food intake and promote weight loss (Figure 1.4) (Cowley et al., 2001; Raffan et al., 2016). Targeted deletion of MC4R and mutations in the POMC gene induced hyperphagia and decreased energy expenditure, leading to obesity in mice (Raffan et al., 2016). Furthermore, selective knockdown of the

insulin receptor in POMC neurones in mice increased HGP and insulin resistance (Hill et al., 2010; Ruud et al., 2017).

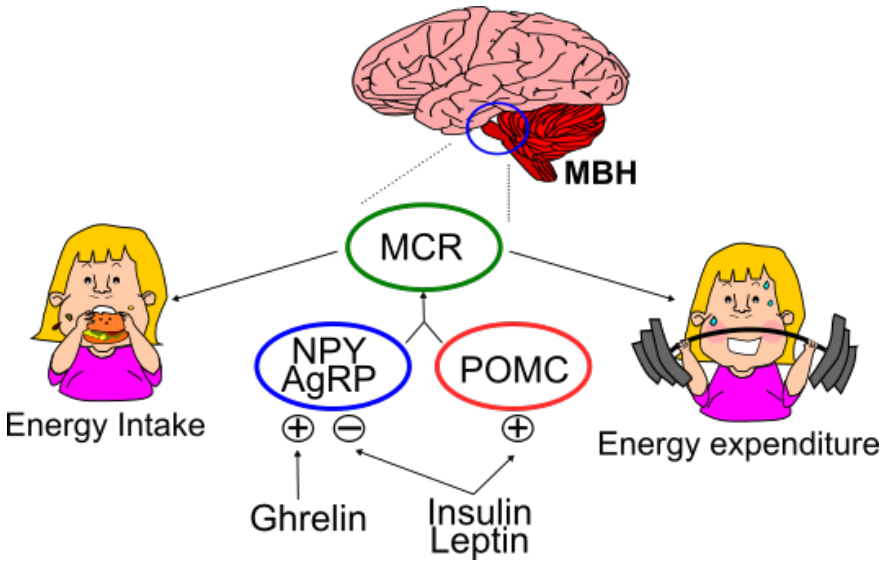

Figure 1.4 Regulation of energy balance by the MBH.

Increased levels of circulating insulin and leptin signal to POMC neurones to increase energy expenditure. In addition, insulin and leptin inhibit AgRP and NPY neurones to decrease food intake. On the other hand, ghrelin, an orexigenic hormone, signals to AgRP and NPY neurones to increase food intake. Defects in secretions of these hormones lead to an increase in food intake leading to obesity and T2DM.

AgRP promotes feeding by competing with α-MSH released from POMC neurones to bind to MC3R and MC4R (Krashes et al., 2014). Activation of AgRP neurones decreased insulin-stimulated glucose uptake and impaired insulin sensitivity and glucose tolerance (Ollmann et al., 1997; Steculorum et al., 2016). Ablation of NPY and AgRP neurones in mice caused a significant decrease in food intake and body weight (Ruud et al., 2017). Central administration of NPY stimulated rapid feeding and insulin resistance in mice (Ruud et al., 2017). In obese insulin-resistant models, insulin neuronal input is reduced due to higher activation of NPY and AgRP neurones inducing hyperphagia (Schwartz, 2005).

Such findings, highlight the critical role of NPY and AgRP neurones in promoting food intake.

Evidence of central action of insulin on glucose regulation and food intake was documented in a primate model, where intracerebroventricular (ICV) infusion of a low dose of insulin resulted in a decrease in food intake and body weight (Woods et al., 1980). A few decades later, knockdown of the insulin receptor in mice resulted in an increase in body weight and food intake, while administration of insulin into the third ventricle decreased HGP. It was therefore postulated that insulin had an integral role in the central regulation of energy and glucose homeostasis (Brüning, 2000; Obici et al., 2002a; Pocai et al., 2005).

When insulin binds to its receptors in the MBH it activates the PI3K and AKT signalling pathway and activation of K_{ATP} channels, leading to hyperpolarisation of neurones. This initiates a cascade of events which leads to a decrease in the expression of phosphoenolpyruvate carboxykinase (PEPCK) and G6PASE in the liver, thus inhibiting gluconeogenesis (Obici et al., 2002b; Pocai et al., 2005). Overnutrition can affect the ability of insulin to lower glucose production, for example, three days of HFD can negate the glucose lowering effect of acute infusion into the MBH (Filippi et al., 2012b). In diabetic rats PI3K expression was reduced in the hypothalamus, however, PI3K signalling in these diabetic rats was restored by overexpression of IRS-2 or PKB, this re-established hypothalamic insulin ability to decrease blood glucose (Gelling et al., 2006). Chronic activation of S6 kinase, a ribosomal protein inhibit PIP3, leads to inhibition of insulin signalling through a negative feedback loop by IRS-1. Molecular inhibition of S6 kinase, using an adenovirus, in the MBH supressed HGP and blunted the effect of HFD-diet feeding (Ono et al., 2008). ICV injection of the K_{ATP} channel activator,

diazoxide, lowered glucose production, while infusion of a sulfonylurea to block K_{ATP} channels prevented the ability of insulin to lower glucose production in rats (Pocai et al., 2005).

As mentioned previously, the brain communicates information on nutritional status to the periphery via the vagus nerve. Following hepatic vagotomy which compromised the ability of efferent fibres to exert effects of ICV insulin to decrease hyperglycaemia (Pocai et al., 2005). ICV injection of an insulin receptor antisense oligonucleotide inhibited insulin's central actions impairing HGP in hyperinsulinemic clamps. Furthermore ICV injection of insulin suppressed HGP irrespective of systemic levels of insulin, thereby highlighting the role of CNS insulin in modulating hepatic glucose metabolism (Obici et al., 2002a, 2002b).

1.2.4.2 Dorsal Vagal Complex

The dorsal vagal complex (DVC) of the brainstem, located close to the fourth ventricle, controls energy homeostasis in various different ways. The DVC encompasses the NTS, the dorsal motor nucleus of the vagus (DMX), and the area postrema (AP) which has a leaky BBB (Filippi et al., 2012b; Gelling et al., 2006; Yettefti et al., 1997). The AP can sense circulating hormones released by peripheral organs, it can receive sensory input from vagal afferents originating from the gastrointestinal tract, lastly, it can receive and relay energy-related signals from other areas of the brain via the AP (Schneeberger et al., 2014). The DVC relay signals to and from the periphery via the vagus nerve. Acute and chronic stimulation of the vagal afferents in rats led to a decrease in food intake (Berthoud, 2008). Chemical stimulation of the DMX resulted in an increase in plasma insulin levels, while subdiaphragmatic vagotomy abolished this effect,

connecting the DMX to the pancreas via the vagus nerve to regulate levels of insulin (Ionescu et al., 1983).

POMC neurones in the ARC of the hypothalamus project signals to the NTS where there are high levels of MC4R (Kishi et al., 2003). In addition to this, delivery of a MC4R agonist into the NTS decreased food intake and increased energy expenditure (Kishi et al., 2003). Deletion of MC4R in the DMX, using chat-cre mice, resulted in hyperinsulinemia and weight gain, therefore illustrating a role for the DMX in regulating insulin levels (Berglund et al., 2014; Rossi et al., 2011). POMC neurones in the NTS act differently to those in the ARC, acute activation of POMC neurones in the NTS results in immediate suppression of food intake, whereas in the ARC, chronic activation of POMC is required to inhibit feeding behaviours (Zhan et al., 2013).

As previously mentioned, in the MBH, insulin activates the PI3K/AKT pathway to regulate glucose homeostasis. However, when insulin was injected into the DVC at the same dose that activated the PI3K/AKT pathway in the MBH, it did not activate this pathway, instead the ERK1/2 pathway was activated determined using western blotting methods (Figure 1.5) (Filippi et al., 2012b). In addition to this, chemical and molecular inhibition of DVC ERK1/2 also negated the effect of insulin on glucose homeostasis, confirming that the ERK1/2 pathway is critical in the regulation of glucose homeostasis in the DVC (Filippi et al., 2012b). Furthermore, infusion of the K_{ATP} channel blocker, glibenclamide, alongside insulin into the DVC; negated the ability of the DVC to lower glucose production and increase glucose infusion rate. This demonstrates that changes in HGP in response to DVC insulin are dependent on the activation of K_{ATP} channels via the ERK1/2 pathway in the DVC (Filippi et al., 2012b). Acute infusion of insulin into

the DVC decreased food intake, where molecular inhibition of ERK1/2 increased food intake in healthy male rats, this molecular disruption of signalling induced obesity after two weeks of feeding (Filippi et al., 2014). Together, this highlights the importance of ERK1/2 signalling in the DVC in the regulation of energy balance.

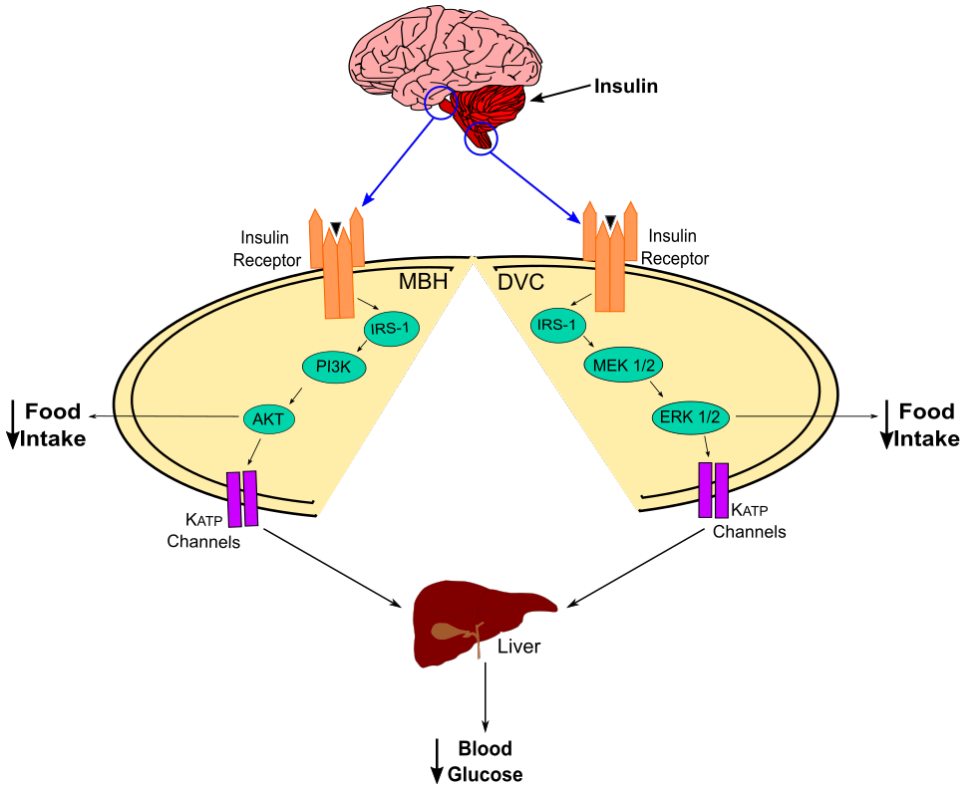

Figure 1.5 Two pathways insulin signalling pathways in the brain resulting in a decrease food intake and HGP.

Insulin in the MBH activates the PI3K/AKT pathway while in the DVC activates ERK1/2 dependent pathway and the K_{ATP} channel to decrease blood glucose by inhibiting HGP

The neuronal populations in the DVC which insulin targets have been shown to be neurones, astrocytes and oligodendrocytes, however the exact mechanism of are not fully understood, a possible way in which information about energy balance are communicated to such neurones could be that astrocytes secrete endozepines, such as octadecaneuropeptide (ODN), which are involved in the regulation food intake (Guillebaud et al., 2017). For example, central administration of ODN decreased food intake in rats, suggesting that ODN could

modify the excitability of NTS neuronal circuits (Guillebaud et al., 2017). Furthermore, activation of astrocytes using DREADDs in the DVC decreased food intake and decreased rebound hyperphagia after fasting (MacDonald et al., 2019).

There are lots of complexities involved in glucose sensing and therefore as yet there are no specific glucose excitatory or glucose inhibitory cells defined in the DVC. It has been previously demonstrated that ERK1/2 dependent insulin signalling activates K_{ATP} channel in the hippocampus, which is also seen in the DVC; K_{ATP} could be a downstream mediator of glucose sensing (Balfour et al., 2006; Filippi et al., 2012b; O'Malley et al., 2003). It is evident that the DVC has an important role in central control of metabolism, further investigation is warranted to fully understand these mechanisms.

1.3 How clinically relevant are insulin's actions in the brain?

There is both *in vivo* and *in vitro* evidence to support that insulin in the brain is a key regulator in peripheral glucose metabolism and feeding behaviours. Many studies have been carried out across species showing that insulin has similar effects on glucose metabolism and feeding (Blázquez et al., 2014). Infusion of insulin in the lateral cerebral ventricle reduced food intake and body weight in baboons, similarly this central administration of insulin has been shown to decrease food intake in rats, sheep, mice and humans (Brüning, 2000; Clegg et al., 2003; Filippi et al., 2012a; Woods et al., 1980). ICV injection of insulin in the third ventricle resulted in a decrease in food intake in male rats but not females (Brüning, 2000). Oral administration of diazoxide, a K_{ATP} channel activator, and somatostatin, to inhibit the release of endogenous insulin, decreased glucose production compared to humans given a placebo, with no effect on glucose

uptake (Kishore et al., 2011). Similarly, ICV injection of diazoxide in rats decreased glucose production, in agreement with previous literature with showed that regulation of endogenous glucose production is mediated by hypothalamic K_{ATP} channels (Kishore et al., 2011; Obici et al., 2002b; Pocai et al., 2005).

Intranasal peptide delivery was developed to understand the effects of insulin in the brain in humans. Intranasal insulin rapidly increases insulin in the cerebrospinal fluid without altering serum insulin, suggesting that insulin directly penetrated from the nasal mucosa to access the brain (Hallschmid et al., 2004). It was found that intranasal insulin significantly suppressed endogenous glucose production in healthy men determined by an arterial pancreatic clamp to maintain euglycemia (Dash et al., 2015). Although the mechanisms of central insulin are not fully understood, a likely mechanism could be the activation of K_{ATP} channels by intranasal insulin to decrease HGP, though this is yet to be determined (Kishore et al., 2011). In addition to this, intranasal insulin administered over eight weeks reduced body fat and weight in healthy men, with consistent findings in rat models (Benedict et al., 2011; Clegg et al., 2003). Intranasal delivery of insulin reduced postprandial appetite in women; in addition, women were less likely to eat palatable food like cookies or chocolate (Guthoff et al., 2010; Hallschmid et al., 2004). There is mounting evidence that insulin's action in the brain can be regulated by both energy and glucose homeostasis, these findings illustrate the potential clinical relevance of the actions of insulin in the brain and insulin actions seen in rats (Spetter and Hallschmid, 2015).

In addition to insulin's role in feeding, research has previously shown the important role in memory formation. Interestingly, intranasal insulin improved cognitive function in humans (Benedict et al., 2008; Spetter and Hallschmid,

2015). Furthermore, systemic inhalation of insulin improved memory in AD patients as measured by story recall; it is thought that insulin can have a direct effect on Apoe4 (Avgerinos et al., 2018). Intranasal insulin is therefore a safe intervention in both diabetes and AD, understanding the mechanisms and efficacy will aid future treatment which can selectively target the brain using pharmacological approaches.

1.4 Insulin resistance

Insulin resistance is characterised by defects in insulin receptor, kinase activity, phosphorylation levels and glucose transport protein translocation, together these lead to the inability to maintain euglycemia, resulting in hyperglycaemia, hyperinsulinemia and dyslipidaemia (Ruud et al., 2017; Saltiel and Kahn, 2001). Deletions of key components of the insulin signalling pathway have been shown to decrease insulin sensitivity leading to T2DM (Saltiel and Kahn, 2001; Schwartz, 2005; Wilcox, 2005).

Insulin resistance can occur in many ways, for example, stress increases inflammatory cytokines and can cause impairments in the insulin signalling pathway in the liver, skeletal muscle and adipose tissue (Mullington et al., 1996). Sleep deprivation increases fasting blood glucose levels and is associated with a decrease in plasma levels of insulin and increased central adiposity (Marette, 2002). Overnutrition is associated with obesity and can be defined as an increase in body mass index and adiposity. Obesity has been linked with endoplasmic reticulum (ER) stress leading to insulin resistance and inflammation (Boden, 2009). It is thought that in obesity, insulin resistance evolves in the muscle, liver and adipose tissue. The adipose tissue produces many cytokines which are associated with the insulin resistance such as interleukins and tumour necrosis

factor (TNF)-α which lead to ER-stress and inflammation (Kahn et al., 2006; Perseghin et al., 2003; Wilcox, 2005).

In pancreatic β-cells the adaptive response to insulin resistance results in an increase in mass and function to maintain euglycemia, however, when β-cells start to become dysfunctional this results in impaired glucose tolerance, increased food intake and can lead to T2DM (Kahn, 2001; Wilcox, 2005). Furthermore, chronic feeding leading to obesity increases non-esterified fatty acids, which can induce insulin resistance and impair β-cell function leading to T2DM, therefore making obesity a risk factor for T2DM (Kahn et al., 2006).

1.4.1 Endoplasmic reticulum stress and insulin resistance

ER stress is a key player in the development of insulin resistance. Abnormal levels of circulating lipids and inflammatory cytokines disrupt insulin signalling and induce insulin resistance. ER stress plays an important role in the development of insulin resistance as it can transduce lipid metabolites and cytokines into stress kinases, which ultimately affects insulin signalling (Salvadó et al., 2015).

The ER is the main cellular organ involved in the synthesis, assembly and secretion of proteins. ER stress occurs when there is an imbalance of protein folding and protein loads, resulting in misfolded proteins (Cunarro et al., 2018; Morris et al., 2018b). ER stress triggers the activation of the unfolded protein response (UPR). The main roles of the UPR are to restore normal function by halting translation, degrade any misfolded proteins and to activate signalling pathways that increase chaperones involved in protein folding. If these mechanisms cannot maintain ER homeostasis the cell undergoes apoptosis. The

loss of UPR signalling can cause diseases such as diabetes and neurodegenerative disorders.

The UPR is mediated by three transmembrane proteins: inositol-requiring enzyme 1 (IRE1), double stranded RNA-activated protein kinase-like ER kinase (PERK) and activating transcription factor 6 (ATF6) (Ron and Walter, 2007; Salvadó et al., 2015; Schröder and Kaufman, 2005). IRE1 monitors ER homeostasis through luminal sensing, under ER stress, binding immunoglobulin protein (BiP), a glucose regulated protein, is released from the lumen of the ER where it acts as a chaperone in the activation of the stress transducers of UPR

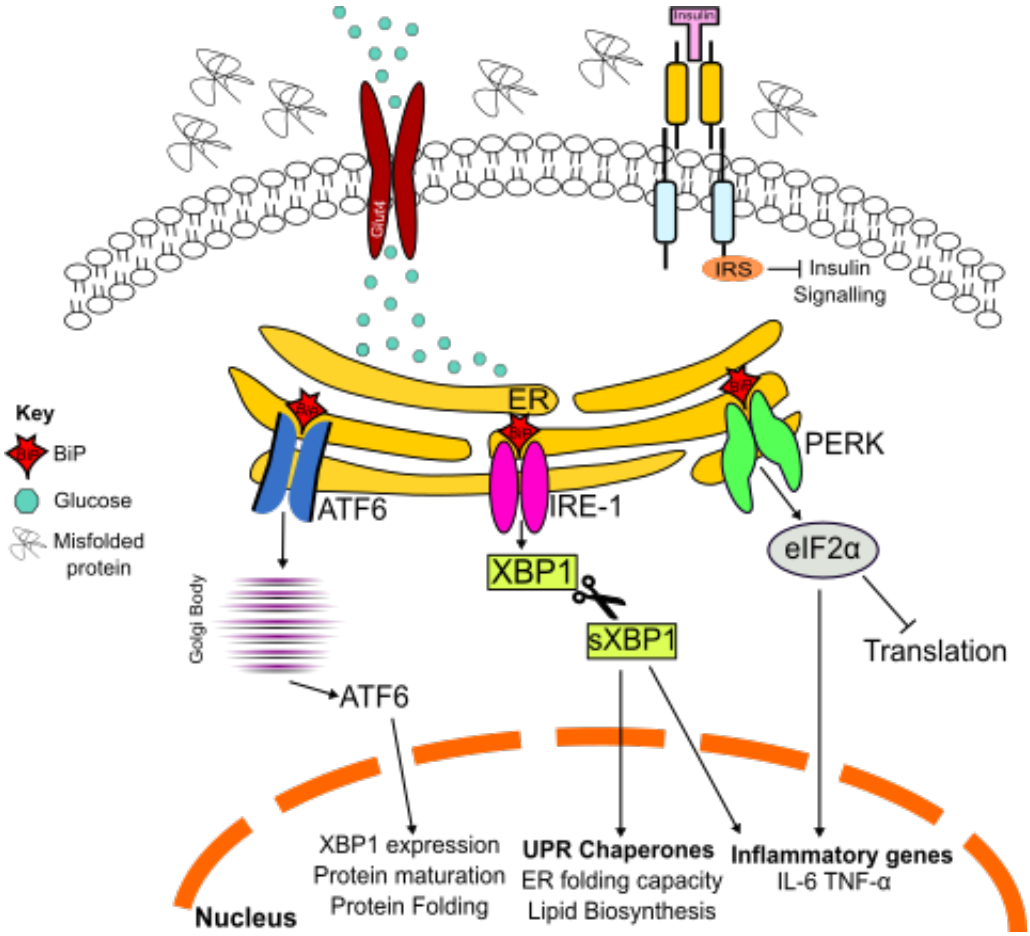

Figure 1.6 The relationship between insulin resistance and ER stress.
Insulin resistance results in misfolded proteins, leading to the activation of the UPR. The UPR has three branches, ATF6, IRE-1 and the PERK, these branches work in unison to try to relieve ER stress, if this is not possible proteins get degraded which leads to inflammation.

(Figure 1.6) (Ron and Walter, 2007; Salvadó et al., 2015). Activation of IRE-1 initiates downstream signalling and the splicing of X-box binding protein 1 (XBP1), which increases transcription of UPR genes and as well as genes involved in inflammation, lipid metabolism and adipogenesis; IRE-1 also produces apoptotic signals (Ron and Walter, 2007; Salvadó et al., 2015). ATF6 senses protein folding status, during ER stress, ATF6 translocates to the Golgi

body to regulate expression of XBP1 and genes involved in folding, maturation and secretion of proteins (Figure 1.6) (Ron and Walter, 2007; Salvadó et al., 2015). PERK can homodimerize and auto-phosphorylate itself under ER stress, this is turn phosphorylates eukaryotic initiating factor 2 alpha (eIF2α) which results in a decrease in the load of newly synthesised proteins and the flux of protein in the ER, therefore reliving stress (Figure 1.6) (Ron and Walter, 2007; Salvadó et al., 2015).

Chronic activation of the UPR can lead to T2DM, obesity, atherosclerosis, heart and liver diseases (Salvadó et al., 2015). HFD-feeding has been shown to increase ER stress in adipose tissue, which in turn increased levels of interleukin-6 and PERK, leading to insulin resistance; in addition it was also demonstrated that PERK can negatively modulate insulin responsiveness in adipose tissue (Figure 1.6) (Bobrovnikova-Marjon et al., 2012). In the liver, ER stress can induce insulin resistance by dysregulating the expression of gluconeogenic genes. Furthermore, XBP1 can initiate degradation of FOXO1 in the liver leading to reduced gluconeogenesis (Lee et al., 2010; Zhou et al., 2011). ER stress also increases the phosphorylation of IRS-1 and -2 via IRE-1 mediated pathways, and as a result induces insulin resistance (Peng et al., 2011a; Salvadó et al., 2013).

It is therefore evident that ER stress plays a dominant role in the pathophysiology of insulin resistance in the body.

1.4.2 Inflammation and insulin resistance

In addition to ER stress, insulin resistance is also associated with low grade inflammation in tissues which is induced by various pro-inflammatory cytokines. TNF-α is a pro-inflammatory cytokine that has been shown to promote insulin resistance by inhibiting tyrosine phosphorylation of IRS-1, this same pathway is also seen in the presence of FFA, demonstrating that both cytokines and FFA act via the same pathway (Figure 1.7) (Hotamisligil et al., 1996). FFA and cytokines stimulate phosphorylation of the serine residues on IRS-1 which in turn dampens insulin signalling. In particular, one serine residue, ser-307, on the IRS-1 substrate is important target for the c-Jun N-terminal kinases (JNK) (Aguirre et al., 2000; Hirosumi et al., 2002). JNKs are a sensing juncture for cellular stress and inflammation, and can phosphorylate IRS-1 at the ser-307 residue (Figure 1.7) (Aguirre et al., 2000). JNK activation has been seen in several models of obesity and insulin resistance; conversely, mice with knockdown of JNK gained less weight and had smaller adipocytes with less fatty livers when fed a HFD, therefore illustrating the role of JNK-mediated phosphorylation of the IRS-1 in the development of insulin resistance (Hirosumi et al., 2002).

An increase in FFA in the blood can result in inflammation leading to insulin resistance. In insulin resistant states, adipocytes release FFA into the bloodstream due to the disruption in the anti-lipolytic effect of insulin, this in turn causes lipotoxicity (Figure 1.7) (Burgos-Morón et al., 2019). Lipotoxicity can lead to β-oxidation and an increase in reactive oxygen species (ROS). An increase in FFA results in an overload to the mitochondria which in turn causes higher levels

of ROS leading ER stress, and ultimately to insulin resistance (Burgos-Morón et al., 2019).

Immune sensors, such as toll like receptors (TLR) play an important role in sensing pathogens and detecting tissue injury including insulin resistance. Activation of TLR initiates a cascade of events leading to the activation of nuclear factor kappa-light-chain enhancer of activated B cells (NF-κB) resulting in the production of inflammatory cytokines (Figure 1.7) (Tanti et al., 2013). TLR also activates ERK1/2 signalling, JNK and ERK (Könner and Brüning, 2011). In particular, TRL4 which has an important role in inflammation and insulin resistance in obesity (Figure 1.7). TLR4 is expressed in macrophages, adipocytes, hepatocytes, muscles and in the hypothalamus (Könner and Brüning, 2011). In obese mice there is a significant increase in TLR4 expression along with a decrease in insulin sensitivity (Könner and Brüning, 2011). Mice with knockdown of TLR4 gained less weight than controls on a HFD and presented with lower levels of inflammation (Shi et al., 2006).

The suppressor of cytokine signalling (SOCS) protein family control the degradation of proteins, and are induced by inflammatory cytokines. SOCS proteins interact with the tyrosine kinase, Janus-activated kinases (JAK), to initiate cytokine mediated signals to inhibit tyrosine phosphorylation (Figure 1.7). SOCS are involved in a negative feedback loop to downregulate the actions of satiety hormones, insulin and leptin (Lebrun and Van Obberghen, 2008; Tanti et al., 2013). SOCS3 has been shown to inhibit insulin signalling by binding to the SH2 domain on the juxtamembrane of the insulin receptor, preventing its interaction with IRS-1 (Emanuelli et al., 2000). In addition, SOCS1 and SOCS6 inhibit tyrosine kinase activity of the insulin receptor, demonstrating the

importance of SOCS proteins in the pathogenesis of insulin resistance (Emanuelli et al., 2000). Inflammation leads to the upregulation of SOCS proteins in many peripheral tissues, where overexpression of SOCS1 and SOCS3 resulted in decreased expression of IRS leading to insulin resistance (Figure 1.7) (Lebrun and Van Obberghen, 2008; Tanti et al., 2013). Mice with a CNS knockdown of SOCS3 were protected against diet-induced obesity and insulin resistance (Howard et al., 2004).

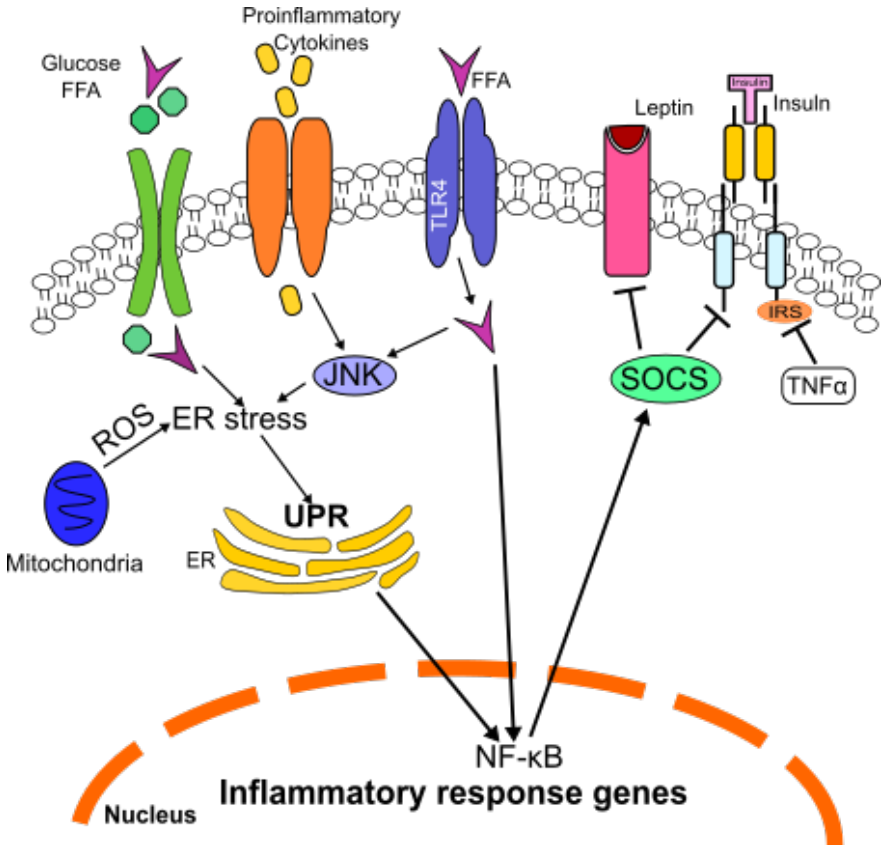

Figure 1.7 The relationship between insulin resistance and inflammation.

Insulin resistance results in an increase in FFA and proinflammatory cytokines, this in turn causes ER stress, mitochondrial stress and the generation of an inflammatory response via activation of many pathways.

1.5 Mitochondria

Mitochondria are intracellular organelles in eukaryotic cells and are deemed the 'powerhouses of the cell' (Annesley and Fisher, 2019; Nunnari and Suomalainen, 2012; Stark and Roden, 2007). As the mitochondria are a primary source of ATP, the major metabolic pathways that occur within these organelles are oxidative phosphorylation, the Krebs cycle and β-oxidation (Stark and Roden, 2007). In addition, mitochondria have an important role in the biosynthesis of cytosolic free calcium (Frey and Mannella, 2000; Nunnari and Suomalainen, 2012; Stark and Roden, 2007). Mitochondria's role in maintaining calcium concentrations is important in cell homeostasis, it helps maintain energy production by buffering and shaping cytosolic calcium to determine the fate of the cells (Contreras et al., 2010). Furthermore, calcium handling is extremely important in the regulation of neuronal and hormonal signalling, highlighting the significance mitochondria play in endocrine function (Stark and Roden, 2007).

To ensure the mitochondrial network is working efficiently to meet energy demands, mitochondria themselves undergo autophagy, which is termed mitophagy (Palikaras et al., 2018). Mitophagy to degrade mitochondria happens in two main steps, first is the initiation of autophagy, followed by the priming of selected mitochondria for removal (Ding and Yin, 2012). The inductive putative kinase (PINK1)-Parkin pathway primarily regulates the priming step in mitophagy, PINK1 accumulates in the outer mitochondrial membrane (OMM) and Parkin translocates to the OMM and mediates ubiquitination of mitochondrial proteins to initiate autophagy of their adaptors thus initiating degradation (Ding and Yin, 2012; Ordureau et al., 2018; Pickles et al., 2018; Sarraf et al., 2013). Basal mitophagy is seen in every cell and occurs at different rates. Extracellular stress

signals affect mitochondrial physiology by inducing mitophagy and altering mitochondria to meet the 'new' metabolic adjustments (Palikaras et al., 2018; Sekine and Youle, 2018).

1.5.1 Mitochondrial dynamics

Organisms can maintain metabolic homeostasis by adjusting the capacity and efficiency of ATP generation to meet energy supply and demand (Gao et al., 2014). Mitochondrial dynamics regulate the morphology, number, distribution and function of the mitochondria, which is critical in the maintenance of mitochondrial homeostasis in response to stress (Gao et al., 2014; Meyer et al., 2017). The changes in mitochondria involve a delicate balance of proteins promoting fusion and fission. Mitochondrial fusion is regulated by mitofusin 1 and 2 (MFN-1 and MFN-2, respectively) and optic atrophy 1 (OPA1), while mitochondrial fission is regulated by dynamin related protein 1 (Drp1) and Fission 1 (Fis1) (Figure 1.8) (Gao et al., 2014; Lee and Yoon, 2016; Meyer et al., 2017). Mitochondrial fusion allows extension of the mitochondrial network to effectively meet high energy demands and allowing increased generation of ATP (Figure 1.8). Conversely, mitochondrial fission serves to eliminate damaged mitochondria from the network by autophagy, demonstrating the importance of this process as a quality control mechanism for the maintenance of mitochondria (Westermann, 2012). Continual fission and fusion of mitochondria is integral to the adaptation to metabolic changes; cells in a fed state maintain fragmented mitochondria, favouring fission, while in a fasted state, mitochondria tend to be fused (Figure 1.8) (Gao et al., 2014; Lee and Yoon, 2016).

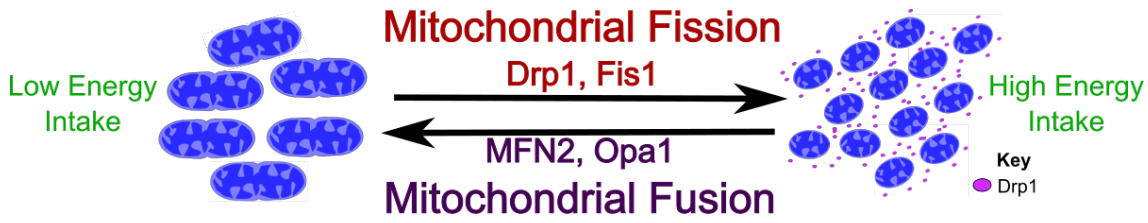

Figure 1.8 An overview of mitochondrial dynamics.

Mitochondrial dynamics are regulated by many proteins, during a low energy intake state mitochondrion favour mitochondrial fusion, aided by regulators MFN2 and Opa1. In high energy intake, mitochondria favour mitochondrial fission regulated by Drp1 and Fis1. (Small dots indicate Drp1)

1.5.1.1 Mitochondrial fusion

Mitochondrial fusion, otherwise known as elongation of mitochondria, is a cell survival mechanism; by increasing respiratory efficacy. Maintaining a network of mitochondria that are hyperfused protects the cells from degrading by autophagy in a nutrient deficient state (Gomes et al., 2011; Meyer et al., 2017; Ramírez et al., 2017). Mitochondrial fusion is tightly regulated by proteins at both the inner mitochondrial membrane (IMM) and the OMM. These proteins have GTPase activity which converts guanosine triphosphate (GTP) to guanosine diphosphate (GDP) and have the ability to self-assemble and remodel membranes (Olichon et al., 2006; Stark and Roden, 2007; Tilokani et al., 2018). Fusion of mitochondria requires merging of the OMM and then the IMM, fusion is regulated by mitofusin GTPases MFN1 and -2 on the OMM. In the IMM, MFN1 is required for mitochondria fusion which is promoted by OPA1. OPA1 mediates IMM fusion and also controls cristae morphogenesis, apoptosis and respiratory capacity (Olichon et al., 2006).

To initiate mitochondrial fusion, two mitochondria outer membranes are tethered together by the transmembrane domain of MFNs (Figure 1.9) (Tilokani et al., 2018). The GTP binding and hydrolysis induce a conformational change in the

MFNs resulting in mitochondrial docking and an increase in membrane contact sites. GTP dependent oligomerisation ensures OMM fusion has taken place (Figure 1.9) (Tilokani et al., 2018), following from this, OPA1 and cardiolipin (CL), an important component of IMM, drive IMM fusion (Tilokani et al., 2018). The interaction between OPA1 and cardiolipin tethers the two IMM and they fuse together following OPA1-dependent GTP hydrolysis; this results in mitochondria fusion (Figure 1.9) (Tilokani et al., 2018).

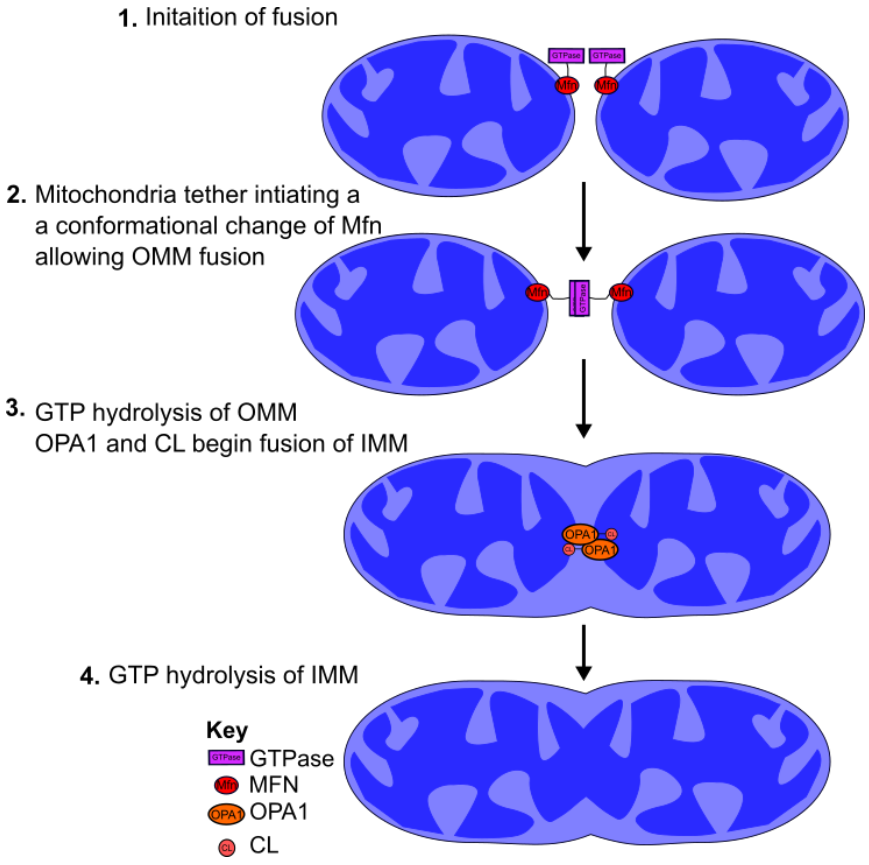

Figure 1.9 Schematic of mitochondrial fusion.

1. The OMM are tethered by the GTPase domains of Mfn2. 2. This induces a conformation change leading to mitochondrial docking. 3. GTPase oligomerises and fuses the OMM. 4. Opa1 and CL tether the two IMMs which fuse together via Opa1 dependent GTP hydrolysis

1.5.1.2 Mitochondrial fission

Mitochondrial fission occurs around the ER site and requires separating the OMM and the IMM, and re-joining these in the correct orientation without losing proteins from the mitochondria matrix. In addition to this, mitochondrial fission has to split mitochondrial proteins and mtDNA to allow the new organelle to function properly (Figure 1.10B) (Scott and Youle, 2010; Sesaki and Jensen, 1999). Mitochondrial fission involves recruitment of a large GTPase, Drp1. Drp1 is a cytosolic protein which is recruited to mitochondrial membranes when they oligomerise and drives the constriction of the membrane.

Drp1 protein has four domains, a GTPase domain (G-domain), middle domain, variable domain and a GTPase effector domain (GED). Drp1 contains a bundle of signalling elements which connect to the GTPase domain allowing recruitment of Drp1 to the OMM, leading to its oligomerisation (Figure 1.10A) (Lee and Yoon, 2016; Tilokani et al., 2018). Mitochondrial fission proteins are regulated by post-translational modifications including phosphorylation, ubiquitination, sumolaytion and nitrosylation. Phosphorylation is an important way in which Drp1 activity is modulated. To date, three different phosphorylation sites have been identified, Ser616, which is phosphorylated by protein kinase C (PKC), Ser693, phosphorylated by glucose synthase kinase 3 beta (GSK3β), and Ser637, phosphorylated by protein kinase A (PKA) and AMP-activated protein kinase (AMPK) (van der Bliek et al., 2013; Chang and Blackstone, 2007, 2010; Li et al., 2015; Wang et al., 2012a). Phosphorylation of Ser616 activates mitochondrial fission as it promotes binding to other fission proteins, such as mitochondrial fission factor (Mff), fission 1 (Fis1), and two docking proteins mitochondrial dynamic proteins 49 and 51 (MiD49 and 51, respectively). Ser637 inhibits

mitochondrial fission by reducing GTPase activity. Both Ser637 and Ser616 are located at the end of the variable domain (Figure 1.10A) (van der Bliek et al., 2013; Chang and Blackstone, 2007, 2010; Wang et al., 2012a). Ser693 is phosphorylated by GSK3β inhibiting mitochondrial fission during apoptosis, this site is located on the GED domain where Drp1 oligomerisation and GTP hydrolysis occurs (Figure 1.10A) (Chou et al., 2012).

Drp1 interacts with several OMM proteins; Fis1 is anchored to the OMM, but it is more uniformly distributed along the mitochondrial tubules. When Fis1 interacts with Drp1 it changes the phosphorylation status of Drp1, it is thought that Fis1 acts under different physiological stress stimuli to increase mitochondrial fission (Sesaki et al., 2014; Wang et al., 2012b). Similarly, Mff is anchored to the OMM and forms punctate structures around mitochondria tubules, when Drp1 interacts with Mff, it results in an enhancement of GTPase activity of Drp1 (Sesaki et al., 2014). MiD49 and -51 are OMM proteins which can interact with both Drp1 and Mff, and serve primarily as adaptors to link together Drp1 and Mff forming a trimeric complex. Low levels of MiD's can increase Drp1 accumulation on mitochondria, however, it has been previously demonstrated that high levels of MiD 49 and -51 can sequester Drp1 in cells and cause elongation of mitochondria; maintaining the equilibrium between mitochondrial fission and fusion (Yu et al., 2017).

The first step of mitochondria fission happens in the matrix when replication of mtDNA triggers the recruitment of ER and initiates constriction by Drp1 (Figure 1.10B). Mff and MiD's recruit Drp1 and accumulate at the ER site, where it oligomerises into a ring like structure. GTP hydrolysis leads to a conformational

change which enhances mitochondrial constriction and cuts the mitochondria into two, leading to two daughter mitochondria (Figure 1.10B) (Tilokani et al., 2018).

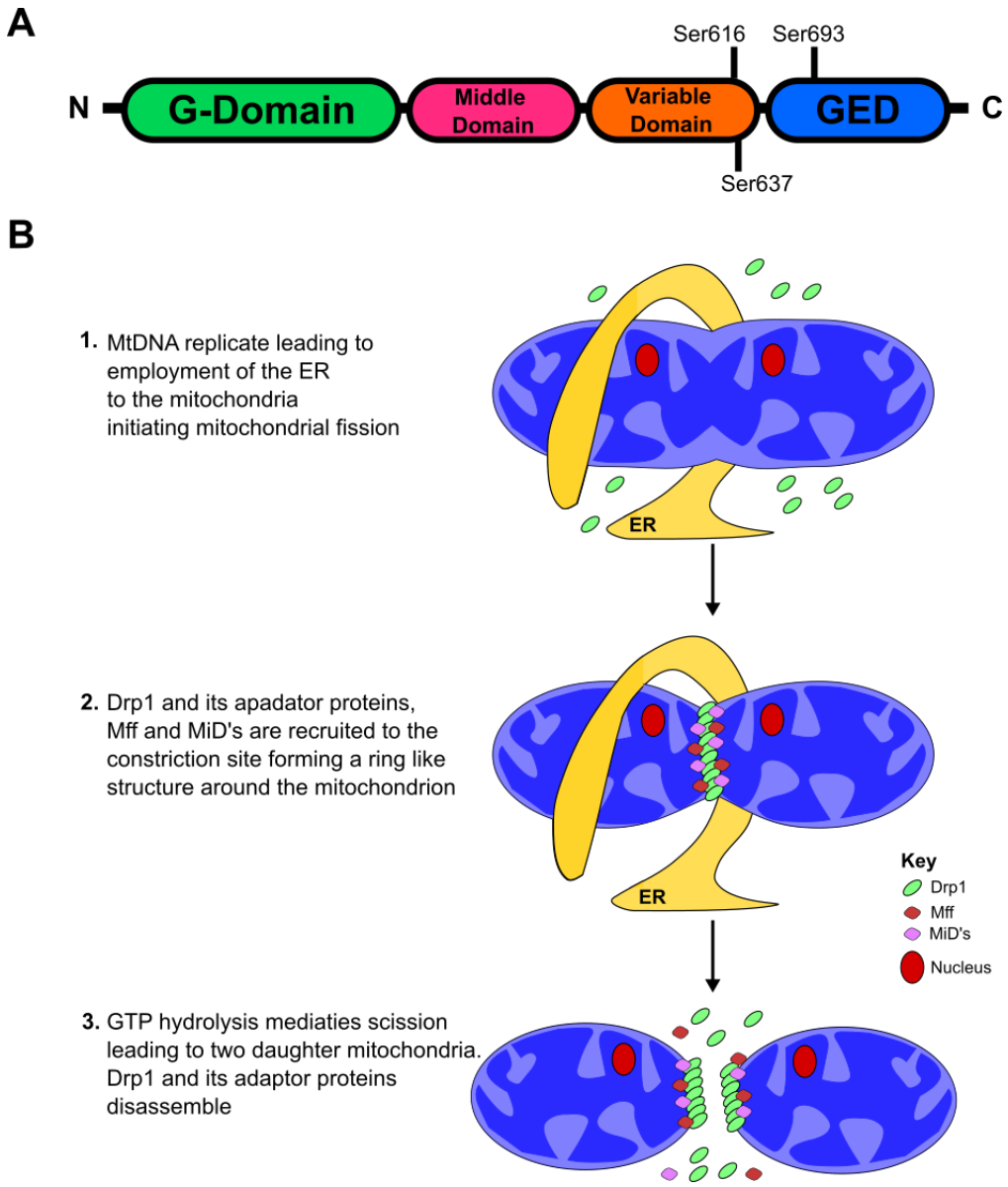

Figure 1.10 Mitochondrial fission

A: Structure of Drp1 encompassing a G-domain, a middle and variable domain and a GED domain. Serine 616 activates mitochondrial fission, where Serine 637 inhibits mitochondrial fission. Ser693 activates mitochondrial fission during apoptosis.

B: Schematic of mitochondrial fission. 1. Replication of MtDNA occurs in the mitochondrial matrix leading to the recruitment of the ER. 2. Drp1 recruits its adaptor proteins which accumulate at the ER leading to oligomerisation in a ring like structure around the mitochondrion to initiate constriction. 3. GTP hydrolysis leads to a conformational change leading to scission of the mitochondrion and Drp1 disassembly.

Abnormal mitochondrial fission leads to mitochondrial dysfunction resulting in ER stress and inflammation (Chang and Blackstone, 2010; Raza et al., 2015; Tilokani et al., 2018).

1.6 Mitochondrial dysfunction

The importance of mitochondrial functionality has been shown in many knockout models where knockout of any of the key genes involved in mitochondrial biogenesis results in embryonic lethality (Bertholet et al., 2016; Davies et al., 2007; Ishihara et al., 2009). There is a fine balance needed between mitochondrial fission and fusion to meet energy demands of cells, when this balance is skewed it results in mitochondrial dysfunction.

Mitochondrial dysfunction is an imbalance of mitophagy and mitochondrial biogenesis, resulting in mitochondrial stress, energy depletion and increased levels of ROS, ultimately leading to cell death (Palikaras et al., 2015). Dysfunctional mitochondria are targeted by vesicles called autophagosomes and are transported to lysosomes for degradation by mitophagy (Palikaras et al., 2015). During cell death and stress mitochondria tend to be less elongated which is associated with mitochondrial fission (Zemirli et al., 2018). Mitochondrial dysfunction increases phosphorylation of Mff increasing the recruitment of Drp1, resulting in mitochondrial fission and the degradation of damaged mitochondria (Toyama et al., 2016). Physiological changes have been associated with mitochondrial dysfunction including insulin resistance and ageing, which can lead to conditions such as Parkinson's disease and metabolic and cardiovascular diseases (Lee and Yoon, 2016; Tilokani et al., 2018; Zemirli et al., 2018).

1.6.1 Mitochondrial dysfunction induces insulin resistance

There is a lot of evidence that links mitochondrial dysfunction and insulin resistance, many studies have shown a decrease in mitochondrial function and an increase in ROS in models of insulin resistance (Filippi et al., 2017; Jheng et al., 2012; de Mello et al., 2018; Rovira-Llopis et al., 2017; Wang et al., 2015). Generation of excessive ROS induces oxidative damage to DNA, lipids and proteins, leading to insulin resistance. An increase in oxidative stress can directly interfere with insulin signalling pathways promoting insulin resistance (Anderson et al., 2009). Insulin has pivotal role in mitochondrial function, the regulation of mitochondria biogenesis and mitophagy. Systemic glucose production fuels the majority of the ATP that is generated in mitochondria via oxidative phosphorylation (Cheng et al., 2010). High circulating glucose levels can lead to mitochondrial dysfunction, as demonstrated by the finding that in T2DM patients present with decreased mitochondrial oxidative phosphorylation and lower mitochondrial content in skeletal muscle (Szendroedi et al., 2012). In caloric excess, a lipid overload activates mitochondrial fission, leading to mitochondrial uncoupling and ATP depletion, and ultimately mitochondrial dysfunction (Gao et al., 2014). The relationship between mitochondrial dysfunction and insulin resistance has been demonstrated in skeletal muscle, liver and the brain (Filippi et al., 2017; Jheng et al., 2012; Koves et al., 2008; Raza et al., 2015; Schneeberger et al., 2014; Yu et al., 2017).

1.6.1.1 Mitochondrial dysfunction in the brain

Diet-induced obesity in rats resulted in increased levels of ROS and mitochondrial dysfunction in the brain. In the hypothalamus, ROS levels can affect the regulation of neuronal function in POMC and AgRP/NYP neurones (Dietrich et

al., 2013; Ramírez et al., 2017). Mutant mice with deletion of MFN2 in POMC neurones exhibited hyperglycaemia, hyperinsulinemia and insulin resistance after 12 weeks of HFD-feeding, they were also hyperphagic and had reduced activity of BAT, leading to obesity (Schneeberger et al., 2013). In addition to this, mice with MFN2 knockout in POMC neurones had dysregulation of glucose homeostasis due to defective insulin secretion from the pancreas (Ramírez et al., 2017). Mitochondria in POMC neurones had a greater aspect ratio, the ratio between the centreline and width of the mitochondrion, in fed rats compared to fasted rats, along with decreased expression of Drp1. Inducible deletion of Drp1 in POMC neurones resulted in improved glucose responsiveness, increased mitochondrial size and decreased ROS production in RC-chow-fed mice (Santoro et al., 2017). POMC-Cre-specific inactivation of apoptosis inducing factor (AIF) in transgenic mice prevented the effects of a HFD by increasing the firing of POMC neurones rather than silencing them, this resulted in an increase in energy expenditure, improved glucose metabolism and insulin sensitivity (Timper et al., 2018).

Glucose-induced Drp1-dependent mitochondrial fission in the hypothalamus is an upstream regulator and key mechanism of glucose sensing in the brain, as evidenced in rats with a knockdown of Drp1, by delivering a small interfering RNA of Drp1, in the hypothalamus presented with a decrease in food intake and insulin secretion in response to glucose (Carneiro et al., 2012). Furthermore, high-fat, high-sugar fed rats, presented with an increase in Drp1-dependent mitochondrial fission and increased ROS in the hypothalamus, this resulted in alterations in glucose sensing and altered vagal activity, leading to T2DM (Desmoulins et al., 2019).

Whilst the relationship between insulin resistance and mitochondrial dysfunction in the MBH has been well researched, in the DVC this relationship has not been extensively examined. Using electron microscopy, a three-day HFD increased mitochondrial fission in the DVC, where mitochondria appeared smaller with fewer branches and were less elongated in rats. Chemical inhibition of mitochondrial fission via direct infusion of the Drp1 inhibitor, MDIVI-1, in the DVC of three-day HFD-fed rats reversed HFD-induced morphological changes in mitochondria (Filippi et al., 2017).

A three-day HFD abolished the glucoregulatory effect of DVC insulin-infusion, however co-infusion of insulin and MDIVI-1 during a pancreatic-euglycemic clamp restored ability of DVC insulin to regulate glucose (Filippi et al., 2017). These data demonstrate that a HFD can increase mitochondrial fission in the DVC inducing insulin resistance. In the DVC of HFD-fed rats there were lower phosphorylation levels of Ser637, resulting in an increase in the activation of Drp1. Three-day HFD-fed insulin resistant rats were protected from HFD-dependent DVC insulin resistance by molecular inhibition of Drp1 in the DVC (by expressing a catalytically inactive mutant of Drp1, Drp1-K38A). Furthermore, the expression of an active form of Drp1, using an adenovirus expressing a constitutively active form of Drp1, Drp1-S637A, in the DVC of RC-fed rats, was sufficient to induce insulin resistance, thus demonstrating that targeting Drp1 in the DVC can recapitulate the effects of a HFD on insulin sensitivity (Filippi et al., 2017).

1.6.2 The relationship between mitochondrial dysfunction and ER stress

Mitochondrial dysfunction and ER stress are critical components in the development of insulin resistance (Cunarro et al., 2018; Lim et al., 2009). ER stress and mitochondria are both major sources of ROS generation which promotes insulin resistance and inflammation (Boden, 2009). Mitochondria integrate metabolic signals, including, ATP levels, oxidative stress and ER stress to maintain key elements in insulin signalling (Lim et al., 2009; Morris et al., 2018b).

In the pancreas, activation of Drp1, by treating cells with a constitutively active form of Drp1, Drp1-S637A, promoted ER stress-induced β-cell apoptosis and resulted in an increase in ROS. Conversely, inhibition of Drp1 in β-cells under ER stress conditions prevented apoptosis and ROS in these tissues (Peng et al., 2011b; Wikstrom et al., 2013). MFN2 plays an important role in the response to ER stress. MFN2 knockdown in mice was shown to induce ER stress in the liver and in skeletal muscle (Filadi et al., 2018; Sebastián et al., 2012). In addition to this, under basal conditions silencing of the UPR arm, PERK in MFN2 ablated cells rescued this phenotype, suggesting that MFN2 is a modulator of PERK (Muñoz et al., 2013). Furthermore, liver ablation of MFN2 in mice resulted in glucose intolerance and impairment of insulin signalling in the liver and muscle. Furthermore, disruption of Opa1 in skeletal muscle induced ER stress and inflammation (Tezze et al., 2017).

Rats with deletion of MFN2 in POMC neurones had an increase in food intake and a decrease in energy expenditure leading to obesity (Schneeberger et al.,

2013). These mice also had significant alterations to mitochondrial-ER contact sites, changes in mitochondrial morphology, and enhanced ROS and ER stress. However, this phenotype was only seen in mice with an MFN2 knockdown not MFN1 (Schneeberger et al., 2013). HFD-induced Drp1-dependent mitochondrial fission in the DVC increases ER-stress, this effect was reversed with a chemical inhibitor of ER stress, 4-phenylbuty-rate. Furthermore, activation of Drp1 in RC-fed rats increased ER stress and resulted in insulin resistance, thus it can be argued that ER stress is a downstream effector of mitochondrial fission which subsequently leads to insulin resistance (Filippi et al., 2017). However, the mechanisms which link ER stress to insulin resistance in the DVC of the brain are currently unknown.

1.7 Inducible nitric oxide synthase

It is evident that mitochondrial dysfunction can induce ER stress, leading to insulin resistance, however, how mitochondrial dysfunction leads to ER stress is not fully understood; a possible mediator of this is inducible nitric oxide synthase (iNOS) (Bratic and Trifunovic, 2010; Förstermann and Sessa, 2012). Nitric oxide (NO) is the smallest messenger molecule and has many molecular targets. NO is ubiquitously expressed and controls regulatory functions such as neurotransmission and vascular tone, it can also regulate gene transcription and induces post-translational modifications of proteins (Evans and Goldfine, 2013; Pautz et al., 2010). NO is highly reactive and can be synthesised rapidly, meaning there are multiple regulatory sites for NO to be synthesised intracellularly (Evans and Goldfine, 2013; Pautz et al., 2010). NOS reacts with a superoxide anion to form the oxidant peroxynitrite ($OONO^{\cdot}$), a form of reactive nitrogen species (RNS), which results in oxidative damage and tyrosine nitration of proteins, lipids

and DNA. NO is generated by three different isoforms of the enzyme NO synthase (NOS), these are known as neuronal NOS (nNOS or NOS1), endothelial NOS (eNOS or NOS3) and iNOS (NOS2) (Förstermann and Sessa, 2012; Li and Förstermann, 2000).

NO is generated in by nNOS and eNOS through the interaction of calcium influx with calmodulin, a calcium binding protein (Ghasemi et al., 2018). nNOS is constitutively expressed in neurones in the central nervous system where it has numerous functions, including regulation of synaptic plasticity and central control of blood pressure (Figure 1.11) (Förstermann and Sessa, 2012). In the peripheral nervous system, NO produced by nNOS acts as a neurotransmitter, in addition, nNOS is also involved in learning and memory in the CNS (Förstermann and Sessa, 2012). On the other hand, NO produced from eNOS acts as a vasodilator and vasoprotector; NO prevents the release of platelet-aggregation and platelet-derived growth factors to prevent thrombosis and smooth muscle proliferation, respectively (Figure 1.11). In addition, eNOS-derived NO can inhibit DNA synthesis, mitogenesis, and can reduce influx of low density lipo-proteins to the vascular wall aiding in the prevention of atherogenesis (Förstermann and Sessa, 2012). Unlike, nNOS and eNOS, NO produced by iNOS is independent of calcium (Ghasemi et al., 2018). NO is produced by the enzymatic conversion of the guanidino nitrogen of L-arginine by iNOS (Pautz et al., 2010; Yun et al., 1997). iNOS-derived NO acts as a signalling molecule for synaptic transmission, it can cause changes in protein signalling and can be induced by many cells in response to inflammatory cytokines (Figure 1.11) (Pautz et al., 2010; Yun et al., 1997).

NO can act as neurotransmitter and is released by neurones, thereby having a direct effect on their electrical activity. It has also been hypothesised that NO can act as a retrograde messenger between pre- and post-synaptic terminals (Amitai, 2010; Nakamura et al., 2013). Principally, nNOS is the main isoform that produces NO, however there is growing evidence that iNOS is involved in modulating neural activity (Amitai, 2010; Ghasemi and Fatemi, 2014; Lee et al., 2018; Raza et al., 2015; Yu et al., 2019). Astrocytes are a group of major cell population in the central nervous system and express all three forms of NOS. Release of NO from astrocytes is upregulated by adaptive and immune responses, and by proinflammatory cytokines (Saha and Pahan, 2006). In aging, astrocytes exhibit an increase in mitochondrial oxidative metabolism and an increased response to inflammatory cytokines resulting in increased NO release (Jiang and Cadenas, 2014).

iNOS is largely involved in the pathophysiology of inflammation, after its induction, iNOS continuously produces NO until the enzyme is degraded. NO produced by iNOS can have many beneficial effects, including being microbicidal, antiviral and antiparasitic. However, abnormal levels of iNOS induction of NO can result in the development of many diseases, such as neurodegeneration, asthma, arthritis and diabetes (Evans and Goldfine, 2013; Förstermann and Sessa, 2012; Pautz et al., 2010; Yun et al., 1997).

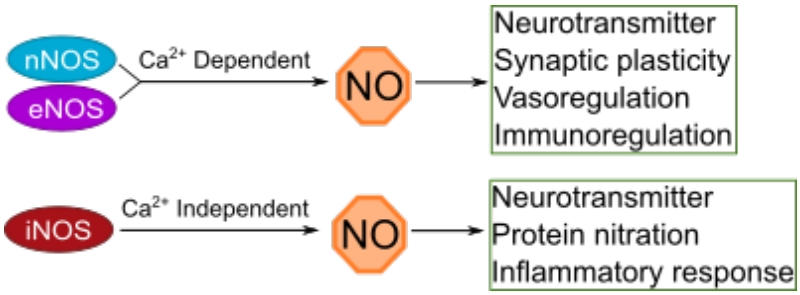

Figure 1.11 Summary function of the different isoforms of NOS

1.7.1 S-nitrosylation and tyrosine nitration

NO influences physiological status predominantly through post-translational modifications, including tyrosine nitration and s-nitrosylation (Figure 1.12) (Anavi and Tirosh, 2020; Förstermann and Sessa, 2012; Hess et al., 2005). S-nitrosylation occurs when a NO group covalently attaches onto a thiol group of a cysteine residue. This reversible post-translational modification influences protein activity, interaction and location, acting as a redox based signal. Several factors depend on protein s-nitrothiols such as hydrophobicity and net charge (Rizza et al., 2014). S-nitrosylation also occurs when there is excessive NO, causing nitrosative stress affecting cellular homeostasis and signalling pathways. Increased oxidative stress and dysregulation of NO production have been implicated in the pathogenesis of insulin resistance (Figure 1.12) (Förstermann and Sessa, 2012; Hess et al., 2005; Shahani and Sawa, 2012).

Tyrosine nitration is a chemical process in which a nitro group replaces a hydrogen group on the third carbon of a tyrosine (Rizza et al., 2014). Unlike s-nitrosylation, tyrosine nitration is an irreversible modification and is accountable for protein damage due an overproduction of NO. Excessive NO reacts with a superoxide anion to form a $OONO^{\cdot}$, inducing tyrosine nitration. Tyrosine nitration

will only occur under nitrosative stress and does not affect signalling, instead, it is a marker of damage (Figure 1.12) (Rizza et al., 2014). Increased levels of tyrosine nitration has been observed in the pathology of many diseases, including neurodegeneration, acute and chronic liver disease, diabetes and obesity (Abdelmegeed and Song, 2014; Bandookwala and Sengupta, 2020; Stadler, 2011).

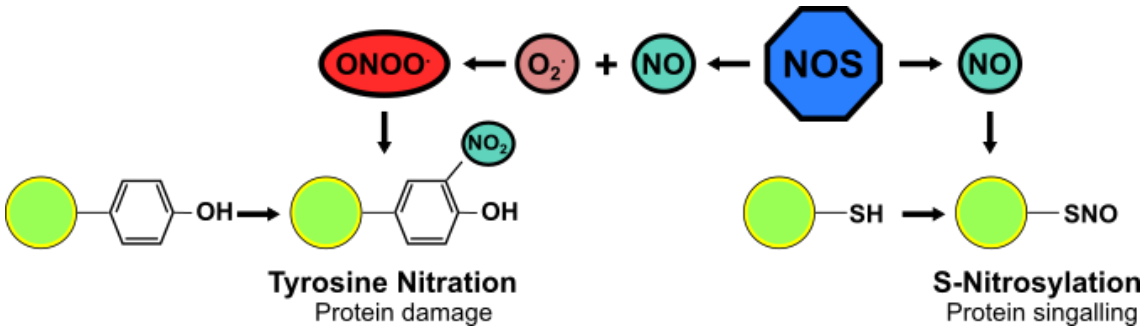

Figure 1.12 Schematic representing the chemical process of tyrosine nitration and s-nitrosylation.

An increase in NO reacts with a superoxide anion to form a peroxynitrite resulting in tyrosine nitration and protein damage. On the other hand, excessive NO leads to nitrosative stress resulting in s-nitrosylation leading to defects in protein signalling.

1.7.2 Nitrosylation and ER stress

Protein s-nitrosylation modulates cellular processes such as vasodilation, proliferation and apoptosis. The accumulation of misfolded proteins leads to activation of the UPR, an increase in NO can s-nitrosylate key stress transducers of the UPR, IRE-1α and PERK (Nakato et al., 2015). S-nitrosylation of IRE-1α inhibits ribosomal activity, which results in increased cell death during ER stress. Furthermore, s-nitrosylation of PERK leads to inhibition of eIF2α and results in an increase in cell death, demonstrating the role of s-nitrosylation of ER stress transducers in cell death (Nakato et al., 2015).

Increased levels of iNOS induce s-nitrosylation of IRE-1α and the insulin receptor, resulted in a decrease in splicing of XBP1 in the liver and insulin resistance in HFD-fed rats (Yang et al., 2015). In addition, obese mice with a nitrosylation-resistant IRE-1α variant in the liver presented improved metabolic effects on glucose homeostasis and hepatic insulin sensitivity (Yang et al., 2015a). In peripheral tissues, genetic inhibition of iNOS resulted in a marked decrease in ER stress in adipose tissue and liver of HFD-fed mice which led to improved insulin sensitivity (Zanotto et al., 2017).

1.7.3 Nitrosylation of key insulin signalling molecules induces insulin resistance

iNOS expression is upregulated by key molecules involved in the development of insulin resistance, such as pro-inflammatory cytokines, FFA, and in situations such as aging and obesity (Anavi and Tirosh, 2020; Förstermann and Sessa, 2012; Hess et al., 2005). In addition, nitrosylation is a key player in the development of ER stress, a process critical in the development of insulin resistance. This leads to the question of whether s-nitrosylation associated with ER stress induces insulin resistance. Induction of iNOS by proinflammatory cytokines is mediated by various signalling pathways, two of these pathways are the AKT/PI3K and the ERK1/2 pathway, which are also major signalling pathways activated by insulin (Anavi and Tirosh, 2020). Increased intracellular levels of NO, which results in nitrosative stress leads to the development of insulin resistance in the liver, skeletal muscle, adipose tissue and brain; this is partly due to s-nitrosylation of key components in the insulin signalling pathway (Carvalho-filho et al., 2005; Katashima et al., 2017; Perreault and Marette, 2001; Ropelle et al., 2013). HFD-feeding in rats resulted in increased levels of iNOS in skeletal muscle

which was associated with s-nitrosylation of IRS-1 and AKT, leading to insulin resistance. Furthermore, rats with a whole body knockdown of iNOS, fed a HFD did not exhibit s-nitrosylation of insulin signalling molecules showing that iNOS expression is essential for s-nitrosylation (Carvalho-filho et al., 2005; Carvalho-Filho et al., 2009). Similarly, in obese diabetic mice, there was increase in iNOS levels and nitrosative stress in livers, a chemical inhibitor of iNOS, L-NIL, decreased iNOS levels, and reversed hyperglycaemia, with significant increases in the expression levels of IRS-1 and -2 (Fujimoto et al., 2005).

Disruption of the PI3K pathway led to skeletal muscle insulin resistance in HFD-fed mice which was not seen in HFD-fed mice with a knockdown of iNOS, these mice were also prevented from developing diet-induced obesity (Perreault and Marette, 2001). iNOS-induced tyrosine nitration of IRS-1 in skeletal muscle resulted in insulin resistance and an increase in peroxynitrite, whereas inhibition of iNOS restored insulin sensitivity (Pilon et al., 2010). Peroxynitrite treatment in skeletal muscle cells altered PI3K activity and glucose uptake, while exposure to lipopolysaccharide (LPS) in skeletal muscles cells expressing the ShRNA for the iNOS protein prevented insulin resistance (Pilon et al., 2010). Furthermore, in aging mice, there were significantly higher levels of iNOS expression and s-nitrosylation of major insulin signalling proteins. Aged mice with a knockout of iNOS were protected from s-nitrosylation and increased NOS levels, highlighting that insulin resistance is mediated partly through s-nitrosylation of the insulin signalling pathway (Ropelle et al., 2013).

A hyperinsulinemic-euglycemic clamp demonstrated that infusion of lipids into the carotid artery in wild type mice for six hours led to elevated HGP and insulin resistance, in the liver (Charbonneau and Marette, 2010). In addition, these mice

exhibited high levels of iNOS which was associated with tyrosine nitrosylation of the insulin receptor and IRS-1 and -2, and decreased activation of AKT; mice with a knockout of iNOS were protected from six hour lipid-induced effects on insulin sensing (Charbonneau and Marette, 2010). S-nitroglutathione reductase (GSNOR) plays an important role in reversing protein s-nitrosylation, where dysfunction of GSNOR activity was seen in the liver of mice fed a HFD (Qian et al., 2018; Yang et al., 2015a). Hepatic deletion of GSNOR led to a significant decrease in hepatic insulin function, phosphorylation of the β-subunit of the insulin receptor and AKT was decreased, and there was also an associated increase in lipid accumulation (Qian et al., 2018). Overexpression of GSNOR in obese mice restored insulin sensitivity and improved glucose homeostasis. In addition, GSNOR levels were decreased in livers of human with T2DM or obesity, demonstrating that obesity impairs GSNOR leading to a decrease in protein denitrosylation capacity in the liver (Qian et al., 2018).

Mice overexpressing iNOS in the liver were hyperglycaemic, hyperinsulinemic and insulin resistant when compared to wild type mice. In addition, AKT and IRS-1 were s-nitrosylated, resulting in decreased activation of these signalling molecules in the liver (Shinozaki et al., 2011). HFD-fed obese mice displayed an increase in iNOS activation in ARC macrophages; inhibition of iNOS in macrophages in the hypothalamus decreased macrophage accumulation and improved glucose metabolism and insulin sensing (Lee et al., 2018). Furthermore, mice fed a HFD had elevated blood pressure and resistance to insulin's actions on blood glucose, these mice also had elevated levels of ROS and iNOS. The glucoregulatory effects of insulin were restored in mice with a homozygous knockdown of iNOS fed a HFD. However these mice still developed

high blood pressure, highlighting that iNOS is an important target in glucose regulation and insulin sensitivity but not on blood pressure (Noronha et al., 2005).

Rats given an ICV injection of S-nitroglutathione (GSNO), a NO donor, into the hypothalamus caused development of insulin resistance and increased food intake and body weight (Katashima et al., 2017). Furthermore, HFD-feeding induced s-nitrosylation of hypothalamic AKT and the insulin receptor, while chemical of inhibition of iNOS or inhibition of s-nitrosylation prevented from the development of hypothalamic insulin resistance and decrease body weight (Katashima et al., 2017). These data highlight the importance of s-nitrosylation and iNOS in the development of insulin resistance in the brain.

1.7.4 Dynamin-related protein 1 is modulated by nitrosylation

It is apparent that nitrosative stress plays an important role in the development of insulin resistance and neurodegenerative diseases. An increase in nitrosative stress can result in aberrant s-nitrosylation of Drp1, leading to increased enzymatic activity and resulting in higher mitochondrial fragmentation (Cho et al., 2009; Lee and Kim, 2018). In addition, decreasing GSNOR in mouse neuronal primary cells resulted in s-nitrosylation of Drp1 and Parkin, leading to an increase in nitrosative stress and mitophagy (Rizza et al., 2018). Higher levels of peroxynitrite activated the PINK1/Parkin pathway triggering tyrosine nitration of Drp1 and leading to mitophagy in stroke models. It is therefore evident that both s-nitrosylation and tyrosine nitration are both important post-translational modifications which can alter mitochondrial dynamics (Feng et al., 2018).

Mitochondrial fission regulates ROS in activated microglial cells, for example, LPS-induced mitochondrial fission caused a dephosphorylation of Ser637 in Drp1

resulting in an increase in the activation of Drp1. In addition mRNA levels of iNOS were decreased in BV2 microglial cells treated with LPS in the presence of an inhibitor of Drp1, MDIVI-1 (Park et al., 2013). Inhibition of iNOS in hippocampal neurones decreased activated Drp1 resulting in elongation of mitochondria and a decrease in neuronal necrosis (Lee and Kim, 2018). In addition to this, activation of mitochondrial fission in PC12 cells increased ER stress. A three-day HFD increased iNOS levels in the DVC of the brain, this effect was negated with an injection MDIVI-1. Furthermore, molecular activation of Drp1 in the DVC increased levels of iNOS compared to GFP control, demonstrating that activation of Drp1-dependent mitochondrial fission can increase iNOS expression in the DVC (Filippi et al., 2017). Together, these data illustrate a clear relationship between iNOS levels and mitochondria fission and provide a basis for further investigation into the effect mitochondrial dynamics on iNOS in the brain.

1.8 Aims and Objectives

Obesity and T2DM are becoming epidemics. In the UK, obesity affects around 27% of the adult population and accounts for around 44% of type II diabetes cases (Zakeri and Batterham, 2018). Being obese or having type II diabetes can increase your risk for many other ailments such as cardiovascular disease, cancer and Alzheimer's disease (Ferreira et al., 2018; Han and Boyko, 2018). Thus, there is a greater need than ever to explore alternative therapeutic avenues for the treatment of obesity and type II diabetes.

Overnutrition leads to an increase in circulating levels of glucose, FFA and pro-inflammatory cytokines which ultimately leads to insulin resistance. An increase in such circulating levels can induce ER stress and mitochondrial stress, which occurs in both the peripheral tissue and in the CNS (Hotamisligil et al., 1996;

Tanti et al., 2013; Wilcox, 2005). The CNS is extremely important in the regulation of glucose metabolism and food intake, it receives signals from the periphery to maintain energy balance (Brüning, 2006; Filippi et al., 2012b; Obici et al., 2002b; Pocai et al., 2005). Alterations in this cross talk between the CNS and the periphery can lead to metabolic disorders, such as insulin resistance.

It has previously been demonstrated that the DVC is an important region of the brain that regulates glucose metabolism and food intake (Filippi et al., 2012b). The NTS of the DVC senses insulin and triggers a cascade of neural events to decrease HGP and food intake, though the neural populations involved have not yet been determined (Filippi et al., 2012b). Furthermore, a three-day HFD was shown to induce insulin resistance and Drp1-dependent mitochondrial fission in the DVC (Filippi et al., 2017). In addition to this, injection of a molecular and chemical inhibitor of Drp1 into the DVC restored insulin resistance and glucose homeostasis in HFD-fed rats, while an injection of a molecular activator of Drp1 into the DVC induced insulin resistance in RC-fed rats (Filippi et al., 2017). It is therefore evident that Drp1 has an important effect on insulin and glucose metabolism, however the effect on feeding behaviours and body weight is yet to be elucidated.

HFD-fed rats had an activation of Drp1 and increased levels in ER stress and iNOS in the DVC (Filippi et al., 2017). It has been previously demonstrated that iNOS can induce s-nitrosylation of key signalling molecules in the insulin signalling pathway (Yang et al., 2015b; Yasukawa et al., 2005). Therefore, it could be hypothesised that an increase in NO by iNOS expression results in an increase in s-nitrosylation that links mitochondrial fission, ER stress and insulin resistance in the DVC. Much of the work investigating Drp1-dependent

mitochondrial fission has looked into ways to prevent HFD-dependent insulin resistance (Filippi et al., 2017), however, whether inhibition of Drp1 in the DVC can restore the hypophagic effect of insulin and affect body weight in a diet-induced obese model is yet to be studied.

With this in mind, it has led to my main aims for this project (Figure 1.13):

1. Investigate the effects of mitochondrial dynamics on feeding behaviours, body weight gain and the hypophagic effect of insulin
2. Discover the molecular mechanism that are implicated with insulin resistance in the DVC and how it affects feeding behaviours and body weight
3. Assess which different cell type/s in the DVC that are involved in the hypophagic effect of insulin
4. Determine whether a DVC-specific targeted approach to restore the hypophagic effect of insulin is sufficient to ameliorate the metabolic status of a diet-induced obese model

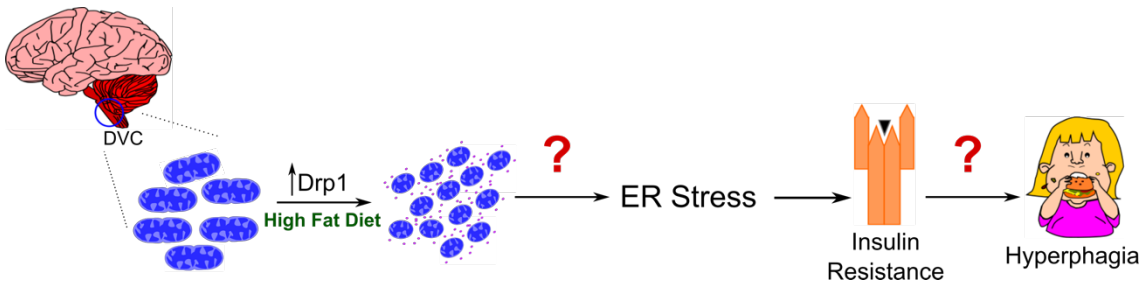

Figure 1.13 Working hypothesis

Can an increase in HFD-dependent Drp1 activation lead to hyperphagia, and what are the molecular players involved in this pathway?

2 General Methods

2.1 Materials

2.1.1 Buffers

Tris-buffered saline (TBS)

50 mM Tris base (MP Biomedical TRIS01KG), 150 mM sodium chloride (Fisher S/3160/63), pH 7.6

Tris-buffered saline

Tween50 mM Tris base, 150 mM sodium chloride, 0.1% Tween 20 (VWR Chemicals 6663684B) pH 7.6

Resolving buffer

1.5 M Tris base, pH 8.6

Stacking buffer

2 M Tris base, pH 6.8

Tris-glycine sodium dodecyl sulphate (SDS) electrophoresis buffer

25 mM Tris base, 192 mM glycine (Sigma G8790), 0.1% (w/v) SDS (Sigma 05030)

Tris-glycine transfer buffer

48 mM Tris base, 39 mM glycine, 20% methanol (Honeywell 179337)

5X Sample buffer

250mM Tris-hydrochloric acid (HCl), pH 6.8, 5% SDS, 50% glycerol (VWR 356350), 0.1% bromophenol blue (Alfa Aesar A18469), 20% 2-mercaptoethanol (Sigma M6250)

Lysis buffer

50 mM Tris-HCl pH 7.5, 1 mM ethylene glycol-bis(beta-aminoethyl ether)-N,N,N',N'-tetraacetic acid tetrasodium salt (EGTA) (Fisher Scientific 428570500), 1 mM ethylenediaminetetraacetic acid (EDTA) (Sigma EDS), 1% (w/v) octyl phenoxypolethoxylethanol 40 (NP-40) (Biobasics LA60), 1 mM sodium orthovanadate (Sigma S6508), 50 mM sodium fluoride (Sigma PHR1408), 5 mM sodium pyrophosphate (Sigma 71501), 0.27 M sucrose (Sigma S7903), 1 mM dithiothreitol (DTT) (ThermoFisher Scientific R0861), Pierce protease inhibitor tablets (ThermoScientific 88266)

Hens Buffer

100mM HEPES, pH 7.8,1mM EDTA, 0.1mM Neocuprione, 1% SDS (ThermoScientific 90106)

Elution Buffer

ThermoScientific 90104 (TMT Elution Buffer)

Wash Buffer

Cell BioLabs Inc. 90002 (Adenovirus purification kit)

Elution Buffer

50mM Tris, pH 7.5, 5 mM magnesium chloride, 2 M sodium chloride. Cell BioLabs Inc. 90003 (Adenovirus purification kit)

Phosphate buffered saline (PBS)

137 mM sodium chloride, 2.7 mM potassium chloride, 10 mM disodium phosphate, 1.8 mM monopotassium phosphate (Hyclone SH30256)

Phosphate buffered saline triton (PBST)

137 mM sodium chloride, 2.7 mM potassium chloride, 10 mM disodium phosphate, 1.8 mM monopotassium phosphate, 0.3% or 0.1% triton (Sigma X100)

Phosphate Buffer (PB)

0.1M PB in double distilled water

4% Paraformaldehyde (4% PFA)

25% 0.1M PB, 50% 8% paraformaldehyde

30% Sucrose

Sucrose in distilled water

Cryoprotectant

0.1 M PB, 30% EGTA (Flourochem 045172), 1% Polyvinyl-pyrrolidine (PVP-40), 30% sucrose

2.1.2 Antibodies

Table 2.1 Primary antibodies

Antibody	Application	Dilution	Species	Catalogue Number
Anti-β-Actin	Western Blotting	1: 50,000	Mouse	Cell Signalling Technology 3700
Anti-Flag	Immunohistochemistry (IHC)	1:500	Rabbit	Sigma F7425
Anti-Flag M2	Western Blotting	1:3000	Mouse	Sigma F1804
Anti-Glial Fibrillary Acidic Protein (GFAP)	IHC	1:1000	Rabbit	AbCam ab7260
Anti-Green Fluorescent Protein (GFP)	Western Blotting	1: 20,000	Mouse	Aviva System Biology OAE00007
Anti-Hexon	AdenoTitre Assay	1:1000 (PBS)	Rabbit	Cell Biolabs VPK-109
Anti-Huc/D	IHC	1:1000	Rabbit	ProteinTech 55047-1-AP

Anti-Iba1	IHC	1:1000	Rabbit	Wako 019-19741
Anti-iNOS	Western Blotting	1:50 (2% milk/ TBST)	Rabbit	AbCam ab15323
Anti-iNOS	IHC	1:250	Rabbit	AbCam ab3523
Anti-Neuronal Nuclei (NeuN)	IHC	1:2000	Guinea Pig	MERCK Millipore ABN90
Anti-Phosphorylated - Double Stranded RNA Activated Protein Kinase-like ER Kinase (PERK)	IHC	1:250 (0.3% PBST)	Rabbit	Biobryt obr128012
Anti-Phosphorylated-PERK	Western Blotting	1:500	Rabbit	Cell Signalling Technology 3179
Anti-Tandem Mass Tag (TMT)	Western Blotting	1:000	Mouse	Invitrogen 90075

Anti-Total PERK	Western Blotting	1:1000	Rabbit	Cell Signalling Technology 3192

All primary antibodies for western blotting were made up in 5% bovine serum albumin (BSA) (Sigma A7906), unless stated otherwise in the table. IHC primary antibodies made up in 0.1% TBST unless stated otherwise in the table.

Table 2.2 Secondary antibodies

Secondary Antibody	Application	Dilution	Catalogue Number
Donkey anti-mouse IgG Alexa Fluor 555	IHC	1:1000	Invitrogen A-31570
Donkey anti-rabbit IgG Alexa Fluor 555	IHC	1:1000	Invitrogen A-13572
Donkey anti-mouse IgG Alexa Fluor 488	IHC	1:1000	Invitrogen A-21202
Donkey anti-rabbit IgG Alexa Fluor 488	IHC	1:1000	Invitrogen A-21206
Donkey anti-sheep IgG Alexa Fluor 488	IHC	1:1000	Invitrogen A-11015
Donkey anti-rabbit IgG Biotin	IHC	1:200	Invitrogen A-16039

Donkey anti-mouse IgG Biotin	IHC	1:200	Invitrogen A-16021
Donkey anti-guinea pig IgG Biotin	IHC	1:200	Invitrogen A18773
Streptavidin Alexa Fluor 555	IHC	1:1000	Invitrogen S-532355
Streptavidin Alexa Fluor 448	IHC	1:1000	Invitrogen S-532354
Donkey anti-rabbit IgG HRP conjugate	Western Blotting	1:5000	Novex A16029
Donkey anti-mouse IgG HRP conjugate	Western Blotting	1:5000	Novex A16011

All antibodies for IHC were made up in PBS. Secondary antibodies for IHC were made up in 5% skimmed milk in TBST.

2.2 Cell Culture

2.2.1 HEK293AD cells

The HEK293 cell line is from primary embryonic human kidney transformed with a human adenovirus type 5 DNA. The cell line 293AD is derived from the parental line HEK293 but specifically selected for adenoviral applications (Cell Biolab Inc., AD-100). Cells were grown in a 37°C, 5% CO_2 incubator and kept in Dulbecco's modified eagle medium (DMEM) high glucose (Lonza 12-604F), 10% fetal bovine serum (Gibco 2024-01), 0.1mM minimum essential medium (MEM) non-essential amino acids (NEAA) (Gibco 11140-035), 1% Penicillin Streptavidin (Sigma P0781), known as complete media. Cells were kept at 37°C, 5% carbon dioxide (CO2). Cells were detached using 0.05% trypsin-EDTA (Gibco 25300-054) and

frozen in 10% dimethyl sulfoxide (DMSO) (G Bioscience BKC-17) in complete media.

2.2.2 PC12 Cells

PC12 cells are derived from a transplantable rat pheochromocytoma (AddexBio, C0032002). Cells were grown in F-12K medium (Gibco 21127-022) with 2.5% FBS, 15% horse serum (Gibco 1011-07) and 1% Penicillin Streptavidin, also known as complete medium and kept at 37°C, 5% CO2. Cells were detached using 0.05% trypsin-EDTA and frozen in 10% DMSO in complete media.

2.3 Viral Amplification and Purification

In order to increase mitochondrial fission in the DVC of the brain, an adenoviral system was used to deliver a CMV promotor expressing a FLAG-tagged constitutively active form of Drp1 in the residue of S637 to A (S637A). This mimics Drp1's non-phosphorylated state, inducing an over-expression of Drp1 and causes an increase in mitochondrial fission in the DVC. A CMV promotor expressing a FLAG-tagged dominant negative form of Drp1, mutated in the residue of K38 to A (K38A), resulting in a defective GTP binding site, resulting in inhibition of Drp1-dependent mitochondrial fission. As control, a CMV promoter expressing green protein florescent (GFP) virus was utilised (Table 2.3) (Filippi et al., 2017). A lentiviral system was used to deliver a ShRNA of the iNOS protein (ShiNOS), 3-target specific ShRNA to knockdown gene expression or a control scramble ShRNA (ShControl) (Santa Cruz Biotechnology, sc-29417-V and sc-108080 respectively) was used to decrease iNOS expression in the DVC (Table 2.3). To inhibit Drp1 specifically in astrocytes of the DVC, Dr Joanne Griffiths in the Filippi lab created an adenoviral system under the GFAP promotor to express

a FLAG-tagged dominant negative form of Drp1, mutated in the residue of K38 to A (K38A), Drp1-K38A::GFAP or to express GFP as a control, GFP::GFAP (Table 2.3).

HEK293AD cells were used to amplify the adenoviruses, Drp1-S637A, Drp1-K38A and GFP. Cells were infected at an 80% confluency, at a multiplicity of infection (MOI) of 5 for Drp1-S637A, Drp1-K38A and GFP and were left for up to 48 hours. When small cell plaques formed in the dishes cells and media were collected and spun down at 2000 rotation per minute (RPM) for 5 minutes, the pellets were resuspended in a small amount of media collected from the viral infected plates. Pellets were subjected to 3 cycles of freezing on dry ice and thawing at 37°C, and then spun down at 3000 RPM for 15 minutes, to release the virus. The supernatant, viral stock, was collected and cell debris was discarded. To determine the concentration of the viral amplification, a viral titration was performed using a 3,3'-Diaminobenzidine (DAB) assay (Cell Biolab Inc., VPK-109). HEK293AD cells were plated on a 24-well plate, 8 hours later cells were infected with varying concentrations of both media and virus stock, the plate was then left for 48 hours 37°C.

After 48 hours, cells were fixed with methanol and left at -20°C for 20 minutes, excess methanol was washed 3 times with PBS. Wells were blocked with 1% BSA in PBS for 1-hour and anti-Hexon primary antibody was made up in PBS and left for 1 hour at RT on an orbital shaker. After one-hour wells were washed 3 times with PBS, followed by a secondary antibody of horseradish peroxidase (HRP) (Cell Biolabs 10902) made up in PBS, wells were washed 5 times with PBS. A 1X DAB working solution was made to detect immunostaining of infected cells. Positive stained cells were counted at 10X magnification, 4 random areas

of each well were counted and averaged to determine the plaque forming unit (PFU) of each virus preparation.

ViraBind adenovirus purification kit (Cell Biolab Inc., VPK-100) was used to purify the viruses. The collected supernatants were filtered with a 0.45 μm sterile filter to clarify the virus. Wash buffer was added to the purification filter to pre-rinse the filter. To ensure that there was maximum recovery of each virus, the viral supernatants were passed through the purification filter by gravity flow. Once the viruses had been passed through the purification filter, the liquid collected, known as the flow-through, was passed back though the same purification filter and aliquoted for use in infections. The purification filter was washed 3 times with 1X wash buffer using gravity flow. Elution buffer passed through the purification filter by gravity flow and pure virus was collected, aliquoted and stored at -80°C for viral injection. Another viral titration was performed to determine final viral concentration of flow through and elution.

Table 2.3 Table of viral preps

Name of virus	Type of Virus	Action
GFP	Adenovirus	GFP under the CMV promotor (control)
Drp1-S637A	Adenovirus	Constitutively active form of Drp1 under the CMV promoter
Drp1-K38A	Adenovirus	Dominant negative form of Drp1 under the CMV promotor
ShiNOS	Lentivirus	Knocking down iNOS
ShControl	Lentivirus	A control used for ShiNOS experiments
GFAP::Drp1-K38A	Adenovirus	Dominant negative form of Drp1 under the GFAP promotor
GFAP::GFP	Adenovirus	GFP under the GFAP promotor (control)

2.4 Rat Preparation

All experiments were carried out under the UK animals (Scientific Procedures) Act 1986 and in line with the ethical standards set out by the University of Leeds Ethical Review Committee. Every effort was made to minimise number of rats and their suffering after surgical procedures including administration of analgesics, recovering on a warm plate and observations before placing back into cage holder. Rats were singly housed and given ad libitum access to food and water, with 12-hour light-dark cycle (06:30-18:30). Nine-week-old male Sprague Dawley (SD) rats weighing between 270-300 g (Charles River Laboratories) were used for experiments.

Rats were fed on one of three different diets. Diet 1 was a regular chow (RC), from BioSystems Cooperation BEEKAY rat and mouse (BK001), total calories of 3.91 kcal/g and comprised of 4.73% fat, 8.68% protein, 3.48% fibre, 5.38% ash and 58.73% carbohydrates. Diet 2 was a control RC from Datesand Group (F4031) the composition of this RC had a total calorie content of 3.93 kcal/g, which, 7.2% was fat, 20.5% protein, 3.5% ash and 61.6% carbohydrate. Diet 3 was a high fat diet (HFD), Datesand Group (F3282), differs from the control RC, with 36% being fat, 20.5% protein, 3.5% ash, 36.2% carbohydrate and total calories of 5.51 kcal/g.

2.4.1 Surgery

Rats were anesthetised by intraperitoneal injection of ketamine (60 mg/kg) (Ketamidor) and xylazine (8 mg/kg) (Rompun). Rats were placed in a stereotactic frame (75-1086, Elevated U-frame Stereotaxic Instrument, Harvard Apparatus) where each rat was implanted with a 26-gauge bilateral catheter (PlasticsOne C235G-0.8-SPC) targeting the nucleus of the solitary tract (NTS) within the DVC, and an internal dummy was inserted to prevent backflow of injections in future experiments (PlasticsOne C235DC-SPC). Measurements of the bregma and lambda were used to ensure the skull was levelled, from the lambda the measurement of occipital suture was taken (Figure 2.1A). The bilateral cannula was implanted at 0.0 mm on the occipital suture, 0.4 mm lateral to the midline and 7.9 mm below the skull surface (Filippi et al., 2014), targeting the NTS in the DVC (Figure 2.1B). The cannula was glued with Loctite® 454 kept in place with Unifast TRAD cement and liquid (0990607 and 4160803 respectively). Rats were given saline (Hypaclens 202/09) and meloxicam (5 mg/ml) (Metacam), an

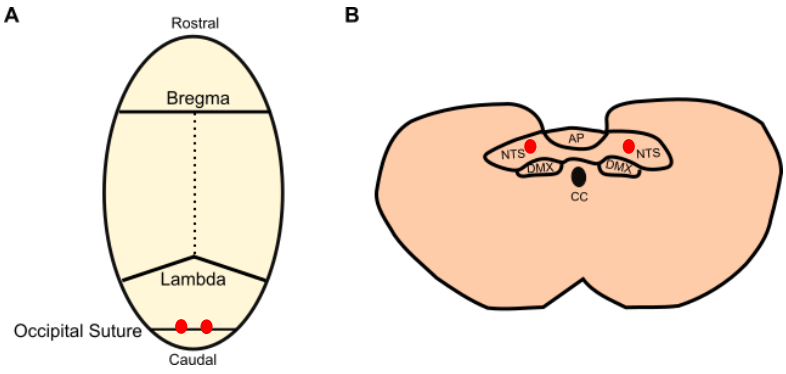

Figure 2.1 Anatomical landmarks used in stereotactic surgery targeting the DVC

A: Highlighting the landmarks used to target the NTS in the DVC in stereotactic brain surgery. Measurements of the Bregma and Lambda are taken before measuring the value of the occipital suture

B: Schematic of a coronal section of the brainstem, highlighting main areas of the DVC, including the NTS, area postrema (AP), dorsal motor nucleus (DMX) and central canal (CC) Red dots mark position of canula

analgesic, as post-operative care. To confirm surgeries were in the correct place, during sacrifice, 2 μl of bromophenol blue was infused into each side of the canula.

2.4.2 Viral Injections

To inject viruses, lines of fine bore polythene tubing (0.58mm inner diameter) were cut and a bilateral internal canula inserted on the end (PlasticsOne C2351-SPC). These lines with the internal canula inserted were attached to 50 μl Hamilton's (80401) and flushed with double distilled water (ddH2O) to ensure no bubbles were in the lines. Syringes were pushed to 5 μl and pulled back to 10 μl to create a small bubble, preventing dilution of the virus. The virus was loaded from the front and syringes were pushed to create a small drop. The internal canula was then inserted into the external canula on the head of rats and slowly 2.5 μl of virus on each side was injected into the NTS. The animal was left with the lines with the internal canula attached to its head for 5 minutes to prevent any backflow of the virus and ensure proper delivery. Rats were then carefully monitored for 10 minutes to make sure there were no adverse reactions.

2.5 Feeding Studies

2.5.1 Chronic Feeding Studies

Rats underwent stereotactic brain surgery on day 0, and viral injections were given on day 0, directly after the surgery for ShiNOS and ShControl rats and on day 1 for the Drp1-S637A, Drp1-K38A and GFP (Figure 2.2). Food intake and body weight were measured at similar times each day to keep consistency in measurements. Rats expressing the activator of Drp1 or GFP expressing control,

were referred to as cohort 1, these rats received Diet 1, a regular chow. Rats expressing either the dominant negative form of Drp1, Drp1-K38A, or the knockdown of iNOS, ShiNOS, were given Diet 2, a regular chow until day 3 and diets were changed to Diet 3, a HFD until the end of the study (Figure 2.2B).

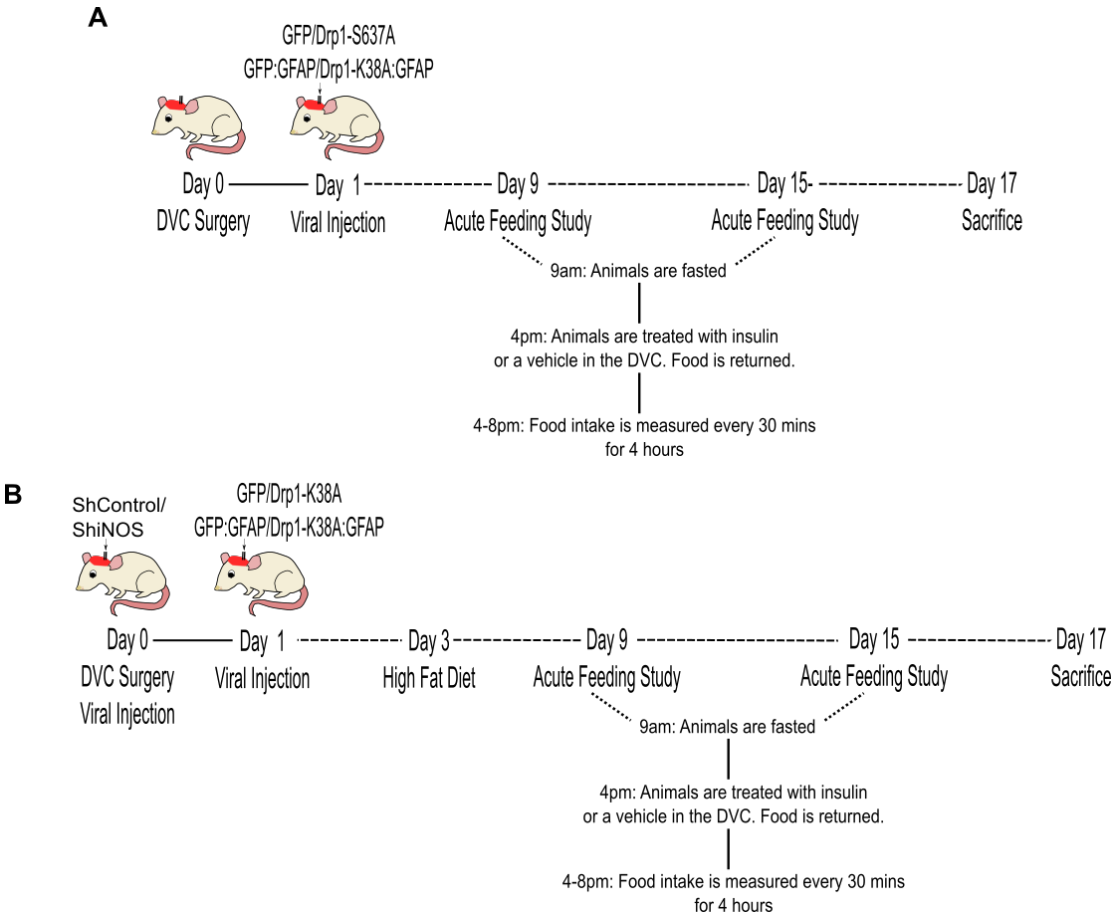

Figure 2.2 Experimental designs including feeding study in rats expressing Drp1-S637A, Drp1-K38A, ShiNOS and Drp1-K38A::GFAP

A: Experimental designs for rats injected with Drp1-S637A and Drp1-K38A::GFAP fed a RC diet

B: Experimental designs for rats either injected with Drp1-K38A, ShiNOS and Drp1-K38A::GFAP fed a HFD

2.5.2 Acute Feeding Studies

These same rats were subjected to an acute feeding study where insulin was infused bilaterally into the DVC. On day nine and day 14 an acute feeding study

was carried out. At 10am body weight and food intake were measured, rats were then fasted with access to water (Figure 2.2). At 4pm rats were bilaterally infused with 2mU/μl insulin (Sigma I-5523) or a vehicle into the DVC, a total of 0.2 μl was infused over 5 minutes (0.04 μl/minute). Food was returned after infusion, and food intake was monitored every half an hour for 4 hours and then again at 12, 24, 36 hours. Body weight was measured, pre-infusion, at 4pm, then again at 12, 24 and 36 hours.

In some instances the cap containing the bilateral cannula was lost before feeding studies, these rats were used as a vehicle control for the acute feeding study. The rats were handled similarly to as if the rats were to get an infusion, to induce mild stress. To ensure this did not skew that data presented, the graph below highlights that that there was no difference in food intake in rats which received the vehicle injection compared to the rat who lost their caps (Figure 2.3).

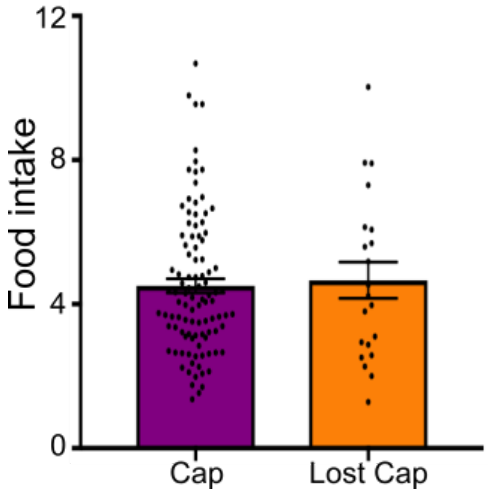

Figure 2.3 Comparing average food intake of rats who had their caps and rats who had lost their caps prior to the feeding studies

All data are expressed as mean ± SEM *n*=101 rats with cap *n*=21 with rats with no cap.
Statistical test: unpaired T-test

2.5.3 Obese Model

Six-week-old male SD rats weighing between 170-190 g were used. From day 0 these rats were subjected to Diet 3, HFD or Diet 2, RC for 28 days (Figure 2.4). On day 28 rats were implanted with a bilateral catheter targeting the NTS within the DVC (see section 2.4.1). The first cohort used for these experiments were injected with the lentivirus expressing the ShRNA for iNOS in order to knockdown of iNOS, ShiNOS or its control, ShControl. Viral injection was administered on day 28 and the acute feeding studies took place on day 37 and 41 (see section 2.5.2). The second cohort we used were injected with an adenovirus either expressing an inactive form of Drp1, Drp1-K38A or GFP expressing control, on day 29, and acute feeding studies were carried out on day 38 and 42 (see section 2.5.2). Rats were sacrificed on day 43 and the DVC and epididymal, retroperitoneal, visceral white adipose tissue and brown adipose tissue were weighed and small volumes were taken.

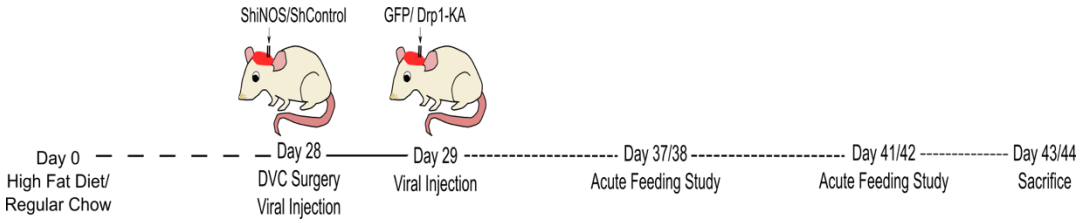

Figure 2.4 Obese model protocol

2.6 Western Blotting

2.6.1 Sample Preparation

In order to determine protein expression and phosphorylation of either tissues or cell lysates, western blotting techniques were used. Pre-frozen eppendorfs were used to weigh tissues, keeping the tissues on dry ice where possible. Samples

were lysed using lysis buffer (see section 2.1.1), the volume of lysis buffer used was determined by the weight of the tissue and multiplied by 7.5, this was the volume in microliters required. Tissues were lysed using a Pellet Pestle Mortar (Kimble 749540-000) on ice until the tissue had completely broken down. Samples were centrifuged at 12,000 RPM for 15 minutes at 4°C, the supernatant collected in eppendorfs and the pellet discarded. A Pierce 660nm Protein Assay (Thermo 22660) was performed to determine protein concentration and samples were made up to at least 2 μg/μl and sample buffer was added. Samples were boiled at 90°C for 2 minutes, ready to be run in an SDS page.

Cells were collected, centrifuged at 2000 RPM for 5 minutes at RT, the supernatant was discarded. PBS was added to the pellet, to wash the cells, cells were centrifuged at 2000 RPM for 5 minutes and RT and the PBS aspirated off. Lysis buffer was added to the cells, the volume of lysis buffer was dependent on cell number, and lysed on ice. Samples were centrifuged at 12,000 RPM for 15 minutes at 4°C, the supernatant collected in eppendorfs and the pellet discarded. A Pierce 660nm Protein Assay (Thermo 22660), was performed to determine protein concentration and samples were made up to at least 1 μg/μl and 5 X sample buffer was added, of which would be one fifth of the sample. Samples were boiled at 90°C for 2 minutes, ready to be run in an SDS page.

2.6.2 SDS Page

Samples were run on an SDS page, this allowed separation of molecules in an electrical field by molecular weight. A Mini-PROTEAN® Tetra Vertical Electrophoresis Cell by BioRad was used to run the SDS page. The gel consisted of two parts, a resolving gel pH 8.6 and a stacking gel pH 6.6. The resolving gel

were made up at either 8% and 10% (Table 2.4), this was dependent on the molecular weight of the protein that was to be looked at. Both resolving and stacking gels contained acrylamide (Thermo 16110158), SDS, ammonium persulphate (APS) (Thermo 17874) which acted as a catalyst for tetramethylethylenediamine (TEMED) (VWR 443083G) to polymerise the gel.

Table 2.4 Composition of resolving and stacking gels

8% Resolving Gel	10% Resolving Gel	Stacking Gel
8% acrylamide v/v	10% acrylamide v/v	4% Acrylamide v/v
0.31 M Tris/HCl pH 8.6	0.31 M Tris/HCl pH 8.6	0.5 M Tris/HCl pH 6.6
0.08% SDS v/v	0.08% SDS v/v	0.4% SDS v/v
0.08% APS w/v	0.08% APS w/v	0.2% APS w/v
0.2% TEMED v/v	0.2% TEMED v/v	0.1% TEMED v/v

First, the resolving gel was made, once polymerised, the stacking gel was added. Once the stacking gel had polymerised, the comb was removed, wells were cleaned with ddH2O and then placed into the cassette.

The cassette was filled with running buffer, samples were loaded, the volume of sample loaded was dependent on the concentration of protein needed that was optimal for the antibody to bind. The molecular weight ladder (Badrilla A010-601) was loaded at the end of samples. Samples were run at 100 Volts (V) until passed the stacking gel and voltage was increased to 120 V and run until dyed had run off. Gels were then transferred to a nitrocellulose membrane. The transfer

cassette, sponges, 3mm blotting paper (Life Sciences 3030-912) and 0.45 μm nitrocellulose membrane (Life Sciences 106002), were soaked in transfer buffer. The transfer was run for 2 hours and 30 minutes at constant 0.75 Amps at 4°C.

Once transfer was complete membranes were stained with Ponceau red to check that the samples were transferred homogeneously (Cell Signalling Technology 598035). Membranes were blocked in 5% BSA in TBST, except for blots for antibodies iNOS and TMT which were blocked in 5% skimmed milk in TBST, for 1 hour on an orbital shaker. Membranes were placed in primary antibodies, to the optimal working concentration (Table 2.1). Unless otherwise stated, primary antibodies were made up using 5% BSA in TBST. Primary antibodies were left on overnight at 4°C on a roller. To remove any excess primary antibody membranes were washed in TBST 3 times for 5 minutes on an orbital shaker. To visualise protein expression, secondary antibody was added to the membrane and left on an orbital shaker for 1 hours at RT. Secondary antibodies were made up at a dilution of 1:5000 in 5% skimmed milk (Serva 42590) in TBST (see Table 2.3). Membranes were washed 5 times for 5 minutes at RT with TBST. Proteins were detected using BioRad Clarity Western enhance chemiluminescence (ECL) and imaged on BioRad ChemiDoc™ MP Imagining System or Genesys G-BOX Genesyn.

2.6.3 Data Analysis

Total protein expression or phosphorylation levels were analysed using ImageJ (Fiji). In brief files were converted to a .tiff file from either a .scn file (BioRad ChemiDoc™ MP Imagining System) or a .sgd file (images taken on Genesys G-BOX Genesyn). Images were opened in ImageJ (Fiji) and image was inverted.

Total protein expression or phosphorylated protein expression was determined by the intensity of the band, these were then standardised by using either β-actin or the total protein of the phosphorylated protein. All images used to quantify were not over saturated signals. Data was transferred to Microsoft Excel for analysis.

2.6.4 Immunohistochemistry

At the end of the experiment rats were anesthetised by intraperitoneal injection of ketamine (60 mg/kg) and xylazine (8 mg/kg). Once fully anesthetised, the chest cavity was opened using blunt scissors, cuts were made along the ribcage to expose the heart. With care a cannula was inserted into the left ventricle and a small cut was made in the right atrium to allow transcardial perfusion of 0.1 M PB to flush the circulatory system, followed by 4% PFA to fix the tissue. The brains were carefully dissected out and left in 4% PFA for 48 hours to fix at 4°C. The 4% PFA was removed and 30% sucrose was added, once the brains had sunk to the bottom of the tube, the brain stem was cut out and frozen in Frozen Section Compound (FSC) (Leica, 3801480). Brain stem was left at -80°C overnight. The brain stem was cut using the Cryostat, sections were frozen in cryoprotectant in preparation for staining.

The correct anatomical sections for the DVC were selected for staining. The iNOS sections was subjected to antigen retrieval, 10 mM of sodium citrate (VWR 436072K), 6.5 pH was added to each section, sections were left at 80°C for 20 minutes. All sections were blocked in 10% donkey serum (Sigma D9663) in PBS for 1 hour at RT. Following this, all sections were place in primary antibodies, to the optimal working concentration (Table 1.1). Unless otherwise stated, primary antibodies were made up using 0.1% PBST to enable tissue permeabilization,

sections were left overnight on an orbital shaker at 4°C. After primary antibody incubation, sections were washed three times in PBS for a total time of 30 minutes to remove any excess primary antibody. Antigens were visualised with the appropriate secondary antibody, Table (1.2), which were left at RT for 2 hours. Sections which were stained for iNOS and NeuN antibodies were enhanced using Biotin-Streptavidin methods, the biotin was incubated at a dilution of 1:200 for two hours, the biotin removed, a conjugated streptavidin antibody was used to visualise the biotin-antibody, enhancing signalling. Sections were protected from light during secondary antibody incubation to prevent bleaching of the fluorescent probes. Sections were washed three times for ten minutes each time on an orbital shaker at RT before being mounted on glass slides using a fine paintbrush. Slides were left to air dry away from light before adding Vectashield plus 4',6-diamidino-2-phenylindole (DAPI) (Vector Laboratories, H-1200) to sections and covering with coverslips with a sealing of nail polish around the edges.

Sections were imaged by Dr. Lauryn New, using the Zeiss LSM880 upright confocal laser scanning microscope with Airyscan equipped with argon and He-Ne lasers and 40x and 63x Fluor oil objective. Each image was taken with the same gain and digital offset for each rat to allow fair comparisons. The Carl Zeiss Zen Software tile scans were used to image the entire DVC. Images were processed and exported using ZEN software, figures presented as a single plane image. Images were counted using 3 random tiles of each slice, 3 slices were used per rat, an average of all counts were taken demonstrated by quantification graphs. No oversaturated signals over exposure images were used in any of the quantifications between each rat.

2.7 Tandem Mass Tag (TMT) Assay

2.7.1 Protocol

Initially, control experiments were performed to optimise how the assay conditions. PC12 cells were collected and spun down at 2,000 RPM for 5 minutes, the supernatant was collected. The volume of the pellet was measured and four times the pellet volume of HENS buffer was added to the pellet to lyse cells. Once the HENS buffer was added, the cells were lysed on ice to stop degradation of proteins, cell lysates were moved to clean eppendorfs. Cell lysates were sonicated for three times for 10 seconds on ice, this was to ensure the samples did not overheat. Samples were centrifuged at 10,000 g for 10 minutes at 4°C.

Two positive controls of 200 μM S-nitroglutathione (GSNO) (Santa Cruz CAS 57564-91-7) or 5 mM DTT (Forrester et al., 2009) and one negative control of 200 μM glutathione were added to the cell pellets. DTT is a reducing agent, DTT opens all the disulphide bonds, resulting in the sample being fully labelled by iodoTMT. One DTT sample was treated with MMTS blocking all of the disulphide bonds, this was used as a negative control. GSNO works by increasing the number of s-nitrosylated cysteines by increasing the levels of NO, making it a positive control. Of note, GNSO is liable to light, samples were kept in the dark to prevent denaturing. Glutathione, works as a good negative control as it inhibits modifications to cysteine thiols. Sample were treated with either DTT, GSNO or glutathione for 90 minutes at room temperature on a shaker. Samples were then put through a Zeba Desalting Spin Column (Thermo 89882), three times to ensure maximum recovery. A bicinchoninic acid assay (BCA) (Thermo 23227) was incubated at 37°C for 30 minutes and protein concentration was determined.

When treating the cell lysates with GSNO, there was a significant loss in the amount of protein recovered in the Zeba Spin Column. PC12 cells were then treated with 250μM GSNO (Kaliyaperumal et al., 2015). Cells were plated at 80% confluency, 8 hours later cells were treated with 250μM GSNO, 12 hours later the media removed and new complete medium with 250μM of GSNO was left for another 12 hours. Cells were collected, spun down at 2000 RPM for 5 minutes and washed with PBS ready for the TMT assay.

Proteins were prepared at 1 mg/ml in 100μl of HENS buffer. To each 100μl of sample 0.04 M of MMTS (Chem Cruz sc-211882) was added, this was vortexed for at least 1 minute, samples were left for 90 minutes on the shaker at 800 RPM, to block any free sulfhydryl bonds. Six volumes of pre-chilled acetone (Fisher A10560117) were then added to each sample, and left at -20°C for 30 minutes, this removes any excess MMTS. The acetone was discarded and the pellet was left to dry in a fume hood. Pellets were resuspended in HENS buffer to give the final concentration to 1 μg/μl; to ensure that pellets were fully resuspended the samples were centrifuged at 6000 RPM for 3 minutes, to make sure there was no precipitate left.

To every 100 μl of sample, 0.4 mM of iodoTMT labelling reagent (Thermo 90101) was added and vortexed for at least one minute and left to sit for one minute. Samples were selectively reduced by 0.04 M sodium ascorbate (Sigma PHR1279) to each 100 μl of sample, vortexed for one minute, and left at room temperature for two hours on a shaker at 1000 RPM. To check that the sodium ascorbate selectively reduced part of the sample was taken out before adding the sodium ascorbate. Five times sample buffer was added to each sample, boiled at 90°C in preparation to run an SDS page. Twenty-five μl of each sample was in

a 10% gel (see section 2.6), after transferred membrane was blocked in 5% skimmed milk in TBST and then left in the anti-TMT antibody overnight on a shaker at 4°C. The membrane was developed in methods stated in section 2.6.

Once the assay had been optimised, PC12 cells were seeded at $10x10^6$ in a $10cm^2$ dish, cells were left overnight at 37°C. The next day the media was changed and cells were infected with either GFP virus at a MOI of 50, Drp1-S637A virus at a MOI of 70 or Drp1-K38A virus at a MOI of 50. After 48 hours, cells were collected. The assay was repeated as per the protocol described above. A 100 μg of GFP lysate was treated with either 200 μM of GSNO or 200 μM of glutathione and 5 mM of DTT in addition to a 100 μg of GFP lysate, to give positive and negative controls.

2.7.2 Production of a PC12-ShiNOS Cell Line (ShRNA inducible nitric oxide synthase (shiNOS) Transduction)

In order to determine whether iNOS was involved in Drp1-dependent S-nitrosylation, a PC12 cell line expressing the ShRNA for iNOS was selectively used to knockdown iNOS. A puromycin titration was carried out, to determine which concentration was toxic to PC12 cells after a few days. The puromycin resistance gene is carried by lentivirus needed to express the shiNOS, once cells had taken up the virus they are puromycin resistance. PC12 cells were plated at a 70% confluency in a 12-well plate, once cells were attached, a range of 2-10 μg/ml of puromycin (Biovision 1860-25) was used to treat the cells. Cells were monitored until there was 90% detachment of cells after a few days, it was determined that the ideal puromycin concentration was 3.5 μg/ml.

PC12 cells were plated in a 12 well plate to ensure that in 24 hours cells would be 50% confluent. Twenty-four hours later, medium was removed in each well and 1ml of a mixture of complete medium with 5 μg/ml of Polybrene (Santa Cruz, sc-134220) and 20 μl of either knockdown iNOS (shiNOS) lentivirus or a control scramble ShRNA (shControl) lentivirus (Santa Cruz Biotechnology, sc-29417-V and sc-108080 respectively) was added to a well and left for 24 hours. The complete medium with Polybrene (Santa Cruz sc-134220) and virus was removed and replaced with complete medium and left for 24 hours. Cells were passaged 1 in 3 in complete medium for 24 hours to recover. After 24 hours the complete medium was removed and complete medium with 3.5 μg/ml puromycin was added to the well. Cells were monitored until the well with the control cells had detached, once fully detached the viable viral expressing cells were passaged into a 6 cm^2 dishes and maintained in the complete medium with puromycin. After a few passages, cells for both PC12 ShControl and PC12 ShiNOS were collected and subjected to western blotting to confirm a decrease in iNOS levels. Following this the s-nitrosylation assay was repeated with these cell lines.

2.7.2.1 Infection

To determine if the Drp1-dependent s-nitrosylation is due iNOS, the stable cell lines, ShiNOS and ShControl were infected with Drp1-S637A, Drp1-K38A and GFP viruses. Initially, cells were infected at a 70% confluency with a MOI of 70 for Drp1-S637A, a MOI 50 Drp1-K38A and a MOI 50 GFP, however after 24 hours cells were detaching across both cell lines infected with GFP and Drp1-K38A. Following this, in order to get similar expression in all viruses in both cell lines a viral titration or a transfection using plasmids expressing Drp1-S637A, Drp1-

K38A and GFP proteins was done to determine which was the best way to prevent the cells dying.

Similarly, to the viral infection (section 2.3), PC12 ShControl and PC12 ShiNOS cells were plated so that in 24 hours cells would be 80% confluent. 24 hours later cells were infected with varying MOI of 10, 20, 30, 50 and 70 for all GFP, Drp1-S637A and Drp1-K38A. Cells were monitored for 48 hours, cells starting to detach before the 48 hours were collected early. At 48 hours samples were collected and prepared for western blotting methods as described in 2.7.1.

2.7.3 Immunoprecipitation

Immunoprecipitation was used to capture and elute the peptides that were labelled with TMT reagent labelled. Protein samples collected from the TMT-assay were precipitated in six volumes of acetone at -20°C overnight, the samples were then centrifuged twice at 4,000 g for 10 minutes at 4°C, the acetone was removed and the pellet was left to dry in a fume hood. The immunoprecipitation reaction was carried out using Immobilised Anti-TMT Resin and TMT Elution Buffer (Thermo Scientific, 90076 and 90104 respectively). Pellets were resuspended in lysis buffer to give the final concentration of 1 μg/μl, to ensure the whole pellet was resuspended, the samples were briefly centrifuged at 6,000 RPM to check for residue pellet. For every 1 mg of sample, 100 μl of settled resin was needed, the slurry was made up with 50% settled resin. To release the settle resin, the slurry was centrifuged at 3000 RPM for 3 minutes at room temperature (RT), the supernatant removed. The pellet was then washed 3 times with PBS at 3000 RPM for 3 minutes at 4°C. The resin was added to the 1 μg/μl sample and left on a wheel overnight at 4°C.

Samples were then centrifuged at 3000 RPM for 3 minutes at 4°C, the supernatant was collected, 5 X sample buffer was added. The pellet was washed with lysis buffer without protease inhibitor tablets and DTT, three times at 3000 RPM at 4°C, the supernatant for the first wash was kept and 5 X sample buffer was added to the wash. Elution buffer was added to each sample, the same volume as the settled resin and left on a shaker at 1000 RPM at 4°C for 1 hour. Samples were centrifuged at 3000 RPM for 3 minutes at 4°C and supernatant collected, known as elution 1, 5 X sample buffer was added. The elution was repeated two additional times the same volume of elution buffer was added to the resin pellet. To the resin pellet, 1 X sample buffer was added to the sample which was equivalent of the elution buffer. All samples were boiled at 90°C, and ran on an SDS page. Protein expression was determined by TMT antibody.

2.8 Statistical Analysis

All data are expressed as the mean ± SEM. Data were inputted on Microsoft Excel and analysed using GraphPad Prism 7 software. A significant difference was determined by using multiple T-tests or unpaired T-Test for fat deposition and western blot analysis quantification, this test was used to compare the average of the different treatments. Statistical significance for acute feeding studies was determined by two-way ANOVA (post-hoc test: Sidak or Tukey), this test was used to do determine treatment with food intake at either the 4 hr or 12 hr time point. All chronic data significance was determined by a two-way ANOVA (post-hoc test: Tukey or Sidak), this test was used to compare two variable treatments with either body weight or food intake each day. *n* refers to the number

of rats used. $P < 0.05$ was considered to be statistically significant. Significance was defined by: (*) $P < 0.05$; (**) $P < 0.01$; (***) $P < 0.001$; (****) $P < 0.0001$.

3 Changes in mitochondrial dynamics can alter feeding behaviours, body weight and insulin sensitivity in the DVC

3.1 Introduction and rationale

Mitochondria are highly dynamic and can change morphology to meet energy demands, via fission and fusion, these two opposing processes are regulated by several proteins (Jheng et al., 2012; Ramírez et al., 2017). Mitochondrial fusion is regulated by MFN-1, MFN-2 and Opa1 while mitochondrial fission is regulated by Drp1, Fis1 and Mff (Jheng et al., 2012). A fine balance of these processes are needed to maintain mitochondria functionality (Filippi et al., 2017).

Mitochondrial dysfunction can lead to insulin resistance, there are many mechanisms that link the development of insulin resistance to alterations of mitochondrial function (Filippi et al., 2017; Gao et al., 2014; Jheng et al., 2012). For example, in adipose tissue, mitochondrial dysfunction can increase oxidative stress in tissues, leading to an increase in fat oxidation and lipid accumulation which is associated with insulin resistance (Gao et al., 2014). Furthermore an increase in active Drp1 can lead to ER stress, and mitochondrial fission in skeletal muscle has led to insulin resistance in obese rats (Jheng et al., 2012). In addition to this, transgenic mice with the deletion of Drp1 in the liver prevented these mice from developing diet induced insulin resistance (Wang et al., 2015). In the DVC an increase in mitochondrial fission leads to an increase in ER stress, ultimately leading to insulin and impairing its ability to control glucose metabolism (Filippi et al., 2017).

Insulin activates its receptors in the DVC to lower hepatic glucose production (Filippi et al., 2012b), and also decrease food intake and body weight in healthy male rats (Filippi et al., 2014). In rats a 3-day HFD induces insulin resistance, and as a result the DVC loses the ability to regulate hepatic glucose production, subsequently leading to an increase food intake (Filippi et al., 2014). This is

because a HFD increases the activation of mitochondrial fission protein, Drp1, as well as inducing insulin resistance in the DVC (Filippi et al., 2017).

In rats fed a HFD, mitochondria appear smaller and are present at a higher frequency in the DVC than in RC control littermates (Filippi et al., 2017). This effect was dependent on the mitochondrial fission protein Drp1, as chemical inhibition of mitochondrial fission using MDIVI-1 reversed the effects of a HFD on mitochondrial morphology (Filippi et al., 2017). Furthermore, a 3 day HFD depleted the glucoregulatory effect of DVC insulin, this effect was negated when insulin was infused with MDIVI-1, determining that mitochondrial fission can induce insulin resistance in the DVC (Filippi et al., 2012b, 2017). This raises the possibility that Drp1-dependent mitochondrial fission is necessary in HFD-dependent insulin resistance in the DVC.

Activation of Drp1 in the DVC induced insulin resistance with rats failing to maintain euglycemia determined by pancreatic euglycemic clamp, similar to the effect a 3-day HFD had on rats (Filippi et al., 2017). In contrast, molecular inhibition of mitochondrial fission protected 3-day HFD-fed rats from insulin resistance (Filippi et al., 2017). The effects of mitochondrial fission on glucose metabolism has been well characterised, however the effect mitochondrial fission has on feeding behaviours is not well understood. Previous data has shown that Drp1-dependent mitochondrial fission induces insulin resistance, using these data as a foundation I hypothesised that activating Drp1-dependent mitochondrial fission in the DVC of RC-fed rats would increase food intake and body weight gain, as well as inducing insulin resistance. Conversely, according to this hypothesis, inhibiting Drp1-dependent mitochondrial fission, would prevent insulin resistance in HFD-fed rats.

3.1.1 Aims

Aim 1: Is Drp1-dependent mitochondrial fission in the DVC sufficient to induce insulin resistance and affect feeding behaviours and body weight in RC-fed rats?

Aim 2: Can inhibiting Drp1-dependent mitochondrial fission in the DVC protect HFD-fed rats from developing insulin resistance and decrease food intake?

3.2 Results

3.2.1 Targeting NTS using an adenoviral delivery system

To the effects of mitochondrial dynamics, an adenoviral delivery system was used to target the NTS of the DVC. An adenovirus expressing a constitutively active form of Drp1 in the residue of S637 to A (S637A), which mimics its non-phosphorylated state, resulting in an over expression of Drp1. An adenovirus expressing a dominant negative form of Drp1, mutated in the residue of K38 to A (K38A), resulting in a defective GTP binding site, causing a decrease Drp1 dependent mitochondrial fission, and finally a control of GFP. The adenoviral systems expressing the different forms of Drp1 were tagged with the FLAG protein to allow specific labelling for IHC and western blotting.

To characterise cell populations which expressed Drp1-S637A, Drp1-K38A and GFP, IHC was performed as detailed in section 2.7[1]. Rats underwent brain surgery on day 0 to specifically target the NTS. On day 1 rats were either injected with adenoviruses expressing Drp1-S637A or GFP and were given Diet 1 RC for 14 days, or were injected with Drp1-K38A or GFP and were given Diet 2 RC for

Figure 3.1 Perfusion protocol for rats to investigate expression of Drp1-S637A, Drp1-K38A and GFP

Rats underwent surgery on day 0 and were injected with either Drp1-K38A, Drp1-S637A or GFP the following day, food intake and body weight were observed every day for 14 days, on day 14 rats underwent perfusion

[1] IHC was done in collaboration with Dr. Lauryn E New in the Filippi Las

rats were monitored daily and were perfused on day 14 as described in section 2.6.4. Sections obtained from these rats were used to confirm that the NTS was specifically targeted (Figure 3.2A) and also to characterise cell types that were co-localised with the viruses. The IHC confirms the accuracy of the surgery, in rats expressing GFP (Figure 3.2B), Drp1-S637A (Figure 3.2C) and Drp1-K38A (Figure 3.2D).

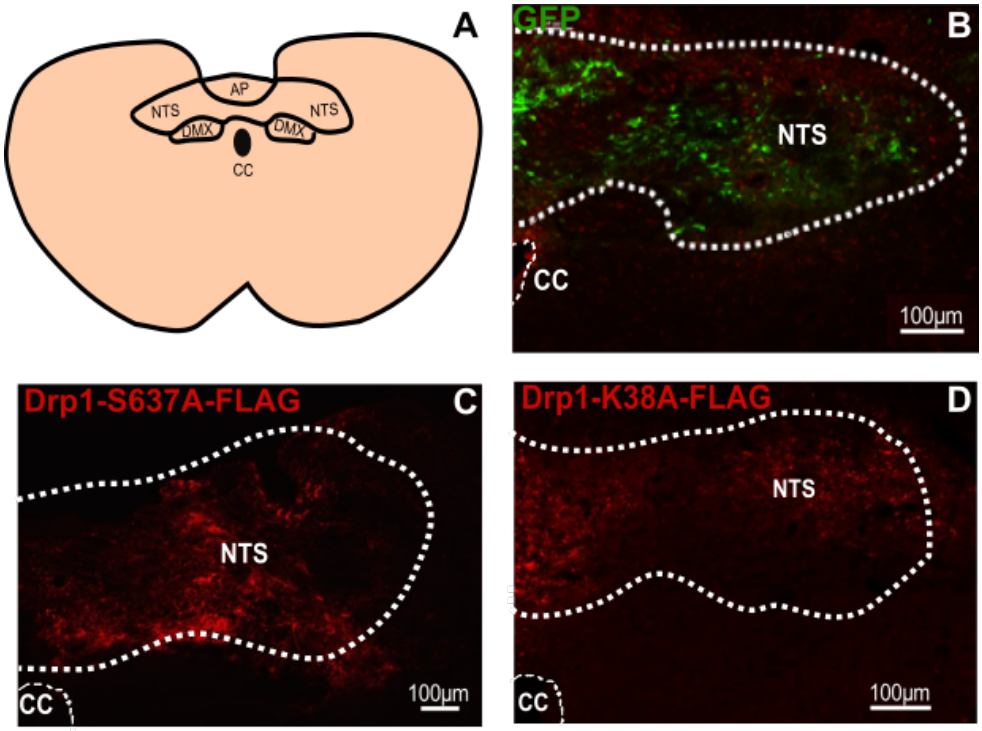

Figure 3.2 IHC demonstrating successful targeting of the NTS

A: Schematic of the DVC highlighting the NTS targeted in surgery
B: GFP expression in the NTS of DVC, green, dual-labelled with GFAP to label astrocytes, red
C: The constitutively active form of Drp1, Drp1-S637A FLAG tagged expression in the NTS, red
D: The dominant negative form of Drp1, Drp1-K38A FLAG tagged expression in the NTS, red

3.2.2 GFP is expressed in astrocytes and oligodendrocytes

In order to characterise the cell populations targeted by the adenoviruses Drp1-S637A, Drp1-K38A and GFP, IHC was carried out in collaboration with Dr Lauryn New as described in section 2.7. GFP staining was used to characterise the dominant cell population infected by the adenoviral system, GFP expression is cytosolic unlike the Drp1-S637A and Drp1-K38A staining meaning it is difficult to accurately determine the frequency of co-localisation of markers with FLAG expression. The GFP adenovirus has the same CMV promoter as both the Drp1-S636A and Drp1-K38A adenoviruses, therefore infection of neurones, astrocytes and oligodendrocytes would likely occur at the same frequency as that of the GFP control expression.

We determined that the cell types expressing GFP within the DVC were neurones, astrocytes and oligodendrocytes. Dual staining with NeuN to label mature neurones showed that 22.1% of GFP expressing cells were neurones (*n* = 3 rats, Figure 3.3A-Aii). Co-labelling with the astrocytic antibody against GFAP with GFP expression, showed that 39.1% of GFP labelled cells were astrocytes (*n* = 4 rats, Figure 3.3B-Bii). In addition to neurones and astrocytes, myelin forming oligodendrocytes are also present within the central nervous system. To determine the expression of oligodendrocytes in the DVC, an antibody against PanQKi was used in GFP expressing sections, it was found that, 36.2% of GFP stained cells were co-localised with PanQKi (*n* = 3 rats, Figure 3.3C-Cii).

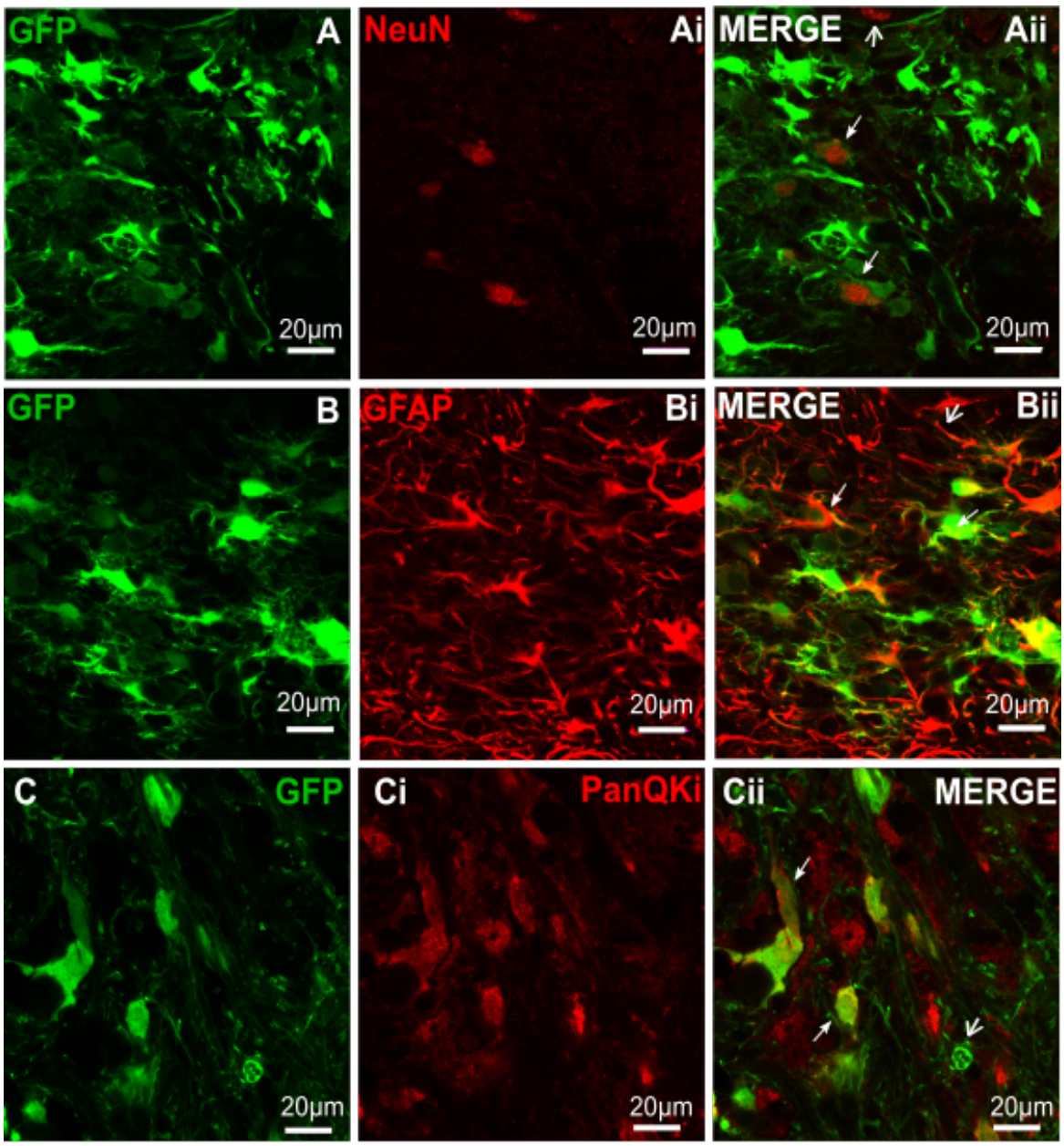

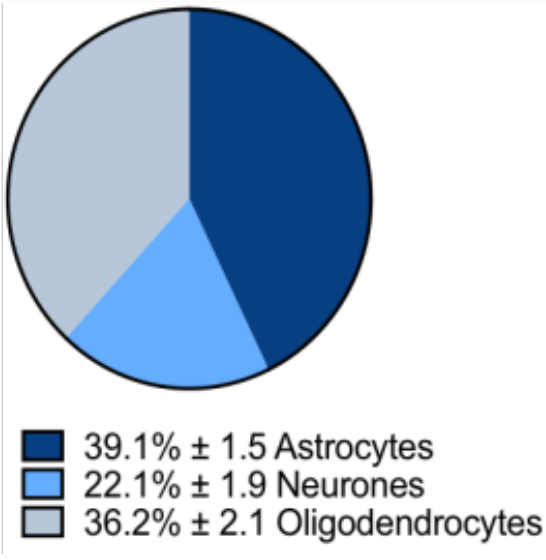

Figure 3.3 GFP expression in neural cell types

A-Aii: Representative confocal images illustrating labelling of GFP expression in (A), NeuN (Ai) and dual labelling for both (A-Ai) in the DVC

B-Bii: Representative confocal images illustrating labelling of GFP expression in (B), GFAP (Bi) and dual labelling for both (B-Bi) in the DVC

C-Cii: Representative confocal images illustrating labelling of GFP expression in (C), PanQKi (Ci) and dual labelling for both (C-Ci) in the DVC

Closed arrows denote colocalised cells (*n*= 3 for NeuN and PanQKi, *n*= 4 for GFAP, *n* = number of rats, per rat 3 tiles of each image were counted of 3 slices)

3.2.2.1 Drp1-S637A and Drp1-K38A are expressed in multiple cell types in the DVC

As mentioned previously as the GFP adenovirus possess the same CMV promoter as Drp1-S637A and Drp1-K38A viruses, the types of cells infected by these Drp1-expressing adenoviruses is likely to be similar. The Drp1-expressing adenoviruses are tagged with FLAG, therefore expression of Drp1-S637A and Drp1-K38A could be seen using an anti-FLAG antibody However, due to the nature of the staining of the Drp1-S637A-FLAG and Drp1-K38A-FLAG, quantification of the number of cells with FLAG tagged Drp1-S637A and Drp1-K38A with cell markers was not possible. Nevertheless, IHC performed on sections confirmed that there was co-localisation of Drp1-S637A or Drp1-K38A with different neural markers (Figure 3.4).

Unlike GFP staining which can be nuclear and cytoplasmic, Drp1-S637A staining was more diffuse along fibres and Drp1-K38A expression appearing more punctate (Figure 3.4). Similarly, with the GFP staining, there is co-localisation with mature neuronal cell marker, NeuN, we demonstrated that Drp1-S637A and Drp1-K38A are expressed around NeuN positive cell bodies (Figure 3.4A-Aii,Figure 3.4B-Bii). Double labelling with anti-GFAP, to label astrocytes, has also shown that there is co-localisation of Drp1-S637A staining with GFAP positive astrocytes in the DVC (Figure 3.4C-Cii), this was also seen in Drp1-K38A expressing cells (Figure 3.4D-Dii). Staining for microglial cells, using an antibody against Iba1, demonstrated expression with Drp1-S637A and Drp1-K38A in microglia processes (Figure 3.4E-Eii, Figure 3.4F-Fii).

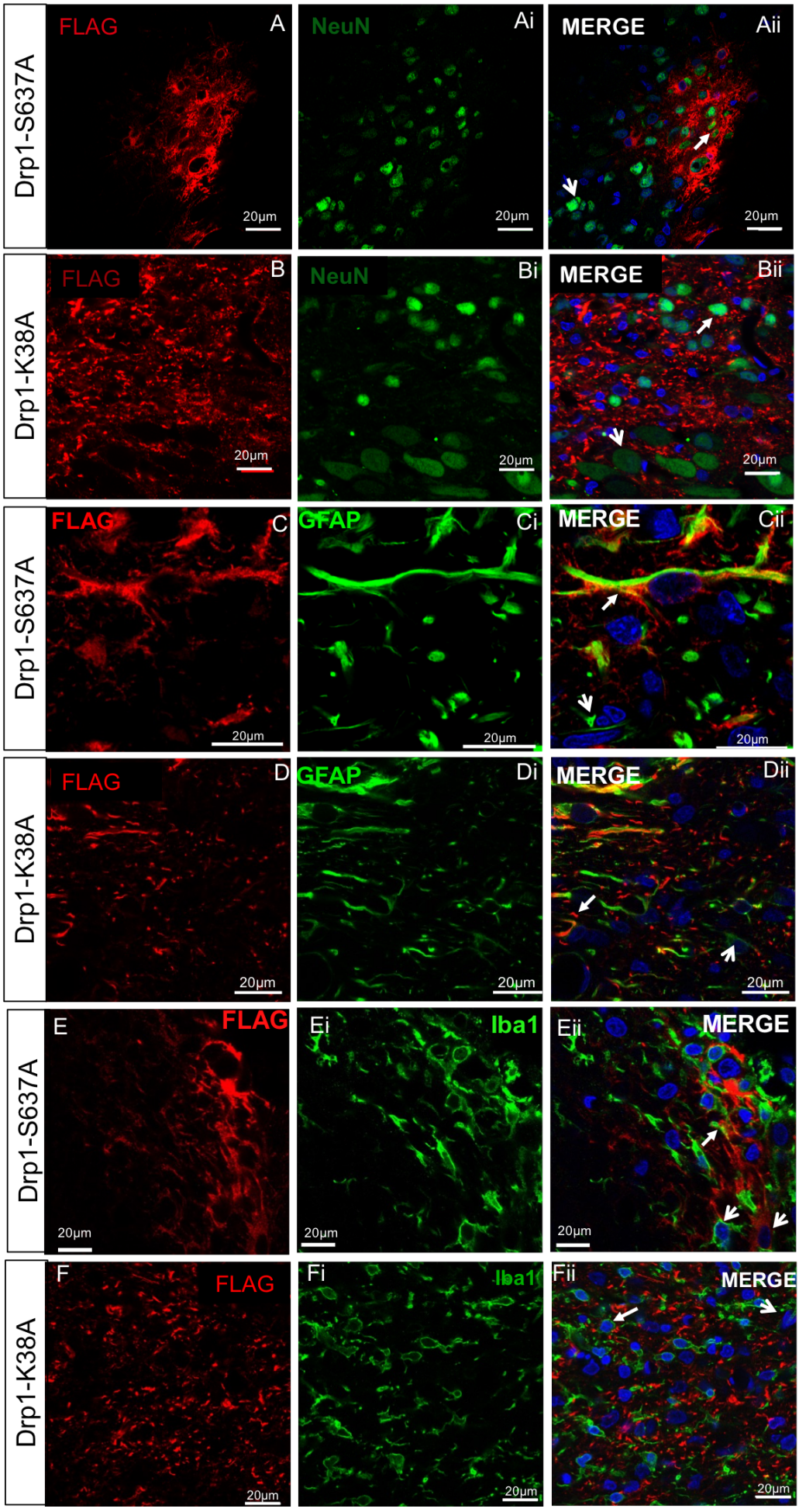
Drp1-S637A
FLAG
A
NeuN
Ai
MERGE
Aii
20μm
Drp1-K38A
FLAG
B
NeuN
Bi
MERGE
Bii
20μm
Drp1-S637A
FLAG
C
GFAP
Ci
MERGE
Cii
20μm
Drp1-K38A
FLAG
D
GFAP
Di
MERGE
Dii
20μm
Drp1-S637A
E
FLAG
Ei
Iba1
Eii
MERGE
20μm
Drp1-K38A
F
FLAG
Fi
Iba1
Fii
MERGE
20μm

Figure 3.4 Expression of the constitutively active form of Drp1, Drp1-S637A and the dominant negative form of Drp1, Drp1-K38A

A-Aii: Representative confocal images illustrating the expression Drp1-S637A (A), NeuN (Ai) and dual labelling for both (A-Ai) in the DVC

B-Bii: Representative confocal images illustrating the expression of Drp1-K38A (B), NeuN (Bi) and dual labelling for both (B-Bi) in the DVC

C-Cii: Representative confocal images illustrating the expression of Drp1-S637A (C), GFAP (Ci) and dual labelling for both (C-Ci) in the DVC

Open arrows denote non-colocalised cells

D-Dii: Representative confocal images illustrating the expression of Drp1-K38A (D), GFAP (Di) and dual labelling for both (D-Di) in the DVC

E-Eii: Representative confocal images illustrating the expression of Drp1-S637A (E), Iba1 (Ei) and dual labelling for both (E-Ei) in the DVC

F-Fii: Representative confocal images illustrating the expression Drp1-K38A (F), Iba1 (Fi) and dual labelling for both (F-Fi) in the DVC

Closed arrows denote colocalised cells

3.2.3 Activation of Drp1 in the DVC induces insulin resistance, hyperphagia and increases body weight in RC-fed rats

3.2.3.1 Activation of Drp1 in the DVC induces insulin resistance

To investigate whether Drp1-dependpent mitochondrial fission affected insulin sensitivity in the DVC, I performed stereotactic brain surgery in rats to insert a bilateral cannula into the NTS of the DVC (as described in section 2.4.1). On the day after surgery (day one), an adenovirus expressing Drp1-S637A or GFP was injected into the DVC of rats (Filippi et al., 2017). On day nine and day 14 an acute feeding study was carried out, where insulin was infused bilaterally into the DVC of fasted rats and feeding behaviours were monitored for four hours (as detailed in section 2.5.2). Rats were sacrificed on day 16, the experimental paradigm is highlighted in Figure 3.5 below.

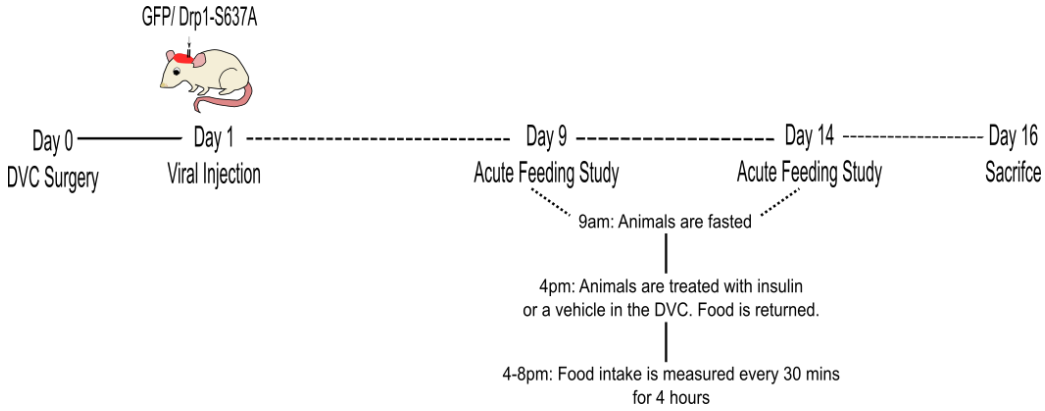

Figure 3.5 Drp1-S367A feeding study protocol

On day 0 rats underwent brain surgery to inset a double cannula, on day one, these rats were injected with Drp1-S637A or GFP. On day 9 and 14 an acute feeding study was performed to observe feeding behaviour. These rats were sacrificed on day 16.

Rats underwent a feeding study as detailed in Figure 3.5, rats were fasted for 6 hours and then infused bilaterally into the DVC with a total 0.2 μl of 2 mU insulin or a vehicle over 5 minutes. Food was then returned and food intake was observed every half hour for 4 hours and a final reading was taken at 12 hours.

GFP expressing rats infused with insulin in the DVC had a significant decrease in food intake compared to their vehicle infused controls. At the four-hour point insulin treated GFP expressing rats had a 50.6% decrease in food intake compared to vehicle treated rats (Figure 3.6A). These results therefore show that these rats were insulin sensitive. At 12-hours, the effect of insulin on feeding behaviours was lost in GFP expressing rats (Figure 3.6B).

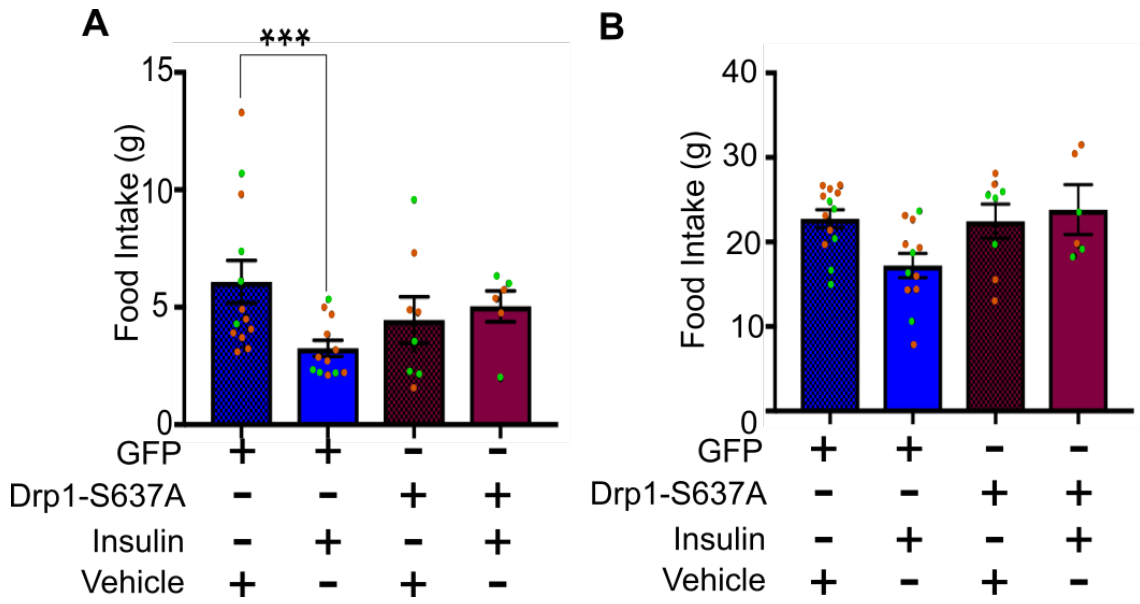

Figure 3.6 Food intake during acute feeding study in rats expressing Drp1-S637A and GFP

A: Total food intake taken at the 4 hour time point, as there was no difference in the food intake in the feeding studies performed on day nine and fourteen, the figure shows the average food intake over both feeding studies

B: Total food intake taken at the 12 hour time point, as there was no difference in the food intake in the feeding studies performed on day nine and fourteen, the figure shows the average food intake over both feeding studies

Data are expressed as a mean± SEM of n=13 for GFP vehicle, *n*=12 for GFP insulin, *n*=8 for Drp1-S637A vehicle, *n*=6 for Drp1-S637A insulin. Orange dots represent data gained from day 9, green dots represent data gained from day 14.

Statistical Test: Two Way Anova (post-hoc test: Sidak) [*** p<0.001]

RC-fed rats expressing the constitutively active form of Drp1, Drp1-S637A, who were treated with insulin, had similar food intake to vehicle treated littermates at four hours (Figure 3.6A). The average food intake of Drp1-S637A expressing rats

infused with the vehicle was 4.45g compared to Drp1-S637A expressing insulin treated food intake which was 4.9g, therefore insulin had no effect on feeding behaviours in rats expressing Drp1-S637A in the DVC (Figure 3.6A). There was no difference in food intake at 12 hours in both insulin and vehicle treated groups (Figure 3.6B). This cohort has confirmed that rats expressing the active form Drp1 in the DVC are insulin resistant in line with previous research which has shown that activation of Drp1 in the DVC can induce insulin resistance[2i] (Filippi et al., 2017).

[2] Referring to the loss of insulin-induced hypophagia when stating rats are insulin resistant in data

3.2.3.2 Chronic activation of Drp1 in DVC induced hyperphagia and increased in body weight in RC-fed rats

The effects of chronic activation of Drp1 on food intake and body weight were also investigated. Each rat had their food intake (to the nearest g) and body weight taken at a 9 am of each day to keep data as consistent as possible. Rats expressing Drp1-S637A had an increase in food intake over the two-week period, with data becoming significant from day 10 (Figure 3.7A). Furthermore, activation of Drp1 in the DVC resulted in an increase in body weight gain compared to GFP expressing controls (Figure 3.7B), this difference was statistically significant from day 7. In summary, activation of Drp1 in the DVC induces insulin resistance and increases in food intake and body weight gain.

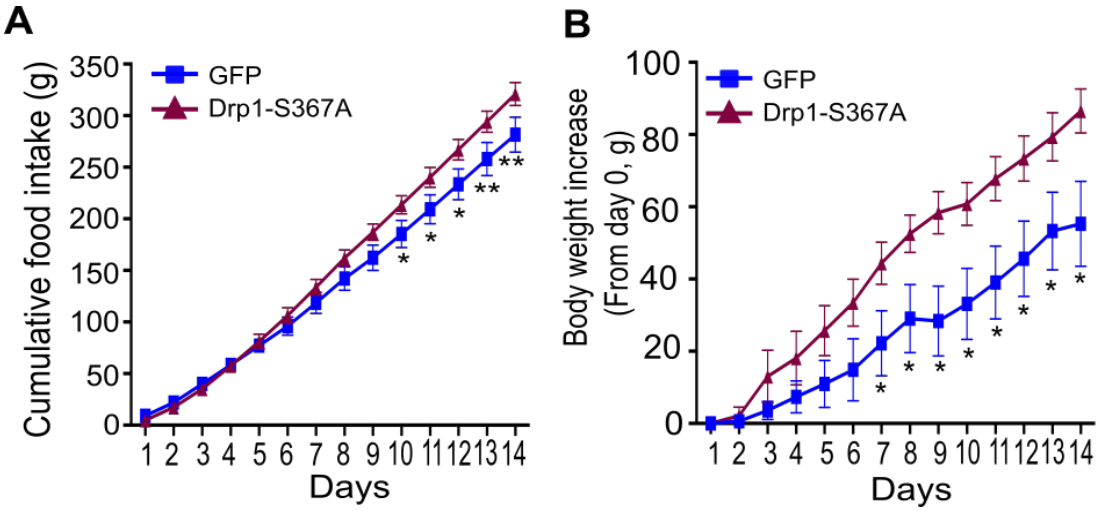

Figure 3.7 Cumulative food intake and body weight increases during the study in Drp1-S637A-expressing rats

A: Cumulative food intake in GFP and Drp1-S637A-expressing rats from day of viral injection (day 1)

B: Body weight increase in GFP and Drp1-S637A-expressing rats from day of viral injection (day 1)

All data are expressed as mean ± SEM *n*=8 for both GFP and Drp1-S637A.

Statistical Test: two-way ANOVA (post-hoc test: Tukey) [*p < 0.05, **p <0.01]

3.2.3.3 Activation of Drp1 in the DVC results in an increase in the total amount of WAT in rats

I have demonstrated that activation of Drp1 in the DVC causes an increase in body weight gain, next, I wanted to investigate the effect of chronic activation of Drp1 on WAT. On the day of sacrifice, day 16, tissues were collected for analysis. Along with the DVC, different types of WAT were dissected and weighed to see if there was a difference in WAT deposition in rats expressing GFP and Drp1-

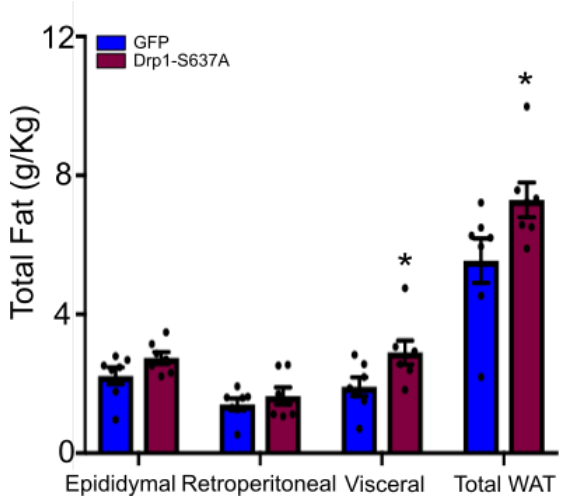

Figure 3.8 Weight of white adipose tissue in Drp1-S637A rats compared to GFP control rats

All data are expressed as mean ± SEM *n*=8 for both GFP and Drp1-S637A cohorts. Statistical test: multiple T-test [*p < 0.05]

S637A. The types of adipose tissue collected included; epididymal fat from the groin area in male rats, retroperitoneal fat, from around the kidney and visceral fat which surrounds the intestines. All fat was collected and weighed to the nearest 0.01 g. Rats expressing Drp1-S637A in the DVC had a significant increase in the total WAT compared to GFP expressing controls (Figure 3.8). The Drp1-expressing rats also had a significantly higher level of visceral fat compared to the GFP expressing rats (Figure 3.8).

3.2.3.4 Activation of Drp1 increases ER-stress and iNOS levels in the DVC

On the day of sacrifice the DVC was collected and snap frozen, DVC tissue was lysed in preparation for western blotting (as described in section 2.6). An increase in active Drp1 has been associated with inflammation and ER stress (Filippi et al., 2017; Gao et al., 2014; Santoro et al., 2017). In order to establish the successful delivery Drp1-S637A, the Drp1 protein was tagged with FLAG (Figure 3.9). An increase in phosphorylation levels of PERK is an indicator of ER stress, here I have shown that an over expression of Drp1 in the DVC increased ER-stress indicated by phosphorylation levels of PERK compared to their GFP-expressing controls (Figure 3.9A). This confirms previous data demonstrating that Drp1 activation increase ER-stress levels in the DVC (Filippi et al., 2017).

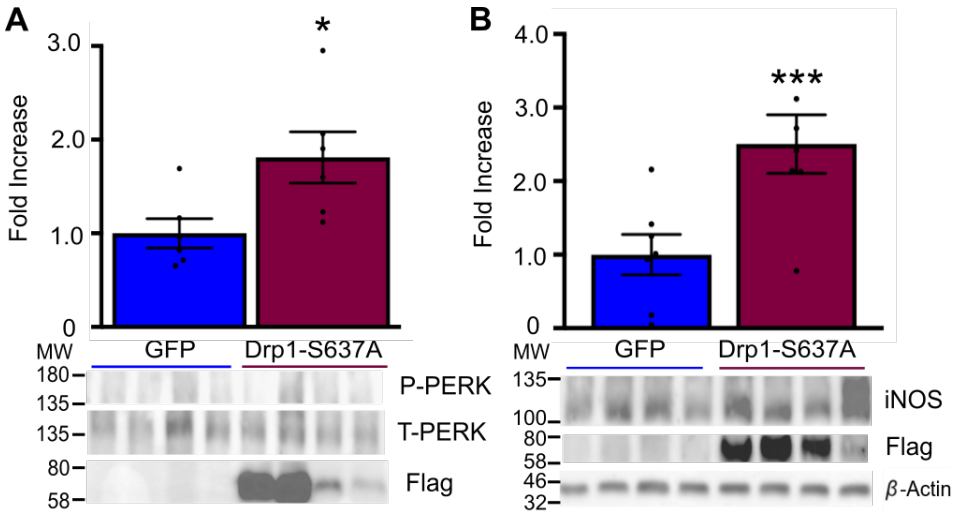

Figure 3.9 Activation of Drp1 leads to an increase in ER stress and iNOS levels in the DVC

A: A representative western blot showing changes in phosphorylation levels of the ER stress marker PERK in the DVC in rats Drp1-S637A compared to control GFP rats (Data were analysed using fiji ImageJ)

B: A representative western blot show levels of iNOS levels in the DVC in rats Drp1-S636A compared to GFP controls (Data were analysed using fiji ImageJ)

All data are expressed as mean ± SEM *n*=8 for both GFP and Drp1-S637A (P-PERK: phosphorylated PERK, T-PERK: total-PERK) Fold increase from control.

iNOS is a mediator of inflammation, higher levels of iNOS results in an increase in the release of nitric oxide (Fujimoto et al., 2005). It has previously been demonstrated that an increase in iNOS levels have been associated with Drp1-dependent mitochondrial fission, next, I wanted to investigate if there was an upregulation in iNOS levels (Filippi et al., 2017; Park et al., 2013). I have found rats expressing Drp1-S637A had a significant increase in iNOS levels compared to their GFP expressing counterparts (Figure 3.9B).

In conclusion, over expression of Drp1 in the DVC of the brain can induce insulin resistance (Figure 3.6), cause an increase in food intake, body weight gain (Figure 3.7) and WAT deposition (Figure 3.8), leading to an increase in ER stress and iNOS in the DVC (Figure 3.9).

3.2.4 Inhibition of mitochondrial fission in the DVC prevents insulin resistance, hyperphagia and body weight gain in HFD-fed rats

3.2.4.1 Inhibition of Drp1 in the DVC prevents the development of insulin resistance in HFD-fed rats

The data I have presented demonstrates that an activation of Drp1 leads to insulin resistance. Next, I wanted to determine whether inhibition of Drp1-dependent mitochondria fission, using an adenovirus expressing the dominant negative form of Drp1, Drp1-K38A, could prevent the development of insulin resistance in HFD-fed rats. Similarly to Drp1-S637A viral delivery, Drp1-K38A was injected a day after surgery (day one) (Filippi et al., 2017), on day three post-brain surgery (Figure 3.10) rats were given HFD for the remainder of the study.

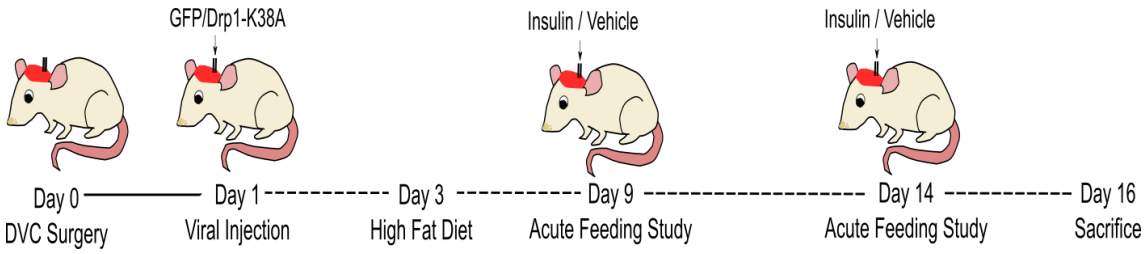

Figure 3.10 Drp1-K38A study timeline.

Rats underwent brain surgery on day 0, on day 1 each rat was injected with Drp1-K38A or GFP, on day 3 rats were put on a HFD. Acute feeding study was done on day 9 and 14.

Drp1-K38A and GFP expressing rats were subjected to feeding studies on day nine and day 14 (as previously described in section 2.5). I have found that at 4 hours the HFD-fed GFP-expressing rats failed to decrease food intake when infused with insulin in the DVC compared with vehicle treated GFP controls, average GFP-expressing vehicle food intake 4.2g vs GFP-expressing insulin treated food intake 3.8g (Figure 3.11A). This effect was also seen at the 12-hour time point (average GFP expressing vehicle food intake 15.8g vs GFP expressing

insulin treated food intake 14.2g) (Figure 3.11B), therefore determining that a HFD can induce insulin resistance.

On the contrary, the rats expressing the dominant negative form of Drp1, Drp1-K38A, exhibited a 59.1% decrease in food intake at the 4-hour point when treated with insulin compared to Drp1-K38A-expressing vehicle treated littermates (Figure 3.11A). At the 12-hour time point, effect of insulin on feeding behaviours was lost in Drp1-K38A expressing insulin treated rats (Figure 3.11B). This is in contrast to the effect of insulin against vehicle treatment in the GFP expressing

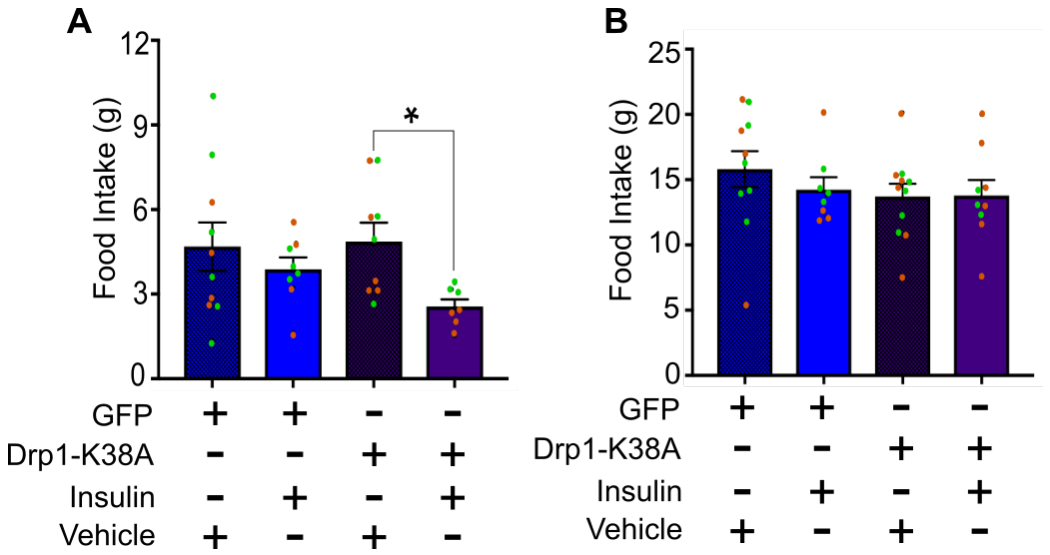

Figure 3.11 Acute feeding study in Drp1-K38A and GFP rats

Rats were fasted for 6 hours and then infused bilaterally into the DVC with a total 0.2ul of insulin (total 2mU) or a vehicle over 5 minutes. Food was returned and food intake was measured every half of an hour for 4 hours, a final reading was taken at 12 hours.

A: Total food intake taken at the 4 hour time point, since there was no difference in the food intake in the feeding studies performed on day nine and fourteen, the figure shows the average food intake over both feeding studies

B: Total food intake taken at the 12 hour time point, from feeding studies, since there was no difference in the food intake in the feeding studies performed on day nine and fourteen, the figure shows the average food intake over both feeding studies

Data are expressed as a mean± SEM of *n*=11 for GFP vehicle, *n*=8 for GFP insulin, *n*=9 for Drp1-K38A vehicle, *n*=8 for Drp1-K38A insulin. Orange dots represent data gained from day 9, green dots represent data gained from day 14.

Statistical Test: Two-way ANOVA (post-hoc test: Tukey) [*p<0.05]

control rats upon food intake at 12 hours. Overall, these data highlights that inhibiting mitochondrial fission in the DVC can prevent insulin resistance[3] in HFD-fed rats.

3.2.5 Chronic inhibition of Drp1 in the DVC prevents hyperphagia and a decrease in food intake

I have shown that a decrease in the expression of Drp1 in the DVC can prevent insulin resistance from occurring in HFD-fed rats (Figure 3.11). I next wanted to understand the effect of chronic inhibition of Drp1 on food intake and body weight gain. A significant decrease in the cumulative food intake in the rats expressing the dominant negative form of Drp1, Drp1-K38A, compared with GFP-expressing HFD-fed controls from day 8 (Figure 3.12A). Drp1-K38A expressing rats also had

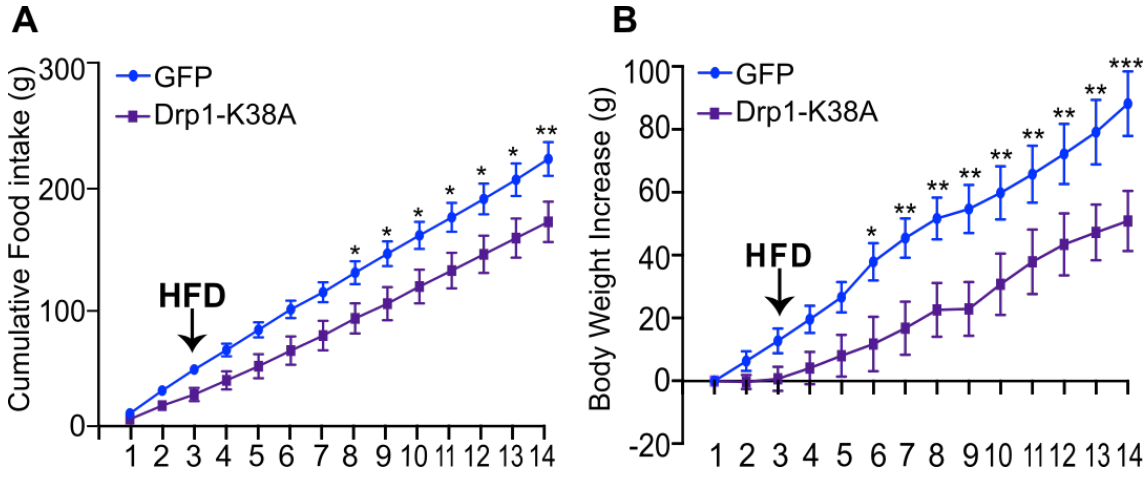

Figure 3.12 Cumulative food intake and body weight in the HFD-fed Drp1-K38A and GFP rats

A: Cumulative food intake in Drp1-K38A and GFP- control rats over the 14-day study, where day 1 is the day of viral injection

B: Body weight increase in Drp1-K38A and GFP- control rats over the 14-day period, where day 1 is the day of viral injection

All data are expressed as mean ± SEM *n*=8 for both GFP and Drp1-K38A

Statistical test: Two way ANOVA (post-hoc test: Sidak) [*p < 0.05, **p <0.01, *** p<0.001]

[3] Referring to the loss of insulin-induced hypophagia when stating rats are insulin resistant in data

an overall lower body weight gain compared to the GFP-expressing rats (Figure 3.12).

3.2.5.1 Chronic inhibition of Drp1 in the DVC results in a decrease in the total weight of WAT in rats

As inhibition of Drp1 in the DVC can decrease body weight gain in HFD-fed rats, I wanted to determine if this had an effect on fat deposition. The weight of the WAT was measured on the day of sacrifice (as previously described in section 3.2.2). Drp1-K38A-expressing rats had significantly less total amount of WAT compared to their GFP-expressing controls, there was also significantly lower amounts of retroperitoneal fat in these rats (Figure 3.13). These data highlight that inhibiting mitochondrial fission in HFD rats is sufficient to prevent the loss of insulin-induced hypophagia, leading to a decrease body weight gain, thus leading to a decrease in WAT deposition compared to HFD-fed controls.

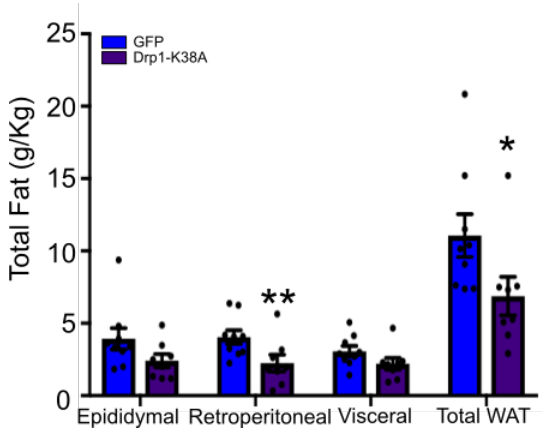

Figure 3.13 White adipose tissue deposition in Drp1-K38A and GFP rats

All data are expressed as mean ± SEM *n*=8 for both GFP and Drp1-K38A

Statistical Test: multiple T-test[*p < 0.05, **p <0.01, *** p<0.001]

3.2.5.2 Inhibition of Drp1 resulted in lower levels of ER-stress and iNOS in the DVC

Inhibition of Drp1 prevents insulin resistance and hyperphagia in HFD-fed rats. To understand what was happening on a molecular level, the DVC of the rats were lysed and a western blot was run to determine if there were changes in ER stress and iNOS levels (as detailed in section 2.6). Rats expressing Drp1-K38A had a decrease in ER stress as determined by phosphorylation levels of PERK compared to GFP expressing control littermates (Figure 3.14A). In addition, Drp1-K38A expressing rats also had a significant decrease in iNOS levels compared to GFP expressing controls (Figure 3.14B). The data presented highlights that inhibiting Drp1-dependent mitochondrial fission in the DVC can lower ER stress in HFD-fed rats. Furthermore, inhibition of mitochondrial fission can decrease iNOS levels in HFD-fed rats.

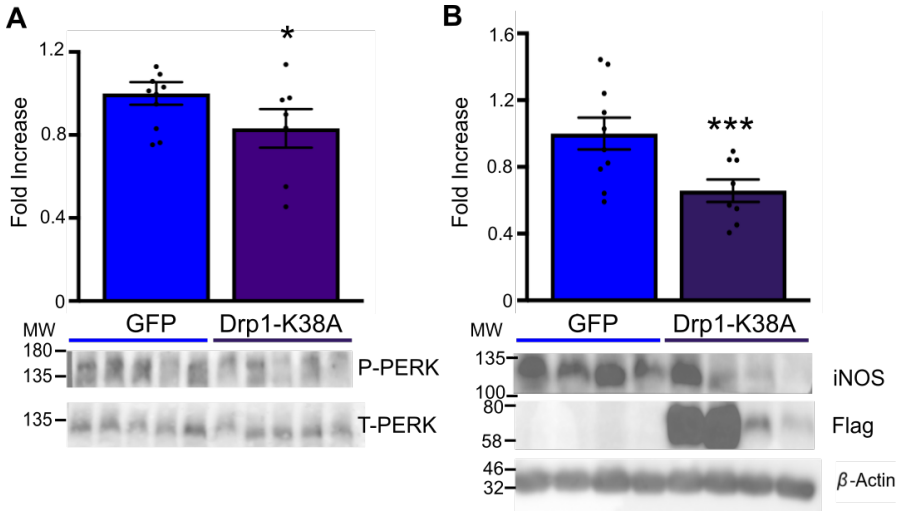

Figure 3.14 Inhibition of Drp1 in the DVC decrease ER-stress and iNOS in HFD-fed rats in the DVC

A: A representative western blot showing ER stress levels determined by phosphorylation levels of PERK in Drp1-K38A-expressing and GFP-expressing rats

B: A representative western blot of iNOS levels in rats expressing GFP or a dominant negative form of Drp1

All data are expressed as mean ± SEM *n*=8 for both GFP and Drp1-K38A (P-PERK: phosphorylated PERK, T-PERK: total-PERK) Statistical test: unpaired T-test [*p < 0.05, **p <0.01, *** p<0.001] Fold increase compared to control.

In summary, it is evident that inhibiting mitochondrial fission in the DVC can prevent insulin resistance (Figure 3.11), decrease cumulative food intake (Figure 3.12A), body weight (Figure 3.12B) and WAT deposition (Figure 3.13) in HFD-fed rats. In addition, inhibiting Drp1 can lower ER stress and iNOS levels (Figure 3.14).

3.3 Discussion

The data I have presented has demonstrated that an activation of Drp1-dependent mitochondrial fission in the DVC induces insulin resistance, hyperphagia and body weight gain in RC-fed rats. Previous work has shown that Drp1-dependent mitochondrial fission results in a decrease in ATP production and higher levels of mitochondrial fragmentation, which leads to reduced insulin mediated glucose uptake in muscles (Touvier et al., 2015). In genetic and diet induced obese mouse models, there is an increase in Drp1 dependent mitochondrial fission which includes insulin resistance in skeletal muscle (Jheng et al., 2012). Such results illustrate that mitochondrial dynamics are important in energy metabolism and insulin sensitivity (Bratic and Trifunovic, 2010; Maechler, 2013). For example overexpression of Drp1 in transmitochondrial cybrid cells decreased the mitochondrial network and increased mitochondrial ROS, which led to a decrease in the activation of the insulin signalling pathway (Lin et al., 2018). In addition, a decrease in the mitochondrial network has also been seen in the skeletal muscle of insulin resistant obese Zucker rats, highlighting the importance of mitochondrial dynamics in the development of insulin resistance (Bach et al., 2003).

In this study I have shown that inhibition of Drp1 in the DVC prevented the development of insulin resistance in HFD-fed rats. Previously it has been shown

that in an obese Zucker rat (fa/fa) model, which exhibit insulin resistance, hyperphagia and hyperlipidaemia, there is a decrease in glucose uptake and lower levels of mitochondrial fusion proteins such as MFN-2 in skeletal muscle (Putti et al., 2015). In the hypothalamus loss of the MFN-1 in POMC neurons impaired glucose sensing and insulin release, furthermore, in POMC neurones with the selective deletion of MFN-1 exhibit defective insulin sensing and an increase in ROS (Santoro et al., 2017; Schneeberger et al., 2013). On the other hand, deletion of Drp1 in POMC neurons was found to improve glucose metabolism (Santoro et al., 2017; Schneeberger et al., 2013).

Inhibition of MFN1 and -2 in Agrp neurons in the hypothalamus prevented diet induced obesity in rats fed a HFD (Dietrich et al., 2013), demonstrating that alterations that change mitochondrial dynamics in the hypothalamus can affect feeding behaviours. Inducible deletion of Drp1 in POMC neurons showed a significant increase in mitochondrial size, and resulted in better responsiveness to glucose (Santoro et al., 2017). Mitochondrial uncoupling protein 2 (UCP2) impairs glucose stimulated ATP production, where UCP2 negatively regulates glucose sensing in POMC neurones (Zhang et al., 2001). Genetic knockdown of UCP2 can prevent diet induced obesity and restore insulin sensitivity in ob/ob mice (Parton et al., 2007; Zhang et al., 2001), highlighting the importance of mitochondria in glucose sensing.

Much of the data regarding mitochondria dynamics and metabolism have been produced in the MBH, however, the DVC is also an important centre in the regulation of glucose metabolism, feeding behaviours and insulin sensing (Dash et al., 2015; Filippi et al., 2012b, 2014; MacDonald et al., 2019). It has been previously shown that a HFD can induce Drp1-dependent mitochondrial fission

resulting in insulin resistance, while activation of Drp1 recapitulates these effects in RC-fed rats (Filippi et al., 2017), emphasising the role that mitochondria has in the regulation of insulin sensitivity in the DVC. However, the effects of mitochondrial dynamics on feeding behaviours was not shown. Here for the first time I have shown that over expression of Drp1-S637A in the DVC can induce hyperphagia in the RC-fed rats. Furthermore, inhibiting Drp1-dependent mitochondrial fission in the DVC in HFD-fed rats prevents hyperphagia when compared to HFD-fed control littermates.

There are many cell types which may be involved in the pathophysiology of Drp1-dependent mitochondrial fission in the development of insulin resistance. In our experiments glial cells, such as astrocytes and microglia, as well as neurones were infected with the Drp1-expressing and GFP expressing adenoviruses. Glial cells play a key role in energy balance. acyl-CoA-binding protein-derived (ACBP-derived) endozepines bind to the $GABA_A$ receptor, in the hypothalamus, a knockdown of ACBP in astrocytes resulted in hyperphagia and body weight gain in rats, where viral rescue of ACBP restored these effects, these data suggest the feeding behaviours could be regulated by astrocytes (Bouyakdan et al., 2019). Astrocytes express iNOS and help control the brains microenvironment (Saha and Pahan, 2006). A ten day HFD was sufficient to induce an increase in astrocytes in the hypothalamus, these rats also had a significant increase in body weight and in fat content (Balland and Cowley, 2017). In addition to this, HFD-fed mice had a higher morphological complexity of GFAP labelled cells within the NTS compared to controls, furthermore, activation of astrocytes in the DVC resulted in a decrease of food intake, due to activation of distant and local,

neuronal circuits determining that astrocytes are involved in the homeostatic response to changes in food intake and energy balance (MacDonald et al., 2019).

Inhibition of NF-κB signalling in astrocytes resulted in a decrease in food intake in the first 24 hours (Buckman et al., 2015). Disrupted insulin signalling in astrocytes in the hypothalamus has also been shown to increase in blood glucose levels and appetite (García-Cáceres et al., 2016). A potential mechanism could be that changes in mitochondrial dynamics in astrocytes could affect the neuronal-glial cross-talk which is important in nutrient sensing. A possible way to test this is to target changes in mitochondria within the astrocytes specifically, by expressing Drp1-S637A or Drp1-K38A under the GFAP promoter, I will address this hypothesis in Chapter 5.

I have shown in the DVC changes in mitochondrial dynamics in the DVC can affect food intake and body weight gain. In mammalian cells, nutrient excess impairs autophagic degradation by inhibiting lysosomes and increases mitochondrial fragmentation, leading to mitochondrial dysfunction and resulting in an increase in ROS (Lee et al., 2004). In mice, a decrease in Drp1 expression in muscles resulted in a decrease in body weight in HFD-fed rats compared to controls (Jheng et al., 2012), which is consistent with the data I have presented.

Drp1-dependent mitochondrial fission in the DVC leads to an increase in the total amount of WAT deposition in RC-fed rats, while inhibition of Drp1-dependent mitochondrial fission in HFD-fed rats resulted in a decrease the total amount of WAT deposition compared to HFD-fed control rats. Muscle specific knockout of Drp1 also results in a decrease in the amount of WAT (Favaro et al., 2019). An increase in FFA, increases the oxidation of adipose tissue leading to an accumulation of lipids and mitochondrial dysfunction (Slawik and Vidal-Puig,

2006). Mitochondria dysfunction increases oxidative stress in tissues, leading to an increase in fat oxidation and lipid accumulation which is associated with insulin resistance (Gao et al., 2014). An increase in FFA leads to increased levels of ROS resulting in mitochondrial dysfunction and an increase in body weight (Jheng et al., 2012). These data suggest that rats with an activation of Drp1 in the DVC results in an increase in WAT which could increase in ROS, leading to an increase in fat oxidation. Additionally, an increase in WAT can cause a rise in blood glucose levels; high glucose levels can induce oxidative stress resulting in mitochondrial fragmentation mediated by Drp1 (Smirnova et al., 2001; Sparrow et al., 1986), it would have been interesting to see how inhibition or activation of Drp1 effected blood sugars in these experiments.

The data I have presented demonstrates that inhibiting Drp1-dependent mitochondrial fission in the DVC can reduce ER stress in HFD-fed rats. ER-stress is mediated by ER-resident transmembrane proteins, such as IRE1α and PERK, where an increase in these markers has been associated with metabolic disorders (Schröder and Kaufman, 2005). Mitochondrial dysfunction has been directly linked to ER stress response which can cause disruption to insulin signalling (Lim et al., 2009). In this chapter I have shown that an activation of Drp1 in the DVC of RC-fed rats increased ER stress levels which is in accordance with Filippi et al. 2017. It is well known that a HFD can lead to an increase in ER-stress (Filippi et al., 2017; Wang et al., 2015; Yang et al., 2015a; Zanotto et al., 2017).

An increase in unfolded proteins in the ER causes an increase in ROS leading to higher levels of ER stress, causing an increase in mitochondrial radicals upregulating inflammatory responses (Chaudhari et al., 2014; Green et al., 2004;

Li et al., 2016). A marker of inflammation is iNOS (Fujimoto et al., 2005; Soskić et al., 2011), and I have demonstrated here that an activation of Drp1 in the DVC leads to an increase in iNOS levels. Rats expressing a constitutively active form of Drp1 in the DVC had higher iNOS levels compared to their control littermates.

Rats given a HFD had higher levels of iNOS in the muscles leading to insulin resistance (Perreault and Marette, 2001). In addition, mRNA levels of iNOS were decreased in BV2 microglial cells when treated with LPS in the presence of an inhibitor of Drp1, MDIVI-1 (Park et al., 2013). Altogether these data indicate that iNOS levels are decreased when mitochondrial fission is inhibited. In addition to this, previous work has shown that infusion of nitric oxide, to mimic the effect of iNOS in the hypothalamus resulted in insulin resistance and an increase in food intake (Katashima et al., 2017). Such findings are consistent with the data I have presented here that inhibition of Drp1-dependent mitochondrial fission decreases iNOS levels to protect HFD-fed rats for insulin resistance.

A potential mechanism that could link Drp1-dependent mitochondria fission, ER-stress and insulin resistance is an increase in iNOS levels which increases the release of NO, leading to S-nitrosylation of molecular players involved in ER stress inducing thereby insulin resistance. For example, in muscle, exogenous NO induced s-nitrosylation of the insulin receptor β subunit and IRS-1, induced insulin resistance. In muscle chemical reversal of s-nitrosylation resulted in an improvement in insulin signalling (Carvalho-filho et al., 2005). An increase in hepatic iNOS levels resulted in s-nitrosylation of a key UPR regulator, IRE1α, which increased ER-stress levels resulting in insulin resistance (Yang et al., 2015a). In addition, Drp1 can be s-nitrosylated under high oxidative stress which can increase the rate of mitochondrial fission and cause changes in energy

imbalance (Morris et al., 2018b; Nakamura et al., 2010). Collectively, it is evident that increasing mitochondrial fission results in higher levels of iNOS which induces s-nitrosylation of different markers involved in the insulin signalling pathway. It is yet to be determined if the iNOS induces s-nitrosylation inducing insulin resistance in the DVC.

The experiments presented in this chapter have shown that mitochondrial fission is a key player in the development of insulin resistance, and data has demonstrated that it is highly important in feeding behaviours and body weight gain. In summary, an increase in Drp1-dependent mitochondrial fission increases ER stress and iNOS levels inducing insulin resistance resulting in hyperphagia. It is still unclear the molecular mechanism that links the changes in mitochondria dynamics to ER stress and insulin resistance (Figure 3.15). This will be investigated in the next chapter.

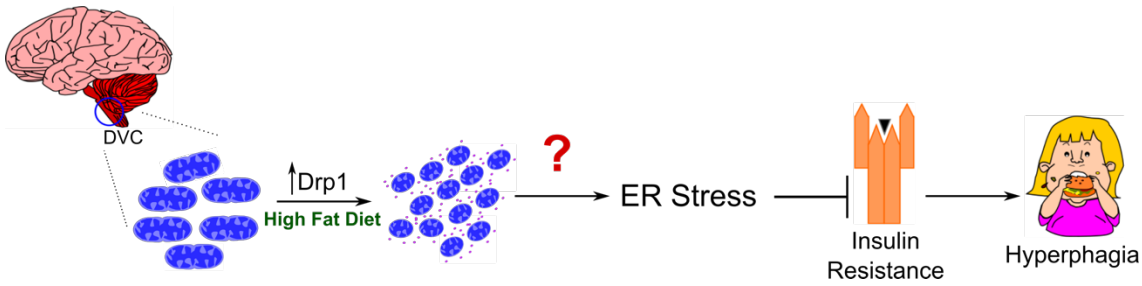

Figure 3.15 Summary of chapter and working hypothesis: Activation of Drp1 in DVC induces insulin resistance and hyperphagia

4 Knocking down iNOS in the DVC of the brain prevents HFD-dependent insulin resistance and hyperphagia

4.1 Introduction

iNOS is a mediator of inflammation and plays an important role in the pathophysiology of insulin resistance (Evans and Goldfine, 2013; Fujimoto et al., 2005). In the DVC, an increase in mitochondrial fission led to an increase in iNOS levels in HFD-fed rats (Filippi et al., 2017), in addition to this, I have previously demonstrated that activation of Drp1 can significantly increase the levels of iNOS in the DVC. However, it is yet to be determined if iNOS is one of the key links between mitochondrial fission and ER stress which leads to hyperphagia and insulin resistance (Figure 4.1). I aim to investigate the effects of iNOS on insulin sensitivity in the DVC.

iNOS is a calcium independent enzyme, which aids in synaptic transmission and can induce inflammation. NO is a small messenger molecule and can control regulatory functions, such as neuronal activation and vasodilation. NO is highly reactive and is synthesised very rapidly, aberrant levels of NO can lead to oxidative damage and tyrosine nitration (Förstermann and Sessa, 2012). NO can also react with sulfhydryl groups on proteins which leads to s-nitrosothiol groups, this reaction is referred to as s-nitrosylation (Hess et al., 2005; Lee and Kim, 2018; Nakamura et al., 2013). S-nitrosylation can change the enzymatic activity of proteins by modulating the cysteine residues (Lee and Kim, 2018). An excess of NO can result in s-nitrosylation of Drp1 and increases GTPase activity, in turn causing excessive mitochondrial fragmentation which has been linked to neurodegenerative diseases (Cho et al., 2009; Soonpaa et al., 2009).

Increased iNOS levels induces S-nitrosylation of key UPR regulators altering ER homeostasis (Yang et al., 2015a). There is growing evidence associating inflammation and ER stress in obesity which can result in the onset of insulin

resistance (Lee and Ozcan, 2014; Yang et al., 2015a; Zanotto et al., 2017). In both obese and HFD-fed mice increased levels of UPR regulators, PERK and IRE-1α were observed in both the liver and adipose tissue (Boden, 2009; Nakatani et al., 2005; Özcan et al., 2006). XBP1, a transcription factor which modulates ER stress. Mice deficient in XBP1 developed insulin resistance and had an increase body weight compared to controls, highlighting the key role ER stress plays in the development of insulin resistance (Özcan et al., 2004; Park and Ozcan, 2013).

In addition to this, an excess of NO can cause aberrant mitochondrial fission and cell death in cortical neurones, however the mechanisms by which this happens is not fully understood (Barsoum et al., 2006; Knott and Bossy-Wetzel, 2009). Protein disulphide isomerase (PDI) is a chaperone in the ER, it can induce s-nitrosylation of Drp1 which alters mitochondrial dynamics in neuronal degeneration. Inhibition of NO or PDI in CA1 neurones significantly improved mitochondrial dynamics in models of epilepsy, however whether s-nitrosylation of Drp1 can induce insulin resistance by a similar mechanism is not well understood (Lee and Kim, 2018). In this chapter, I aim to study whether alterations in mitochondrial dynamics in PC12 cells can induce changes in s-nitrosylation levels, to this aim, I developed an assay which specifically isolated nitrosylated proteins from neuronal cell lysates.

There is evidence to suggest that links increases in NO production and insulin resistance leading to type II diabetes (Foster et al., 2009). This is thought to be due to iNOS dependent s-nitrosylation of key signalling protein of the insulin signalling pathway, such as AKT, the insulin receptor β subunit and IRS-1 as has been demonstrated in diabetic murine models (Carvalho-filho et al., 2005;

Yasukawa et al., 2005). Aging can increase iNOS expression, which in turn can lead to an increase in s-nitrosylation induced insulin resistance, furthermore, when iNOS was inhibited in old mice, mice were protected from iNOS induced s-nitrosylation mediated insulin resistance (Ropelle et al., 2013). In addition to this, iNOS deficiency in skeletal muscle and genetic inhibition of iNOS in adipose tissue and in the liver prevented HFD-induced insulin resistance in mice (Fujimoto et al., 2005; Zanotto et al., 2017). Furthermore, knocking down iNOS in mice ($Nos2^{-/-}$) prevented diet-induced obesity and insulin resistance and preserved skeletal muscle insulin sensitivity in HFD-fed mice (Perreault and Marette, 2001). Infusion of NO into the hypothalamus resulted in insulin resistance and an increase in food intake, where inhibition of NO significantly improved insulin sensitivity and food regulation in HFD-fed rats (Katashima et al., 2017). In this chapter I wanted to investigate the role iNOS in the DVC has on insulin sensing, feeding behaviours and body weight gain in HFD-fed rats.

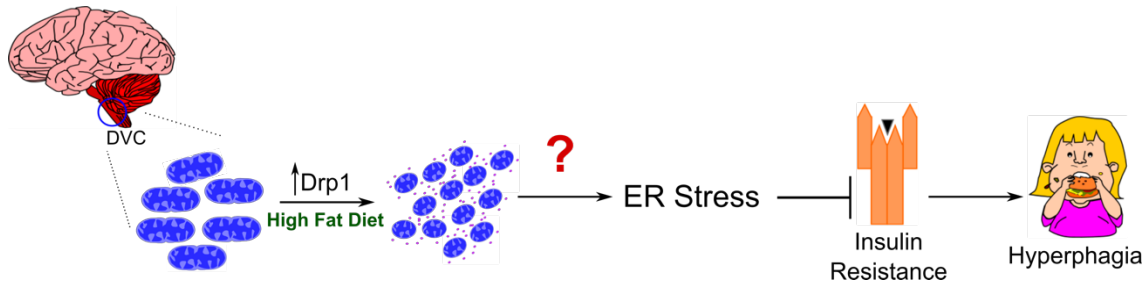

Figure 4.1 Over expression of Drp1 in the DVC can prevent insulin-induced hypophagia, my next aim is to determine if iNOS is the link inducing this?

4.1.1 Aims and objectives

Aim 1: Does over expression of mitochondrial fission protein, Drp1, in PC12 cells increase iNOS levels thus affecting NO production and nitrosylation levels?

Aim 2: Can inhibition of iNOS in the DVC prevent HFD-dependent effects on insulin sensitivity, food intake and body weight gain?

4.2 Results

4.2.1 Determining the correct multiplicity of infection (MOI) to infect PC12 cells

MOI is defined as the number of virions that are added per cell during infection, this ratio can be determined by the concentration of the virus and the number of cells (Thomas, 2001). Firstly, I aimed to examine the expression of each of the Drp1-mutant-FLAG viruses and GFP using western blotting methods (as described in section 2.6), to determine if I had equal expression. PC12 cells, a rat neuronal call line, were infected with varying MOI's of 30, 40, 50 and 70 of Drp1-S637A, Drp1-K38A or GFP and left for 48 hours, to determine protein expression. I found that when treated at a MOI of 30 and 40, the expression in Drp1-mutants determined by FLAG or GFP was not similar to one another (Figure 4.2). From this, I established that I would need a higher MOI for Drp1-S637A than for both Drp1-K38A and GFP. Following this, I decided to infect PC12 cells with a MOI for 70 for Drp1-S637A and a MOI of 50 for both Drp1-K38A and GFP

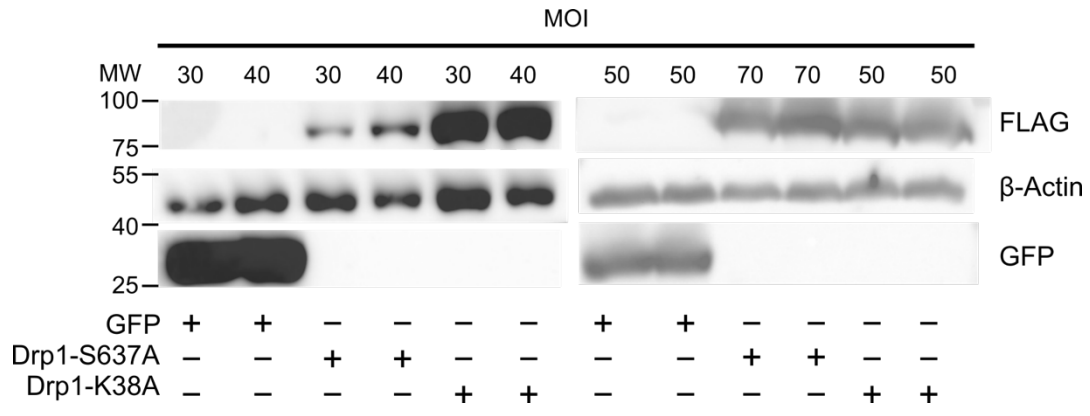

Figure 4.2 Determining the correct MOI to infect PC12 cells

PC12 cells were infected at varying MOIs of either GFP, Drp1-K38A or Drp1-S637A for 48 hours, samples were run on a western blot to determine the expression of the protein (using FLAG) in each sample. Data are shown as a representative western blot

(Figure 4.2). The western blots highlighted a similar expression, it therefore was decided PC12 cells would be infected at these MOI's (Figure 4.2).

4.2.2 Activation of Drp1 in PC12 cells increases iNOS levels

I have previously demonstrated that rats expressing a constitutively active form of Drp1 in the DVC had higher levels of iNOS in the DVC (see section 3.2.3.4). Following on from this, I wanted to understand whether changes in iNOS levels due to Drp1-dependent mitochondrial fission can affect NO production and consequently nitrosylation levels. To replicate the data I found in rats, PC12 cells, were infected with the adenoviruses expressing the constitutively active form of Drp1, Drp1-S637A, the dominant negative form of Drp1, Drp1-K38A or a control of GFP, for 48 hours. Cells were collected, lysed and prepared for western blotting (see section 2.6). PC12 cells expressing Drp1-S637A had a higher level of both iNOS (Figure 4.3) when compared with PC12 cells expressing with catalytically inactive form of Drp1, Drp1-K38A or a control of GFP.

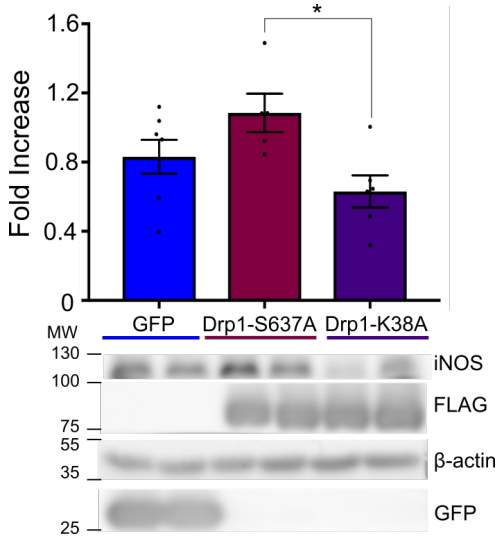

Figure 4.3 Representative western blots for iNOS expression in PC12

Cells infected with either the constitutively active form of Drp1, Drp1-S637A; the dominant negative form of Drp1, Drp1-K38A or a control of GFP iNOS expression of PC12 cells infected with GFP; Drp1-S637A or Drp1-K38A (*n*=7 for GFP; *n*=5 Drp1-S637A and *n*=6 Drp1-K38A). Statistical test: unpaired T-test [*p<0.05]

4.2.3 Development of the S-nitrosylation TMT assay

Activation of Drp1 increased iNOS levels in PC12 cells, furthermore, it has been well established that an increase in iNOS levels can induce s-nitrosylation of thiol groups on cysteine residues (Anavi and Tirosh, 2020; Förstermann and Sessa, 2012; Hess et al., 2005). S-nitrosylation results in nitrosative stress which as a result affect cellular homeostasis and signalling pathways, thereby altering protein activity (Anavi and Tirosh, 2020). Increased levels of iNOS induce s-nitrosylation of key players in the insulin signalling pathway such as AKT and the insulin receptor, resulting in insulin resistance (Anavi and Tirosh, 2020). I set out to look into the effect of Drp1 had on s-nitrosylation levels in PC12 cells and by performing an iodoTMT assay (see section 2.7). In the initial trial of the assay I came across a few problems with the effectiveness and replicability of the assay, to enable maximum capture of nitrosylated proteins, the assay went through troubleshooting. The assay principally has three main steps, the first step is to block any free nitro groups with MMTS, next to selectively reduce s-nitroso groups with sodium ascorbate and finally to selectively label these s-nitroso groups with iodoTMT (Figure 4.4).

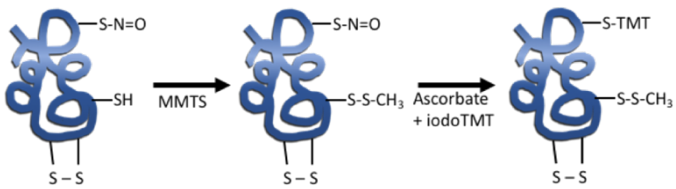

Figure 4.4 IodoTMT S-nitrosylation assay protocol

Samples are blocked with MMTS to block any free sulfhydryl groups, next, s-nitrocysteine groups are selectively reduced using sodium ascorbate and labelling with iodoTMT. iodoTMT can then be examined using western blotting methods with an antibody against TMT to see s-nitrosylated proteins

DTT is a reducing agent that can open all the disulphide bonds, DTT was used as a negative and a positive control to determine the efficacy of iodoTMT labelling. One sample was treated with DTT and blocked with MMTS to act as a negative control and another sample was treated with DTT, but was not blocked with MMTS to allow full labelling by iodoTMT. In addition to this. collected cell lysates were treated with 200 μM of s-nitroglutathione (GSNO) to increase the levels of s-nitroso groups or treated with 200 μM of glutathione (GSH) to inhibit modifications to the cysteines on the thiol groups. As discussed previously, one of the main steps is to selectively reduce s-nitroso groups with sodium ascorbate, to ensure the material that was captured was specifically s-nitrosylated, each sample was split in half and only half was treated with sodium ascorbate for the remaining half nothing was added, to give an additional negative control.

The s-nitrosylation assay demonstrates that treating cell lysates with DTT labels all bonds, while treating cells with DTT and blocking with MMTS successfully managed to block labelling (Figure 4.5). In addition, the data shows that treating cell lysates with GSNO resulted in a small increase in the level of nitrosylated proteins compared to GSH treated cells (Figure 4.5). Furthermore, samples which were not reduced with sodium ascorbate showed no staining, determining that the reduction with sodium ascorbate is essential for the assay to work. In summary, I successfully established the s-nitrosylation assay, next I aimed to apply this assay to assess the nitrosylation levels in PC12 cells expressing the constitutively active form or the dominant negative form of Drp1, Drp1-S637A and Drp1-K38A respectively.

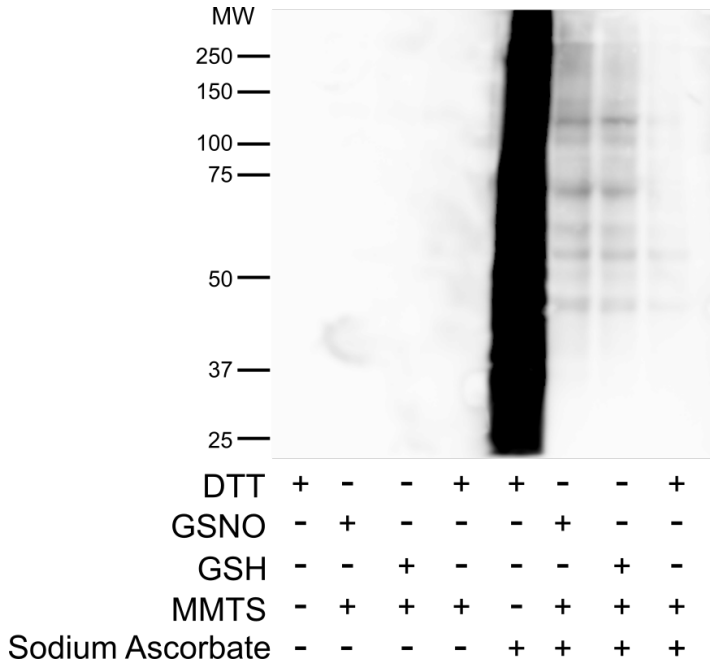

Figure 4.5 A representative western blot of the S-nitrosylation TMT assay levels in initial troubleshooting methods.

Cells treated with GSNO (positive control) had higher nitrosylation levels when compared to cells treated with GSH (negative control). Sodium ascorbate is essential for the reduction of the samples to be specifically labelled by iodoTMT

4.2.4 Immunoprecipitation captures s-nitrosylated proteins

I have demonstrated that the TMT assay labels s-nitrosylated proteins. In order to determine if I could specifically isolate and label s-nitrosylated proteins, I ran an immunoprecipitation experiment (as detailed 2.7.4). Levels of eluted iodoTMT labelled s-nitrosylated proteins were seen using western blotting methods (as described in section 2.6). Samples used were all selectively reduced with sodium ascorbate. The supernatant was collected from the flow through, elution 1 and 2 (Figure 4.6). The results demonstrate that as expected, that largest amount of nitrosylated protein was found in the sample treated with DTT. More interestingly, TMT labelled proteins eluted in the cell lysates treated with GSNO were higher than the GSH TMT labelled proteins eluted (Figure 4.6). In comparison to the

initial lysate that had been through the Pierce S-nitrosylated assay, I have successfully managed to enhance the expression of s-nitrosylated proteins using concentration (Figure 4.6).

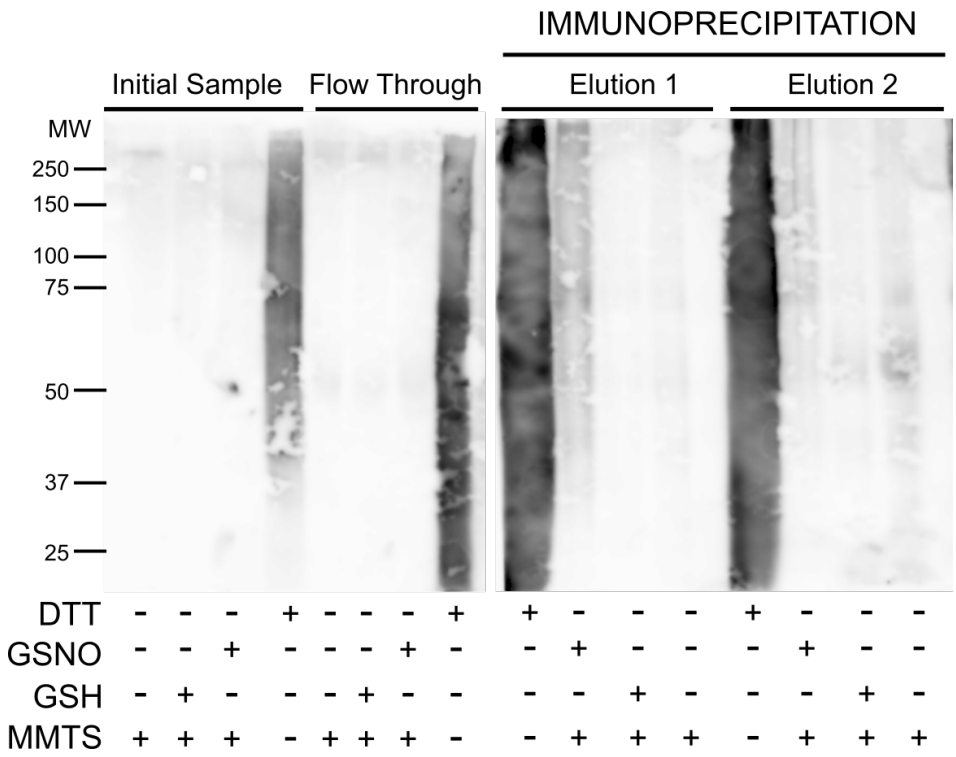

Figure 4.6 Immunoprecipitation specifically isolates iodoTMT labelled s-nitrosylated proteins.

Cells were treated with GSNO, GSH or DTT and a nitrosylation assay was run and samples were labelled with iodoTMT. Following this, immunoprecipitation was carried out using the anti TMT antibody with labelled samples. The immunoprecipitation determined by Elution 1 and 2 demonstrate that cells treated with GSNO had higher levels of s-nitrosylated proteins compared with GSH treated samples.

4.2.5 Activation of Drp1 increases s-nitrosylation levels in PC12 cells

I have successfully troubleshooted the TMT assay to capture and label s-nitrosylated proteins. Using these same methods, I wanted to investigate the effect that mitochondrial fission had on nitrosylation levels. PC12 cells were infected at a MOI of 70 for Drp1-S637A or 50 for Drp1-K38A and GFP, cells were left for 48 hours and then collected. The TMT s-nitrosylated assay was carried out as described in section 2.7. Using western blotting methods to look into s-nitrosylation levels, it is evident that when cell lysates were treated with GSNO, there was a higher level of nitrosylation levels compared to cell lysates which were treated with GSH. More interestingly, cells infected with Drp1-S637A (the

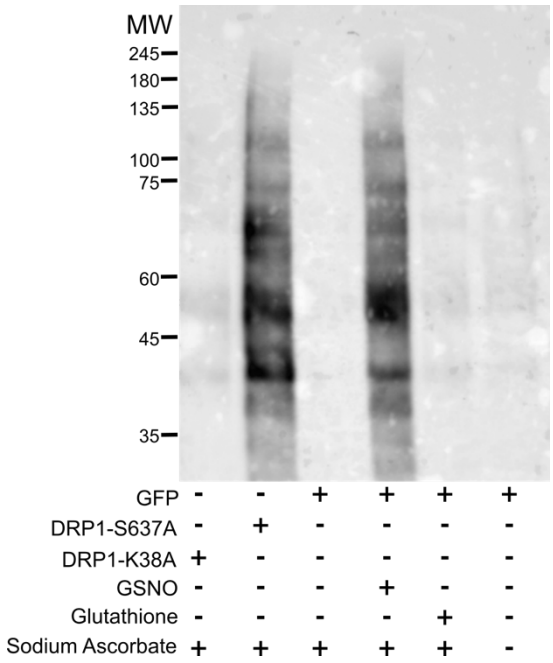

Figure 4.7 The effect changes in mitochondrial dynamics have on nitrosylation levels in PC12 cells

PC12 cells were infected with Drp1-S637A, Drp1-K38A or GFP for 48 hours and were collected to run a nitrosylation assay to determine levels of nitrosylation using western blotting methods. Activation of Drp1 in PC12 cells, using Drp1-S637A adenovirus, increased nitrosylation levels when compared to PC12 cells infected with Drp1-K38A or GFP. GSNO and GSH were used as positive and negative control, respectively.

constitutively active from of Drp1) had higher levels of nitrosylation levels when

compared with cells infected with both Drp1-K38A (the catalytically inactive form of Drp1) and GFP (Figure 4.7). These data highlights that activation of Drp1 can increase the levels of s-nitrosylation in PC12 cells.

4.2.6 Knocking down iNOS in the PC12 cells decreases levels of S-nitrosylation

Activating Drp1 in PC12 cells increased levels of s-nitrosylation, next I wanted to confirm whether these changes in nitrosylation were due to changes in iNOS levels. To this aim, I decided to knock down iNOS in PC12 cells. I created a stable PC12 cell line expressing ShRNA for iNOS to selectively knockdown iNOS (ShiNOS) or a control of a scrambled ShRNA (ShControl) (as described in section 2.7.3). There was a significant decrease of 58% in iNOS protein levels in the PC12 cells expressing ShiNOS when compared to the control cell line (Figure 4.8).

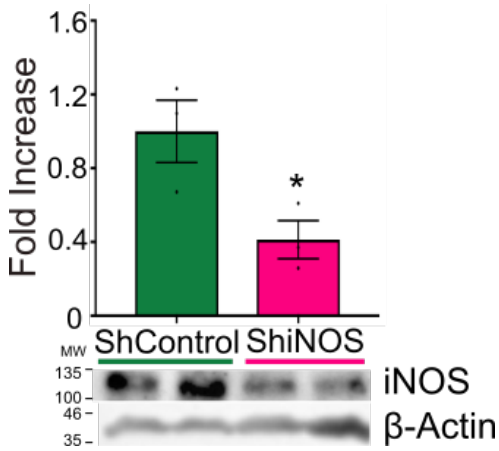

Figure 4.8 A representative western blot to show successful knockdown of iNOS in PC12 cells.

All data are expressed as mean ± SEM *n*=3 for ShControl and ShiNOS-expressing cells
Statistical Test: Unpaired T-test [*p < 0.05]

From the literature, it is evident that iNOS can induce the post-translational modification, s-nitrosylation (Förstermann and Sessa, 2012). The nitrosylation assay was repeated with cell lysates of PC12 cells expressing the knockdown of iNOS, ShiNOS or the control, ShControl. The western blot shows that ShiNOS-expressing PC12 cells had a decrease in s-nitrosylation levels compared with ShControl-expressing PC12 cells, supporting literature that decreasing iNOS levels can reduce s-nitrosylation levels (Figure 4.9).

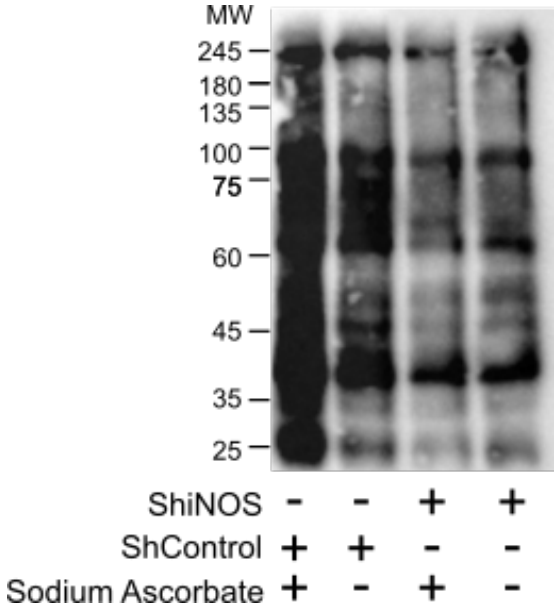

Figure 4.9 Decreasing iNOS expression in PC12 cells decreased the levels of s-nitrosylation

Representative western blot of S-nitrosylation iodoTMT assay in PC12 cells expressing ShiNOS or ShControl. Cell lysates were either selectively reduced with sodium ascorbate or without to act as a negative control.

4.2.7 Knocking down iNOS in the DVC prevents HFD dependent insulin resistance

In previous chapters I have demonstrated that activation of Drp1 can increase iNOS levels in the DVC of rats and in addition to this, an increase s-nitrosylation levels in-vitro were seen in cells infected with Drp1-S637A. Following this, I wanted to investigate the effect decreasing iNOS levels in the DVC had on feeding behaviours, body weight gain and insulin sensitivity in HFD-fed rats. Stereotactic surgery was performed where a bilateral cannula was inserted into the NTS of the DVC, at the same time, a lentiviral system was used to deliver a ShRNA against iNOS mRNA to knockdown the protein (ShiNOS) or a control (ShControl) (day 0) (Figure 4.10). An acute feeding study was carried out on day nine and 16 where insulin was infused into the DVC of fasted rats, food intake was measured every half an hour for four hours (Figure 4.10).

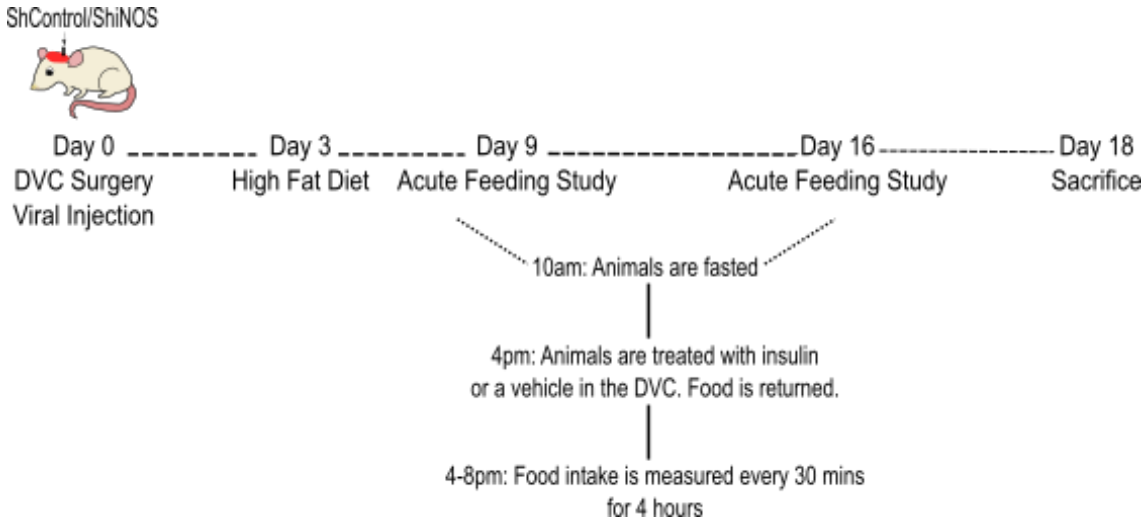

Figure 4.10 Feeding protocol for ShiNOS and ShControl cohort

Rats were implanted with bilateral cannula and injected with either ShiNOS or ShControl on day 0, these rats were then changed to HFD on day 3. On day 9 and 16 these rats underwent a feeding studying to monitor acute feeding behaviours. On day 16 these rats were sacrificed.

To determine I had successful delivery of the lentiviral system to knockdown iNOS in the DVC, both western blot (as detailed in section 2.4) and IHC (as detailed in 2.7) were used to confirm a decrease in iNOS expression. The data shows a significant 52% decrease in iNOS levels in the rats expressing ShiNOS, compared to ShControl expressing littermates (Figure 4.11A). Furthermore, using IHC, I have also demonstrated that there is a decrease in the staining of iNOS in the NTS of DVC. These data highlight the specificity of the surgery and lentiviral delivery (Figure 4.11B).

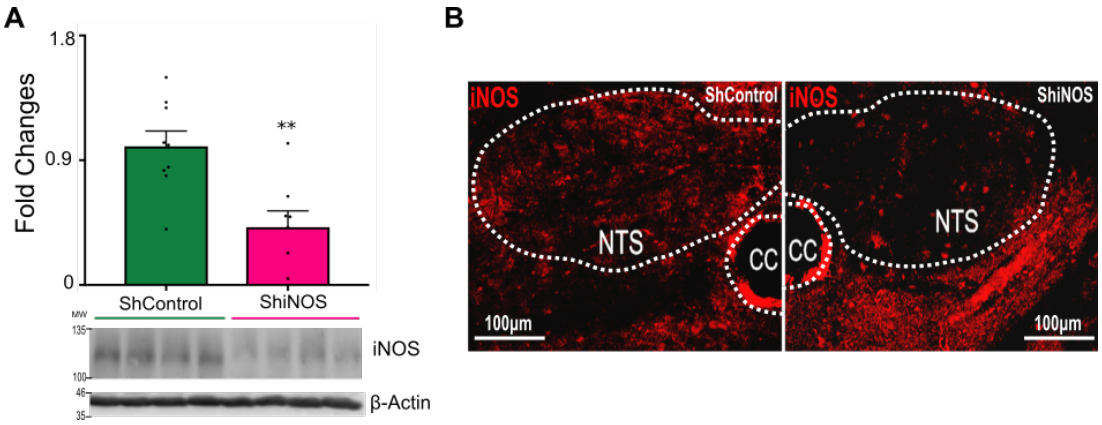

Figure 4.11 Confirmation of decreased iNOS expression in the DVC of rats injected with ShiNOS or ShControl in the NTS

A: A representation of the successful knockdown of iNOS in the DVC. *n*=10 for control, *n*=8 for shiNOS.

B: A representative confocal image of iNOS labelling in rats expressing the knockdown of iNOS (ShiNOS) or the control (shControl) in the NTS of the DVC.

[*p < 0.05, **p <0.01, *** p<0.001, ****p<0.0001]

On day nine and 14 I carried out an acute feeding study where insulin or a vehicle were infused into the bilateral cannula targeting the NTS of DVC in fasted rats. Their food intake was observed every half an hour for four hours. The data I obtained shows rats expressing ShControl, failed to decrease their food intake when treated with insulin (insulin treated ShControl ate an average of 3.94g compared to vehicle treated ShControl who on average ate 4.10g), demonstrating that these rats are insulin resistant (Figure 4.12A). On the other

hand, rats expressing ShiNOS in the DVC, were still sensitive to insulin and demonstrated a significant 53% decrease in food intake compared to their vehicle treated littermates. These data show that decreasing iNOS levels in the DVC is sufficient to protect rats from developing HFD-dependent insulin resistance[4] (Figure 4.12A). ShiNOS-expressing rats also had a significant 30% decrease in food intake at 12 hours (Figure 4.12B).

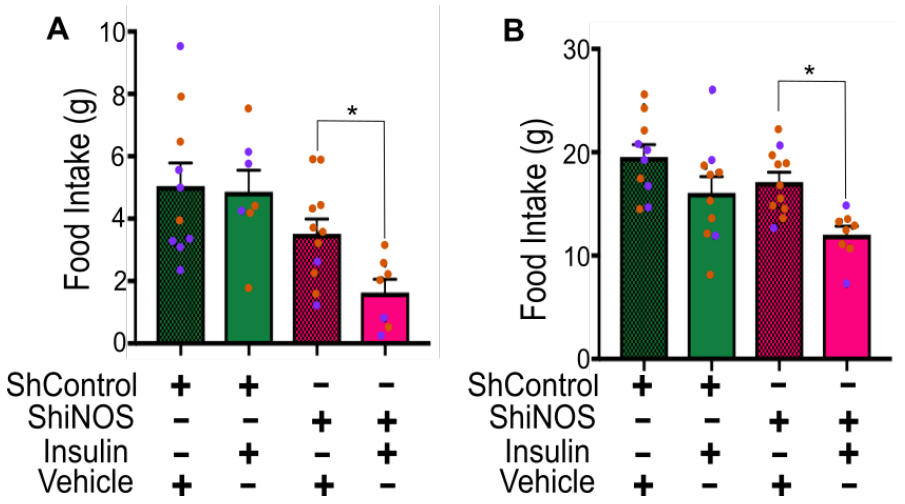

Figure 4.12 Food intake during acute feeding studies in rats expressing ShiNOS versus a control, ShControl

Rats were fasted for 6 hours and then infused bilaterally into the DVC with a total 0.2ul of 2mU insulin or a vehicle over 5 minutes. Food was then returned and food intake was observed every half hour for 4 hours and a final reading was taken at 12 hours.

A: Total food intake taken at the 4 hour time point, since there was no difference in the food intake in the feeding studies performed on day nine and fourteen, the figure shows the average food intake over both feeding studies

B: Total food intake taken at the 12 hour time point, since there was no difference in the food intake in the feeding studies performed on day nine and fourteen, the figure shows the average food intake over both feeding studies

Data are expressed as a mean ± SEM *n*=10 for control vehicle, *n*=7 control insulin, *n*=11 for shiNOS vehicle, *n*=7 for shiNOS insulin. Orange dots represent data gained from day 9, purple dots represent data gained from day 14.

Statistical test: two-way ANOVA (post-hoc test: Sidak) [*p < 0.05]

[4] Referring to the loss of insulin-induced hypophagia when stating rats are insulin resistant in data

4.2.8 Decreasing iNOS expression in the DVC can decrease food intake and body weight in HFD-fed rats

Knocking down iNOS in the DVC was sufficient to prevent insulin resistance in HFD-fed rats. Next, I wanted to determine the effect that knocking down iNOS had on food intake and body weight. Rats had their body weight and food intake taken at a similar time each day, to keep data consistent. The ShiNOS-expressing rats ate less food when compared with control littermates, where significance was reached at day 7 (Figure 4.13A). In addition, ShiNOS-expressing rats had an overall decrease in body weight, which is significant from day 12 (Figure 4.13B). Overall, I have demonstrated that knocking down iNOS in the NTS of the DVC can decrease food intake and body weight increase in HFD-fed rats.

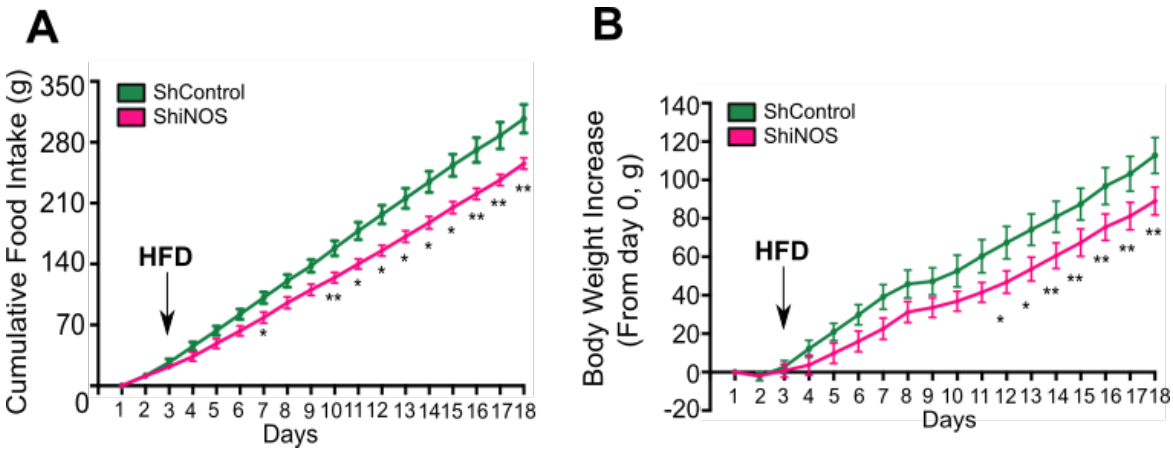

Figure 4.13 Cumulative food intake and body weight increase during the study in ShControl-expressing rats compared to ShiNOS-expressing rats

A: Cumulative food intake in ShiNOS and ShControl-expressing rats from day of viral injection (day 0)

B: Body weight increase in ShiNOS and ShControl-expressing rats from day of viral injection (day 0)

All data are expressed as mean ± SEM *n*=10 for ShControl-expressing rats and *n*=8 ShiNOS-expressing rats

Statistical Test: two way ANOVA (post-hoc test: Sidak) [*p < 0.05, **p <0.01]

4.2.9 Decreasing iNOS expression in the DVC of the brain decreases total WAT in HFD-fed rats

Decreasing iNOS expression in the DVC resulted in a decrease in food intake and body weight gain in HFD-fed rats, following from this, I wanted to investigate the effect of iNOS on WAT distribution. On day 18, the day of sacrifice, epididymal, retroperitoneal and visceral fats were collected and weighed. Knocking down iNOS in the DVC significantly decreased the total weight of the WAT and visceral fat, in addition, there was a significant decrease in the weight of epididymal and retroperitoneal fat specifically when compared to HFD-fed ShControl-expressing rats (Figure 4.14A). BAT energy expenditure is regulated by neural circuitry, vagal nerve stimulation has helped decrease weight gain in humans, to this end, BAT was weight from this cohort (Berthoud, 2008; Morrison

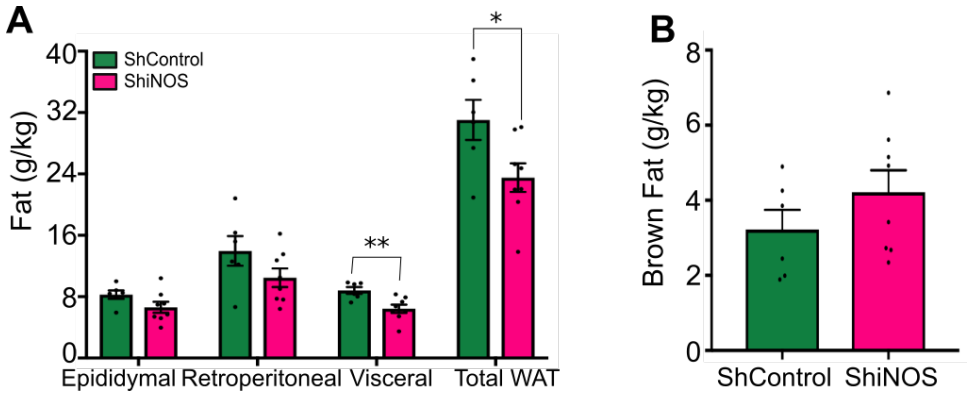

Figure 4.14 Weight of white adipose tissue and brown adipose tissue

A: Weight of white adipose tissue expressing a knockdown of iNOS, ShiNOS or a control, ShControl

B: Weight of brown adipose tissue in rats expressing a knockdown of iNOS, ShiNOS, or a control, ShControl

Body weight was divided by the weight of fat to establish fat distribution (g/kg). All data are expressed as mean ± SEM *n*=10 for ShControl expressing rats and *n*=8 ShiNOS-expressing rats

Statistical Test: multiple T-test [*p < 0.05, **p <0.01]

and Madden, 2014). Rats expressing ShiNOS had no changes in BAT compared to HFD-fed controls, ShControl-expressing rats (Figure 4.14B).

4.2.10 Knocking down iNOS in HFD-fed rats decreases levels of ER-stress in the DVC

I have demonstrated that knocking down iNOS in the DVC can prevent HFD-dependent loss of insulin-induced hypophagia and can also decrease food intake, body weight gain and WAT deposition. Since it has been previously demonstrated that HFD-fed rats had increased levels of ER-stress in the DVC (Filippi et al., 2017), next, I wanted to investigate the effects of iNOS levels on ER stress. On the day of sacrifice the DVC of rats was collected and snap frozen, and ER stress levels were analysed using western blotting methods (as described in section 2.4). Decreasing iNOS expression in the DVC of ShiNOS-expressing rats significantly decreased the levels of ER stress levels determined by the phosphorylation levels of PERK compared to HFD-fed rats (Figure 4.15).

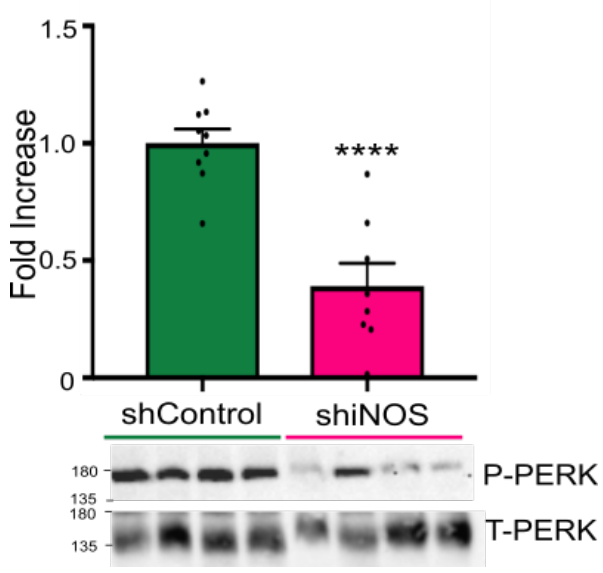

Figure 4.15 Knocking down iNOS in the DVC of HFD-fed rats decreases phosphorylation levels of PERK

All data are expressed as mean ± SEM *n*=10 for ShControl expressing rats and *n*=8 ShiNOS-expressing rats. (P-PERK: phosphorylated PERK, T-PERK: total-PERK) Statistical test: unpaired T-test [****p<0.0001]

In summary, I have demonstrated the knocking down iNOS in HFD-fed rats can decrease ER stress levels, fat mass, food intake and body weight gain and can also prevent HFD-dependent insulin resistance compared to HFD-fed controls.

4.3 Discussion

I have previously shown that an over expression in Drp1 increased iNOS levels in the DVC, where inhibition of Drp1 in HFD-fed rats decreased the levels of iNOS. These data led me to investigate the effects of iNOS on insulin sensing and feeding behaviours. My data demonstrates that knocking down iNOS in the DVC prevented the development in insulin resistance in HFD-fed rats. This is in agreement with previous work which shows that subcutaneous injections of L-arginine, which increase NO, increased food intake in fasted mice, where inhibition of NO, decreased food intake in these mice (Morley and Flood, 1991). In the brain, infusion of NO into the hypothalamus resulted in insulin resistance and an increase in food intake (Katashima et al., 2017). Similarly, ICV administration of s-nitroglutathione increased s-nitrosylation in the hypothalamus, but also inhibited hypothalamic insulin signalling in rats, leading to insulin resistance (Katashima et al., 2017).

Higher levels of iNOS in the liver have been associated with insulin resistance, in obese mice, where inhibition of iNOS in the liver, increased protein expression of IRS-1 and -2 by 2-fold, and significantly improved insulin sensitivity and decreased food intake (Fujimoto et al., 2005). In muscle, induction of iNOS is an essential mechanism in the development of insulin resistance, where inhibition of iNOS in the muscle significantly improved insulin signalling in HFD-fed mice (Zanotto et al., 2017). Furthermore, an increase in s-nitrosylation of the insulin signalling pathway has been seen in obese rats, where ICV injection of an

inhibitor of iNOS restored hypothalamic insulin sensitivity in HFD-fed rats (Katashima et al., 2017). It is therefore apparent that iNOS is a key player in the development of insulin resistance.

I have shown that decreasing iNOS expression in the DVC can prevent HFD-dependent insulin resistance. Knocking down iNOS in HFD-fed mice ($Nos2^{-/-}$) protected them from diet induced obesity and insulin resistance, and preserved skeletal muscle insulin sensitivity (Perreault and Marette, 2001). This was due to disruption of the PI3K pathway leading to skeletal muscle insulin resistance in HFD-fed mice which was not seen in HFD-fed $Nos2^{-/-}$ mice (Perreault and Marette, 2001). mRNA levels of iNOS were decreased in BV2 microglial cells when treated with lipopolysaccharide (LPS) in the presence of an inhibitor of Drp1, Mdivi-1 (Park et al., 2013). In addition to this ICV injection of streptozotocin (a toxic drug which impairs insulin receptor and glucose uptake in the brain), in rats, induced insulin resistance by inactivating Akt by S-nitrosylation, which in turn upregulated ROS and induced neurotoxicity in the hypothalamus (Crunfli et al., 2018). Together with this, and the data I have presented, it could be deduced that inhibiting iNOS in the DVC prevents the underlying effect of HFD dependent nitrosative stress, which in turns prevents s-nitrosylation of key players in the insulin signalling pathway, thus preventing the development of insulin resistance.

HFD control rats displayed high levels of ER stress compared with rats expressing the knockdown of iNOS. Obesity is widely associated with ER stress, this plays an integral role in the development of insulin resistance by activation of IRE-1α and inhibition of insulin signalling, suggesting that there is a causal relationship between the status of the ER and insulin resistance (Ozcan, 2004; Özcan et al., 2006). Treatment with small chemical chaperones which reduce ER

stress in cells, in obese and diabetic mice resulted in normalisation of glycemia and insulin sensitivity in muscle, liver and adipose tissue (Özcan et al., 2006). Furthermore, activation of Drp1 in the DVC resulted in insulin resistance and ER stress, inhibition of ER stress via the inhibitor 4-phenylbuty rate into the DVC alleviated the effects of HFD-dependent insulin resistance, demonstrating that ER stress is a downstream effector of Drp1-dependent insulin resistance (Filippi et al., 2017). Chronic activation of the UPR has been seen in the liver and adipose tissue of obese rats (Pagliassotti et al., 2017). In peripheral tissues, genetic inhibition of iNOS showed marked decrease in ER stress in adipose tissue and liver of HFD-fed mice (Zanotto et al., 2017).

Elevated levels of nitrosative stress in the liver and skeletal muscle have been associated with obesity and insulin resistance in both murine and human models (Qian et al., 2018; Zahedi Asl et al., 2008). Interestingly, mice fed a HFD had lower levels of s-nitroglutathione reductase, a protein denitrosylase, which has provided a link between inflammation and type II diabetes (Qian et al., 2018). In the liver, overexpression of s-nitroglutathione reductase in obese mice enhanced autophagy and improved insulin actions and glucose homeostasis (Qian et al., 2018). My data has shown rats expressing ShiNOS had a significant decrease in ER stress levels, furthermore PC12 cells treated with the ShRNA of iNOS had lower levels of s-nitrosylation. It would therefore be interesting to look into the levels of s-nitroglutathione reductase in the DVC to see if these levels correlate with insulin sensitivity in the brain as is seen in the liver.

An increase in nitrosative stress can causes S-nitrosylation of Drp1 leading to excessive mitochondrial fragmentation; in this chapter I have demonstrated activation of Drp1 in PC12 cells can increase the levels of s-nitrosylation. (Cho et

al., 2010). It has been well demonstrated that s-nitrosylation of Drp1 is essential in the pathophysiology of neurodegenerative diseases, such as Parkinson's and Alzheimer's disease (Cho et al., 2009; Ghasemi et al., 2018; Lee and Kim, 2018; Zorzano and Claret, 2015). NO in excess can lead to s-nitrosylation of Drp1, resulting in neurotoxicity and neurodegenerative diseases (Cho et al., 2010). Taking this into consideration and the data I have presented, a potential negative feedback mechanism may exist to increase s-nitrosylation, due to an increase in mitochondrial fission, which lead to a surge in the s-nitrosylation of Drp1 exacerbating the insulin resistant phenotype. It would be interesting to look into nitrosylation levels Drp1 and insulin signalling molecules in the DVC of insulin resistant rats.

ER stress and inflammation are associated with many diseases, the UPR alters ER homeostasis. In obesity, iNOS can cause s-nitrosylation of key UPR regulator, IRE1α, which increased ER-stress and induced insulin resistance (Yang et al., 2015a). Furthermore, in both genetic and dietary models of obesity, rats had a decrease in hepatic IRE1α (Yang et al., 2015a). *In vitro* I have shown an increase in s-nitrosylation levels in PC12 cells expressing Drp1-S637A and a decrease in s-nitrosylation levels in PC12 expressing ShiNOS. It would have been interesting however to see which potential markers underwent change in s-nitrosylation, such as IRE1α.

There is growing evidence to suggest a link between NO and protein nitrosylation with insulin resistance in type II diabetes. For example marked levels of iNOS were seen in mouse models of diabetes, while knockout of iNOS in HFD-fed mice had improved glucose tolerance and insulin sensitivity in skeletal muscle (Foster et al., 2009; Perreault and Marette, 2001). iNOS dependent S-nitrosylation of

AKT and IRS-1 abolishes the action of insulin upon its signalling pathway, in addition, following an excess of iNOS, s-nitrosylation of the insulin receptor β subunit can decrease the tyrosine kinase activity (Carvalho-filho et al., 2005; Sugita et al., 2005; Yasukawa et al., 2005). An increase in s-nitrosylation of these key players in insulin signalling have been seen in diabetic mouse models (Carvalho-filho et al., 2005; Perreault and Marette, 2001; Sugita et al., 2005; Yasukawa et al., 2005). Whether the aforementioned signalling molecules were nitrosylated in this system and if decreasing iNOS levels could prevent it still warrants further investigation.

Increasing the activity of Drp1 in PC12 cells caused significantly higher levels of iNOS and s-nitrosylation, these preliminary data are a good indication that an increase in s-nitrosylation is involved in the development of Drp1-dependent insulin resistance. However further investigation is needed to confirm this. If time permitted, I would have carried out an immunoprecipitation on Drp1-expressing samples, to isolate nitrosylated proteins, next, mass spectrometry would be carried out on these samples to find specific target molecules which were s-nitrosylated. With these target proteins, I could further investigate the effects of these nitrosylated proteins on the insulin resistant phenotype.

In the brain, basal levels of iNOS are low, where certain stimuli such as inflammation or infection can increase iNOS expression in astrocytes and microglia (Ghasemi and Fatemi, 2014). I have shown that decreasing the expression of iNOS in the DVC can significantly decrease levels of ER stress; furthermore, infecting PC12 cells with the ShiNOS-expressing virus, decreased the levels of ER-stress compared to control cells expressing ShControl. These data highlight the importance of iNOS in the ER-stress and the development of

insulin resistance. It has been previously determined that a HFD can induce hypothalamic inflammation, where hypothalamic microglia are activated following exposure to a HFD (Lee et al., 2018; Perry et al., 2010). Furthermore, iNOS activation in macrophages can contribute to hypothalamic inflammation in HFD-fed rats, where ICV injection of an inhibitor of iNOS decreased macrophage activation and improved glucose metabolism in HFD mice (Lee et al., 2018). Ablation of the insulin receptors in astrocytes reduced the activation of POMC neurones and impaired glucose availability, determining that insulin signalling in astrocytes controls central glucose sensing and glucose uptake (García-Cáceres et al., 2016).

In conclusion, I have demonstrated that mitochondrial fission can increase s-nitrosylation in PC12 cells, and inhibition of iNOS can decrease levels of s-nitrosylation. Furthermore, I have shown that knocking down iNOS in the DVC of HFD-fed rats can prevent the development of insulin resistance, decrease food intake and body weight gain. Together with these data, I propose a hypothesis by a HFD can induce mitochondrial fission which increases iNOS release which in turn results in ER stress and insulin resistance (Figure 4.16).

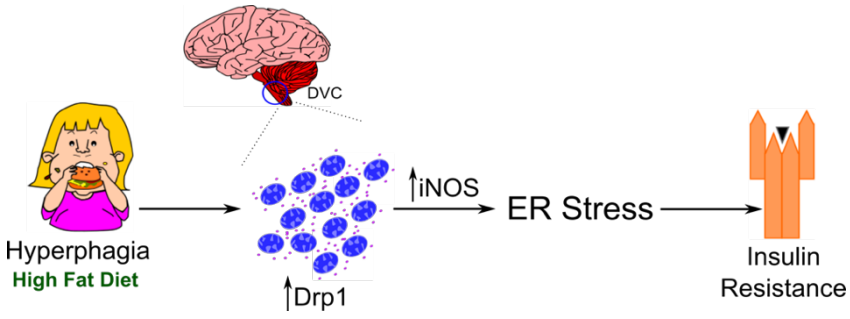

Figure 4.16 In summary, an increase in HFD can induce Drp1-dependent mitochondrial fission, leading to an increase in iNOS levels resulting in insulin resistance

5 Inhibition of mitochondrial fission specifically in astrocytes of the DVC prevents HFD-dependent insulin resistance, body weight gain and hyperphagia

5.1 Introduction

Activation of Drp1 in the DVC induced insulin resistance and increases iNOS expression (see section 3.2.3.4). In addition to this inhibition of iNOS in the DVC was sufficient to prevent HFD-dependent insulin resistance (see section 4.2.8). It is still unclear which neural cell populations in the DVC are involved in insulin sensing and in the development of insulin resistance. My approach up until now was to target all the cell populations in the DVC by expressing Drp1 under a CMV promoter. When I analysed the cellular localisation of the adenovirus, I could see that we preferentially targeted astrocytes at 39.1% and oligodendrocytes 36.2% of infected cells (see section 3.2.2). Considering astrocytes are important in the maintenance of the microenvironment and have also been implicated with feeding, I aimed to look into the effect of inhibition of mitochondrial fission in astrocytes specifically (Buckman et al., 2015; García-Cáceres et al., 2012; MacDonald et al., 2019; Saha and Pahan, 2006).

Astrocytes are the most abundant neural cell type in the brain, they regulate many aspects of neuronal function, including synaptic plasticity, survival, metabolism and neurotransmission (García-Cáceres et al., 2012). Astrocytes are responsible for synthesising and releasing NO, and in this way they can communicate with surrounding neurones (Amitai, 2010). Aberrant levels of iNOS in astrocytes, leading to astrogliosis, has shown to increase levels of neuroinflammation and neurotoxicity (Liberatore et al., 1999). Astrogliosis, an abnormal level of astrocytes, is a result from CNS damage, from situations such as immune responses, stroke or infection (Sofroniew, 2015). Astrogliosis has been seen in the hypothalamus of diet induce or genetically modified models of obesity, however the exact mechanism of this is not well understood (Buckman et al.,

2013; Horvath et al., 2010). In the ARC nucleus of diet induced obesity there was a significant astrogliosis, interestingly, treatment with an iNOS inhibitor, L-NIL, by ICV injection, inhibited HFD-induced astrogliosis, suggesting that iNOS activation may induce hypothalamic inflammation (Lee et al., 2018).

Astrocytes can respond to levels of nutrients, thereby acting as metabolic sensors, their location between vessels and neurones put them in good stead to control glucose changes within the CNS and the periphery (García-Cáceres et al., 2012). Astrocytes in the NTS of the DVC respond to acute nutritional overload, by increasing their network to integrate peripheral satiety signals to decrease food intake (MacDonald et al., 2019). In addition to this, astrocytes are involved in the regulation of feeding and glucose homeostasis (Buckman et al., 2015; García-Cáceres et al., 2016; MacDonald et al., 2019). Altogether these data lead me to hypothesise that the effects of mitochondrial dynamics in the DVC could be largely due to the effect on astrocytes.

Therefore, I aimed to specifically inhibit mitochondrial fission in astrocytes in order to determine whether the effects seen on insulin sensitivity, food intake, body weight gain and fat deposition were due to astrocyte mediated mechanisms. To this end, we produced adenoviruses[5] expressing GFP or Drp1-K38A under the control of the GFAP promoter (GFP::GFAP and Drp1-K38A::GFAP, respectively).

[5] Adenoviruses were engineered and produced by Dr Joanne Parkes in the Filippi Lab

5.1.1 Aims and objectives

Aim 1: Can inhibiting mitochondrial fission specifically in astrocytes in the DVC prevent HFD-induced insulin resistance, body weight gain and food intake?

Aim 2: Can inhibiting mitochondrial fission specifically in astrocytes in the DVC improve insulin sensitivity and decrease body weight and food intake in RC-fed rats?

5.2 Results

5.2.1 Inhibition of Drp1 in astrocytes of the DVC prevents HFD-dependent insulin resistance

On day 0 rats underwent stereotactic surgery where a bilateral canula was inserted into the NTS of DVC of the brain, on day one rats were injected with GFP::GFAP or Drp1-K38A::GFAP. On day three these rats were given HFD (Diet 3). To confirm that the adenovirus specifically targets astrocytes, IHC[6] was performed (as described in section 2.7), where we analysed the extent of co-localisation between GFP::GFAP or Drp1-K38A::GFAP expression with either an astrocytic marker (GFAP) or a neuronal marker (NeuN). Both GFP::GFAP and Drp1-K38A::GFAP proteins are tagged with FLAG, therefore expression could be determined using an anti-FLAG antibody (Figure 5.1A-Aii and Figure 5.1B-Bii, respectively). Dual labelling using anti-GFAP to label astrocytes demonstrates that there is co-localisation with both GFP::GFAP and Drp1-K38A::GFAP expressing cells in the DVC (Figure 5.1C-Cii and Figure 5.1D-Dii, respectively). Double staining against NeuN showed that there was no co-localisation with both GFP::GFAP and Drp1-K38A::GFAP expressing cells, determining the specificity of this adenoviral delivery system.

[6] All IHC experiments were performed in collaboration with Dr Lauryn New in the Filippi Lab

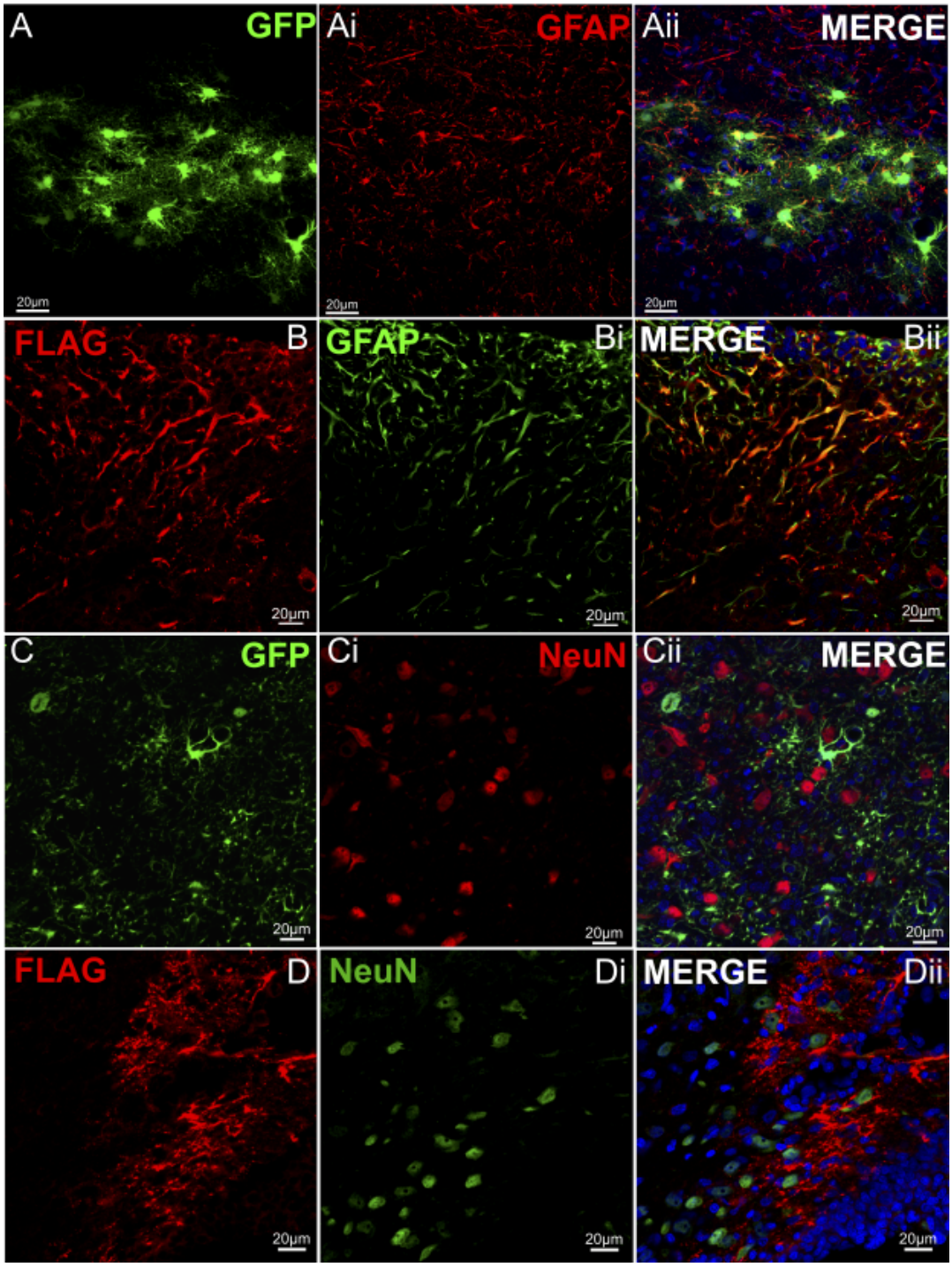

Figure 5.1 GFP::GFAP and Drp1-K38A::GFAP expression astrocytes and neurones

A-Aii: Representative confocal images illustrating expression of GFP::GFAP (A), GFAP (Ai) and dual labelling for both in the DVC

B-Bii: Representative confocal images illustrating expression of GFP:Drp1-K38A::GFAP (B), GFAP (Bi) and dual labelling for both (Bii) in the DVC

C-Cii: Representative confocal images illustrating expression of GFP::GFAP (C), NeuN (Ci) and dual labelling for both (Cii) in the DVC

D-Dii: Representative confocal images illustrating expression of Drp1-K38A::GFAP (D), NeuN (Di) and dual labelling for both (Dii) in the DVC

The feeding study was performed on day nine and 14, fasted rats were injected with insulin or a vehicle bilaterally into the DVC, and food intake was taken every half an hour for four hours. The data shows that rats expressing Drp1-K38A::GFAP had a significant 43% decrease in food intake compared to GFP::GFAP-expressing rats (Figure 5.2A). At the 12 hour point however the effect of insulin on food intake is lost (Figure 5.2B).

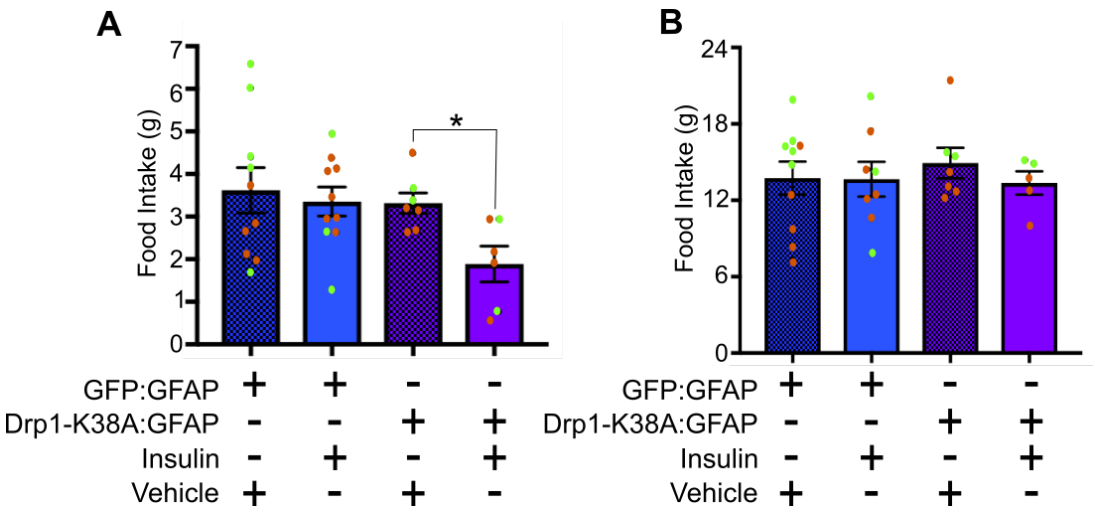

Figure 5.2 Food intake during acute feeding study in HFD-fed rats expressing GFP::GFAP or Drp1-K38A::GFAP

Rats were fasted for 6 hours and then infused bilaterally into the DVC with a total 0.2ul of 2mU insulin or a vehicle over 5 minutes. Food was then returned and food intake was observed every half hour for 4 hours and a final reading was taken at 12 hours.

A: Total food intake taken at the 4 hour time point, since there was no difference in the food intake in the feeding studies performed on day nine and fourteen, the figure shows the average food intake over both feeding studies

B: Total food intake taken at the 12 hour time point, since there was no difference in the food intake in the feeding studies performed on day nine and fourteen, the figure shows the average food intake over both feeding studies total food intake at 4 hours comparing rats treated with insulin or a vehicle in the DVC.

Data are expressed as a mean ± SEM *n*=11 for GFP::GFAP vehicle, *n*=8 GFP::GFAP insulin, *n*= 7 for Drp1-K38A::GFAP vehicle, *n*=5 for Drp1-K38A::GFAP insulin. Orange dots represent data gained from day 9, green dots represent data gained from day 14.

Statistical test: two way ANOVA (post-hoc test: Tukey) [*$p < 0.05$]

5.2.2 Inhibiting Drp1 in astrocytes of the DVC decreases food intake and body weight in HFD-fed rats

Inhibiting Drp1 in astrocytes of the DVC in HFD-fed rats had a significant acute effect on feeding behaviours, over a four-hour period. Next, I wanted to investigate whether inhibiting Drp1-dependent mitochondrial fission in astrocytes had an effect on chronic feeding behaviours and body weight gain. Rats had their body weight and food intake taken at a similar time each day. The data shows that rats expressing Drp1-K38A::GFAP had a decrease in food intake, with data becoming significant from day 4, when compared with GFP::GFAP-expressing rats (Figure 5.3A). In addition to this, Drp1-K38A::GFAP-expressing rats also had a significant decrease in body weight, which was significant from day 3 (Figure 5.3B). These data show that inhibiting Drp1 in the astrocytes of DVC can have a significant effect on food intake and body weight gain in HFD-fed rats.

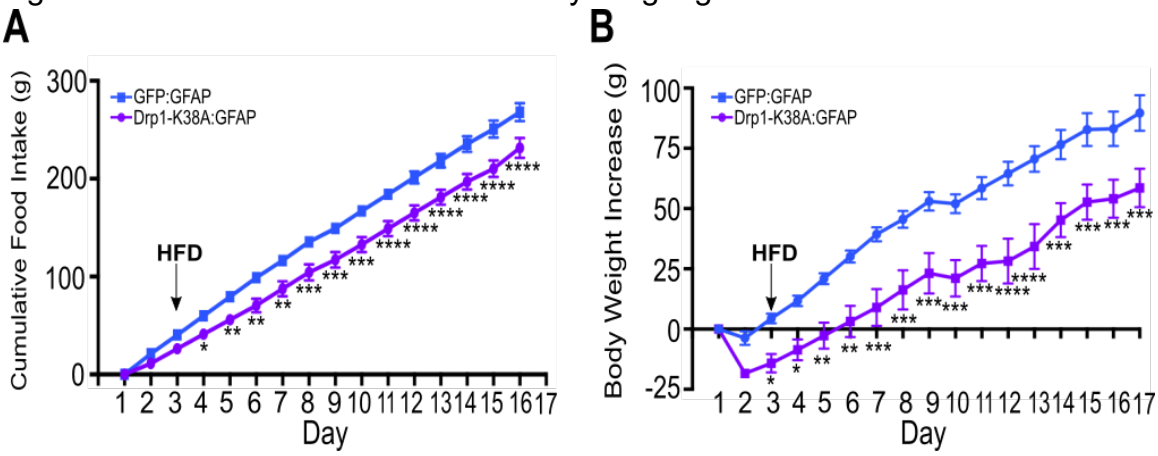

Figure 5.3 Cumulative food intake and body weight increase in the during of the study in HFD-fed Drp1-K38A::GFAP expressing rats compared to GFP::GFAP expressing rats

A: Cumulative food intake in Drp1-K38A::GFAP and GFP::GFAP expressing rats from day of viral injection (day 1)

B: Body weight increase in Drp1-K38A::GFAP and GFP::GFAP expressing rats from day of viral injection (day 1)

All data are expressed as mean ± SEM *n*=12 for GFP::GFAP expressing rats and *n*= 12 Drp1-K38A::GFAP expressing rats Statistical test: Two way ANOVA (post-hoc test: Tukey) [*p < 0.05, **p <0.01, *** p<0.001, **** p<0.0001]]

5.2.3 Inhibiting Drp1 in the astrocytes of the DVC in HFD-fed rats decreases fat deposition

Inhibition of Drp1 in astrocytes can decrease food intake and body weight gain in HFD-fed rats, next I wanted to look into the effect this had on fat deposition. On the day of sacrifice, day 17, rats WAT and BAT were collected and weighed (as described in section 3.2.3.3). Rats expressing the catalytically inactive form of Drp1, Drp1-K38A, under the GFAP promoter, had significantly lower levels of epididymal and total WAT tissue compared to GFP::GFAP-expressing control rats (Figure 5.4A). In addition to WAT, BAT was also collected, where data shows that there was no significant difference in the weight of BAT in the Drp1-K38A::GFAP-expressing rats compared to control GFP::GFAP-expressing littermates (Figure 5.4B).

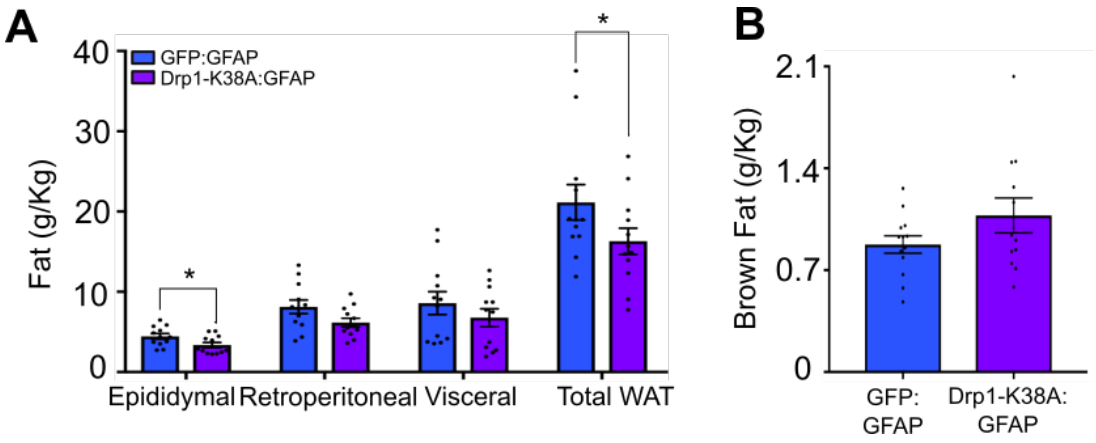

Figure 5.4 Weight of white adipose tissue and brown adipose tissue

A: Weight of white adipose tissue expressing Drp1-K38A::GFAP and GFP::GFAP

B: Weight of brown adipose tissue in rats Drp1-K38A::GFAP and GFP::GFAP

Body weight was divided by the weight of fat to establish fat distribution (g/kg). All data are expressed as mean ± SEM *n*=12 for GFP::GFAP expressing rats and *n*=12 Drp1-K38A::GFAP expressing rats

Statistical test: multiple T-test [*p < 0.05]

5.2.4 Inhibition of Drp1 in astrocytes decreases iNOS levels in the DVC of HFD-fed rats

On the day of sacrifice, day 17, the DVC was collected and snap frozen, in preparation for western blotting (as described in section 2.6). Astrocytes are important in the synthesis and the release of NO, where an increase of iNOS dependent release of NO can lead to neurotoxicity and inflammation (Liberatore et al., 1999). Here I have shown that an inhibition of Drp1 in astrocytes of the DVC significantly decreases iNOS levels compared to controls (Figure 5.5).

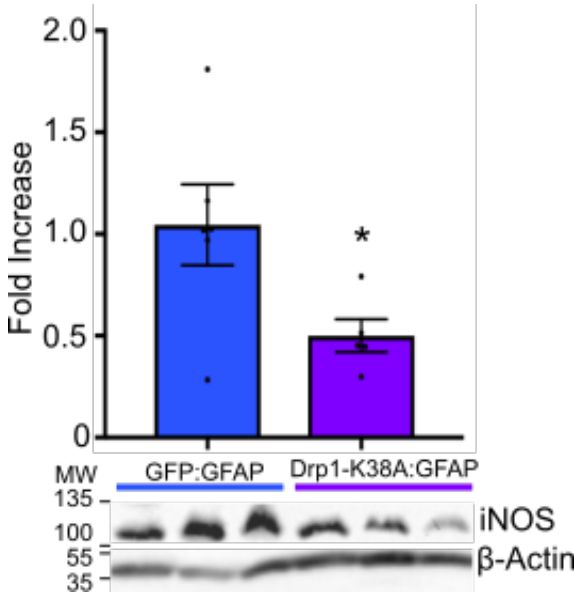

Figure 5.5 Inhibition of Drp1 in the astrocytes in the DVC decreases iNOS levels

A representative western blot show iNOS levels in the DVC of HFD-fed rats expressing Drp1-K38A::GFAP compared to GFP::GFAP

All data are expressed as mean ± SEM *n*=12 for both GFP::GFAP and Drp1-K38A::GFAP

Statistical test: unpaired test [*p < 0.05]

In summary, my data shows that inhibiting Drp1 in astrocytes of the DVC specifically prevents HFD-dependent insulin resistance[7] as well as decreasing body weight gain, food intake, WAT deposition and iNOS levels.

[7] Referring to loss of insulin-induced hypophagia when stating rats are insulin resistant in data

5.2.5 Inhibition of Drp1-dependent mitochondrial fission in astrocytes in the DVC moderately improves insulin sensitivity in RC-fed rats

I have shown that inhibiting mitochondrial fission in the DVC and specifically within astrocytes of the DVC, prevented HFD-dependent insulin resistance. I next wanted to see if inhibiting mitochondrial fission in astrocytes of the DVC of RC-fed rats could improve insulin sensing and have an effect on feeding behaviours. Rats underwent stereotactic surgery to implant a bilateral cannula targeting the NTS in the DVC, on day one, rats were injected with either an adenovirus to express Drp1-K38A::GFAP or GFP::GFAP in the DVC (Figure 5.6). These rats were fed with RC (Diet 1).

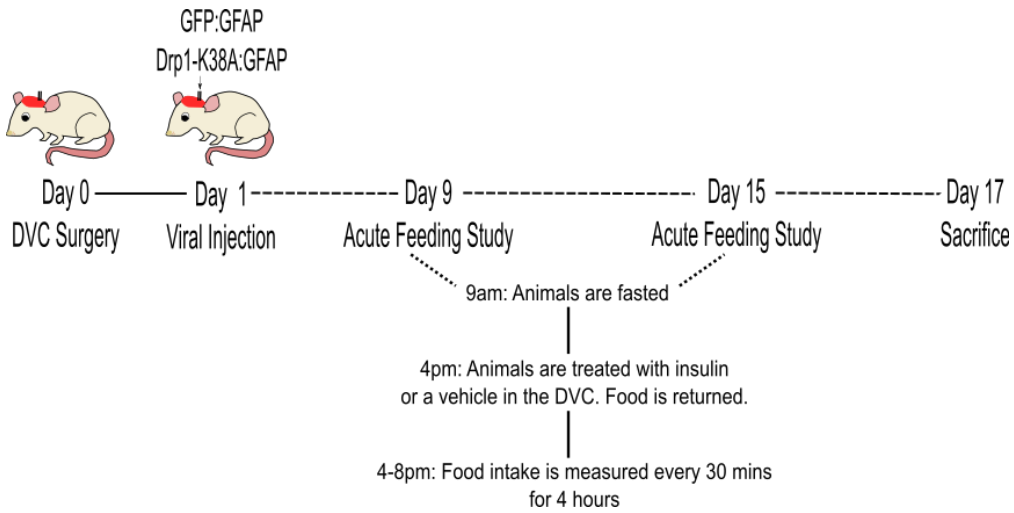

Figure 5.6 Protocol used in feeding study Drp1-K38A::GFAP and GFP::GFAP RC-fed rats.

On day 0 rats underwent brain surgery where a bilateral cannula was inserted into the NTS of the DVC. On day one rats were injected with an adenoviral system to deliver GFP::GFAP or Drp1-K38A::GFAP. On day nine and 15 rats were subjected to a feeding study where acute food intake was recorded. Rats were sacrificed on day 17

On day nine and 14 rats were subjected to a feeding study as previously described above. RC-fed rats expressing GFP::GFAP who were infused with insulin had a significant 29.1% decrease in food intake over four hours compared with vehicle infused littermates (Figure 5.7A). Similarly, Drp1-K38A::GFAP-expressing rats infused with insulin had a significant 41.1% decrease in food intake over four hours compared to Drp1-K38A::GFAP-expressing vehicle infused rats. The Drp1-K38A::GFAP treated with insulin ate 10% less than GFP::GFAP controls who were treated with insulin, the difference between these amounts eaten is not significant (Figure 5.7A). At 12 hours the effect of insulin

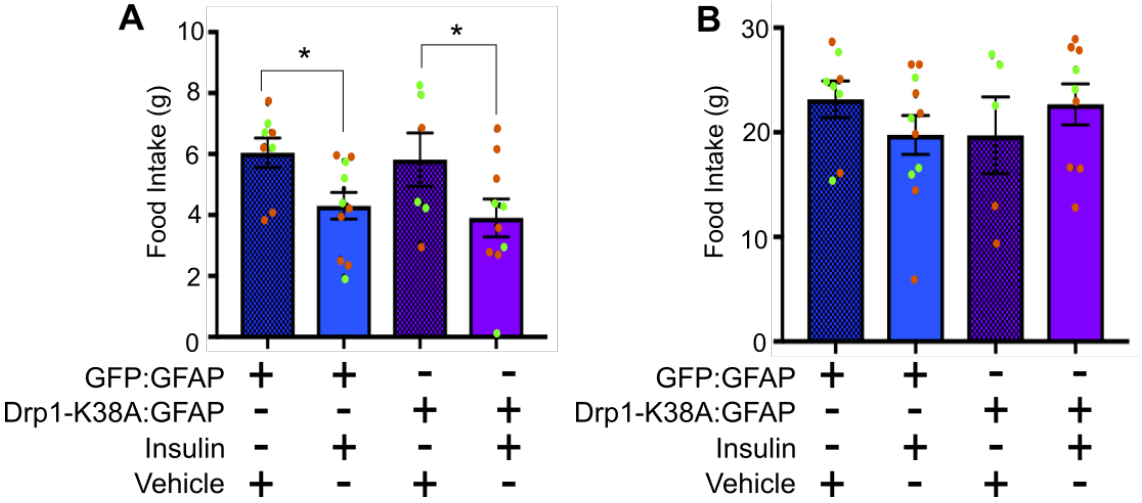

Figure 5.7 Food intake during acute feeding study in RC-fed rats either expressing GFP::GFAP or Drp1-K38A::GFAP

Rats were fasted for 6 hours and then infused bilaterally into the DVC with a total 0.2ul of 2mU insulin or a vehicle over 5 minutes. Food was then returned and food intake was observed every half hour for 4 hours and a final reading was taken at 12 hours.

A: Total food intake taken at the 4 hour time point, since there was no difference in the food intake in the feeding studies performed on day nine and fourteen, the figure shows the average food intake over both feeding studies

B: Total food intake taken at the 12 hour time point, since there was no difference in the food intake in the feeding studies performed on day nine and fourteen, the figure shows the average food intake over both feeding studies total food intake at 4 hours comparing rats treated with insulin or a vehicle in the DVC.

Data are expressed as a mean ± SEM n=8 for GFP::GFAP vehicle, *n*=11 GFP::GFAP insulin, *n*= 5 for Drp1-K38A::GFAP vehicle, *n*=9 for Drp1-K38A::GFAP insulin. Orange dots represent data gained from day 9, green dots represent data gained from day 14. Statistical test: Two way ANOVA (post-hoc test: Tukey) [*$p < 0.05$]

was lost in both Drp1-K38A::GFAP and GFP::GFAP-expressing rats (Figure 5.7B).

5.2.6 Inhibition of Drp1 in astrocytes of the DVC decreases food intake and body weight in RC-fed rats

Inhibition of Drp1 in the astrocytes of the DVC resulted had little improvement on insulin sensing in RC-fed rats. I next wanted to look at the effect that inhibition of Drp1 in astrocytes had on food intake and body weight in RC-fed rats. Each rat's food intake and body weight were taken at a similar time each day. These data demonstrate that inhibition of mitochondrial fission in astrocytes of the DVC can decrease food intake and body weight where data for both becomes significant from day two (Figure 5.8A and Figure 5.8B, respectively).

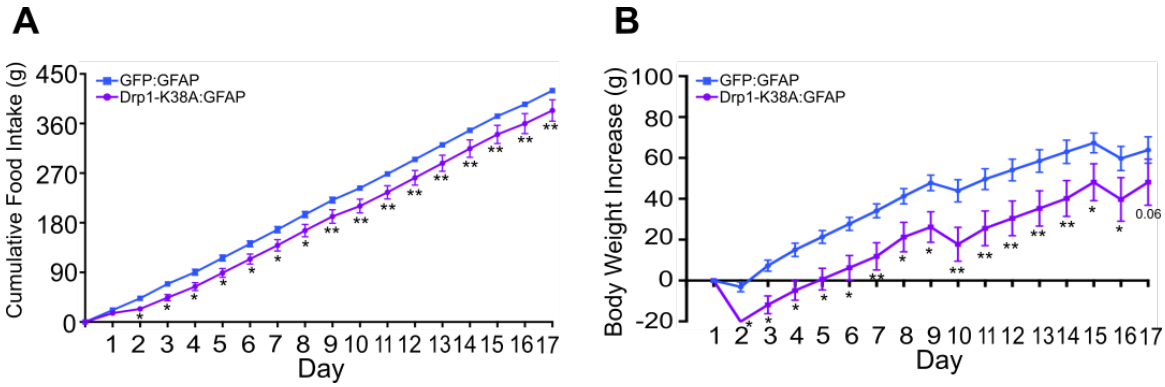

Figure 5.8 Cumulative food intake and body weight increase in the during of the study RC-fed rats expressing Drp1-K38A::GFAP compared to GFP::GFAP expressing RC-fed rats

A: Cumulative food intake in Drp1-K38A::GFAP and GFP::GFAP expressing rats from day of viral injection (day 1)

B: Body weight increase in Drp1-K38A::GFAP and GFP::GFAP expressing rats from day of viral injection (day 1)

All data are expressed as mean ± SEM *n*=12 for GFP::GFAP expressing rats and *n*= 12 Drp1-K38A::GFAP expressing rats

Statistical test: two way ANOVA (post-hoc test: Tukey) [*p < 0.05, **p <0.01]

5.2.7 Inhibition of Drp1 in astrocytes in the DVC has no effect on WAT and BAT deposition

I have found that inhibition of Drp1 in astrocytes can decrease food intake and body weight compared to RC-fed controls, I next wanted to investigate the effect on fat deposition. On the day of sacrifice WAT and BAT was collected from each rat and weighed. There was no difference in the weight and the different types of WAT between Drp1-K38A::GFAP and GFP::GFAP-expressing rats (Figure 5.9A). Interestingly, rats expressing Drp1-K38A::GFAP had a higher weight of BAT compared to control GFP::GFAP expressing littermates (Figure 5.9B).

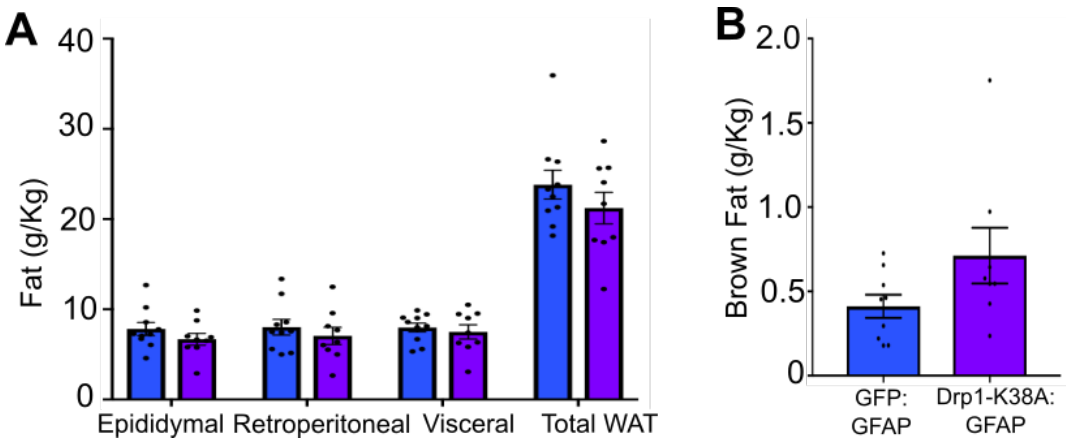

Figure 5.9 Weight of white adipose tissue and brown adipose tissue

A: Weight of white adipose tissue from rats expressing Drp1-K38A::GFAP and GFP::GFAP
B: Weight of brown adipose tissue in rats Drp1-K38A::GFAP and GFP::GFAP
The weight of fat was divided by the body weight to establish fat distribution (g/kg). All data are expressed as mean ± SEM *n*=9 for GFP::GFAP expressing rats and *n*=8 Drp1-K38A::GFAP expressing rats.
Statistical test: multiple T-test

In summary, I have found that inhibiting mitochondrial fission in astrocytes of the DVC of RC-fed rats had a significantly improved body weight gain and a decrease in food intake but no effect was seen in insulin sensitivity or fat deposition.

5.3 Discussion

Altogether the data suggest that specific inhibition of Drp1 in the astrocytes of the DVC can significantly decrease body weight gain and food intake in HFD-fed rats. In addition to this I have shown inhibition of Drp1 in the astrocytes can prevent HFD-dependent insulin resistance compared to HFD controls. Previously it has been shown that astrocytic insulin signalling is involved in glucose sensing in the hypothalamus; ablation of the insulin receptor in astrocytes resulted in alteration in glial morphology, mitochondrial function in astrocytes and connectivity of astrocytes in the hypothalamus (García-Cáceres et al., 2016). In addition to this, mice with a knockdown of the insulin receptor in astrocytes, failed to respond to elevated glucose levels, as a result, astrocytes elevated mitochondrial in β-oxidation as a compensatory mechanism. The mitochondria in these astrocytes had reduced aspect ratio and fewer elongated mitochondria compared to controls, favouring mitochondrial fission (García-Cáceres et al., 2016).

It has been previously demonstrated that 10 days of HFD-feeding can increase astrocyte complexity in the ARC nucleus, which was sufficient to induce astrogliosis, which is thought to be due to metabolic changes in fat content and body mass, leading to an increase in inflammatory factors such as IL-6 and TNF-α (Balland and Cowley, 2017). In addition to this, astrocytes play an important role in the hypothalamic response to insulin, where ablation of the insulin receptor in astrocytes resulted in impairment of physiological changes to glucose availability (García-Cáceres et al., 2016). An increased nutritional overload resulted in upregulation of GFAP expression and morphological complexity astrocytes in the DVC, which in turn resulted in a decrease in food intake (MacDonald et al., 2019).

Astrocytes have been shown to induce iNOS in response to inflammation, however the exact pathway leading to this are not well understood, it has been suggested that an increase in NO leads to ROS which in turn causes defects in. signalling pathways (Liberatore et al., 1999). Previously I have demonstrated that an activation of Drp1 increase iNOS levels in the DVC, and here, I have shown that inhibition of Drp1 in astrocytes of the DVC decreased iNOS levels determining the relationship between iNOS and astrocytic Drp1 in the pathogenesis of insulin resistance.

Astrocytes provide metabolic and structural support to neurones and play an active role in neurotransmission which may be involved in energy balance. For example, chemogenetic activation of astrocytes in the DVC of mice led to the recruitment of local downstream neuronal circuits which in turn maintained energy homeostasis (MacDonald et al., 2019). There are distinct neuronal population which are involved in feeding, some of which include POMC and cholecystokinin receptor (cholecystokinin is a hormone which is produced in the gut) expressing neurones, it has been proposed that activation of astrocytes through feeding recruit such neurones to inhibit feeding (D'Agostino et al., 2016; MacDonald et al., 2019). In addition to this, inflammatory responses generated by astrocytes can affect neuronal function by imposing on intercellular signals from NO. It has also been demonstrated that NO can act as an intracellular mediator in neuronal function (Jiang and Cadenas, 2014). Here, I have shown that inhibition of mitochondrial fission in the astrocytes of the DVC reduced food intake and body weight in both HFD and RC-fed rats, perhaps there is a neuronal glial cross talk in which astrocytes sense changes within the network and

communicate to feeding related neurones to regulate energy homeostasis, which could be mediated by the release of iNOS dependent NO.

In conclusion, I have demonstrated that mitochondrial dynamics specifically in astrocytes in the DVC have a central role in energy homeostasis and insulin sensitivity. From these data I propose two potential mechanisms by which HFD-dependent Drp1-activation induces insulin resistance in the DVC:

1. Astrocytes directly act by increasing iNOS dependent NO which increases ER stress inducing insulin resistance.

2. Alternatively an increase in iNOS dependent NO from astrocytes acts as a gaseous neurotransmitter to neurones inducing insulin resistance

or if these work in tandem, is still yet to be determined (Figure 5.10).

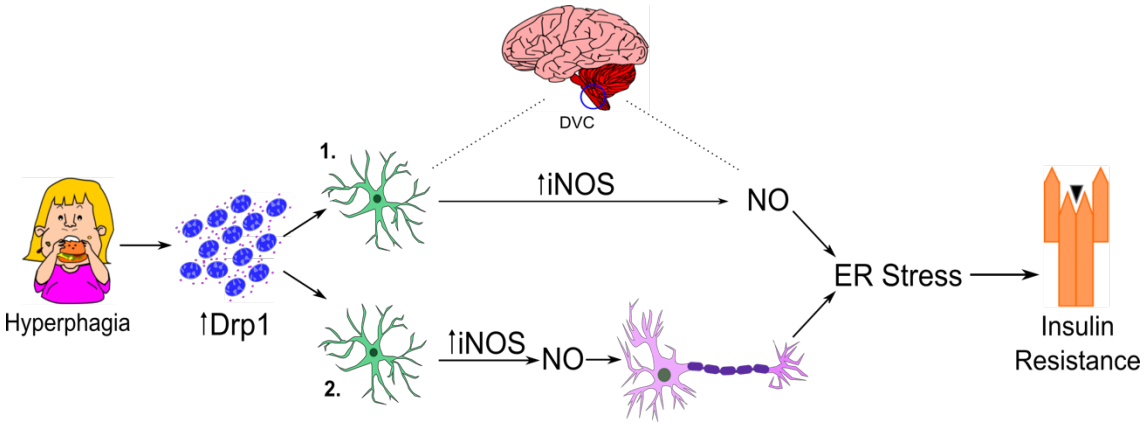

Figure 5.10 Two potential mechanisms by which HFD dependent Drp1 activated insulin resistance in the DVC may occur

1. An increase in Drp1 activity in the astrocytes results in an increase in iNOS produced NO which in turn leads to ER-stress leading to insulin resistance

2. Drp1 activation in astrocytes results in an increase in NO produced by iNOS which acts as a neurotransmitter to signal to neurones inducing ER stress and insulin resistance.

6 Inhibition of Drp1-dependent mitochondrial fission or a decrease in iNOS expression in the DVC restores insulin sensitivity in overweight and hyperphagic rats

6.1 Introduction

Short term HFD-feeding dysregulates glucose metabolism and induces insulin resistance in rats (Balland and Cowley, 2017; Filippi et al., 2017; Maurer et al., 2017). Furthermore, three-day HFD-feeding can increase Drp1-dependent mitochondrial fission in the DVC, leading to changes in mitochondrial morphology which in turn induces insulin resistance (Filippi et al., 2017). I have demonstrated in previous chapters that inhibiting Drp1 in the DVC is a preventative method in the development of HFD-dependent insulin resistance, hyperphagia and body weight gain. In addition to this, I have presented data that confirms that knocking down iNOS in the DVC can decrease body weight gain and food intake, and also the development of HFD-induced insulin resistance in rats.

Following chronic HFD-feeding (16 weeks), mice presented with larger pancreatic islet size, as well as greater mass gain, insulin resistance and hepatic liver disease (Fraulob et al., 2010). Mice given a HFD for 12 months had significantly higher levels of blood glucose, with increased circulating blood glucose levels, which presented within the first weeks of the study (Winzell and Ahren, 2004). In both human and rat models of HFD-feeding an increase in WAT mass can lead to adipose tissue inflammation which has been associated with glucose metabolism dysfunction and insulin resistance (Burhans et al., 2019). HFD-feeding can cause primary hyperinsulinemia through activation of the β-cells of the pancreas, this in turn raises FFA levels (Czech, 2017). When insulin secretion cannot compensate for insulin resistance and high blood glucose levels, this ultimately leads to type two diabetes (Czech, 2017; Yang et al., 2018).

In the pathology of obesity, nutritional intake is greater than energy output, this can be referred to as metabolic flexibility, whereby metabolism changes to meet needs of substrate availability (Smith et al., 2018; Yang et al., 2018). Given the crucial role of mitochondria in energy metabolism, mitochondrial dysfunction acts as a key regulator in the pathophysiology of obesity (Chan, 2012; Dai and Jiang, 2019). Metabolic flexibility is linked to mitochondria and their ability to change to meet metabolic needs, in situation of caloric excess mitochondria change their morphology, favouring fission, as there is no need for energy utilisation from glucose, fatty acids or amino acids instead substances are stored, which can lead to an increase in inflammation and ER stress (Muoio, 2014; Smith et al., 2018; Yang et al., 2018).

I have previously demonstrated that activation of Drp1 can increase iNOS levels in RC-fed rats (see figure 3.13). It has previously been demonstrated that HFD can lead to an increase in ER stress and increase iNOS levels in adipose tissue (Kawasaki et al., 2012). In addition to this, knocking down iNOS in muscle can restore insulin sensitivity in HFD-fed rats (Perreault and Marette, 2001). Furthermore, I have demonstrated that inhibiting Drp1 or knocking down iNOS in the DVC, can prevent the loss of insulin-induced hypophagia I HFD-fed rats (see section 3.2.4.1 and 4.2.7).

A four-week HFD-feeding can induce a significant 9-15% increase in body weight, higher blood glucose levels and hyperinsulinemia compared with RC-fed littermates (Maurer et al., 2017; Yue et al., 2016). In addition a 28 day HFD-feeding increases body weight, adiposity and peripheral insulin resistance in rats compared to control RC-fed rats, (Côté et al., 2015). Together with these data, I determined that a 28-day HFD was an effective model to induce hyperphagia and

insulin resistance in rats. As 28 days of HFD-feeding can induce insulin resistance and body weight gain, and the fact that inhibition of Drp1 or a knockdown of iNOS can prevent HFD-dependent insulin resistance, I wanted to investigate if inhibition of Drp1 or iNOS in the DVC could restore insulin sensitivity in 28-day HFD-fed rats.

6.1.1 Aims and objectives

Aim 1: Can inhibiting mitochondrial fission in the DVC restore insulin sensitivity and change feeding behaviours in HFD-fed overweight and hyperphagic rats?

Aim 2: Can decreasing expression of iNOS in the DVC restore insulin sensitivity, decrease food intake and body weight gain in overweight and hyperphagic HFD-fed rats?

6.2 Results

6.2.1 Rats given HFD for 28 days had an increase in food intake, body weight gain and blood glucose levels

The aim of this chapter was to understand if I could restore insulin sensitivity in overweight and hyperphagic HFD-fed rats by inhibiting Drp1 or decreasing iNOS levels in the DVC. Rats were given either Diet 2 RC or Diet 3 HFD for 28 days (Figure 6.1A). Daily monitoring was carried out at a similar time each morning, to keep data consistent. These data show that rats fed a HFD for 28 days had a significant 7% increase in cumulative food intake at day 28 compared to RC-fed rats (Figure 6.1B) and a significant 9.4% increase in body weight gain at day 28 compared to RC-fed rats (Figure 6.1C). At day 28, the body weight increase was

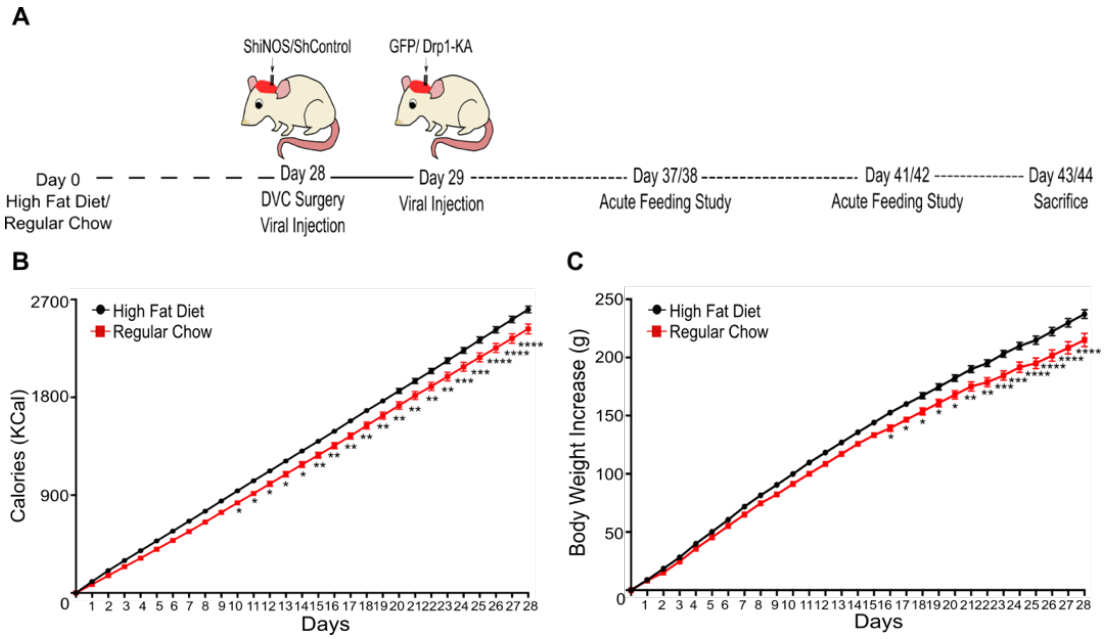

Figure 6.1 Cumulative food intake and body weight gain in 28-days prior to brain surgery in rats either given a HFD or RC

A: 28-day HFD study protocol
B: Cumulative food intake (in calories) in rats fed either a HFD or RC
C: Body weight increase in rats fed either a HFD or RC
(B-C Data are expressed as mean ± SEM, *n*=10 RC, *n*=24)
Statistical test: two way ANOVA (post-hoc test: Tukey)[*p <0.05, **p <0.01, *** p<0.001, ****p<0.0001]

greater than 9% compared to RC-fed rats, I will therefore refer to this model from now on as the obese model as detailed in Maurer et al. 2017.

On the morning of surgery on day 28, blood glucose measurements were taken from each rat. A small prick was applied to the tail and a small amount of blood was taken from the rat to compare glucose levels in the RC and HFD cohorts. Rats fed a HFD had a significant increase in blood glucose levels compared to RC-fed controls over 28 days, HFD-fed rats had an average of 5.9 mmol/L compared to RC-fed rats who had an average blood glucose of 5.4 mmol (Figure 6.2).

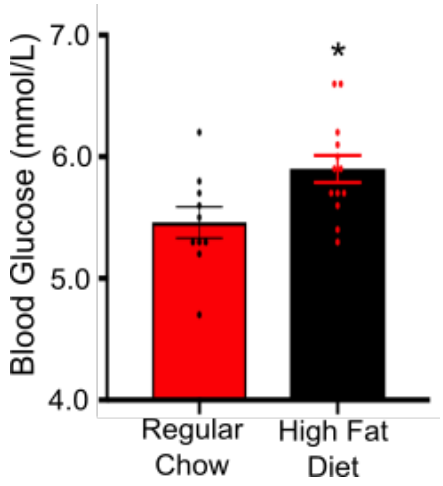

Figure 6.2 Average blood sugar of RC-fed versus HFD-fed rats on day 28
Data are expressed as mean ± SEM, *n*=6 RC, *n*=16, Statistical test: unpaired T-test

6.2.2 Inhibition of mitochondrial fission in the DVC restored insulin sensitivity and decreases body weight in obese rats

6.2.2.1 Inhibition of mitochondrial fission in the DVC restores insulin sensitivity in HFD-fed obese rats

Previously, I have demonstrated that inhibiting Drp1 in the DVC could prevent HFD-dependent insulin resistance from occurring in rats. Next, I wanted to investigate whether inhibiting mitochondrial fission in overweight rats could restore insulin sensitivity. Rats underwent stereotactic brain surgery on day 28 where a bilateral canula was inserted into the DVC (detailed in section 2.4). On day 29 rats received a viral injection in the DVC where either a dominant negative form of Drp1, mutated in the residue of K38 to A (K38A), resulting in a decrease in Drp1 dependent mitochondrial fission or a control of GFP was delivered (Filippi et al., 2017). Rats were subjected to acute feeding studies on day 38 and 42, where insulin was infused into the DVC of fasted rats and food intake was taken every half an hour for four hours (as described in section 2.5.2).

GFP-expressing RC-fed rats infused with insulin exhibited a significant 59% decrease in food intake at 4 hours compared to their vehicle infused GFP-expressing RC controls (Figure 6.3A). However, the HFD-fed GFP-expressing rats did not decrease food intake when infused with insulin at the four-hour point compared to their vehicle infused controls (Figure 6.3A), determining that insulin did not have an effect on feeding behaviours as demonstrated in the RC-fed littermates. Interestingly, HFD-fed rats expressing the catalytically inactive form of Drp1, Drp1-K38A, who were infused with insulin, had a significant 62% reduction in food intake at four hours compared with vehicle infused controls. This effect is similar to the effect seen in GFP-expressing RC insulin infused rats

(Figure 6.3A). These data highlight that inhibiting Drp1 in HFD-fed hyperphagic rats can restore insulin sensitivity[8].

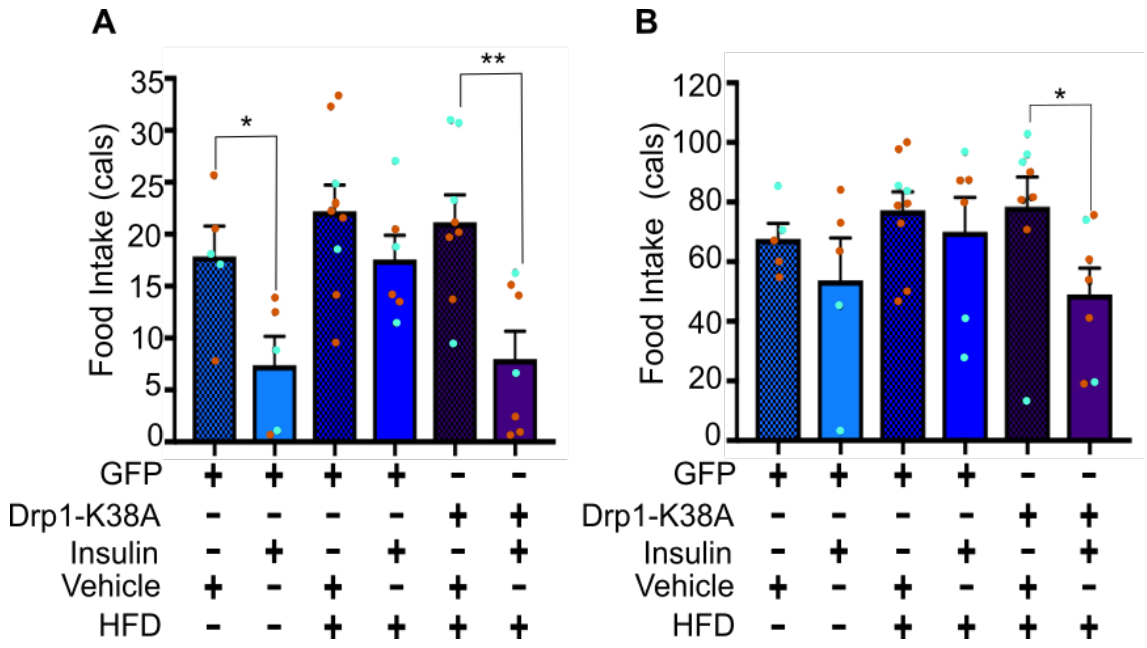

Figure 6.3 Food intake during acute feeding study in 28-day RC or HFD-fed rats expressing Drp1-K38A and GFP

Rats were fasted for 6 hours and then infused bilaterally into the DVC with a total 0.2ul of 2mU insulin or a vehicle over 5 minutes. Food was then returned and food intake was observed every half hour for 4 hours and a final reading was taken at 12 hours.

A: Total food intake taken at the 4 hour time point, as there was no difference in the food intake in the feeding studies performed on day 38 and 42, the figure shows the average food intake over both feeding studies

B: Total food intake taken at the 12 hour time point, as there was no difference in the food intake in the feeding studies performed on day 38 and 42, the figure shows the average food intake over both feeding studies

Data are expressed as a mean ± SEM *n*=5 for RC GFP vehicle, *n*=5 RC GFP insulin, *n*=9 for HFD GFP vehicle, *n*=6 for HFD GFP insulin, *n*=8 for HFD Drp1-K38A vehicle, *n*=6 for HFD Drp1-K38A insulin. Orange dots represent data gained from day 9, blue dots represent data gained from day 14. Statistical test: Two way ANOVA (post-hoc test: Tukey)[*p <0.05, **p <0.01]

At the 12 hours, the effect of insulin was lost in both RC-fed and HFD-fed GFP-expressing rats, however there is still a significant decrease in food intake effect

[8] Restoration of insulin sensitivity refers to restoring insulin-induced hypophagia

seen in Drp1-K38A-expressing rats infused with insulin (Figure 6.3B). In summary, inhibition of Drp1 in hyperphagic HFD rats can restore insulin sensitivity.

6.2.2.2 Inhibition of Drp1 in the DVC decreased food intake, body weight gain and blood glucose levels in obese HFD-fed rats

Inhibiting Drp1 in the DVC restored insulin sensitivity in HFD-fed obese rats (Figure 6.3). Next, I wanted to understand the effects that inhibiting Drp1 had on food intake, body weight and blood glucose levels in HFD-fed rats. Each rat's food intake and body weight were taken each morning at a similar time. Blood glucose of each rats was taken before each feeding study and on the day of sacrifice, blood glucose levels are shown as an average of each time point as blood glucose levels did not differ.

Over the 14-day experiment HFD-fed rats expressing GFP in the DVC cumulatively ate more food in calories than both GFP-expressing RC-fed rats and Drp1-K38A-expressing HFD-fed rats (Figure 6.4A). From day 13, GFP-expressing-HFD-fed rats had a significant increase in food intake compared to Drp1-K38A-expressing rats (Figure 6.4A). In summary, I have shown that inhibiting Drp1 in the DVC decreases hyperphagia compared to HFD-fed controls.

There was variability in body weight gain within each cohort, initially, GFP-expressing RC-fed rats recovered better from surgery and viral injection when compared to both HFD-fed groups (Figure 6.4B). GFP-expressing and Drp1-K38A-expressing HFD-fed rats cohorts did not reach pre-surgical body weight until day four unlike the GFP-expressing RC-fed rats who reached pre-surgical body weight at day two (Figure 6.4B). By the end of the study, day 14 after surgery, GFP RC-fed and GFP HFD-fed rats had overall gained the same amount of body weight (Figure 6.4B). From day seven, Drp1-K38A-expressing rats and GFP-HFD-fed expressing rats, had reached pre-surgical body weight.

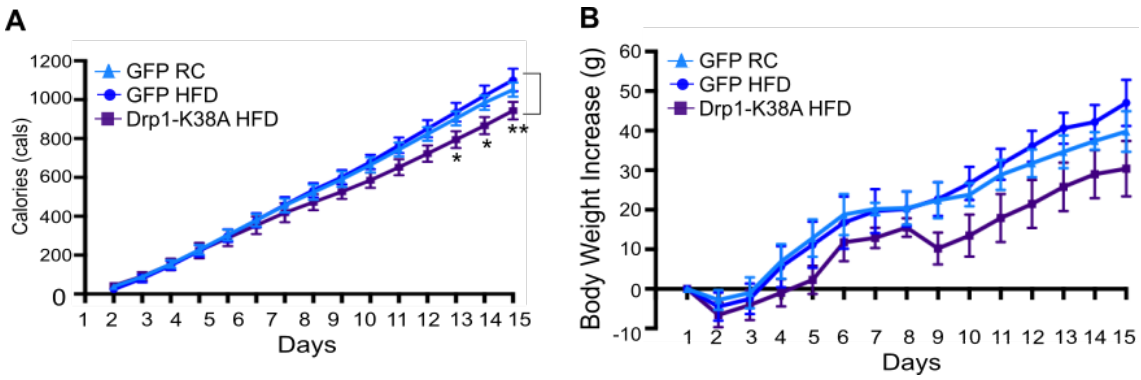

Figure 6.4 Cumulative food intake and body weight increase over the 14 days post-surgery in rats expressing Drp1-K38A and GFP

A: Cumulative food intake (in calories) in RC-fed GFP-expressing, HFD-fed GFP- expressing and Drp10K38A-expressing rats from day of viral injection

B: Body weight increase in RC-fed GFP-expressing, HFD-fed GFP-expressing and Drp1-K38A-expressing rats from day of viral injection

Data are expressed as mean ± SEM, *n*=5 GFP RC, *n*=6 GFP HFD, *n*=10 Drp1-K38A HFD [*p <0.05, **p <0.01] Significance is shown between Drp1-K38A-expressing and GFP-expressing HFD cohorts. Statistical test: TWO way ANOVA (post-hoc test: Tukey)

As mentioned previously, the blood glucose levels of rats were taken before each acute feeding study and on the day of sacrifice. There was no changes in bloody glucose levels across the three cohorts (Figure 6.5).

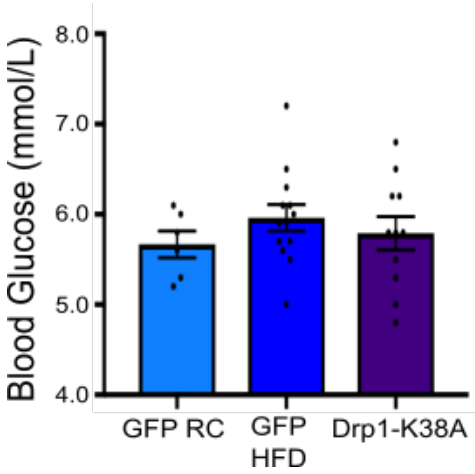

Figure 6.5 Average blood glucose during the study post-surgery

Data are an average of readings taken before feeding studies and day of sacrifice. Data are expressed as mean ± SEM, *n*=6 GFP RC, *n*=15 GFP HFD, *n*=12 Drp1-K38A HFD. Statistical Test: unpaired T-test

6.2.2.3 Inhibition of Drp1 in the DVC decreased the total white adipose tissue and increases the weight of brown fat in obese HFD-fed rats

I have demonstrated that inhibition of Drp1 in hyperphagic rats can restore insulin sensitivity to a similar level of a RC-fed rats. On the day of sacrifice, day 44, WAT and BAT were collected and weighed to look into the effect that inhibiting mitochondrial fission in the DVC has on fat distribution in obese rats.

HFD-fed rats expressing the catalytically inactive form of Drp1, Drp1-K38A, had significantly lower levels of visceral fat and total WAT and less epididymal and visceral fat than GFP-expressing HFD-fed controls (Figure 6.6A). RC-fed GFP-expressing rats had significantly lower level of epididymal fat, and lower levels of retroperitoneal and visceral fat compared to GFP-expressing HFD-fed rats (Figure 6.6A)

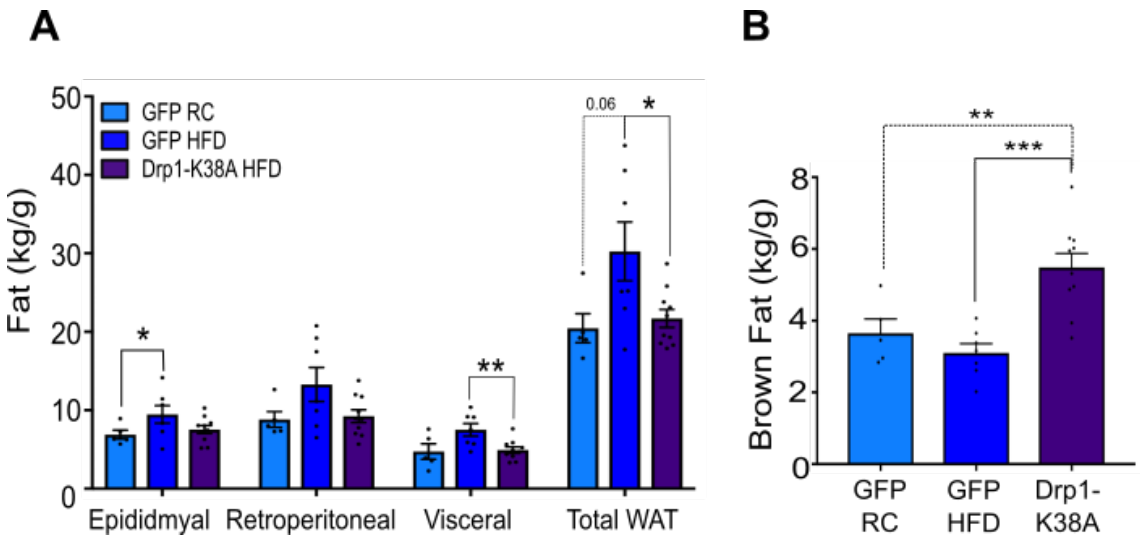

Figure 6.6 Weight of white adipose tissue and brown adipose tissue on the day of sacrifice in Drp1-K38A and GFP-expressing rats

A: Weight of epididymal, retroperitoneal, visceral and total WAT in rats expressing GFP or Drp1-K38A

B: Weight of BAT in rats expressing GFP or Drp1-K38A

Data are expressed as mean ± SEM, *n*=5 GFP RC, *n*=6 GFP HFD, *n*=10 Drp1-K38A HFD

Statistical test: multiple T-test [*p <0.05, **p <0.01, *** p<0.001]

In this cohort the BAT was also collected as I wanted to investigate whether altering mitochondrial fission in the DVC could have an effect on BAT. Intrascapular BAT was collected from between the shoulder blades and weighed. Rats expressing Drp1-K38A had a significant 43% and 33% greater volumes of BAT than both HFD-fed and RC-fed expressing rats, respectively (Figure 6.6).

It is evident that inhibiting Drp1 in the DVC of obese rats can decrease the volumes of WAT, and can significantly increase the volume of BAT.

6.2.3 Inhibition of iNOS in the DVC restores insulin sensitivity and decreased body weight in obese HFD-fed rats

6.2.3.1 Inhibition of iNOS in the DVC restored insulin sensitivity in HFD-fed rats

Previously I have shown that knocking down iNOS in the DVC prevented the development of HFD-dependent insulin resistance and that inhibiting Drp1 in the DVC can decrease iNOS levels in obese rats following chronic HFD-feeding. Next, I wanted to investigate whether knocking down iNOS in the DVC could restore insulin sensitivity in obese-insulin resistant rats. On day 28 (Figure 6.1A), rats underwent stereotactic brain surgery where a bilateral canula was inserted into the NTS of the DVC, on the same day a lentiviral system was used to deliver a ShRNA for the mRNA of the iNOS protein (ShiNOS) or a control scrambled ShRNA (ShControl) (as described in section 2.4). Rats were subjected to feeding studies on day 37 and 41 (Figure 6.1A), where they were fasted for six hours, and then given an injection of insulin or a vehicle into the DVC. Food intake was measured every half an hour for four hours (as describe in section 2.5.2).

RC-fed ShControl-expressing rats infused with insulin had a significant 60% decrease in food intake at four hours compared to their RC-fed vehicle infused controls (Figure 6.7A). On the contrary, ShControl-expressing HFD-fed rats who were treated with insulin had a no effect on food intake at the four-hour time point (Figure 6.7A). HFD-fed rats expressing ShiNOS in the DVC who were treated with insulin had a significant 54% decrease in food intake at four hours, similar to RC-fed ShControl littermates (Figure 6.7A)

The effect of insulin at 12 hours had been diminished in HFD-fed and RC-fed ShControl expressing and in ShiNOS expressing rats (Figure 6.7B). In summary, it is evident that decreasing iNOS expression in the DVC can restore insulin sensitivity[9] in HFD-fed hyperphagic rats.

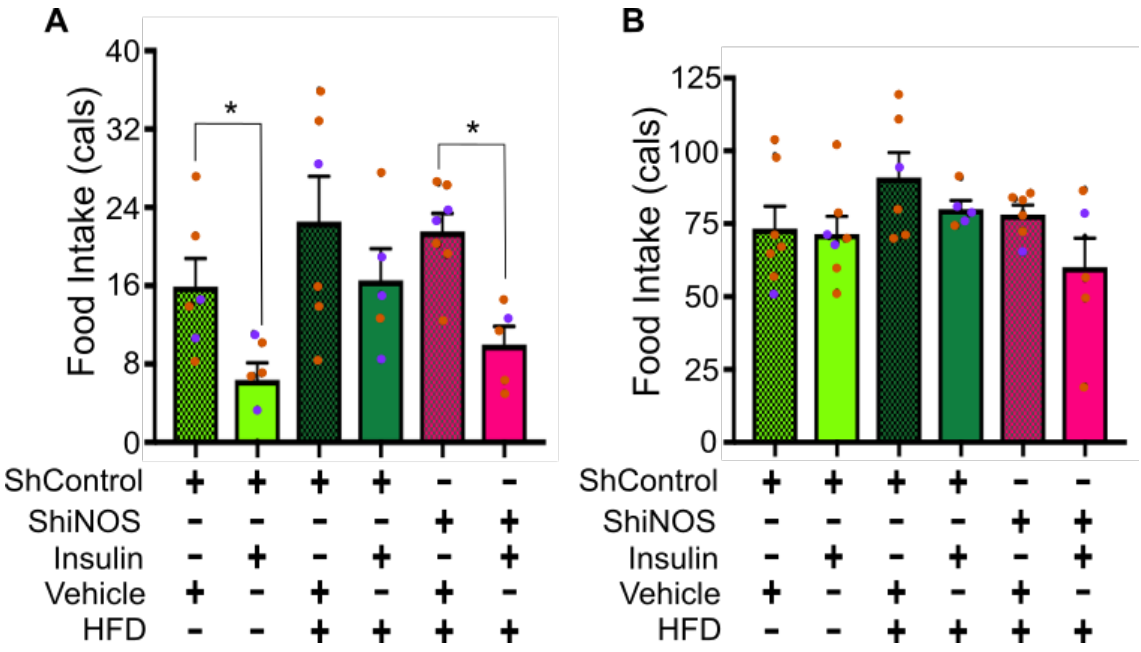

Figure 6.7 Food intake during acute feeding studies in 28-day RC or HFD-fed rats expressing ShiNOS and ShControl

Rats were fasted for 6 hours and then infused bilaterally into the DVC with a total 0.2ul of 2mU insulin or a vehicle over 5 minutes. Food was then returned and food intake was observed every half hour for 4 hours and a final reading was taken at 12 hours.

A: Total food intake taken at the 4 hour time point, since there was no difference in the food intake in the feeding studies performed on day 37 and 41, the figure shows the average food intake over both feeding studies

B: Total food intake taken at the 12 hour time point, since there was no difference in the food intake in the feeding studies performed on day 37 and 41, the figure shows the average food intake over both feeding studies

Data are expressed as a mean ± SEM *n*=6 for RC ShControl vehicle, *n*=6 RC ShControl insulin, *n*=6 for HFD ShControl vehicle, *n*=5 for HFD ShControl insulin, *n*=7 for HFD ShiNOS vehicle, *n*=5 for HFD ShiNOS insulin Orange dots represent data gained from day 9, purple dots represent data gained from day 14. Statistical test: two way ANOVA (post-hoc test: Tukey) [*p <0.05]

[9] Restoration of insulin sensitivity refers to insulin-induced hypophagia

6.2.3.2 Decreased iNOS expression in DVC reduces food intake and body weight gain in HFD-fed obese rats

The data above demonstrates that knocking down iNOS can restore insulin sensitivity in the DVC in HFD-fed rats compared to HFD-fed ShControl-expressing rats. Chronic daily monitoring was carried out to monitor changes in food intake and body weight. From day 12, we start to see a significant difference in the food intake in ShiNOS-expressing rats and ShControl-expressing HFD-fed rats (Figure 6.8A). ShiNOS-expressing rats ate less than ShControl-expressing RC rats, where there is a significant difference from day 15 (Figure 6.8A). Over the 14 days post-surgery, ShControl-expressing HFD-fed rats had consumed the largest number of calories (Figure 6.8A). To determine whether the changes in body weight were due to the treatment and due to with the welfare of the rats, daily checks were carried out to look for any signs of distress. Overall, knocking down iNOS in the DVC can decrease food intake in hyperphagic HFD-fed rats.

HFD-fed ShiNOS-expressing rats had similar pattern body weight gain to RC-fed ShControl-expressing rats (Figure 6.8B). From day six, the body weight gained per day in ShiNOS-expressing rats started to plateau slowly much like RC-fed ShControl expressing rats (Figure 6.8B). Comparing the body weight gain in the ShControl expressing HFD-fed and RC-fed cohorts, there is a more noticeable trend in the changes in body weight gain over the 14 days post-surgery, HFD-fed ShControl-expressing rats gained weight more rapidly over the study period, however there is no significant difference between the ShiNOS-expressing HFD-fed and the ShControl-expressing RC-fed (Figure 6.8B) Overall, the ShControl expressing HFD-fed cohort gained the most body weight over the 14-day period, there is a clear difference in body weight gained being seen from day three

comparatively with ShiNOS expressing rats (Figure 6.8B). There is quite high variance within cohorts, resulting in a lack of significant difference between these data.

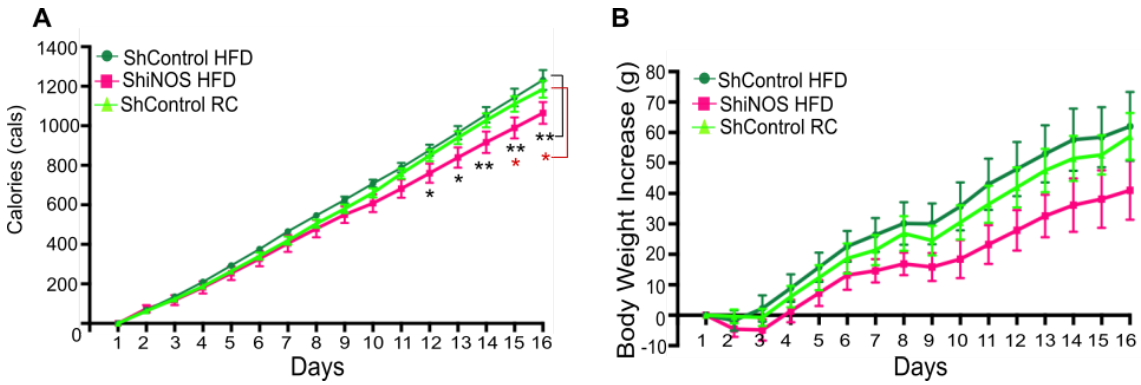

Figure 6.8 Cumulative food intake and body weight increase in ShiNOS and ShControl expressing rats

A: Cumulative food intake (in calories) in RC-fed ShControl expressing, HFD-fed ShControl expressing and ShiNOS expressing rats from day of viral injection

B: Body weight increase in RC-fed ShControl expressing, HFD-fed ShControl expressing and ShiNOS expressing rats from day of viral injection

Data are expressed as mean ± SEM, *n*=8 ShControl RC, *n*=8 ShControl HFD, *n*=7 ShiNOS HFD. Significance is shown between ShControl expressing HFD-fed and ShiNOS expressing cohorts in black, and ShControl expressing RC-fed and ShiNOS expressing cohorts in red. Statistical test: two way ANOVA (post-hoc test: Tukey) [*p <0.05, **p <0.01]

On the day of each feeding study, day 37 and 41, and on the day of sacrifice day 43, the blood glucose of each rat was taken. During the study there was a significantly lower blood glucose levels in the RC-fed ShControl expressing rats compared with the HFD-fed ShControl expressing rats (Figure 6.9). There was no difference in blood glucose in ShiNOS-expressing rats compared to ShControl-expressing HFD-fed rats (Figure 6.9).

In conclusion, I have demonstrated that knocking down iNOS in the DVC can decrease feeding behaviours and in turn reduce body weight gain comparatively against HFD-fed controls.

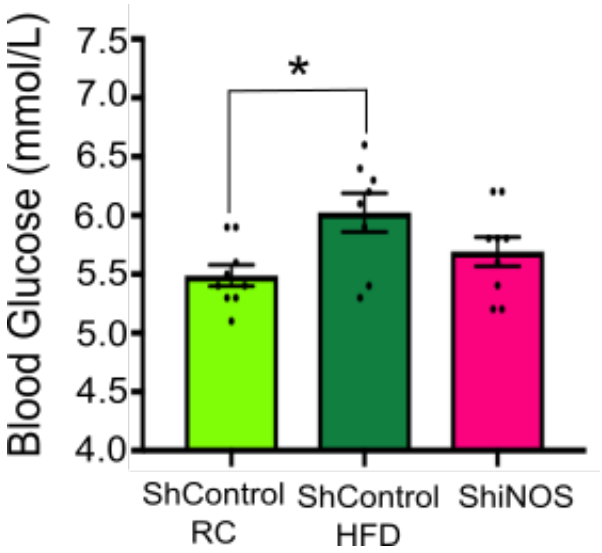

Figure 6.9 Average blood glucose during the study post-surgery in ShiNOS expressing and ShControl rats

Data are an average of readings taken before feeding studies (day 37 and 41) and day on sacrifice (day 43). Data are expressed as mean ± SEM, *n*=9 for ShControl RC, ShControl HFD, ShiNOS HFD. Statistical test: unpaired T-test [*p <0.05]

6.2.3.3 Decreasing expression of iNOS in the DVC had no effect on WAT and BAT deposition in obese rats

Previously, I have shown that knocking down iNOS in the DVC can decrease WAT deposition in 14 days compared to controls, next, I wanted to investigate the effect knocking down iNOS had on fat distribution in obese rats. The ShControl-expressing RC-fed rats, had significant decrease in the weight of epididymal and retroperitoneal fat compared to the HFD-fed ShControl-expressing rats (Figure 6.10A). However, there was no difference in the WAT deposition when comparing ShiNOS-expressing rats and ShControl-expressing HFD-fed rats (Figure 6.10A). There was no effect on BAT in rats expressing ShiNOS in the DVC compared to both HFD and RC-fed ShControl-expressing rats (Figure 6.10B).

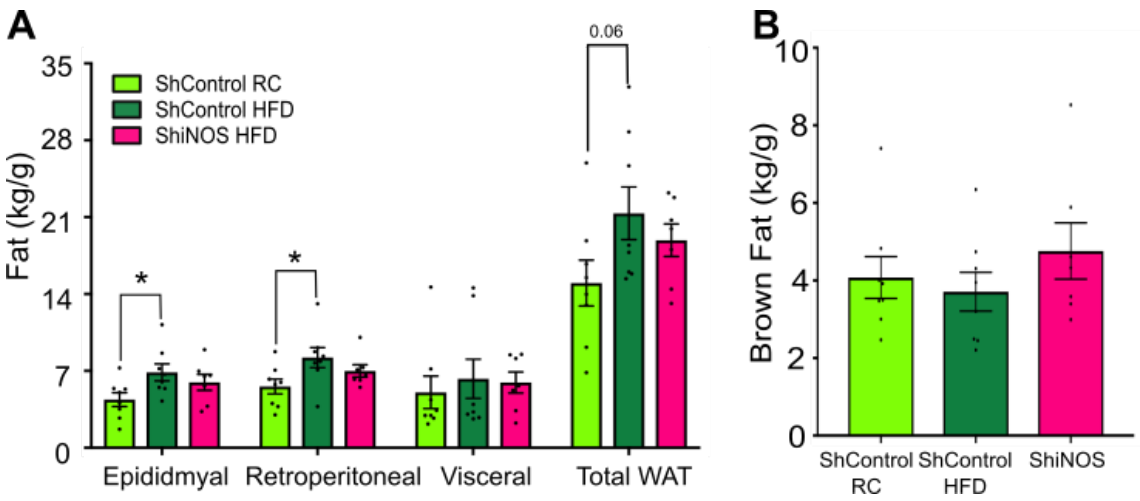

Figure 6.10 Weight of white adipose tissue and brown adipose tissue on the day of sacrifice in ShControl expressing RC and HFD-fed rats and in ShiNOS expressing rats

A: Weight of epididymal, retroperitoneal, visceral and total WAT in RC and HFD-fed ShControl or ShiNOS-expressing rats

B: Weight of BAT in RC and HFD-fed ShControl or ShiNOS-expressing rats

Data are expressed as mean ± SEM, n=8 ShControl RC, *n*=8 ShControl HFD, *n*=7 ShiNOS HFD. Statistical test: multiple T-test [*p <0.05]

6.3 Discussion

Studies have shown that obesity is associated with mitochondrial dysfunction which can lead to insulin resistance in the brain (Anderson et al., 2009; Jheng et al., 2012; Koves et al., 2008; Raza et al., 2015), here I have demonstrated that inhibiting mitochondrial fission in the DVC in obese rats, can successfully decrease food intake and body weight gain. It has been previously shown that HFD consumption increased levels of Drp1 by 50%, while decreasing fusion regulatory proteins such as Opa1 by 20%, furthermore ob/ob leptin deficient mice presented with significantly higher levels of Drp1 (Jheng et al., 2012; Liu et al., 2014). In addition to this, the data I have presented highlights that inhibiting mitochondria fission in the DVC can restore insulin sensitivity in HFD-fed hyperphagic rats, a possible mechanism by which this happens by decreasing levels of ROS and inflammation in the DVC (Filippi et al., 2017).

Increased caloric consumption caused impairment of mitochondrial function in the brain, and as a result increased ROS production and activation of UPR (Pipatpiboon et al., 2012; Pratchayasakul et al., 2015). Zucker rats have reduced functionality of their mitochondria which correlated with a decrease in ATP production and an increase in fission proteins, Drp1 (Raza et al., 2015). By knocking down iNOS in the DVC, I have successfully managed to restore insulin sensitivity in 28-day HFD-fed rats. A similar effect has also been seen in obese mice with a whole body knockout of iNOS, these rats exhibited improved glucose homeostasis and were more sensitive to insulin than their obese control counterparts (Perreault and Marette, 2001). Obese rats had an increase in s-nitrosylation of key insulin signalling pathways, AKT and IRS-1, in the hypothalamus (Katashima et al., 2017). These data demonstrate that iNOS plays

an important factor in the development of insulin resistance, a possible mechanism this may be due to an increase in s-nitrosylation of insulin signalling molecules.

Inhibition of iNOS in the hypothalamus in leptin deficient (*ob/ob)* rats resulted in a decreased body weight, as well as changes in feeding behaviours and energy homeostasis (Katashima et al., 2017). Obese iNOS knockout mice were protected from HFD-dependent insulin resistance and glucose homeostasis. In addition, these rats also had less NO in the vasculature (Noronha et al., 2005). Furthermore *ob/ob* mice which received an intraperitoneal injection of a chemical inhibitor of iNOS had improved insulin sensitivity and increase in IRS-1 in the livers compared to controls, suggesting that iNOS plays an important role in the development of insulin resistance (Fujimoto et al., 2005). Here, I have shown knocking down iNOS in the DVC can improve the hypophagic effect of insulin in obese rats. It has been previously demonstrated that intraperitoneal injection of an iNOS inhibitor, L-NIL, increased nodose ganglion excitability which in turn restored afferent sensitivity to satiety signalling, reduced food intake and lower levels of epididymal fat (Yu et al., 2019). It would be interesting to investigate the effect of inhibiting iNOS in the DVC and the relationship with afferent signals via the nodose ganglion in the regulation of body weight gain.

Chronic consumption of HFD increases the macrophage pool in the ARC in the hypothalamus, where the increase in macrophages was due to an higher levels of iNOS in obese rats (Lee et al., 2018). iNOS inhibition in the ARC abolished macrophage accumulation, inflammatory cytokines and astrogliosis, suggesting the critical role of iNOS in the hypothalamic inflammation (Lee et al., 2018). It would be interesting to look into the levels of ER-stress in the model and nitrite

levels in DVC to see if there is any more release of NO in the control HFD-fed hyperphagic rats, which could be an indicator of nitrosylation of proteins.

Inhibition of Drp1 in the DVC of obese rats caused a significant decrease in fat deposition, to levels similar to a RC-fed rat, however there was not a significant difference in body weight. This discrepancy may be due to high energy expenditure in the rats, which may be related to an increase in muscle mass in the rats expressing the inhibitor of Drp1, a finding which has been previously reported (Bach et al., 2003; Liesa and Shirihai, 2013). Using metabolic cages would allow a better understanding of how inhibition of mitochondrial fission effects energy expenditure. HFD-fed rats present with marked increased levels of ER stress in adipose tissue, which is induced by FFA ROS which results in an increase in inflammatory cytokines causing chronic inflammation (Kawasaki et al., 2012). Chemical treatment with chemical chaperones decreased the levels of ER stress in the obese adipose tissues (Kawasaki et al., 2012). Considering there is a significant decrease in the total volume of WAT in rats expressing the inhibitor of Drp1, it would be interesting to further investigate ER stress markers in the WAT specifically.

It would appear that BAT plays an important role in preventing obesity related complications. When HFD-fed rats were given a BAT transplant from healthy RC-fed rats and immune cell profiled four weeks later, HFD-fed BAT transplanted rats had a decrease in many different proinflammatory macrophages in the epididymal WAT. In addition, these rats also had a decrease in food intake and increase insulin sensitivity (Shankar et al., 2019; Stanford et al., 2013). I have demonstrated that decreasing mitochondrial fission in the DVC can increase the total weight of BAT. Interestingly, there is a significant increase in BAT mass in

rats expressing the inhibitor of Drp1, Drp1-K38A, it would therefore be interesting to look into the activity of BAT and the mitochondria morphology in these rats. It could be possible that inhibiting mitochondrial fission in the DVC improves insulin sensitivity, which in turn increases BAT activity due to the increase in caloric intake in HFD-feeding.

Ablation of iNOS in leptin deficient (*ob/ob)* mice resulted in a decrease in food intake and increased expression of BAT adipogenesis transcriptional regulators as well as uncoupling proteins 1 and 3, enabling the recovery of the BAT phenotype (Becerril et al., 2010). Furthermore, rats with a leptin deficiency (*ob/ob*) and a knockout of iNOS had improved insulin sensitivity, decreased adipose tissue inflammation and also a down-regulation in proinflammatory genes (Becerril et al., 2018). Although there was no effect on the weight of the BAT tissue collected from the ShiNOS expressing rats, it would be interesting to investigate the activity of the BAT and to see if any regulators of adiposity are upregulated in this model.

While there was a clear restoration of insulin sensitivity following either inhibition of Drp1 or knockdown of iNOS in the DVC of HFD-fed overweight and insulin resistant rats, I could not see a clear effect on food intake and body weight. A possible reason that this could be due to poor recovery from both surgery and viral injection when rats are fed a HFD. In both cases, the Drp1-expressing cohort and ShiNOS-expressing cohort, it is apparent that the recovery is not as fast as their RC-fed littermates; where I saw faster recovery in previous experiments, when HFD was given after the viral injections (see section 3.2.4.2 and 4.2.6). However, from day 8 in both cohorts, there is a clear trend in the body weight gain in HFD control rats versus HFD experimental treated counterparts (those

injected with either Drp1-K38A or ShiNOS). Since the study concluded 2 weeks after the viral treatment, it would be interesting to see whether the trend we see becomes significant after a longer period.

In conclusion it is evident that inhibiting Drp1 or decreasing the expression of iNOS in the DVC can restore insulin sensitivity in hyperphagic rats. Inhibiting Drp1 decreased WAT deposition and increased the amount of BAT compared to their HFD-fed controls (Figure 6.11).

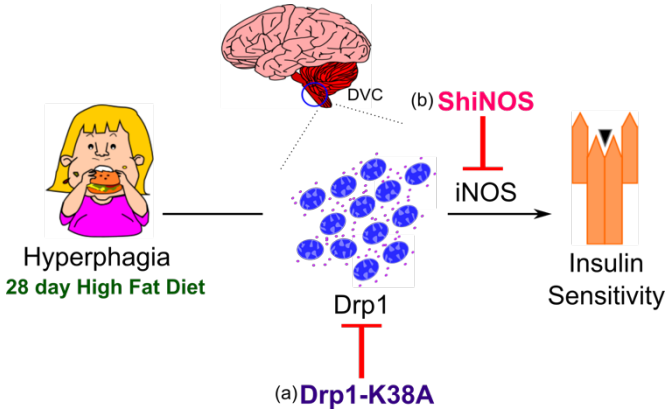

Figure 6.11 Inhibition of Drp1 (a) and knocking down iNOS (b) in the DVC can restore insulin-induced hypophagia in HFD-fed rats

7 General Discussion

7.1 Summary of findings

It has been well established that the brain plays an important role in central metabolism, in particular the MBH has been extensively researched in its contribution to the essential function of energy homeostasis. At the beginning of my project, I aimed to look into another region of the brain which is known to play an important role in central regulation of metabolism, the DVC. It has been well defined that the DVC helps regulate food intake and HGP through activation of the ERK1/2 pathway. In addition to this, three days of HFD-feeding is sufficient to induce insulin resistance and change mitochondrial morphology in the DVC (Filippi et al., 2017). This led to my first aim to understand how mitochondrial dynamics in the DVC affect feeding behaviour and body weight gain in rats.

My data has demonstrated that over expression of Drp1 in the DVC prevented hypophagia induced by insulin and increased body weight and food intake in RC-fed rats, in addition to this, expression of the dominant negative form of Drp1 in the DVC prevented loss of insulin induced-hypophagia and decreased body weight gain and food intake compared to controls. It has been previously shown that an increase in the activation of Drp1 in muscle, liver and adipose tissue can induce insulin resistance (Bach et al., 2003; Favaro et al., 2019; Gao et al., 2014; Jheng et al., 2012). These results therefore highlight the importance of Drp1 in the development of insulin resistance.

Furthermore, activation of Drp1 *in vitro* has been shown to increase ROS and decrease activation of insulin signalling pathway molecules such as AKT and the insulin receptor (Lin et al., 2018). In support of this, my data demonstrates that not only does an activation of Drp1 in the DVC induce insulin resistance, it also increases iNOS levels. iNOS is a mediator of inflammation and has been

associated with insulin resistance (Carvalho-Filho et al., 2006). I have presented data which shows that inhibiting mitochondrial fission in rats fed HFD reduced iNOS levels in the DVC of rats. This led to my next aim which was to determine if iNOS plays a role in the pathway linking Drp1-dependent mitochondrial fission, ER stress and insulin resistance.

Excessive endogenous NO can induce S-nitrosylation which is an important chemical process, involving an addition of an NO group onto the cysteine residue of a thiol group, this in turn affects signalling pathways, such as insulin signalling (Rizza et al., 2014). It has previously been demonstrated that aberrant NO induces s-nitrosylation of the insulin receptor and IRS-1 which in turn causes insulin resistance in skeletal muscle, where chemical reversal of s-nitrosylation improved insulin signalling (Carvalho-Filho et al., 2006). In addition to this, Drp1 activity is modulated by s-nitrosylation, leading to increase in mitochondrial fragmentation (Cho et al., 2009). To this end, I first wanted to look into the effects mitochondrial fission had on nitrosylation levels in PC12 cells by establishing a nitrosylation assay. I managed to successfully determine that activation of Drp1 in PC12 cells increased iNOS levels as well as levels of s-nitrosylation. My data supports previous research which has shown that activation of Drp1 increased the mRNA levels of iNOS in microglial cells, emphasising that the cross talk between iNOS and Drp1 is involved in the development of insulin resistance, while inhibition of iNOS decreased Drp1 activity, perhaps there is a feeding back loop where Drp1 control iNOS levels which modulates activity levels of Drp1 (Lee and Kim, 2018; Park et al., 2013).

My data thus far, had shown that activation of Drp1 in the DVC increased iNOS levels in RC-fed rats, while inhibition of Drp1 in the DVC in HFD-fed rats

decreased iNOS, which led to investigate the effect of knocking down iNOS in the DVC of HFD-fed rats had on feeding behaviours, body weight gain and insulin sensitivity. My data demonstrated that decreasing iNOS levels in the DVC prevented HFD-dependent insulin resistance and decreased food intake and body weight gain. These data are in agreement with previous work where inhibition of iNOS via subcutaneous injection of an iNOS inhibitor, L-nitro arginine, decreased food intake mice (Morley and Flood, 1991). Furthermore, mice with a specific iNOS knockdown in skeletal muscle were protected from HFD-dependent diet induced obesity and insulin resistance (Perreault and Marette, 2001). Indeed, in the hypothalamus, ICV injection of GSNO induced s-nitrosylation of insulin signalling molecules leading to inhibition of insulin signalling, leading to an increase in food intake (Katashima et al., 2017). Together with these data, it could be deduced that iNOS plays a critical role in energy metabolism and insulin sensing, which is most likely to be due to nitrosylation of key components of the insulin signalling pathway. Thus far, I had found that activation of Drp1 in the DVC in RC-fed rats increased iNOS levels, furthermore, inhibition of iNOS in the DVC in HFD-fed rats prevented HFD-dependent insulin resistance.

My next aim was to identify what neural populations are involved in this pathway, by identifying the neural population involved and their target aids in the understanding of the pathogenesis of insulin resistance. Using an adenovirus expressing recombinant protein under a CMV promoter, we could not distinguish between the cell population that could be involved in the development of insulin resistance in the DVC. With a detailed analysis we could see that roughly 40% of the cells we could target were astrocytes. Since astrocytes are an important cells

for the production of NO and can increase iNOS levels are seen with an activation of mitochondrial fission, I tested the hypothesis that by specifically inhibiting mitochondrial fission in astrocytes of the DVC I could protect the rats from the HFD-dependent insulin resistance. To this end an adenoviral system was created to specifically target mitochondrial fission in astrocytes. Drp1-K38A was expressed under the GFAP promoter, to specifically target GFAP positive astrocytes in the DVC in order to understand the effect inhibiting mitochondrial fission in astrocytes had on feeding behaviours, body weight gain and insulin resistance in HFD-fed rats.

I found that inhibition of Drp1 in astrocytes of the DVC decreased food intake, body weight, iNOS levels and also prevented HFD-dependent insulin resistance. It has previously been demonstrated that in astrocytes knocked down of the insulin receptor, mitochondria failed to respond to an increase in glucose uptake, in addition these mitochondria appeared smaller, suggesting mitochondrial fission (García-Cáceres et al., 2016). More specifically, in the DVC, HFD-feeding initiated an upregulation of GFAP expression and an increase in the morphological complexity of astrocytes, which in turn inhibited food intake (MacDonald et al., 2019). Thus, suggesting that astrocytes play an integral role in the regulation of feeding behaviours in the DVC. Here I propose a novel mechanism in which changes in mitochondria dynamics in astrocytes can induce insulin resistance and affect the ability of the DVC to control metabolic functions. A potential mechanism could involve neuronal glial cross talk which allows astrocytes to sense metabolic changes within their network and communicate such information to neurones of the DVC to regulate energy homeostasis.

All the data thus far have investigated methods for the prevention of HFD-dependent insulin resistance. I next wanted to determine if these preventative methods could be used as a means to restore insulin sensitivity in obese rats. Obesity leads to the plethora of problems, I aimed to understand if altering a consequence in the development of obesity, such as mitochondrial fission or iNOS induced inflammation could alleviate some of these problems including insulin resistance and hyperphagia. My data has shown that both cohorts were able to acutely decrease food intake when treated with insulin compared to their HFD-fed controls. A similar effect has been seen previously, where a whole body knockout of iNOS improved glucose uptake and these rats were insulin sensitive compared to their obese control counterparts (Perreault and Marette, 2001). Rats expressing Drp1-K38A also successfully managed to acutely decrease food intake, however the chronic effects seen in both cohorts were not significant.

7.2 Future work

The data I have presented demonstrates that both inhibition of Drp1-dependent mitochondrial fission and decreasing iNOS in the DVC can prevent HFD-induced insulin resistance and metabolic changes. My work has provided a foundation that will help aid future research toward a deeper understanding of the pivotal role of the DVC in energy regulation and insulin sensing. If time permitted during my research project, I would have finished off the molecular analysis for the obese model cohorts, by running western blots to look into changes in certain molecular markers. My data shows a clear effect on restoration of insulin sensing after 28 days of HFD-feeding in both Drp1-K38A and ShiNOS-expressing cohorts compared to their HFD controls, however, whether there were changes in iNOS levels and ER-stress is yet to be determined. From previous research, there is

clear evidence that a decrease in iNOS in obese rats can decrease ER-stress levels and improve insulin sensing (Fujimoto et al., 2005; Perreault and Marette, 2001). Furthermore, an increase in mitochondrial fission has been associated with obesity (Dai and Jiang, 2019). While there was a clear restoration of insulin sensitivity with both inhibition of Drp1 or knockdown of iNOS in HFD-fed overweight and insulin resistant rats, I could not see a clear effect on food intake and body weight.

In this project I established an assay to specifically label s-nitrosylated proteins. In addition to this, I demonstrated that an activation of Drp1 in PC12 cells resulted in an increase in s-nitrosylation in cells. Following on from this, it would have been interesting to immunoprecipitate these samples to isolate and capture s-nitrosylated proteins. Using this assay in the future, using mass spectrometry, I would be able to identify specific molecular markers which are s-nitrosylated due to changes in mitochondrial dynamics. In particular, previously it has been demonstrated that an accumulation of misfolded proteins due to high levels of ER stress results in s-nitrosylation of key stress transducers of the UPR; PERK and IRE-1 (Nakato et al., 2015; Yang et al., 2015a). In addition to this, it has been well described that changes in iNOS levels can induce s-nitrosylation of key molecules in the insulin signalling pathway (Carvalho-Filho et al., 2006; Qian et al., 2018; Yasukawa et al., 2005). It could therefore be hypothesised that a potential relationship exists between activation of Drp1 and induction of insulin resistance which is due to an increase in nitrosylation of ER stress transducers and insulin signalling pathway molecules. S-nitrosylation is a reversible reaction leading to defects in signalling pathways, another form of nitrosylation is tyrosine nitration, which causes irreversible protein damage (Rizza et al., 2014). It would

be interesting to look into the effect of activation of Drp1 on tyrosine nitration in both *in vivo*, using the tissue samples from all of the cohort, and *in vivo,* using neuronal cell lysates. Following on from this to investigate the effect of iNOS-mediated tyrosine nitration of key insulin signalling molecules in the DVC on insulin sensing.

Inhibition of Drp1 in astrocytes of the DVC prevented the effect of HFD-dependent insulin resistance, body weight gain and hyperphagia. If time permitted, it would have been interesting to investigate the effect of activation of Drp1 in astrocytes of the DVC, by using an adenoviruses expressing Drp1-S637A under the GFAP promotor, to see if the effect on food intake, body weight gain and insulin is greater than targeting all neural populations of the DVC, as I saw with Drp1-K38A::GFAP expressing rats. At the end of chapter 5, I proposed two hypotheses, one of which was that an increase of Drp1 in astrocytes results in an iNOS-dependent increase in NO which acts as a neurotransmitter to neurones to induce insulin resistance in the DVC.

By using live slices of the DVC with altered mitochondrial dynamics in astrocytes we could look into the levels of NO using a fluorescent NO dye compared to controls. In addition to this, another important mechanism that needs to exploring is whether effecting astrocytes effects the way neurones respond to insulin, to this end, acute slices of the DVC where mitochondrial dynamics in astrocytes are altered, could be used to record neuronal activity in response to insulin

It would be interesting to explore the effects of mitochondrial dynamics in oligodendrocytes and neurones on feeding behaviours and insulin sensing furthermore to understand the pathways in the DVC which induce these behavioural changes. A possible way investigate the neuronal pathway would be

to specifically target mitochondrial dynamics in the neurones themselves, by expressing Drp1-K38A or Drp1-S637A under the synapsin I promotor (SYN), which is a neurone specific promotor (Hioki et al., 2007), in the DVC. If the SYN promotor demonstrated a clear effect of feeding and insulin sensing, I could go even further to specifically target certain types of neurones, whether inhibitory or excitatory. The future work I have proposed would help provide a better understanding to bridge the gap between mitochondrial fission and insulin resistance in the DVC.

7.3 How is my data clinically relevant?

Obesity and T2DM are epidemics with cases around the world rising at exponential rates, both conditions are also a risk factor for many other ailments. According to Public Health England, 7 out of 10 males and 6 out of 10 females in the United Kingdom are overweight or obese, while costing the National Health Service over £6.1 billion to treat obesity related illnesses (NHS Digital, 2019; Public Health England, 2017); now more than ever we need new therapeutic avenues in the prevention and treatment of obesity and T2DM. The CNS receives and processes signals in the periphery to maintain energy balance, making it an important area to research to gain a better understanding of the pathogenesis of these metabolic disorders (Hotamisligil et al., 1996; Tanti et al., 2013; Wilcox, 2005). My data has highlighted the importance of Drp1-dependent mitochondrial fission in DVC in the development of insulin resistance and hyperphagia. These findings are in line with much of the literature which demonstrates an increase of Drp1 is associated with insulin resistance in models of obesity (Jheng et al., 2012; Kelley et al., 2002; Wang et al., 2015). It could be proposed that a way to potentially prevent the onset of these metabolic diseases is by specifically

targeting mitochondrial dynamics to enhance mitochondrial fusion, or inhibit mitochondrial fission proteins, to reduce ER stress and mitophagy.

More specifically, my data has created a foundation for future research to look into the neural populations which are involved in the central action of insulin and the markers involved in the progression of insulin resistance in the brain. Intranasal drug delivery is a novel treatment an effective and non-invasive way to deliver drugs to CNS. By unveiling the potential molecular markers involved, it would allow for the generation of an intranasal drug delivery system to possibly inhibit said markers to restore insulin sensitivity in the brain and effectively the periphery. The DVC plays a critical role in the regulation of energy metabolism, in this project I have delved into molecular mechanisms involved in Drp1-dependent insulin resistance, and for the first time the effect of Drp1 in the DVC has on feeding behaviours has been reported, thereby laying a foundation for future research and novel therapies.

7.4 Final conclusions

In conclusion, my project has validated the role Drp1 in the DVC has on feeding behaviours, where a key molecular player of this mechanism is iNOS. In addition to this, I have determined for the first time that astrocytes are an important neural cell population in the pathogenesis of Drp1-dependent mechanisms of insulin resistance in the DVC. Finally, not only have I demonstrated that expressing a dominant negative form of Drp1 or knocking down iNOS in the DVC prevented the development of HFD-induced insulin resistance, I have shown that these methods are able to restore insulin sensitivity and reverse the effects of HFD-induced loss of insulin-induced hypophaia.

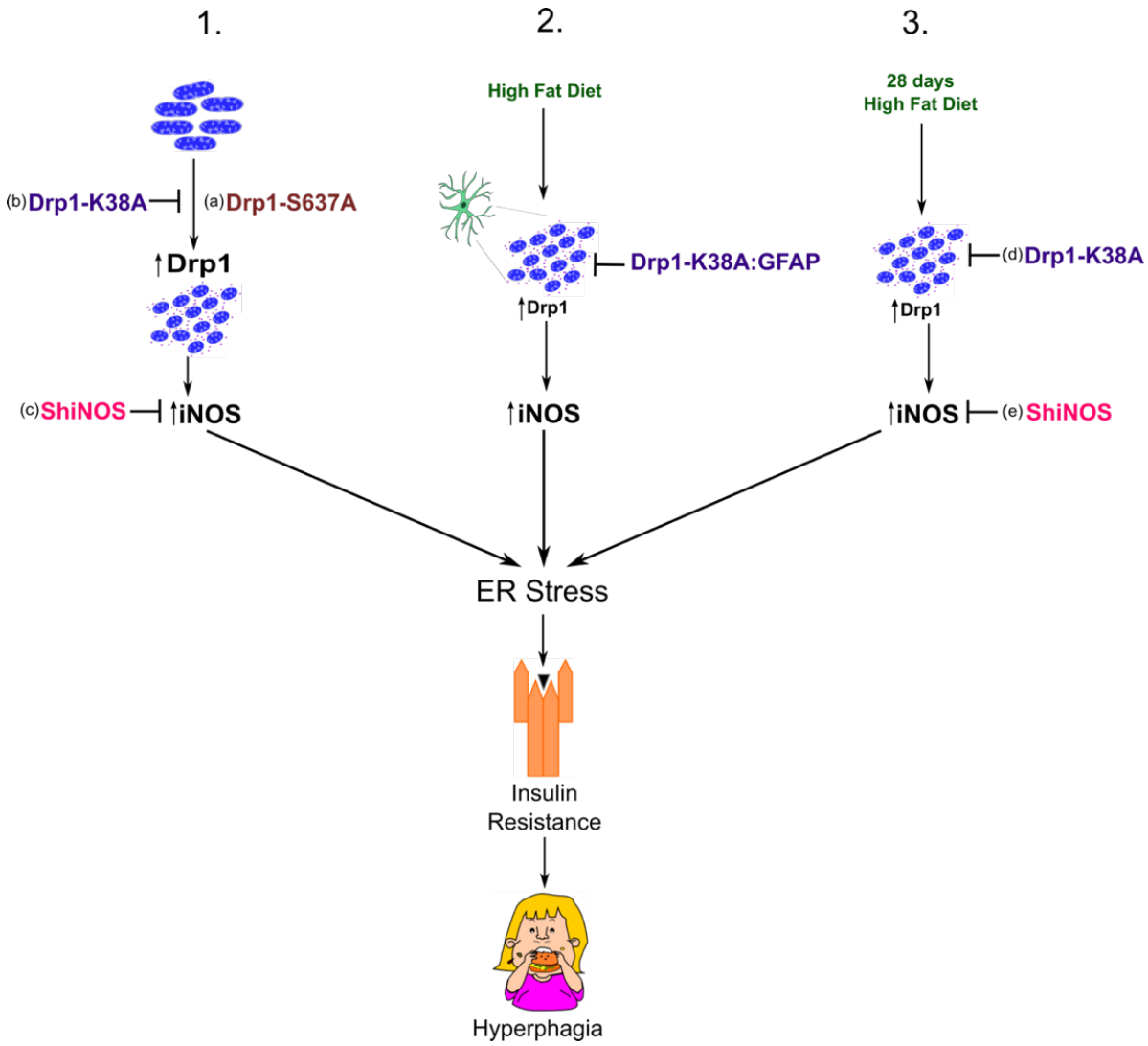

Figure 7.1 Summary figure of the main findings

1. Activation of Drp1, (a) Drp1-S637A, increases iNOS levels which in turn induces ER stress leading to insulin resistance in the DVC and hyperphagia. Inhibition of Drp1, using an adenovirus expressing a catalytically inactive form of Drp1, (b) Drp1-K38A or (c) inhibition of iNOS, using a lentiviral system to deliver a ShRNA of the mRNA of the iNOS proteins, ShiNOS, prevents HFD induced ER stress leading to insulin resistance in the DVC

2. Inhibition of Drp1 in the astrocytes of, Drp1-K38A::GFAP decreased iNOS levels and prevented HFD-dependent insulin resistance and hyperphagia

3. Inhibition of Drp1(d) or iNOS (e) in the DVC in 28-day HFD-fed rats restored insulin sensitivity and decreased food intake

8 References

Abdelmegeed, M.A., and Song, B.J. (2014). Functional roles of protein nitration in acute and chronic liver diseases. Oxid. Med. Cell. Longev. *2014*.

Adams, M.J., Blundell, T.L., Dodson, E.J., Dodson, G.G., Vijayan, M., Baker, E.N., Harding, M.M., Hodgkin, D.C., Rimmer, B., and Sheat, S. (1969). Structure of rhombohedral 2 zinc insulin crystals. Nature *224*, 491–495.

Aguirre, V., Uchida, T., Yenush, L., Davis, R., and White, M.F. (2000). The c-Jun NH2-terminal kinase promotes insulin resistance during association with insulin receptor substrate-1 and phosphorylation of Ser307. J. Biol. Chem. *275*, 9047–9054.

Amitai, Y. (2010). Physiologic role for “Inducible” nitric oxide synthase: A new form of astrocytic-neuronal interface. Glia *58*, 1775–1781.

Anavi, S., and Tirosh, O. (2020). iNOS as a metabolic enzyme under stress conditions. Free Radic. Biol. Med. *146*, 16–35.

Anderson, E.J., Lustig, M.E., Boyle, K.E., Woodlief, T.L., Kane, D.A., Lin, C.-T., Price, J.W., Kang, L., Rabinovitch, P.S., Szeto, H.H., et al. (2009). Mitochondrial H2O2 emission and cellular redox state link excess fat intake to insulin resistance in both rats and humans. J. Clin. Invest. *119*, 573–581.

Annesley, S.J., and Fisher, P.R. (2019). Mitochondria in Health and Disease. Cells *8*, 680.

Araki, E., Lipes, M.A., Patti, M., Brüning, J.C., Haag III, B., Johnson, R.S., and Kahn, C.R. (1994). Alternative pathway of insulin signalling in mice with targeted disruption of the IRS-1 gene. Nature *372*, 186–190.

Avgerinos, K.I., Kalaitzidis, G., Malli, A., Kalaitzoglou, D., Myserlis, P.G., and Lioutas, V.A. (2018). Intranasal insulin in Alzheimer’s dementia or mild cognitive impairment: a systematic review. J. Neurol. *265*, 1497–1510.

Bach, D., Pich, S., Soriano, F.X., Vega, N., Baumgartner, B., Oriola, J., Daugaard, J.R., Lloberas, J., Camps, M., Zierath, J.R., et al. (2003). Mitofusin-2 determines mitochondrial network architecture and mitochondrial metabolism: A

novel regulatory mechanism altered in obesity. J. Biol. Chem. *278*, 17190–17197.

Balfour, R.H., Hansen, A.M.K., and Trapp, S. (2006). Neuronal responses to transient hypoglycaemia in the dorsal vagal complex of the rat brainstem. J. Physiol. *570*, 469–484.

Balland, E., and Cowley, M.A. (2017). Short-term high-fat diet increases the presence of astrocytes in the hypothalamus of C57BL6 mice without altering leptin sensitivity. J. Neuroendocrinol. *29*, 1–7.

Bamshad, M., Song, C.K., and Bartness, T.J. (1999). CNS origins of the sympathetic nervous system outflow to brown adipose tissue. Am. J. Physiol. - Regul. Integr. Comp. Physiol. *276*.

Bandookwala, M., and Sengupta, P. (2020). 3-Nitrotyrosine: a versatile oxidative stress biomarker for major neurodegenerative diseases. Int. J. Neurosci. *0*, 1–16.

Banks, W.A. (2008). The blood-brain barrier: Connecting the gut and the brain. Regul. Pept. *149*, 11–14.

Barsoum, M.J., Yuan, H., Gerencser, A.A., Liot, G., Kushnareva, Y., Gräber, S., Kovacs, I., Lee, W.D., Waggoner, J., Cui, J., et al. (2006). Nitric oxide-induced mitochondrial fission is regulated by dynamin-related GTPases in neurons. EMBO J. *25*, 3900–3911.

Bartlett, K., and Eaton, S. (2004). Mitochondrial β-oxidation. Eur. J. Biochem. *271*, 462–469.

Becerril, S., Rodríguez, A., Catalán, V., Sáinz, N., Ramaaírez, B., Collantes, M., Peñuelas, I., Gómez-Ambrosi, J., and Frühbeck, G. (2010). Deletion of inducible nitric-oxide synthase in leptin-deficient mice improves brown adipose tissue function. PLoS One *5*, 1–12.

Becerril, S., Rodríguez, A., Catalán, V., Méndez-Giménez, L., Ramírez, B., Sáinz, N., Llorente, M., Unamuno, X., Gómez-Ambrosi, J., and Frühbeck, G. (2018). Targeted disruption of the iNOS gene improves adipose tissue inflammation and fibrosis in leptin-deficient ob/ob mice: role of tenascin C. Int. J. Obes. *42*, 1458–1470.

Benedict, C., Kern, W., Schultes, B., Born, J., and Hallschmid, M. (2008). Differential sensitivity of men and women to anorexigenic and memory-improving effects of intranasal insulin. J. Clin. Endocrinol. Metab. *93*, 1339–1344.

Benedict, C., Brede, S., Schiöth, H.B., Lehnert, H., Schultes, B., Born, J., and Hallschmid, M. (2011). Intranasal insulin enhances postprandial thermogenesis and lowers postprandial serum insulin levels in healthy men. Diabetes *60*, 114–118.

Berglund, E.D., Liu, T., Kong, X., Sohn, J.W., Vong, L., Deng, Z., Lee, C.E., Lee, S., Williams, K.W., Olson, D.P., et al. (2014). Melanocortin 4 receptors in autonomic neurons regulate thermogenesis and glycemia. Nat. Neurosci. *17*, 911–913.

Bertholet, A.M., Delerue, T., Millet, A.M., Moulis, M.F., David, C., Daloyau, M., Arnauné-Pelloquin, L., Davezac, N., Mils, V., Miquel, M.C., et al. (2016). Mitochondrial fusion/fission dynamics in neurodegeneration and neuronal plasticity. Neurobiol. Dis. *90*, 3–19.

Berthoud, H.R. (2008). The vagus nerve, food intake and obesity. Regul. Pept. *149*, 15–25.

Biddinger, S.B., Hernandez-Ono, A., Rask-Madsen, C., Haas, J.T., Alemán, J.O., Suzuki, R., Scapa, E.F., Agarwal, C., Carey, M.C., Stephanopoulos, G., et al. (2008). Hepatic Insulin Resistance Is Sufficient to Produce Dyslipidemia and Susceptibility to Atherosclerosis. Cell Metab. *7*, 125–134.

Blázquez, E., Velázquez, E., Hurtado-Carneiro, V., and Ruiz-Albusac, J.M. (2014). Insulin in the brain: Its pathophysiological implications for states related with central insulin resistance, type 2 diabetes and alzheimer's disease. Front. Endocrinol. (Lausanne). *5*, 1–21.

van der Bliek, A.M., Shen, Q., and Kawajiri, S. (2013). Mechanisms of mitochondrial fission and fusion. Cold Spring Harb. Perspect. Biol. *5*.

Bobrovnikova-Marjon, E., Pytel, D., Riese, M.J., Vaites, L.P., Singh, N., Koretzky, G.A., Witze, E.S., and Diehl, J.A. (2012). PERK Utilizes Intrinsic Lipid Kinase Activity To Generate Phosphatidic Acid, Mediate Akt Activation, and Promote

Adipocyte Differentiation. Mol. Cell. Biol. *32*, 2268–2278.

Boden, G. (2006). Fatty acid - Induced inflammation and insulin resistance in skeletal muscle and liver. Curr. Diab. Rep. *6*, 177–181.

Boden, G. (2009). Endoplasmic reticulum stress: Another link between obesity and insulin resistance/inflammation? Diabetes *58*, 518–519.

Boucher, J., Kleinridders, A., and Kahn, C.R. (2014). Insulin Receptor Signaling in Normal. Cold Spring Harb Perspect Biol 2014 *6*, a009191.

Bouyakdan, K., Martin, H., Liénard, F., Budry, L., Taib, B., Rodaros, D., Chrétien, C., Biron, É., Husson, Z., Cota, D., et al. (2019). The gliotransmitter ACBP controls feeding and energy homeostasis via the melanocortin system. J. Clin. Invest. *129*, 2417–2430.

Boyt, A.A., Taddei, K., Hallmayer, J., Helmerhorst, E., Gandy, S.E., Craft, S., and Martins, R.N. (1999). The effect of insulin and glucose on the plasma concentration of Alzheimer's amyloid precursor protein. Neuroscience *95*, 727–734.

Brand, M.D. (2010). The sites and topology of mitochondrial superoxide production. Exp. Gerontol. *45*, 466–472.

Bratic, I., and Trifunovic, A. (2010). Mitochondrial energy metabolism and ageing. Biochim. Biophys. Acta - Bioenerg. *1797*, 961–967.

Brown, M.S., and Goldstein, J.L. (2008). Selective versus Total Insulin Resistance: A Pathogenic Paradox. Cell Metab. *7*, 95–96.

Browning, K.N., and Travagli, R.A. (2011). Plasticity of vagal brainstem circuits in the control of gastrointestinal function. Auton. Neurosci. *161*, 6–13.

Brüning, J.C. (2000). Role of Brain Insulin Receptor in Control of Body Weight and Reproduction. Science (80-.). *289*, 2122–2125.

Brüning, L.P.B.F.B.J.C. (2006). Central insulin action in energy and glucose homeostasis. J. Clin. Invest. *116*, 1761–1766.

Buckman, L.B., Thompson, M.M., Moreno, H.N., and Ellacott, K.L.J. (2013).

Regional astrogliosis in the mouse hypothalamus in response to obesity. J. Comp. Neurol. *521*, 1322–1333.

Buckman, L.B., Thompson, M.M., Lippert, R.N., Blackwell, T.S., Yull, F.E., and Ellacott, K.L.J. (2015). Evidence for a novel functional role of astrocytes in the acute homeostatic response to high-fat diet intake in mice. Mol. Metab. *4*, 58–63.

Burgos-Morón, Abad-Jiménez, Marañón, Iannantuoni, Escribano-López, López-Domènech, Salom, Jover, Mora, Roldan, et al. (2019). Relationship Between Oxidative Stress, ER Stress, and Inflammation in Type 2 Diabetes: The Battle Continues. J. Clin. Med. *8*, 1385.

Burhans, M.S., Hagman, D.K., Kuzma, J.N., Schmidt, K.A., and Kratz, M. (2019). Contribution of adipose tissue inflammation to the development of type 2 diabetes mellitus. Compr. Physiol. *9*, 1–58.

Carneiro, L., Allard, C., Guissard, C., Fioramonti, X., Tourrel-Cuzin, C., Bailbé, D., Barreau, C., Offer, G., Nédelec, E., Salin, B., et al. (2012). Importance of Mitochondrial Dynamin-Related Protein 1 in Hypothalamic Glucose Sensitivity in Rats. Antioxid. Redox Signal. *17*, 433–444.

Carvalho-filho, M.A., Ueno, M., Hirabara, S.M., Seabra, A.B., Carvalheira, B.C., Oliveira, M.G. De, Velloso, A., Curi, R., and Saad, M.J.A. (2005). S-Nitrosation of the Insulin Receptor , Insulin Receptor. Diabetes *54*, 959–967.

Carvalho-Filho, M.A., Ueno, M., Carvalheira, J.B.C., Velloso, L.A., and Saad, M.J.A. (2006). Targeted disruption of iNOS prevents LPS-induced S-nitrosation of IRβ/IRS-1 and Akt and insulin resistance in muscle of mice. Am. J. Physiol. - Endocrinol. Metab. *291*, 476–482.

Carvalho-Filho, M.A., Ropelle, E.R., Pauli, R.J., Cintra, D.E., Tsukumo, D.M.L., Silveira, L.R., Curi, R., Carvalheira, J.B.C., Velloso, L.A., and Saad, M.J.A. (2009). Aspirin attenuates insulin resistance in muscle of diet-induced obese rats by inhibiting inducible nitric oxide synthase production and S-nitrosylation of IRβ/IRS-1 and Akt. Diabetologia *52*, 2425–2434.

Chadt, A., and Al-Hasani, H. (2020). Glucose transporters in adipose tissue, liver, and skeletal muscle in metabolic health and disease. Pflugers Arch. Eur. J.

Physiol. *472*, 1273–1298.

Chan, D.C. (2012). Fusion and Fission: Interlinked Processes Critical for Mitochondrial Health. Annu. Rev. Genet. *46*, 265–287.

Chang, C.R., and Blackstone, C. (2007). Cyclic AMP-dependent protein kinase phosphorylation of Drp1 regulates its GTPase activity and mitochondrial morphology. J. Biol. Chem. *282*, 21583–21587.

Chang, C.R., and Blackstone, C. (2010). Dynamic regulation of mitochondrial fission through modification of the dynamin-related protein Drp1. Ann. N. Y. Acad. Sci. *1201*, 34–39.

Charbonneau, A., and Marette, A. (2010). Inducible nitric oxide synthase induction underlies lipid-induced hepatic insulin resistance in mice: Potential role of tyrosine nitration of insulin signaling proteins. Diabetes *59*, 861–871.

Chaudhari, N., Talwar, P., Parimisetty, A., d'Hellencourt, C.L., and Ravanan, P. (2014). A molecular web: Endoplasmic reticulum stress, inflammation, and oxidative stress. Front. Cell. Neurosci. *8*, 1–15.

Cheng, Z., Tseng, Y., and White, M.F. (2010). Insulin signaling meets mitochondria in metabolism. Trends Endocrinol. Metab. *21*, 589–598.

Cherrington, A.D. (1999). Banting Lecture 1997. Control of glucose uptake and release by the liver in vivo. Diabetes *48*, 1198 LP – 1214.

Cherrington, A.D., Moore, M.C., Sindelar, D.K., and Edgerton, D.S. (2007). Insulin action on the liver in vivo. Biochem. Soc. Trans. *35*, 1171–1174.

Cho, D.-H., Nakamura, T., Fang, J., Cieplak, P., Godzik, A., Gu, Z., and Lipton, S.A. (2009). S-Nitrosylation of Drp1 Mediates β-Amyloid-Related Mitochondrial Fission and Neuronal Injury. Science (80-.). *324*, 102–105.

Cho, D.H., Nakamura, T., and Lipton, S.A. (2010). Mitochondrial dynamics in cell death and neurodegeneration. Cell. Mol. Life Sci. *67*, 3435–3447.

Chou, C.H., Lin, C.C., Yang, M.C., Wei, C.C., Liao, H. De, Lin, R.C., Tu, W.Y., Kao, T.C., Hsu, C.M., Cheng, J.T., et al. (2012). GSK3beta-Mediated Drp1 Phosphorylation Induced Elongated Mitochondrial Morphology against Oxidative

Stress. PLoS One *7*.

Cignarelli, A., Genchi, V.A., Perrini, S., Natalicchio, A., Laviola, L., and Giorgino, F. (2019). Insulin and insulin receptors in adipose tissue development. Int. J. Mol. Sci. *20*, 1–20.

Claude, B. (1855). Leçons de physiologie expérimentale appliquée à la médecine. Faites Au Collège Fr. *XXX*.

Clegg, D.J., Riedy, C.A., Smith, K.A.B., Benoit, S.C., and Woods, S.C. (2003). Differential Sensitivity to Central Leptin and Insulin in Male and Female Rats. Diabetes *52*, 682 LP – 687.

Contreras, L., Drago, I., Zampese, E., and Pozzan, T. (2010). Mitochondria: The calcium connection. Biochim. Biophys. Acta - Bioenerg. *1797*, 607–618.

Costello, D.A., Claret, M., Al-Qassab, H., Plattner, F., Irvine, E.E., Choudhury, A.I., Giese, K.P., Withers, D.J., and Pedarzani, P. (2012). Brain deletion of insulin receptor substrate 2 disrupts hippocampal synaptic plasticity and metaplasticity. PLoS One *7*, 30–34.

Côté, C.D., Rasmussen, B.A., Duca, F.A., Zadeh-Tahmasebi, M., Baur, J.A., Daljeet, M., Breen, D.M., Filippi, B.M., and Lam, T.K.T. (2015). Resveratrol activates duodenal Sirt1 to reverse insulin resistance in rats through a neuronal network. Nat. Med. *21*, 498–505.

Cowley, M.A., Smart, J.L., Rubinstein, M., Cerdán, M.G., Diano, S., Horvath, T.L., Cone, R.D., and Low, M.J. (2001). Leptin activates anorexigenic POMC neurons through a neural network in the arcuate nucleus. Nature *411*, 480–484.

Crunfli, F., Mazucanti, C.H., De Moraes, R.C.M., Costa, A.P., Rodrigues, A.C., Scavone, C., and Torrão, A.D.S. (2018). NO-Dependent Akt Inactivation by S-Nitrosylation as a Possible Mechanism of STZ-Induced Neuronal Insulin Resistance. J. Alzheimer's Dis. *65*, 1427–1443.

Cunarro, J., Casado, S., Lugilde, J., and Tovar, S. (2018). Hypothalamic mitochondrial dysfunction as a target in obesity and metabolic disease. Front. Endocrinol. (Lausanne). *9*, 1–10.

Czech, M.P. (2017). Insulin action and resistance in obesity and type 2 diabetes. Nat. Med. *23*, 804–814.

D'Agostino, G., Lyons, D.J., Cristiano, C., Burke, L.K., Madara, J.C., Campbell, J.N., Garcia, A.P., Land, B.B., Lowell, B.B., Dileone, R.J., et al. (2016). Appetite controlled by a cholecystokinin nucleus of the solitary tract to hypothalamus neurocircuit. Elife *5*, 1–15.

Dai, W., and Jiang, L. (2019). Dysregulated Mitochondrial Dynamics and Metabolism in Obesity, Diabetes, and Cancer. Front. Endocrinol. (Lausanne). *10*, 1–10.

Dash, S., Xiao, C., Morgantini, C., Koulajian, K., and Lewis, G.F. (2015). Intranasal Insulin Suppresses Endogenous Glucose Production in Humans Compared With Placebo in the Presence of Similar Venous Insulin Concentrations. Diabetes *64*, 766 LP – 774.

Davies, V.J., Hollins, A.J., Piechota, M.J., Yip, W., Davies, J.R., White, K.E., Nicols, P.P., Boulton, M.E., and Votruba, M. (2007). Opa1 deficiency in a mouse model of autosomal dominant optic atrophy impairs mitochondrial morphology, optic nerve structure and visual function. Hum. Mol. Genet. *16*, 1307–1318.

Desmoulins, L., Chrétien, C., Paccoud, R., Collins, S., Cruciani-Guglielmacci, C., Galinier, A., Liénard, F., Quinault, A., Grall, S., Allard, C., et al. (2019). Mitochondrial Dynamin-Related Protein 1 (DRP1) translocation in response to cerebral glucose is impaired in a rat model of early alteration in hypothalamic glucose sensing. Mol. Metab. *20*, 166–177.

Dietrich, M.O., Liu, Z.W., and Horvath, T.L. (2013). Mitochondrial dynamics controlled by mitofusins regulate agrp neuronal activity and diet-induced obesity. Cell *155*, 188.

Dimitriadis, G., Mitron, P., Lambadiari, V., Maratou, E., and Raptis, S.A. (2011). Insulin effects in muscle and adipose tissue. Diabetes Res. Clin. Pract. *93*, 52–59.

Ding, W.X., and Yin, X.M. (2012). Mitophagy: Mechanisms, pathophysiological roles, and analysis. Biol. Chem. *393*, 547–564.

Dohm, G.L., Tapscott, E.B., Pories, W.J., Dabbs, D.J., Flickinger, E.G., Meelheim, D., Fushiki, T., Atkinson, S.M., Elton, C.W., and Caro, J.F. (1988). An in vitro human muscle preparation suitable for metabolic studies. Decreased insulin stimulation of glucose transport in muscle from morbidly obese and diabetic subjects. J. Clin. Invest. *82*, 486–494.

Edgerton, D.S., Lautz, M., Scott, M., Everett, C.A., Stettler, K.M., Neal, D.W., Chu, C.A., and Cherrington, A.D. (2006). Insulin's direct effects on the liver dominate the control of hepatic glucose production. J. Clin. Invest. *116*, 521–527.

Emanuelli, B., Peraldi, P., Filloux, C., Sawka-Verhelle, D., Hilton, D., and Van Obberghen, E. (2000). SOCS-3 is an insulin-induced negative regulator of insulin signaling. J. Biol. Chem. *275*, 15985–15991.

Evans, J.L., and Goldfine, I.D. (2013). Aging and insulin resistance: Just say iNOS. Diabetes *62*, 346–348.

Favaro, G., Romanello, V., Varanita, T., Andrea Desbats, M., Morbidoni, V., Tezze, C., Albiero, M., Canato, M., Gherardi, G., De Stefani, D., et al. (2019). DRP1-mediated mitochondrial shape controls calcium homeostasis and muscle mass. Nat. Commun. *10*.

Feng, J., Chen, X., Guan, B., Li, C., Qiu, J., and Shen, J. (2018). Inhibition of Peroxynitrite-Induced Mitophagy Activation Attenuates Cerebral Ischemia-Reperfusion Injury. Mol. Neurobiol. *55*, 6369–6386.

Ferreira, L.S.S., Fernandes, C.S., Vieira, M.N.N., and De Felice, F.G. (2018). Insulin Resistance in Alzheimer's Disease. Front. Neurosci. *12*, 26–40.

Ferris, H.A., and Kahn, C.R. (2016). Unraveling the paradox of selective insulin resistance in the liver: The brain-liver connection. Diabetes *65*, 1481–1483.

Filadi, R., Pendin, Di., and Pizzo, P. (2018). Mitofusin 2: From functions to disease. Cell Death Dis. *9*.

Filippi, B.M., Mighiu, P.I., and Lam, T.K.T. (2012a). Is insulin action in the brain clinically relevant? Diabetes *61*, 773–775.

Filippi, B.M., Yang, C.S., Tang, C., and Lam, T.K.T. (2012b). Insulin activates

Erk1/2 signaling in the dorsal Vagal complex to inhibit glucose production. Cell Metab. *16*, 500–510.

Filippi, B.M., Bassiri, A., Abraham, M.A., Duca, F.A., Yue, J.T.Y., and Lam, T.K.T. (2014). Insulin Signals Through the Dorsal Vagal Complex to Regulate Energy Balance. Diabetes *63*, 892–899.

Filippi, B.M., Abraham, M.A., Silva, P.N., Rasti, M., LaPierre, M.P., Bauer, P. V., Rocheleau, J. V., and Lam, T.K.T. (2017). Dynamin-Related Protein 1-Dependent Mitochondrial Fission Changes in the Dorsal Vagal Complex Regulate Insulin Action. Cell Rep. 3201–2309.

Forrester, M.T., Foster, M.W., Benhar, M., and Stamler, J.S. (2009). Detection of protein S-nitrosylation with the biotin-switch technique. Free Radic. Biol. Med. *46*, 119–126.

Förstermann, U., and Sessa, W.C. (2012). Nitric oxide synthases: Regulation and function. Eur. Heart J. *33*, 829–837.

Foster, M.W., Hess, D.T., and Stamler, J.S. (2009). Protein S-nitrosylation in health and disease: a current perspective. J. Mol. Med. *15*, 391–404.

Fraulob, J.C., Ogg-Diamantino, R., Fernandes-Santos, C., Aguila, M.B., and Mandarim-de-Lacerda, C.A. (2010). A mouse model of metabolic syndrome: Insulin resistance, fatty liver and Non-Alcoholic Fatty Pancreas Disease (NAFPD) in C57BL/6 mice fed a high fat diet. J. Clin. Biochem. Nutr. *46*, 212–223.

Frey, T.G., and Mannella, C.A. (2000). The internal structure of mitochondria. Trends Biochem. Sci. *25*, 319–324.

Fujimoto, M., Shimizu, N., Kunii, K., Martyn, J.A.J., Ueki, K., and Kaneki, M. (2005). A role for iNOS in fasting hyperglycemia and impaired insulin signaling in the liver of obese diabetic mice. Diabetes *54*, 1340–1348.

Gao, A.W., Cantó, C., and Houtkooper, R.H. (2014). Mitochondrial response to nutrient availability and its role in metabolic disease. EMBO Mol. Med. *6*, 580–589.

García-Cáceres, C., Fuente-Martín, E., Argente, J., and Chowen, J.A. (2012).

Emerging role of glial cells in the control of body weight. Mol. Metab. *1*, 37–46.

García-Cáceres, C., Quarta, C., Varela, L., Gao, Y., Gruber, T., Legutko, B., Jastroch, M., Johansson, P., Ninkovic, J., Yi, C.X., et al. (2016). Astrocytic Insulin Signaling Couples Brain Glucose Uptake with Nutrient Availability. Cell *166*, 867–880.

Garvey, W.T., Maianu, L., Zhu, J.H., Brechtel-Hook, G., Wallace, P., and Baron, A.D. (1998). Evidence for defects in the trafficking and translocation of GLUT4 glucose transporters in skeletal muscle as a cause of human insulin resistance. J. Clin. Invest. *101*, 2377–2386.

Gelling, R.W., Morton, G.J., Morrison, C.D., Niswender, K.D., Myers, M.G., Rhodes, C.J., and Schwartz, M.W. (2006). Insulin action in the brain contributes to glucose lowering during insulin treatment of diabetes. Cell Metab. *3*, 67–73.

Ghasemi, M., and Fatemi, A. (2014). Pathologic role of glial nitric oxide in adult and pediatric neuroinflammatory diseases. Neurosci. Biobehav. Rev. *45*, 168–182.

Ghasemi, M., Mayasi, Y., Hannoun, A., Eslami, S.M., and Carandang, R. (2018). Nitric Oxide and Mitochondrial Function in Neurological Diseases. Neuroscience *376*, 48–71.

Girard, J. (2006). The inhibitory effects of insulin on hepatic glucose production are both direct and indirect. Diabetes *55*, 23–25.

Gomes, L.C., Benedetto, G. Di, and Scorrano, L. (2011). During autophagy mitochondria elongate, are spared from degradation and sustain cell viability. Nat. Cell Biol. *13*, 589–598.

Green, K., Brand, M.D., and Murphy, M.P. (2004). Prevention of Mitochondrial Oxidative Damage As A Therapeutic Strategy in Diabetes. Diabetes *53*.

Guillebaud, F., Girardet, C., Abysique, A., Gaigé, S., Barbouche, R., Verneui, J., Jean, A., Leprince, J., Tonon, M.C., Dallaporta, M., et al. (2017). Glial endozepines inhibit feeding-related autonomic functions by acting at the brainstem level. Front. Neurosci. *11*, 1–15.

Guthoff, M., Grichisch, Y., Canova, C., Tschritter, O., Veit, R., Hallschmid, M., Häring, H.U., Preissl, H., Hennige, A.M., and Fritsche, A. (2010). Insulin modulates food-related activity in the central nervous system. J. Clin. Endocrinol. Metab. *95*, 748–755.

Hallschmid, M., Benedict, C., Schultes, B., Fehm, H.L., Born, J., and Kern, W. (2004). Intranasal insulin reduces body fat in men but not in women. Diabetes *53*, 3024–3029.

Han, S.J., and Boyko, E.J. (2018). The evidence for an obesity paradox in type 2 diabetes mellitus. Diabetes Metab. J. *42*, 179–187.

Van Der Heide, L.P., Kamal, A., Artola, A., Gispen, W.H., and Ramakers, G.M.J. (2005). Insulin modulates hippocampal activity-dependent synaptic plasticity in a N-methyl-D-aspartate receptor and phosphatidyl-inositol-3-kinase-dependent manner. J. Neurochem. *94*, 1158–1166.

Hess, D.T., Matsumoto, A., Kim, S.O., Marshall, H.E., and Stamler, J.S. (2005). Protein S-nitrosylation: Purview and parameters. Nat. Rev. Mol. Cell Biol. *6*, 150–166.

Hill, J.W., Elias, C.F., Fukuda, M., Williams, K.W., Berglund, E.D., Holland, W.L., Cho, Y.R., Chuang, J.C., Xu, Y., Choi, M., et al. (2010). Direct Insulin and Leptin Action on Pro-opiomelanocortin Neurons Is Required for Normal Glucose Homeostasis and Fertility. Cell Metab. *11*, 286–297.

Hiltunen, M., Khandelwal, V.K.M., Yaluri, N., Tiilikainen, T., Tusa, M., Koivisto, H., Krzisch, M., Vepsäläinen, S., Mäkinen, P., Kemppainen, S., et al. (2012). Contribution of genetic and dietary insulin resistance to Alzheimer phenotype in APP/PS1 transgenic mice. J. Cell. Mol. Med. *16*, 1206–1222.

Hioki, H., Kameda, H., Nakamura, H., Okunomiya, T., Ohira, K., Nakamura, K., Kuroda, M., Furuta, T., and Kaneko, T. (2007). Efficient gene transduction of neurons by lentivirus with enhanced neuron-specific promoters. Gene Ther. *14*, 872–882.

Hirosumi, J., Tuncman, G., Chang, L., Görgün, C.Z., Uysal, K.T., Maeda, K., Karin, M., and Hotamisligil, G.S. (2002). A central, role for JNK in obesity and

insulin resistance. Nature *420*, 333–336.

Horvath, T.L., Sarman, B., García-Cáceres, C., Enriori, P.J., Sotonyi, P., Shanabrough, M., Borok, E., Argente, J., Chowen, J.A., Perez-Tilve, D., et al. (2010). Synaptic input organization of the melanocortin system predicts diet-induced hypothalamic reactive gliosis and obesity. Proc. Natl. Acad. Sci. U. S. A. *107*, 14875–14880.

Hotamisligil, G. k. S., Peraldi, P., Budavari, A., Ellis, R., White, M.F., and Spiegelman, B.M. (1996). IRS-1-Mediated Inhibition of Insulin Receptor Tyrosine Kinase Activity in TNF-alpha- and Obesity-Induced Insulin Resistance. Science (80-.). *271*, 665–670.

Howard, J.K., Cave, B.J., Oksanen, L.J., Tzameli, I., Bjoørbæk, C., and Flier, J.S. (2004). Enhanced leptin sensitivity and attenuation of diet-induced obesity in mice with haploinsufficiency of Socs3. Nat. Med. *10*, 734–738.

Ionescu, E., Rohner-Jeanrenaud, F., Berthoud, H.-R., and Jeanrenaud, B. (1983). Increases in Plasma Insulin Levels in Response to Electrical Stimulation of the Dorsal Motor Nucleus of the Vagus Nerve*. Endocrinology *112*, 904–910.

Ishihara, N., Nomura, M., Jofuku, A., Kato, H., Suzuki, S.O., Masuda, K., Otera, H., Nakanishi, Y., Nonaka, I., Goto, Y.I., et al. (2009). Mitochondrial fission factor Drp1 is essential for embryonic development and synapse formation in mice. Nat. Cell Biol. *11*, 958–966.

Jheng, H.-F., Tsai, P.-J., Guo, S.-M., Kuo, L.-H., Chang, C.-S., Su, I.-J., Chang, C.-R., and Tsai, Y.-S. (2012). Mitochondrial Fission Contributes to Mitochondrial Dysfunction and Insulin Resistance in Skeletal Muscle. Mol. Cell. Biol. *32*, 309–319.

Jiang, T., and Cadenas, E. (2014). Astrocytic metabolic and inflammatory changes as a function of age. Aging Cell *13*, 1059–1067.

Kadowaki, T., Tamemoto, H., Tobe, K., Terauchi, Y., Ueki, K., Kaburagi, Y., Yamauchi, T., Satoh, S., Sekihara, H., Aizawa, S., et al. (1996). Insulin Resistance and Growth Retardation in Mice Lacking Insulin Receptor Substrate-1 and Identification of Insulin Receptor Substrate-2. Diabet. Med. *13*, 103–108.

Kahn, S.E. (2001). Clinical, review 135: The importance of β-cell failure in the development and progression of type 2 diabetes. J. Clin. Endocrinol. Metab. *86*, 4047–4058.

Kahn, S.E., Hull, R.L., and Utzschneider, K.M. (2006). Mechanisms linking obesity to insulin resistance and type 2 diabetes. Nature *444*, 840–846.

Kaliyaperumal, K., Sharma, A.K., McDonald, D.G., Dhindsa, J.S., Yount, C., Singh, A.K., Won, J.S., and Singh, I. (2015). S-nitrosoglutathione-mediated STAT3 regulation in efficacy of radiotherapy and cisplatin therapy in head and neck squamous cell carcinoma. Redox Biol. *6*, 41–50.

Katashima, C.K., Silva, V.R.R., Lenhare, L., Marin, R.M., and Carvalheira, J.B.C. (2017). INOS promotes hypothalamic insulin resistance associated with deregulation of energy balance and obesity in rats. Sci. Rep. *7*.

Kawasaki, N., Asada, R., Saito, A., Kanemoto, S., and Imaizumi, K. (2012). Obesity-induced endoplasmic reticulum stress causes chronic inflammation in adipose tissue. Sci. Rep. *2*, 1–7.

Kelley, D.E., He, J., Menshikova, E. V., and Ritov, V.B. (2002). Dysfunction of Mitochondria in Human Skeletal Muscle in Type 2 Diabetes. Diabetes *51*, 2944–2950.

Kido, Y., Burks, D.J., Withers, D., Bruning, J.C., Kahn, C.R., White, M.F., and Accili, D. (2000). Tissue-specific insulin resistance in mice with mutations in the insulin receptor, IRS-1, and IRS-2. J. Clin. Invest. *105*, 199–205.

Kishi, T., Aschkenasi, C.J., Lee, C.E., Mountjoy, K.G., Saper, C.B., and Elmquist, J.K. (2003). Expression of melanocortin 4 receptor mRNA in the central nervous system of the rat. J. Comp. Neurol. *457*, 213–235.

Kishore, P., Boucai, L., Zhang, K., Li, W., Koppaka, S., Kehlenbrink, S., Schiwek, A., Esterson, Y.B., Mehta, D., Bursheh, S., et al. (2011). Activation of K ATP channels suppresses glucose production in humans. J. Clin. Invest. *121*, 4916–4920.

Kleinridders, A., Ferris, H.A., Cai, W., and Kahn, C.R. (2014). Insulin action in brain regulates systemic metabolism and brain function. Diabetes *63*, 2232–

2243.

Kleinridders, A., Cai, W., Cappellucci, L., Ghazarian, A., Collins, W.R., Vienberg, S.G., Pothos, E.N., and Kahn, C.R. (2015). Insulin resistance in brain alters dopamine turnover and causes behavioral disorders. Proc. Natl. Acad. Sci. U. S. A. *112*, 3463–3468.

Knott, A.B., and Bossy-Wetzel, E. (2009). Nitric oxide in health and disease of the nervous system. Antioxidants Redox Signal. *11*, 541–553.

Könner, A.C., and Brüning, J.C. (2011). Toll-like receptors: Linking inflammation to metabolism. Trends Endocrinol. Metab. *22*, 16–23.

Könner, A.C., Janoschek, R., Plum, L., Jordan, S.D., Rother, E., Ma, X., Xu, C., Enriori, P., Hampel, B., Barsh, G.S., et al. (2007). Insulin Action in AgRP-Expressing Neurons Is Required for Suppression of Hepatic Glucose Production. Cell Metab. *5*, 438–449.

Koves, T.R., Ussher, J.R., Noland, R.C., Slentz, D., Mosedale, M., Ilkayeva, O., Bain, J., Stevens, R., Dyck, J.R.B., Newgard, C.B., et al. (2008). Mitochondrial Overload and Incomplete Fatty Acid Oxidation Contribute to Skeletal Muscle Insulin Resistance. Cell Metab. *7*, 45–56.

Krashes, M.J., Shah, B.P., Madara, J.C., Olson, D.P., Strochlic, D.E., Garfield, A.S., Vong, L., Pei, H., Watabe-Uchida, M., Uchida, N., et al. (2014). An excitatory paraventricular nucleus to AgRP neuron circuit that drives hunger. Nature *507*, 238–242.

Kusminski, C.M., and Scherer, P.E. (2012). Mitochondrial dysfunction in white adipose tissue. Trends Endocrinol. Metab. *23*, 435–443.

Labbé, S.M., Caron, A., Lanfray, D., Monge-Rofarello, B., Bartness, T.J., and Richard, D. (2015). Hypothalamic control of brown adipose tissue thermogenesis. Front. Syst. Neurosci. *9*, 1–13.

Lebrun, P., and Van Obberghen, E. (2008). SOCS proteins causing trouble in insulin action. Acta Physiol. *192*, 29–36.

Lee, D. shin, and Kim, J.E. (2018). PDI-mediated S-nitrosylation of DRP1

facilitates DRP1-S616 phosphorylation and mitochondrial fission in CA1 neurons. Cell Death Dis. *9*.

Lee, H., and Yoon, Y. (2016). Mitochondrial fission and fusion. Biochem. Soc. Trans. *44*, 1725–1735.

Lee, J., and Ozcan, U. (2014). Unfolded Protein Response Signaling and Metabolic Diseases. J. Biol. Chem. *289*, 1203–1211.

Lee, J., and Pilch, P.F. (1994). The insulin receptor: structure, function, and signaling. Am. J. Physiol. Physiol. *266*, C319–C334.

Lee, C.C., Huang, C.C., and Hsu, K. Sen (2011). Insulin promotes dendritic spine and synapse formation by the PI3K/Akt/mTOR and Rac1 signaling pathways. Neuropharmacology *61*, 867–879.

Lee, C.H., Kim, H.J., Lee, Y.-S., Kang, G.M., Lim, H.S., Lee, S., Song, D.K., Kwon, O., Hwang, I., Son, M., et al. (2018). Hypothalamic Macrophage Inducible Nitric Oxide Synthase Mediates Obesity-Associated Hypothalamic Inflammation. Cell Rep. *25*, 934-946.e5.

Lee, M.W., Chanda, D., Yang, J., Oh, H., Kim, S.S., Yoon, Y.S., Hong, S., Park, K.G., Lee, I.K., Choi, C.S., et al. (2010). Regulation of Hepatic Gluconeogenesis by an ER-Bound Transcription Factor, CREBH. Cell Metab. *11*, 331–339.

Lee, S.H., Zabolotny, J.M., Huang, H., Lee, H., and Kim, Y.B. (2016). Insulin in the nervous system and the mind: Functions in metabolism, memory, and mood. Mol. Metab. *5*, 589–601.

Lee, Y., Jeong, S.-Y., Karbowski, M., Smith, C.L., and Youle, R.J. (2004). Roles of the Mammalian Mitochondrial Fission and Fusion Mediators Fis1, Drp1, and Opa1 in Apoptosis. Mol. Biol. Cell *15*, 5001–5011.

Li, H., and Förstermann, U. (2000). Nitric oxide in the pathogenesis of vascular disease. J. Pathol. *190*, 244–254.

Li, A., Zhang, S., Li, J., Liu, K., Huang, F., and Liu, B. (2016). Metformin and resveratrol inhibit Drp1-mediated mitochondrial fission and prevent ER stress-associated NLRP3 inflammasome activation in the adipose tissue of diabetic

mice. Mol. Cell. Endocrinol. *434*, 36–47.

Li, J., Wang, Y., Wang, Y., Wen, X., Ma, X.N., Chen, W., Huang, F., Kou, J., Qi, L.W., Liu, B., et al. (2015). Pharmacological activation of AMPK prevents Drp1-mediated mitochondrial fission and alleviates endoplasmic reticulum stress-associated endothelial dysfunction. J. Mol. Cell. Cardiol. *86*, 62–74.

Liberatore, G.T., Jackson-Lewis, V., Vukosavic, S., Mandir, A.S., Vila, M., Mcauliffe, W.G., Dawson, V.L., Dawson, T.M., and Przedborski, S. (1999). Inducible nitric oxide synthase stimulates dopaminergic neurodegeneration in the MPTP model of Parkinson disease. Nat. Med. *5*, 1403–1409.

Liesa, M., and Shirihai, O.S. (2013). Mitochondrial dynamics in the regulation of nutrient utilization and energy expenditure. Cell Metab. *17*, 491–506.

Lim, J.H., Lee, H.J., Ho Jung, M., and Song, J. (2009). Coupling mitochondrial dysfunction to endoplasmic reticulum stress response: A molecular mechanism leading to hepatic insulin resistance. Cell. Signal. *21*, 169–177.

Lin, H.-Y., Weng, S.-W., Chang, Y.-H., Su, Y.-J., Chang, C.-M., Tsai, C.-J., Shen, F.-C., Chuang, J.-H., Lin, T.-K., Liou, C.-W., et al. (2018). The Causal Role of Mitochondrial Dynamics in Regulating Insulin Resistance in Diabetes: Link through Mitochondrial Reactive Oxygen Species. Oxid. Med. Cell. Longev. *2018*, 1–14.

Lin, H. V., Plum, L., Ono, H., Gutiérrez-Juárez, R., Shanabrough, M., Borok, E., Horvath, T.L., Rossetti, L., and Accili, D. (2010). Divergent regulation of energy expenditure and hepatic glucose production by insulin receptor in agouti-related protein and POMC neurons. Diabetes *59*, 337–346.

Liu, R., Jin, P., Yu, L., Wang, Y., Han, L., Shi, T., and Li, X. (2014). Impaired mitochondrial dynamics and bioenergetics in diabetic skeletal muscle. PLoS One *9*, 1–8.

MacDonald, A.J., Holmes, F.E., Beall, C., Pickering, A.E., and Ellacott, K.L.J. (2019). Regulation of food intake by astrocytes in the brainstem dorsal vagal complex. Glia 1–14.

Maechler, P. (2013). Mitochondrial function and insulin secretion. Mol. Cell.

Endocrinol. *379*, 12–18.

Mardilovich, K., Pankratz, S.L., and Shaw, L.M. (2009). Expression and function of the insulin receptor substrate proteins in cancer. Cell Commun. Signal. *7*, 1–15.

Marette, A. (2002). Mediators of cytokine-induced insulin resistance in obesity and other inflammatory settings. Curr. Opin. Clin. Nutr. Metab. Care *5*, 377–383.

Margolis, R.U., and Altszuler, N. (1967). Insulin in the Cerebrospinal Fluid. Nature *215*, 1375–1376.

Maurer, L., Tang, H., Haumesser, J.K., Altschüler, J., Kühn, A.A., Spranger, J., and Van Riesen, C. (2017). High-fat diet-induced obesity and insulin resistance are characterized by differential beta oscillatory signaling of the limbic cortico-basal ganglia loop. Sci. Rep. *7*, 1–11.

de Mello, A.H., Costa, A.B., Engel, J.D.G., and Rezin, G.T. (2018). Mitochondrial dysfunction in obesity. Life Sci. *192*, 26–32.

Mering, J., and Minkowski, O. (1890). Diabetes mellitus nach Pankreasexstirpation. Arch. Für Exp. Pathol. Und Pharmakologie *26*, 371–387.

Meyer, J.N., Leuthner, T.C., and Luz, A.L. (2017). Mitochondrial fusion, fission, and mitochondrial toxicity Submitted for consideration for the Special Issue of Toxicology on “Chemical Mitochondrial Toxicity.” Toxicology *391*, 42–53.

Moore, M.C., Coate, K.C., Winnick, J.J., An, Z., and Cherrington, A.D. (2012). Regulation of Hepatic Glucose Uptake and Storage In Vivo. Adv. Nutr. *3*, 286–294.

Morley, J.E., and Flood, J.F. (1991). Evidence that nitric oxide modulates food intake in mice. Life Sci. *49*, 707–711.

Morris, G., Fernandes, B.S., Puri, B.K., Walker, A.J., Carvalho, A.F., and Berk, M. (2018a). Leaky brain in neurological and psychiatric disorders: Drivers and consequences. Aust. N. Z. J. Psychiatry *52*, 924–948.

Morris, G., Puri, B.K., Walder, K., Berk, M., Stubbs, B., Maes, M., and Carvalho, A.F. (2018b). The Endoplasmic Reticulum Stress Response in Neuroprogressive

Diseases: Emerging Pathophysiological Role and Translational Implications. Mol. Neurobiol. *55*, 8765–8787.

Morrison, S.F., and Madden, C.J. (2014). Central nervous system regulation of brown adipose tissue. Compr. Physiol. *4*, 1677–1713.

Mullington, J., Hermann, D., Holsboer, F., and Pollmächer, T. (1996). Age-dependent suppression of nocturnal growth hormone levels during sleep deprivation. Neuroendocrinology *64*, 233–241.

Muñoz, J.P., Ivanova, S., Sánchez-Wandelmer, J., Martínez-Cristóbal, P., Noguera, E., Sancho, A., Díaz-Ramos, A., Hernández-Alvarez, M.I., Sebastián, D., Mauvezin, C., et al. (2013). Mfn2 modulates the UPR and mitochondrial function via repression of PERK. EMBO J. *32*, 2348–2361.

Muoio, D.M. (2014). Metabolic inflexibility: When mitochondrial indecision leads to metabolic gridlock. Cell *159*, 1253–1262.

Nakamura, T., Cieplak, P., Cho, D.H., Godzik, A., and Lipton, S.A. (2010). S-Nitrosylation of Drp1 links excessive mitochondrial fission to neuronal injury in neurodegeneration. Mitochondrion *10*, 573–578.

Nakamura, T., Tu, S., Akhtar, M.W., Sunico, C.R., Okamoto, S. ichi, and Lipton, S.A. (2013). Aberrant Protein S-nitrosylation in neurodegenerative diseases. Neuron *78*, 596–614.

Nakatani, Y., Kaneto, H., Kawamori, D., Yoshiuchi, K., Hatazaki, M., Matsuoka, T.A., Ozawa, K., Ogawa, S., Hori, M., Yamasaki, Y., et al. (2005). Involvement of endoplasmic reticulum stress in insulin resistance and diabetes. J. Biol. Chem. *280*, 847–851.

Nakato, R., Ohkubo, Y., Konishi, A., Shibata, M., Kaneko, Y., Iwawaki, T., Nakamura, T., Lipton, S.A., and Uehara, T. (2015). Regulation of the unfolded protein response via S-nitrosylation of sensors of endoplasmic reticulum stress. Sci. Rep. *5*, 14812.

NHS Digital, L.T. (2019). Health Survey for England 2018.

Noronha, B.T., Li, J.-M., Wheatcroft, S.B., Shah, A.M., and Kearney, M.T. (2005).

Inducible Nitric Oxide Synthase Has Divergent Effects on Vascular and Metabolic Function in Obesity. Diabetes *54*, 1082–1089.

Nunnari, J., and Suomalainen, A. (2012). Mitochondria: In Sickness and in Health. Cell *148*, 1145–1159.

O-Sullivan, I., Zhang, W., Wasserman, D.H., Liew, C.W., Liu, J., Paik, J., Depinho, R.A., Stolz, D.B., Kahn, C.R., Schwartz, M.W., et al. (2015). FoxO1 integrates direct and indirect effects of insulin on hepatic glucose production and glucose utilization. Nat. Commun. *6*.

O'Malley, D., Shanley, L.J., and Harvey, J. (2003). Insulin inhibits rat hippocampal neurones via activation of ATP-sensitive K+ and large conductance Ca2+-activated K+ channels. Neuropharmacology *44*, 855–863.

Obici, S., Feng, Z., Karkanias, G., Baskin, D.G., and Rossetti, L. (2002a). Decreasing hypothalamic insulin receptors causes hyperphagia and insulin resistance in rats. Nat. Neurosci. *5*, 566–572.

Obici, S., Zhang, B.B., Karkanias, G., and Rossetti, L. (2002b). Hypothalamic insulin signaling is required for inhibition of glucose production. Nat. Med. *8*, 1376–1382.

Okada, T., Kawano, Y., Sakakibara, T., Hazeki, O., and Ui, M. (1994). Essential role of phosphatidylinositol 3-kinase in insulin-induced glucose transport and antilipolysis in rat adipocytes. Studies with a selective inhibitor wortmannin. J. Biol. Chem. *269*, 3568–3573.

Olichon, A., Guillou, E., Delettre, C., Landes, T., Arnauné-Pelloquin, L., Emorine, L.J., Mils, V., Daloyau, M., Hamel, C., Amati-Bonneau, P., et al. (2006). Mitochondrial dynamics and disease, OPA1. Biochim. Biophys. Acta - Mol. Cell Res. *1763*, 500–509.

Ollmann, M.M., Wilson, B.D., Yang, Y.K., Kerns, J.A., Chen, Y., Gantz, I., and Barsh, G.S. (1997). Antagonism of Central Melanocortin receptors in vitro and in vivo by agouti-related protein. Science (80-.). *278*, 135–138.

Ono, H., Pocai, A., Wang, Y., Sakoda, H., Asano, T., Backer, J.M., Schwartz, G.J., and Rossetti, L. (2008). Activation of hypothalamic S6 kinase mediates diet-

induced hepatic insulin resistance in rats. J. Clin. Invest. *118*, 2959–2968.

Ordureau, A., Paulo, J.A., Zhang, W., Ahfeldt, T., Zhang, J., Cohn, E.F., Hou, Z., Heo, J.M., Rubin, L.L., Sidhu, S.S., et al. (2018). Dynamics of PARKIN-Dependent Mitochondrial Ubiquitylation in Induced Neurons and Model Systems Revealed by Digital Snapshot Proteomics. Mol. Cell *70*, 211-227.e8.

Ozcan, U. (2004). Endoplasmic Reticulum Stress Links Obesity, Insulin Action, and Type 2 Diabetes. Science (80-.). *306*, 457–461.

Özcan, U., Cao, Q., Yilmaz, E., Lee, A.H., Iwakoshi, N.N., Özdelen, E., Tuncman, G., Görgün, C., Glimcher, L.H., and Hotamisligil, G.S. (2004). Endoplasmic reticulum stress links obesity, insulin action, and type 2 diabetes. Science (80-.). *306*, 457–461.

Özcan, U., Yilmaz, E., Özcan, L., Furuhashi, M., Vaillancourt, E., Smith, R.O., Görgün, C.Z., and Hotamisligil, G.S. (2006). Chemical chaperones reduce ER stress and restore glucose homeostasis in a mouse model of type 2 diabetes. Science (80-.). *313*, 1137–1140.

Pagliassotti, M.J., Kim, P.Y., Estrada, A.L., Stewart, C.M., Gentile, C.L., and Nutrition, H. (2017). Disorders : An Expanded View. *65*, 1238–1246.

Palikaras, K., Lionaki, E., and Tavernarakis, N. (2015). Balancing mitochondrial biogenesis and mitophagy to maintain energy metabolism homeostasis. Cell Death Differ. *22*, 1399–1401.

Palikaras, K., Lionaki, E., and Tavernarakis, N. (2018). Mechanisms of mitophagy in cellular homeostasis, physiology and pathology. Nat. Cell Biol. *20*, 1013–1022.

Park, S.W., and Ozcan, U. (2013). Potential for therapeutic manipulation of the UPR in disease. Semin. Immunopathol. *35*, 351–373.

Park, J., Choi, H., Min, J.S., Park, S.J., Kim, J.H., Park, H.J., Kim, B., Chae, J. Il, Yim, M., and Lee, D.S. (2013). Mitochondrial dynamics modulate the expression of pro-inflammatory mediators in microglial cells. J. Neurochem. *127*, 221–232.

Parton, L.E., Ye, C.P., Coppari, R., Enriori, P.J., Choi, B., Zhang, C.Y., Xu, C., Vianna, C.R., Balthasar, N., Lee, C.E., et al. (2007). Glucose sensing by POMC

neurons regulates glucose homeostasis and is impaired in obesity. Nature *449*, 228–232.

Pautz, A., Art, J., Hahn, S., Nowag, S., Voss, C., and Kleinert, H. (2010). Regulation of the expression of inducible nitric oxide synthase. Nitric Oxide - Biol. Chem. *23*, 75–93.

Peng, G., Li, L., Liu, Y., Pu, J., Zhang, S., Yu, J., Zhao, J., and Liu, P. (2011a). Oleate blocks palmitate-induced abnormal lipid distribution, endoplasmic reticulum expansion and stress, and insulin resistance in skeletal muscle. Endocrinology *152*, 2206–2218.

Peng, L., Men, X., Zhang, W., Wang, H., Xu, S., Xu, M., Xu, Y., Yang, W., and Lou, J. (2011b). Dynamin-related protein 1 is implicated in endoplasmic reticulum stress-induced pancreatic β-cell apoptosis. Int. J. Mol. Med. *28*, 161–169.

Perreault, M., and Marette, A. (2001). Targeted disruption of inducible nitric oxide synthase protects against obesity-linked insulin resistance in muscle. Nat Med *7*, 1138–1143.

Perry, V.H., Nicoll, J.A.R., and Holmes, C. (2010). Microglia in neurodegenerative disease. Nat. Rev. Neurol. *6*, 193–201.

Perseghin, G., Price, T.B., Petersen, K.F., Roden, M., Cline, G.W., Gerow, K., Rothman, D.L., and Shulman, G.I. (1996). Increased Glucose Transport–Phosphorylation and Muscle Glycogen Synthesis after Exercise Training in Insulin-Resistant Subjects. N. Engl. J. Med. *335*, 1357–1362.

Perseghin, G., Petersen, K., and Shulman, G.I. (2003). Cellular mechanism of insulin resistance: Potential links with inflammation. Int. J. Obes. *27*, S6–S11.

Petersen, M.C., and Shulman, G.I. (2018). Mechanisms of insulin action and insulin resistance. Physiol. Rev. *98*, 2133–2223.

Pickles, S., Vigié, P., and Youle, R.J. (2018). Mitophagy and Quality Control Mechanisms in Mitochondrial Maintenance. Curr. Biol. *28*, R170–R185.

Pilon, G., Charbonneau, A., White, P.J., Dallaire, P., Perreault, M., Kapur, S., and Marette, A. (2010). Endotoxin mediated-iNOS induction causes insulin resistance

via ONOO- induced tyrosine nitration of IRS-1 in skeletal muscle. PLoS One *5*, 2–12.

Pipatpiboon, N., Pratchayasakul, W., Chattipakorn, N., and Chattipakorn, S.C. (2012). PPARγ agonist improves neuronal insulin receptor function in hippocampus and brain mitochondria function in rats with insulin resistance induced by long term high-fat diets. Endocrinology *153*, 329–338.

Plum, L. (2006). Central insulin action in energy and glucose homeostasis. J. Clin. Invest. *116*, 1761–1766.

Pocai, A., Obici, S., Schwartz, G.J., and Rossetti, L. (2005). A brain-liver circuit regulates glucose homeostasis. Cell Metab. *1*, 53–61.

Pratchayasakul, W., Sa-nguanmoo, P., Sivasinprasasn, S., Pintana, H., Tawinvisan, R., Sripetchwandee, J., Kumfu, S., Chattipakorn, N., and Chattipakorn, S.C. (2015). Obesity accelerates cognitive decline by aggravating mitochondrial dysfunction, insulin resistance and synaptic dysfunction under estrogen-deprived conditions. Horm. Behav. *72*, 68–77.

Public Health England (2017). Health Matters: obesity and the food environment.

Putti, R., Sica, R., Migliaccio, V., and Lionetti, L. (2015). Diet impact on Mitochondrial Bioenergetics and Dynamics. Front. Physiol. *6*, 1–7.

Qian, Q., Zhang, Z., Orwig, A., Chen, S., Ding, W.X., Xu, Y., Kunz, R.C., Lind, N.R.L., Stamler, J.S., and Yang, L. (2018). S-nitrosoglutathione reductase dysfunction contributes to obesity-associated hepatic insulin resistance via regulating autophagy. Diabetes *67*, 193–207.

Quianzon, C.C., and Cheikh, I. (2012). History of insulin. J. Community Hosp. Intern. Med. Perspect. *2*, 18701.

Raffan, E., Dennis, R.J., O'Donovan, C.J., Becker, J.M., Scott, R.A., Smith, S.P., Withers, D.J., Wood, C.J., Conci, E., Clements, D.N., et al. (2016). A Deletion in the Canine POMC Gene Is Associated with Weight and Appetite in Obesity-Prone Labrador Retriever Dogs. Cell Metab. *23*, 893–900.

Ramírez, S., Gómez-Valadés, A.G., Schneeberger, M., Varela, L., Haddad-

Tóvolli, R., Altirriba, J., Noguera, E., Drougard, A., Flores-Martínez, Á., Imbernón, M., et al. (2017). Mitochondrial Dynamics Mediated by Mitofusin 1 Is Required for POMC Neuron Glucose-Sensing and Insulin Release Control. Cell Metab. *25*, 1390-1399.e6.

Raza, H., John, A., and Howarth, F.C. (2015). Increased oxidative stress and mitochondrial dysfunction in zucker diabetic rat liver and brain. Cell. Physiol. Biochem. *35*, 1241–1251.

Rizza, S., Montagna, C., Di Giacomo, G., Cirotti, C., and Filomeni, G. (2014). S - nitrosation and ubiquitin-proteasome system interplay in neuromuscular disorders. Int. J. Cell Biol.

Rizza, S., Cardaci, S., Montagna, C., Giacomo, G. Di, De Zio, D., Bordi, M., Maiani, E., Campello, S., Borreca, A., Puca, A.A., et al. (2018). S-nitrosylation drives cell senescence and aging in mammals by controlling mitochondrial dynamics and mitophagy. Proc. Natl. Acad. Sci. U. S. A. *115*, E3388–E3397.

Rodríguez, E.M., Blázquez, J.L., and Guerra, M. (2010). The design of barriers in the hypothalamus allows the median eminence and the arcuate nucleus to enjoy private milieus: The former opens to the portal blood and the latter to the cerebrospinal fluid. Peptides *31*, 757–776.

Roh, E., Song, D.K., and Kim, M.S. (2016). Emerging role of the brain in the homeostatic regulation of energy and glucose metabolism. Exp. Mol. Med. *48*.

Ron, D., and Walter, P. (2007). Signal integration in the endoplasmic reticulum unfolded protein response. Nat. Rev. Mol. Cell Biol. *8*, 519–529.

Ropelle, E.R., Pauli, J.R., Cintra, D.E., Da Silva, A.S., De Souza, C.T., Guadagnini, D., Carvalho, B.M., Caricilli, A.M., Katashima, C.K., Carvalho-Filho, M.A., et al. (2013). Targeted disruption of inducible nitric oxide synthase protects against aging, S-nitrosation, and insulin resistance in muscle of male mice. Diabetes *62*, 466–470.

Rosenfeld, L. (2002). Insulin: Discovery and Controversy. Clin. Chem. *48*, 2270 LP – 2288.

Rossi, J., Balthasar, N., Olson, D., Scott, M., Berglund, E., Lee, C.E., Choi, M.J.,

Lauzon, D., Lowell, B.B., and Elmquist, J.K. (2011). Melanocortin-4 receptors expressed by cholinergic neurons regulate energy balance and glucose homeostasis. Cell Metab. *13*, 195–204.

Rovira-Llopis, S., Bañuls, C., Diaz-Morales, N., Hernandez-Mijares, A., Rocha, M., and Victor, V.M. (2017). Mitochondrial dynamics in type 2 diabetes: Pathophysiological implications. Redox Biol. *11*, 637–645.

Ruud, J., Steculorum, S.M., and Bruning, J.C. (2017). Neuronal control of peripheral insulin sensitivity and glucose metabolism. Nat. Commun. *8*.

Saha, R., and Pahan, K. (2006). Signals for the induction of nitric oxide synthase in astrocytes. Neurochem. Int. *49*, 154–163.

Saltiel, A.R., and Kahn, C.R. (2001). Insulin signalling and the regulation of glucose and lipid metabolism. Nature *414*, 799–806.

Salvadó, L., Coll, T., Gómez-Foix, A.M., Salmerón, E., Barroso, E., Palomer, X., and Vázquez-Carrera, M. (2013). Oleate prevents saturated-fatty-acid-induced ER stress, inflammation and insulin resistance in skeletal muscle cells through an AMPK-dependent mechanism. Diabetologia *56*, 1372–1382.

Salvadó, L., Palomer, X., Barroso, E., and Vázquez-Carrera, M. (2015). Targeting endoplasmic reticulum stress in insulin resistance. Trends Endocrinol. Metab. *26*, 438–448.

Santoro, A., Campolo, M., Liu, C., Sesaki, H., Meli, R., Liu, Z.W., Kim, J.D., and Diano, S. (2017). DRP1 Suppresses Leptin and Glucose Sensing of POMC Neurons. Cell Metab. *25*, 647–660.

Sarraf, S.A., Raman, M., Guarani-Pereira, V., Sowa, M.E., Huttlin, E.L., Gygi, S.P., and Harper, J.W. (2013). Landscape of the PARKIN-dependent ubiquitylome in response to mitochondrial depolarization. Nature *496*, 372–376.

Scherer, T., OHare, J., Diggs-Andrews, K., Schweiger, M., Cheng, B., Lindtner, C., Zielinski, E., Vempati, P., Su, K., Dighe, S., et al. (2011). Brain insulin controls adipose tissue lipolysis and lipogenesis. Cell Metab. *13*, 183–194.

Schmitz, L., Kuglin, R., Bae-Gartz, I., Janoschek, R., Appel, S., Mesaros, A.,

Jakovcevski, I., Vohlen, C., Handwerk, M., Ensenauer, R., et al. (2018). Hippocampal insulin resistance links maternal obesity with impaired neuronal plasticity in adult offspring. Psychoneuroendocrinology *89*, 46–52.

Schneeberger, M., Dietrich, M.O., Sebastián, D., Imbernón, M., Castaño, C., Garcia, A., Esteban, Y., Gonzalez-Franquesa, A., Rodríguez, I.C., Bortolozzi, A., et al. (2013). Mitofusin 2 in POMC neurons connects ER stress with leptin resistance and energy imbalance. Cell *155*, 172–187.

Schneeberger, M., Gomis, R., and Claret, M. (2014). Hypothalamic and brainstem neuronal circuits controlling homeostatic energy balance. J. Endocrinol. *220*.

Schröder, M., and Kaufman, R.J. (2005). the Mammalian Unfolded Protein Response. Annu. Rev. Biochem. *74*, 739–789.

Schwartz, M.W. (2005). Diabetes, Obesity, and the Brain. Science (80-.). *307*, 375–379.

Schwartz, M.W. (2006). Central nervous system regulation of food intake. Obesity (Silver Spring). *14 Suppl 1*, 1–8.

Scott, I., and Youle, R.J. (2010). Mitochondrial fission and fusion. Essays Biochem. *47*, 85–98.

Sebastián, D., Hernández-Alvarez, M.I., Segalés, J., Sorianello, E., Muñoz, J.P., Sala, D., Waget, A., Liesa, M., Paz, J.C., Gopalacharyulu, P., et al. (2012). Mitofusin 2 (Mfn2) links mitochondrial and endoplasmic reticulum function with insulin signaling and is essential for normal glucose homeostasis. Proc. Natl. Acad. Sci. U. S. A. *109*, 5523–5528.

Sekine, S., and Youle, R.J. (2018). PINK1 import regulation; a fine system to convey mitochondrial stress to the cytosol. BMC Biol. *16*, 1–12.

Sesaki, H., and Jensen, R.E. (1999). Mitochondrial Shape. J. Cell Biol. *147*, 699–706.

Sesaki, H., Adachi, Y., Kageyama, Y., Itoh, K., and Iijima, M. (2014). In vivo functions of Drp1: Lessons learned from yeast genetics and mouse knockouts.

Biochim. Biophys. Acta - Mol. Basis Dis. *1842*, 1179–1185.

Shankar, K., Kumar, D., Gupta, S., Varshney, S., Rajan, S., Srivastava, A., Gupta, A., Gupta, A.P., Vishwakarma, A.L., Gayen, J.R., et al. (2019). Role of brown adipose tissue in modulating adipose tissue inflammation and insulin resistance in high-fat diet fed mice. Eur. J. Pharmacol. *854*, 354–364.

Shaw, L.M. (2011). The insulin receptor substrate (IRS) proteins: At the intersection of metabolism and cancer. Cell Cycle *10*, 1750–1756.

Shi, H., Cave, B., Inouye, K., Bjørbæk, C., and Flier, J.S. (2006). Overexpression of Suppressor of Cytokine Signaling 3 in Resistance. *55*, 699–707.

Shi, Y.C., Lau, J., Lin, Z., Zhang, H., Zhai, L., Sperk, G., Heilbronn, R., Mietzsch, M., Weger, S., Huang, X.F., et al. (2013). Arcuate NPY controls sympathetic output and BAT function via a relay of tyrosine hydroxylase neurons in the PVN. Cell Metab. *17*, 236–248.

Shinozaki, S., Choi, C.S., Shimizu, N., Yamada, M., Kim, M., Zhang, T., Dong, H.H., Kim, Y.B., and Kaneki, M. (2011). Liver-specific inducible nitric-oxide synthase expression is sufficient to cause hepatic insulin resistance and mild hyperglycemia in mice. J. Biol. Chem. *286*, 34959–34975.

Slawik, M., and Vidal-Puig, A.J. (2006). Lipotoxicity, overnutrition and energy metabolism in aging. Ageing Res. Rev. *5*, 144–164.

Smeets, P.A.M., Charbonnier, L., van Meer, F., van der Laan, L.N., and Spetter, M.S. (2012). Food-induced brain responses and eating behaviour. Proc. Nutr. Soc. *71*, 511–520.

Smirnova, E., Griparic, L., Shurland, D., and van der Bliek, A.M. (2001). Dynamin-related Protein Drp1 Is Required for Mitochondrial Division in Mammalian Cells. Mol. Biol. Cell *12*, 2245–2256.

Smith, R.L., Soeters, M.R., Wüst, R.C.I., and Houtkooper, R.H. (2018). Metabolic flexibility as an adaptation to energy resources and requirements in health and disease. Endocr. Rev. *39*, 489–517.

Sofroniew, M. V (2015). Astrogliosis perspectives. Cold Spring Harb. Perspect.

Biol. *7*, 1–16.

Soonpaa, M.H., Field, L.J., Spalding, K., Bhardwaj, R.D., Buchholz, B., Druid, H., Vries, H. De, Nydal, R., Lovseth, K., Levin, I., et al. (2009). S-Nitrosylation of Drp1 Mediates b -Amyloid – Related Mitochondrial Fission and Neuronal Injury. 102–106.

Soskić, S.S., Dobutović, B.D., Sudar, E.M., Obradović, M.M., Nikolić, D.M., Djordjevic, J.D., Radak, D.J., Mikhailidis, D.P., and Isenović, E.R. (2011). Regulation of Inducible Nitric Oxide Synthase (iNOS) and its Potential Role in Insulin Resistance, Diabetes and Heart Failure. Open Cardiovasc. Med. J. *5*, 153–163.

Sparrow, D., Borkan, G.A., Gerzof, S.G., Wisniewski, C., and Silbert, C.K. (1986). Relationship of Fat Distribution To Glucose Tolerance. *35*, 411–415.

Spetter, M.S., and Hallschmid, M. (2015). Intranasal Neuropeptide Administration To Target the Human Brain in Health and Disease. Mol. Pharm. *12*, 2767–2780.

Stadler, K. (2011). Peroxynitrite-Driven Mechanisms in Diabetes and Insulin Resistance – the Latest Advances. Curr. Med. Chem. *18*, 280–290.

Stanford, K.I., Middelbeek, R.J.W., Townsend, K.L., An, D., Nygaard, E.B., Hitchcox, K.M., Markan, K.R., Nakano, K., Hirshman, M.F., Tseng, Y.-H., et al. (2013). Brown adipose tissue regulates glucose homeostasis and insulin sensitivity. J. Clin. Invest. *123*, 215–223.

Stanley, B.G., and Leibowitz, S.F. (1984). Neuroreptide Y: Stimulation of feeding and drinking by injection into the paraventricular nucleus. Life Sci. *35*, 2635–2642.

Stark, R., and Roden, M. (2007). Mitochondrial function and endocrine diseases. Eur. J. Clin. Invest. *37*, 236–248.

Steculorum, S.M., Ruud, J., Karakasilioti, I., Backes, H., Engström Ruud, L., Timper, K., Hess, M.E., Tsaousidou, E., Mauer, J., Vogt, M.C., et al. (2016). AgRP Neurons Control Systemic Insulin Sensitivity via Myostatin Expression in Brown Adipose Tissue. Cell *165*, 125–138.

Sugita, H., Fujimoto, M., Yasukawa, T., Shimizu, N., Sugita, M., Yasuhara, S., Martyn, J.A.J., and Kaneki, M. (2005). Inducible nitric-oxide synthase and NO donor induce insulin receptor substrate-1 degradation in skeletal muscle cells. J. Biol. Chem. *280*, 14203–14211.

Sun, X.J., Crimmins, D.L., Myers, M.G., Miralpeix, M., and White, M.F. (1993). Pleiotropic insulin signals are engaged by multisite phosphorylation of IRS-1. Mol. Cell. Biol. *13*, 7418–7428.

Szendroedi, J., Phielix, E., and Roden, M. (2012). The role of mitochondria in insulin resistance and type 2 diabetes mellitus. Nat. Rev. Endocrinol. *8*, 92–103.

Tanti, J.F., Ceppo, F., Jager, J., and Berthou, F. (2013). Implication of inflammatory signaling pathways in obesity-induced insulin resistance. Front. Endocrinol. (Lausanne). *3*, 1–15.

Tezze, C., Romanello, V., Desbats, M.A., Fadini, G.P., Albiero, M., Favaro, G., Ciciliot, S., Soriano, M.E., Morbidoni, V., Cerqua, C., et al. (2017). Age-Associated Loss of OPA1 in Muscle Impacts Muscle Mass, Metabolic Homeostasis, Systemic Inflammation, and Epithelial Senescence. Cell Metab. *25*, 1374-1389.e6.

Thomas, E. (2001). Multiplicity of Infection. In Encyclopedia of Genetics, (Elsevier), p. 1258.

Tilokani, L., Nagashima, S., Paupe, V., and Prudent, J. (2018). Mitochondrial dynamics: Overview of molecular mechanisms. Essays Biochem. *62*, 341–360.

Timper, K., and Brüning, J.C. (2017). Hypothalamic circuits regulating appetite and energy homeostasis: Pathways to obesity. DMM Dis. Model. Mech. *10*, 679–689.

Timper, K., Paeger, L., Sánchez-Lasheras, C., Varela, L., Jais, A., Nolte, H., Vogt, M.C., Hausen, A.C., Heilinger, C., Evers, N., et al. (2018). Mild Impairment of Mitochondrial OXPHOS Promotes Fatty Acid Utilization in POMC Neurons and Improves Glucose Homeostasis in Obesity. Cell Rep. *25*, 383-397.e10.

Titchenell, P.M., Lazar, M.A., and Birnbaum, M.J. (2017). Unraveling the Regulation of Hepatic Metabolism by Insulin. Trends Endocrinol. Metab. *28*, 497–

505.

Tokarz, V.L., MacDonald, P.E., and Klip, A. (2018). The cell biology of systemic insulin function. J. Cell Biol. *217*, 1–17.

Touvier, T., De Palma, C., Rigamonti, E., Scagliola, A., Incerti, E., Mazelin, L., Thomas, J.L., D'Antonio, M., Politi, L., Schaeffer, L., et al. (2015). Muscle-specific Drp1 overexpression impairs skeletal muscle growth via translational attenuation. Cell Death Dis. *6*, 1–11.

Toyama, E.Q., Herzig, S., Courchet, J., Jr, T.L.L., Oliver, C., Hellberg, K., Young, N.P., Chen, H., Polleux, F., David, C., et al. (2016). Response To Energy Stress. *351*, 275–281.

Travagli, R.A., Hermann, G.E., Browning, K.N., and Rogers, R.C. (2006). Brainstem Circuits Regulating Gastric Function. Annu Rev Physiol *68*, 279–305.

Vatner, D.F., Majumdar, S.K., Kumashiro, N., Petersen, M.C., Rahimi, Y., Gattu, A.K., Bears, M., Camporez, J.P.G., Cline, G.W., Jurczak, M.J., et al. (2015). Insulin-independent regulation of hepatic triglyceride synthesis by fatty acids. Proc. Natl. Acad. Sci. U. S. A. *112*, 1143–1148.

Wang, L., Ishihara, T., Ibayashi, Y., Tatsushima, K., Setoyama, D., Hanada, Y., Takeichi, Y., Sakamoto, S., Yokota, S., Mihara, K., et al. (2015). Disruption of mitochondrial fission in the liver protects mice from diet-induced obesity and metabolic deterioration. Diabetologia *58*, 2371–2380.

Wang, W., Wang, Y., Long, J., Wang, J., Haudek, S.B., Overbeek, P., Chang, B.H.J., Schumacker, P.T., and Danesh, F.R. (2012a). Mitochondrial fission triggered by hyperglycemia is mediated by ROCK1 activation in podocytes and endothelial cells. Cell Metab. *15*, 186–200.

Wang, W., Wang, Y., Long, J., Wang, J., Haudek, S.B., Overbeek, P., Chang, B.H.J., Schumacker, P.T., and Danesh, F.R. (2012b). Mitochondrial fission triggered by hyperglycemia is mediated by ROCK1 activation in podocytes and endothelial cells. Cell Metab. *15*, 186–200.

Ward, C.W., and Lawrence, M.C. (2011). Landmarks in insulin research. Front. Endocrinol. (Lausanne). *2*, 1–11.

Webb, A.E., and Brunet, A. (2014). FOXO transcription factors: key regulators of cellular quality control. Trends Biochem. Sci. *39*, 159–169.

Westermann, B. (2012). Bioenergetic role of mitochondrial fusion and fission. Biochim. Biophys. Acta - Bioenerg. *1817*, 1833–1838.

Wikstrom, J.D., Israeli, T., Bachar-Wikstrom, E., Swisa, A., Ariav, Y., Waiss, M., Kaganovich, D., Dor, Y., Cerasi, E., and Leibowitz, G. (2013). AMPK regulates ER morphology and function in stressed pancreatic β-cells via phosphorylation of DRP1. Mol. Endocrinol. *27*, 1706–1723.

Wilcox, G. (2005). Insulin and insulin resistance. Clin. Biochem. Rev. *26*, 19–39.

Winzell, M.S., and Ahren, B. (2004). A Model for Studying Mechanisms and Treatment of Impaired Glucose Tolerance and Type 2 Diabetes. Diabetes *237*, 215–219.

Withers, D.J., Gutierrez, J.S., Towery, H., Burks, D.J., Ren, J.M., Previs, S., Zhang, Y., Bernal, D., Pons, S., Shulman, G.I., et al. (1998). Disruption of IRS-2 causes type 2 diabetes in mice. Nature *391*, 900–904.

Woods, S.C., McKay, L.D., and Stein, L.J. (1980). Chronic infusion of insulin reduces food intake and body weight of baboons. Appetite *1*, 89.

Woods, S.C., Lutz, T.A., Geary, N., and Langhans, W. (2006). Pancreatic signals controlling food intake; insulin, glucagon and amylin. Philos. Trans. R. Soc. B Biol. Sci. *361*, 1219–1235.

Yang, L., Calay, E.S., Fan, J., Arduini, A., Kunz, R.C., Gygi, S.P., Yalcin, A., Fu, S., and Hotamisligil, G.S. (2015a). S-Nitrosylation links obesity-associated inflammation to endoplasmic reticulum dysfunction. Science (80-.). *349*, 500–506.

Yang, L., Calay, E.S., Fan, J., Arduini, A., Kunz, R.C., Gygi, S.P., Yalcin, A., Fu, S., and Hotamisligil, G.S. (2015b). S-Nitrosylation links obesity-associated inflammation to endoplasmic reticulum dysfunction. Science (80-.). *349*, 500–506.

Yang, Q., Vijayakumar, A., and Kahn, B.B. (2018). Metabolites as regulators of

insulin sensitivity and metabolism. Nat. Rev. Mol. Cell Biol. *19*, 654–672.

Yasukawa, T., Tokunaga, E., Ota, H., Sugita, H., Martyn, J.A.J., and Kaneki, M. (2005). S-nitrosylation-dependent inactivation of Akt/protein kinase B in insulin resistance. J. Biol. Chem. *280*, 7511–7518.

Yettefti, K., Orsini, J.C., and Perrin, J. (1997). Characteristics of glycemia-sensitive neurons in the nucleus tractus solitarii: Possible involvement in nutritional regulation. Physiol. Behav. *61*, 93–100.

Yu, R., Liu, T., Jin, S.B., Ning, C., Lendahl, U., Nistér, M., and Zhao, J. (2017). MIEF1/2 function as adaptors to recruit Drp1 to mitochondria and regulate the association of Drp1 with Mff. Sci. Rep. *7*, 1–16.

Yu, Y., Park, S.J., and Beyak, M.J. (2019). Inducible nitric oxide synthase-derived nitric oxide reduces vagal satiety signalling in obese mice. J. Physiol. *597*, 1487–1502.

Yue, J.T.Y., Abraham, M.A., Bauer, P. V., Lapierre, M.P., Wang, P., Duca, F.A., Filippi, B.M., Chan, O., and Lam, T.K.T. (2016). Inhibition of glycine transporter-1 in the dorsal vagal complex improves metabolic homeostasis in diabetes and obesity. Nat. Commun. *7*, 1–11.

Yun, H.-Y., Dawson, V.L., and Dawson, T.M. (1997). Nitric oxide in health and disease of the nervous system. Mol. Psychiatry *2*, 300–310.

Zahedi Asl, S., Ghasemi, A., and Azizi, F. (2008). Serum nitric oxide metabolites in subjects with metabolic syndrome. Clin. Biochem. *41*, 1342–1347.

Zakeri, R., and Batterham, R.L. (2018). Obesity: when is specialist referral needed? Br. J. Gen. Pract. *68*, 264–265.

Zanotto, T.M., Quaresma, P.G.F., Guadagnini, D., Weissmann, L., Santos, A.C., Vecina, J.F., Calisto, K., Santos, A., Prada, P.O., and Saad, M.J.A. (2017). Blocking iNOS and endoplasmic reticulum stress synergistically improves insulin resistance in mice. Mol. Metab. *6*, 206–218.

Zemirli, N., Morel, E., and Molino, D. (2018). Mitochondrial dynamics in basal and stressful conditions. Int. J. Mol. Sci. *19*, 1–19.

Zhan, C., Zhou, J., Feng, Q., Zhang, J. en, Lin, S., Bao, J., Wu, P., and Luo, M. (2013). Acute and long-term suppression of feeding behavior by POMC neurons in the brainstem and hypothalamus, respectively. J. Neurosci. *33*, 3624–3632.

Zhang, C.Y., Baffy, G., Perret, P., Krauss, S., Peroni, O., Grujic, D., Hagen, T., Vidal-Puig, A.J., Boss, O., Kim, Y.B., et al. (2001). Uncoupling protein-2 negatively regulates insulin secretion and is a major link between obesity, β cell dysfunction, and type 2 diabetes. Cell *105*, 745–755.

Zhou, Y., Lee, J., Reno, C.M., Sun, C., Park, S.W., Chung, J., Lee, J., Fisher, S.J., White, M.F., Biddinger, S.B., et al. (2011). Regulation of glucose homeostasis through a XBP-1-FoxO1 interaction. Nat. Med. *17*, 356–365.

Zorzano, A., and Claret, M. (2015). Implications of mitochondrial dynamics on neurodegeneration and on hypothalamic dysfunction. Front. Aging Neurosci. *7*, 1–17.

---

i